TECHNISCHE UNIVERSITÄT MÜNCHEN

Lehrstuhl für Lebensmittelverpackungstechnik

Dairy fouling characterization and detection by means of electrochemical and low-field NMR techniques

Olga Fysun

Vollständiger Abdruck der von der Fakultät Wissenschaftszentrum Weihenstephan für Ernährung, Landnutzung und Umwelt der Technischen Universität München zur Erlangung des akademischen Grades eines

Doktors der Naturwissenschaften (Dr. rer. nat.)

genehmigten Dissertation.

Vorsitzender:	Prof. Dr.-Ing. Ulrich Kulozik
Prüfer der Dissertation:	1. Prof. Dr. Horst-Christian Langowski
	2. Prof. Dr.-Ing. Reinhard Kohlus

Diese Dissertation wurde am 28.01.2020 bei der Technischen Universität München eingereicht und durch die Fakultät Wissenschaftszentrum Weihenstephan für Ernährung, Landnutzung und Umwelt am 10.07.2020 angenommen.

Acknowledgements

I would like to thank all those people who greatly contributed to the research work and made this doctoral thesis possible.

First of all, I wish to express my sincere thanks to Prof. Dr. rer. nat. H.-Ch. Langowski for his valuable and constructive suggestions during the planning and development of this research work. Prof. Dr. rer. nat. H.-Ch. Langowski offered his continuous advice and encouragement throughout the PhD program at the Technical University of Munich.

In full gratitude, I would like to acknowledge the second examiner of this thesis, Prof. Dr.- Ing. Reinhard Kohlus, and the chief examiner, Prof. Dr.-Ing. Ulrich Kulozik. In addition, I take this opportunity to express gratitude to all of the Department faculty members for their help and support.

In particular, I would like to express my gratitude to Prof. Dr. Bernd Wilke and Dr. Johannes Rauschnabel for their patient guidance, enthusiastic encouragement and useful critiques through the learning process of this doctoral thesis. During the most difficult times when writing this thesis, they gave me the support and the freedom I needed to move on.

I would like also thank Theresa Anzmann and Dr. Peter Gschwind from University of Hohenheim for their valuable advice and support on nuclear magnetic resonance.

I would like to express my sincere thanks to Dr. Holger Brehm and Dunja Weiss from Robert Bosch Packaging Technology GmbH for their support on sensor technology and microbiology.

Also, I would like to express my heartfelt gratitude to my students, Heike Kern, Alen Maher, Alexander Schmitt, Peter Thomas Auernhammer, Alexander Kleesattel, and Sara Khorshid for the valuable contribution to this doctoral thesis.

My thanks also go to my family and friends for the unceasing encouragement and attention. Many thanks for the friendship and unyielding support through the process of researching and writing this doctoral thesis.

SCIENTIFIC CONTRIBUTIONS

Full papers

The following peer-reviewed publications were generated in the period of this work. These publications are related to the topic of the doctoral thesis and are included in the doctoral thesis:

1. Fysun, O., Kern, H., Wilke, B., Langowski, H.-C. (2019). Formation of dairy fouling deposits on food contact surfaces. International Journal of Dairy Technology, 72(2), 257-265. doi: 10.1111/1471-0307.12580

2. Fysun, O., Kern, H., Wilke, B., Langowski, H.-C. (2019). Evaluation of factors influencing dairy biofilm formation in filling hoses of food-processing equipment. Food and Bioproducts Processing, 113, 39-48. doi: 10.1016/j.fbp.2018.10.009

3. Fysun, O., Anzmann, T., Gschwind, P., Rauschnabel, J., Kohlus, R., Langowski, H.-C. (2019). Biofilm and Dairy Fouling Detection in Flexible Tubing using Low-Field NMR. European Food Research and Technology, 245(11), 2579-2590. doi: 10.1007/s00217-019-03371-4

4. Fysun, O., Anzmann, T., Kleesattel, A., Gschwind, P., Rauschnabel, J., Kohlus, R., Langowski, H.-C. (2019). Detection of *P. polymyxa* biofilm, dairy biofouling and CIP-cleaning agents using low-field NMR. European Food Research and Technology, 245(8), 1719-1731. doi: 10.1007/s00217-019-03288-y

5. Fysun, O., Schmitt, A., Auernhammer, P. T., Rauschnabel, J., Langowski, H.-C. (2019). Electrochemical detection of food-spoiling bacteria using platinum microelectrodes. Journal of Microbiological Methods, 161, 63-70. doi: 10.1016/j.mimet.2019.04.015

6. Fysun, O., Khorshid, S., Rauschnabel, J., Langowski, H.-C. (2019). Electrochemical detection of a *P. polymyxa* biofilm and CIP cleaning solutions by voltammetric microsensors. Engineering in Agriculture, Environment and Food, 12, 232-243. doi: 10.1016/j.eaef.2019.01.004

7. Fysun, O., Khorshid, S., Rauschnabel, J., Langowski, H.-C. (2020). Electrochemical detection of dairy fouling by cyclic voltammetry and square wave voltammetry. Food Science & Nutrition, 8(7), 3070-3080. doi: 10.1002/fsn3.1463

Patent applications

The following patent applications were generated in the period of this work:

1. Fysun, O. (2018). Vorrichtung und Verfahren zur Bestimmung einer Ablagerung biologischen Materials. Offenlegungsschrift DE 10 2016 225 009 A1 2018.06.14, Germany

2. Fysun, O. (2018). Vorrichtung und Verfahren zur Bestimmung von Ablagerung. Offenlegungsschrift DE 10 2017 210 224 A1 2018.12.20, Germany

Further full papers

1. Fysun, O., Maher, A., Brehm, H., Wilke, B., Langowski, H.-C. (2017). Monitoring of Biofilm Development on Surfaces Using an Electrochemical Method. Solid State Phenomena, 262, 492−495. doi: 10.4028/www.scientific.net/SSP.262.492

Oral presentations

1. Fysun, O. (2018). For a healthy and hygienic future – thin-layer electrochemical sensor for real time bacteria detection. 8th Robert Bosch GmbH PhD Conference. Renningen, Germany, 02.10.2018

2. Fysun, O. (2017). Biofilms and biofouling in dairy processing equipment. 7th European Food Safety and Standards Conference. Athens, Greece, 13.11.2017

Poster presentations

1. Fysun, O. (2018). Detection of *P. polymyxa* biofilm and dairy fouling by a portable NIR device. Biofilms 8 International Conference. Aarhus, Denmark, 28.05.2018

2. Fysun, O. (2018). Detection of microbial biofilms in dairy plants using electrochemical methods. 4th HEZagrar PhD Symposium. Freising, Germany, 24.04.2018

3. Fysun, O. (2017). For safety and hygienic future – sensor system for biofilm detection. Robert Bosch GmbH Research & Development Conference 2017. Abstatt, Germany, 17.10.2017

4. Fysun, O. (2017). Monitoring of Biofilm Development on Surfaces Using an Electrochemical Method. 22nd International Biohydrometallurgy Symposium. Freiberg, Germany, 25.09.2017

INDEX

List of abbreviations

α-LA	α-lactalbumin
ATP	Adenosine triphosphate
CFU	Colony forming unit
CHEMFET	Chemically sensitized field effect transistor
CIP	Cleaning-in-Place
CV	Cyclic voltammetry
EET	Extracellular electron transfer
EPS	Extracellular polymeric substance
IUPAC	International Union of Pure and Applied Chemistry
LSV	Linear sweep voltammetry
NMR	Nuclear magnetic resonance
PTFE	Polytetrafluorethylen
QCM	Quartz crystal microbalance
SWV	Square wave voltammetry
β-LG	β-lactoglobulin

1 Introduction

Formation of different types of fouling in food processing equipment is a problem for the food industry particularly due to the risk of the food product contamination and the resulting equipment downtime. Thus, the mechanism of the formation and the detection of non-microbiologically-induced fouling (mineral and organic fouling) and microbiologically-induced fouling (biofouling and biofilm) should be investigated in more detail in order to lower the risk of the contamination in food processing equipment.

According to literature, the presence of fouling on food processing contact surfaces can lead to food spoilage, shortened time between cleaning, contamination of product by non-starter cultures, metal corrosion in pipelines and tanks (Cappitelli et al. 2014; Chmielewski and Frank 2003). In addition, biofilms can become resistant to the effects of cleaning agents due to extracellular polymeric substance (EPS) formation. Due to the EPS, it is difficult to remove biofilms from food processing surfaces and environments. In addition, biofilm formation increases the risk of corrosion and clogging of pipelines in food processing plants as well as it reduces the heat transfer efficiency, resulting in increased operational costs (Chmielewski and Frank 2003). Therefore, real-time fouling detection on different food contact surfaces becomes the focus of attention in food industry.

Several publications have appeared documenting critical parts in food equipment regarding fouling, particularly biofilm formation. For example, the parts containing non-metal material such as open equipment (conveyer belts) and closed equipment (containers, gaskets, membranes, or cutting boards) as well as the equipment containing crevices or dead spaces were considered to be sources of the contamination (Marchand et al. 2012; Chmielewski and Frank 2003). One of the proposed strategies to avoid fouling formation is the application of sensors to monitor fouling formation and cleaning processes in real time. Several approaches for the real-time fouling detection has been applied by using different sensor types. Depending on sensor type, the change of the oxygen content, impedance, temperature, mass, thickness, pressure, or light absorption were recorded and their correlation with the actual fouling formation was investigated. However, many critical parts in food processing equipment are difficult to access. Moreover, in closed systems it is a significant effort to detect different types of fouling and to distinguish between them.

Due to the current lack of early warning systems, the presence of fouling is often still assumed when poor process performance and decreased product quality are observed after production. Moreover, according to literature there is a lack of a reliable monitoring and detecting sensor

system that allows to monitor fouling development and cleaning processes in food processing equipment (Cappitelli et al. 2014; Marchand et al. 2012; Simões et al. 2010). Therefore, new approaches to control fouling and cleaning processes in the food processing equipment should be introduced.

1.1 Fouling

1.1.1 Fouling in processing equipment

Different types of deposits can be found on surfaces of industrial processing equipment. The presence of deposits can lead to the decrease of the equipment's performance and to the contamination of manufactured products. The general definition and classification of deposits was originally adapted from the field of heat exchanger technology (Epstein 1981) and can also be used to classify different deposit types in the food processing equipment. These deposits are generally called *fouling.* Fouling is an unwanted deposit on the industrial surfaces. According to Epstein 1981, the fouling can be classified into the following fouling types:

(1) Mineral fouling − deposition of inorganic materials precipitating on a surface;
(2) Particle fouling − deposition of silica, clay or other substances;
(3) Organic fouling − deposition of organic substances;
(4) Biofouling − adhesion of microorganisms to surfaces and biofilm development.

For the types 1 to 3 (mineral, particle, and organic fouling), fouling layers are formed from deposited abiotic accumulations. Abiotic accumulation originates from the transport of material from liquid phase to the surface. This process can be handled by eliminating these accumulations from the liquid phase (Flemming 2002). The formation of the abiotic type of fouling differs from the formation process of biofouling. In biofouling, the accumulations are microorganisms, which can grow using nutritive substances from the liquid phase. The nutritive substances are converted into metabolic products and biomass (Flemming and Ridgway 2009).

In literature, microbiologically-induced fouling is often named not only *biofouling* but also *biofilm* (Lewandowski and Beyenal 2013). The term *biofilm* stands for a large variety of microbial aggregates. If the formation of biofilms is unwanted, microbial aggregates are addressed then as *biofouling* (Flemming and Ridgway 2009). Biofouling formation is prevalent in food or pharmaceutical processing equipment due to the favourable temperature range for microbial growth and wet surfaces. The development of microbiologically-induced fouling, known as *biofilm* or *biofouling*, has been found on surfaces of various parts in food processing equipment, e.g., storage tanks, filling units, pipelines (Marchand et al. 2012; Chmielewski and Frank 2003; Storgards et al. 1999).

The definition of fouling types proposed by Epstein 1981 is originally limited to the heat exchanger technology. An extended comparison of different fouling types in the food processing equipment has been summarized by Wallhäuser et al. 2012 and is shown in Table 1.

Table 1

Comparison of most common fouling types in the food processing equipment (adapted from Wallhäuser et al. 2012).

Fouling type	Short description	Example of occurrence	Example
(1) Chemical reaction	Decomposition/polymerisation of proteins, hydrocarbons on heat transfer surfaces	Heat exchangers in dairy, food processing industry, crude oil industry	Dairy fouling type A (protein fouling), crude oil fouling
(2) Precipitation	Precipitation/crystallisation of salts, oxides	Heat exchangers in dairy industry, water treatment, desalination	Dairy fouling type B (mineral fouling), calcium, other salts
(3) Biofilm (biofouling)	Growth of algae, bacteria	Water treatment	Bacterial growth on membranes
(4) Particulate / sedimentation	Deposition/accumulation of particles on surfaces	Combustion systems, food processing industry	Colloids, dust

Table 1 summarizes different types of fouling in the food industry and water treatment. From Table 1 it is evident that dairy industry is a sector of the food industry with a high risk of fouling formation (Wallhäußer et al. 2012). The mechanisms of fouling (abiotic accumulations) and biofouling (microbiologically-induced accumulation) formation in the dairy processing equipment are different. In fact, fouling is often a precursor for biofouling due to the equipment's heat exchanging capability loss (Al-Haj 2012). Prior to the attachment of microorganisms, the primary step in dairy fouling formation is the adsorption of a protein monolayer onto the contact surface. Thus, the concentration of nutrients in the liquid closer to the solid surface is higher, as compared to the liquid phase. In addition, the fouling layer can change physical properties of the food contact surfaces, leading to the increase of the bacterial attachment and subsequently to the formation of the biofouling (Fratamico et al. 2009). Biofouling increases the risk for the microbial contamination that can lead to a shorter shelf life of processed foods as well as biofouling can be a reason for the limitation of continuous production time in manufacturing plants (Bhushan 2016; Brooks and Flint 2008; Chmielewski and Frank 2003).

1.1.2 Major fouling types in dairy processing equipment

Fouling formation has become a major concern for the dairy industry due to the current trend to extended production runs and the use of more complex processing equipment (Mogha et al. 2014). It is important to note that fouling does not only occur on heated surfaces. A monolayer of protein can be adsorbed at room temperature. This mechanism of the monolayer formation is often linked with the surface conditioning (Rosmaninho et al. 2007). Once the temperature rises above 65 °C, the fouling formation in dairy processing equipment is enhanced because dairy proteins become thermally unstable above this temperature as they start to denature and to aggregate (Kessler 2006). This leads to a faster adherence, as compared to the native proteins. The components that are mainly responsible for the fouling formation in dairy processing equipment are calcium phosphate and whey proteins, particularly *β*-1actoglobulin (*β*-LG) (Visser and Jeurnink 1997). According to Kessler 2006, there are two types of fouling on heated surfaces in the industrial dairy equipment, which he classifies as Type A and Type B. Type A is relatively soft and bulky and it is formed at temperatures between 70−90 °C and consists of about 60% proteins and 40% minerals. Type B is formed at temperatures between 110−140 °C and consists of less than 20% proteins and up to 80% minerals, of which more than 80% is calcium phosphate (Kessler 2006). At temperatures between 110-140 °C the fouling layer can be divided in two sublayers, a protein rich outer layer and a calcium and phosphorus rich layer near the solid surface (Fratamico et al. 2009).

1.1.3 Biofouling formation

As described in Subchapter 1.1.1, *biofouling* can also be called *biofilm*. *Biofilm* is a term for many microbiologically-induced deposits (Flemming 2011). There are two ways, in which microorganisms exist: (1) planktonic bacteria, existing freely in the bulk solution or (2) bacteria attached to a surface or within the confines of a biofilm (Garrett et al. 2008). Almost all of the bacteria found on the earth are in various stages of biofilms (Costerton et al. 1987). According to the IUPAC definition, *"biofilms are an aggregate of microorganisms in which cells that are frequently embedded within a self-produced matrix of extracellular polymeric substances (EPS) adhere to each other and/or to a surface"* (Vert et al. 2012). Typically, a biofilm matrix has a heterogeneous structure and consists mainly of water (up to 97% of matrix), cells (2 – 5 % of matrix), polysaccharides (1 – 2 % of matrix), protein (1 – 2 % of matrix), and DNA and RNA (1 – 2 % of matrix). Extracellular polymeric substance (EPS) is produced by bacteria and contains bound water, polysaccharides, proteins, or extracellular DNA

(Derlon et al. 2016). EPS is of microbial origin and provides functional and structural cohesion of the biofilm matrix. The architecture and composition of a biofilm is defined by environmental and surface properties as well as by the bacterial gene and the components, which are embedded into the biofilm matrix (Marchand et al. 2012).

The biofilm development shows a characteristic development sequence. There are usually five stages from the first attachment of microorganisms to the releasing of microorganisms from a fully developed biofilm: (1) the reversible attachment, (2) the irreversible attachment, (3) the microcolony formation, (4) the maturation and (5) the dispersion (Sauer et al. 2007).

Figure 1 shows the steps from the first attachment to a fully developed biofilm.

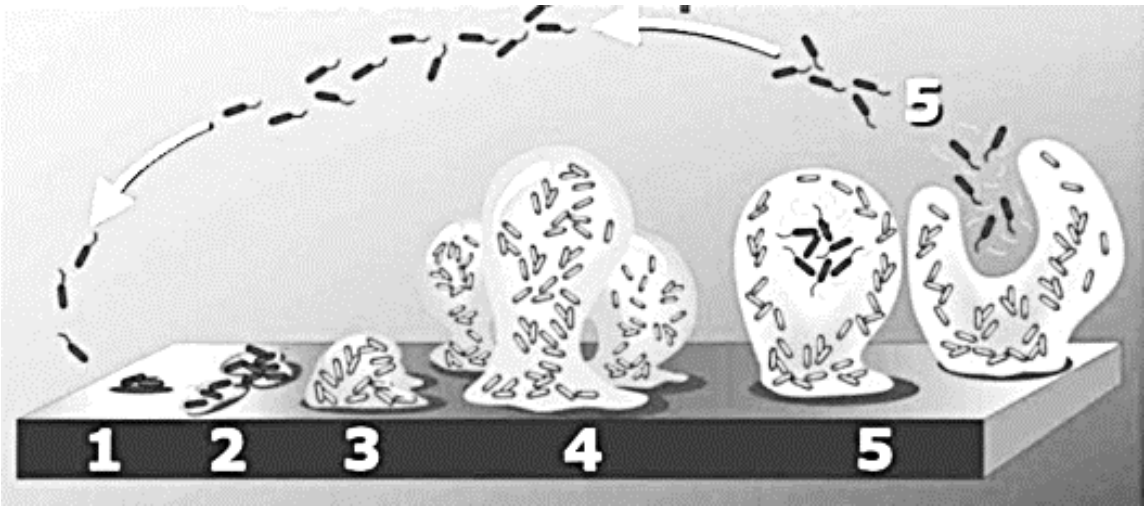

Figure 1 Five steps of the biofilm development: (1) reversible attachment, (2) irreversible attachment, (3) microcolony formation, (4) maturation and (5) dispersion (adapted from Stoodley et al. 2002).

(1) Reversible attachment

The biofilm formation starts with the attachment of single cells. Microorganisms are floating towards a surface either actively via chemotaxis and motility or passively via fluid dynamics. If a microorganism reaches a specific vicinity, the microorganism can attach to the surface depending on the net sum of attractive and repulsive forces between the microorganism and the surface. These forces are electrostatic forces and hydrophobic interactions (Fratamico et al. 2009). In addition, the initial attachment of microorganism to a surface is favoured by van der Waal's attractions. This attachment is unstable and can be reversible (O'Toole et al. 2000).

(2) Irreversible attachment

The forces leading to the irreversible attachment are dipole, ionic, hydrogen, and hydrophobic interactions. The attachment is assisted by bacterial surface structures like flagella or pili. When the attachment to the surface is completed, the production of EPS is induced by genotypic and phenotypic changes (Fratamico et al. 2009). These changes can also lead to the increased resistance to antibiotics and to UV light, as well as to the increased formation of secondary metabolites (O'Toole et al. 2000).

(3) Microcolony formation

Irreversibly attached microorganisms start to multiply while communicating with other cells through chemical signals called *quorum sensing*. Water-filled channels within the structure allow delivering nutrients to the cells (Wilson and Devine 2003; Wilking et al. 2013).

(4) Maturation

The maturation of biofilms starts when the microcolonies of microorganisms are formed. In the maturation stage, the cell density rises. If the availability of nutrients in the immediate environment is limited, the biofilm development is inhibited. The biofilm reaches its dynamic equilibrium and the outermost layers start to generate planktonic cells (Dunne 2002).

(5) Dispersion

In order to colonize new surfaces and to survive, microorganisms are detached and dispersed from the biofilm. The main driving force for the detachment are fluid dynamics and shear effects. Other factors that affect the detachment of microorganisms include EPS-degrading enzymes, generated gas bubbles, activation of lytic bacteriophages and quorum-sensing signals (Fratamico et al. 2009).

1.1.4 Factors influencing biofouling formation in food processing equipment

There are several main factors that can affect biofouling formation in the industrial food processing environment: (1) wide temperature range in many production units, (2) different types of food contact material, (3) hydrodynamics and mass transport, (4) bacterial species, and (5) properties of the manufactured product (Chmielewski and Frank 2003).

(1) Temperature

Dairy products are exposed to a broad scale of different temperatures during the production processes. The temperature can range from 5 °C to 140 °C (Teh et al. 2015). Therefore,

different units of the processing equipment can provide optimum growth conditions for psychrophiles (optimum temperature range 0 °C – 25 °C), psychrotrophic bacteria (0 °C – 40 °C), mesophiles (10 °C – 45 °C), and thermophiles (40 °C – 70 °C). Pasteurized milk can be spoiled by Gram-positive spore-forming bacteria and by Gram-negative psychrotrophic bacteria. Gram-positive spore-forming bacteria can survive the pasteurization process. Gram-negative psychrotrophic bacteria are inactivated during the pasteurization but can recontaminate the dairy-processing equipment during the automatic filling of the retail packages (Eneroth et al. 2000a; Eneroth et al. 2000b; Cousin 1982). Psychotrophic bacteria should be also considered in the quality concern and the shelf life of dairy products, as they can grow rapidly under low temperatures and therefore can grow in the consumer milk packages in retail (Eneroth et al. 2000a; Fratamico et al. 2009). Microorganisms that can shorten the shelf life of milk at around 4 °C are *Pseudomonas* ssp., among others *P. fragi* and *P. lundensis.* As an example, *P. fragi* and *P. lundensis* produce heat-stable extracellular lipases, proteases, and lecithinases that cause the milk spoilage (Mogha et al. 2014).

(2) Properties of food contact material

Food contact materials have different properties that can facilitate the attachment of microorganisms to surfaces. Food grade stainless steel is a contact material usually used for pipelines and tanks in food processing equipment (Chmielewski and Frank 2003; EHEDG 2004). In addition, polymeric materials such as PTFE are often used for processing lining or for gaskets (Hauser 2009; EHEDG 2004). In the literature, it was reported that hydrophobicity and specific roughness profile of the surface could affect the fouling formation. Hydrophobic interactions have long been seen as the reason for cell attachment. Some studies have reported that higher numbers of bacteria attach to hydrophobic surfaces such as PTFE rather than to hydrophilic surfaces such as metals (Pasmore et al. 2010; Teixeira et al. 2005). However, there are conflicting views as only a small part of microbial cells is hydrophobic as for example pili, fimbriae and flagella, while most of the surface of a microbial cell is hydrophilic (Teh et al. 2015; Lewandowski and Beyenal 2013).

Another important factor is the surface finish, e.g., the roughness, which affects the adhesion of particles. The relation of adhesion surface area and surface roughness regarding particle attachment is depicted in Figure 2.

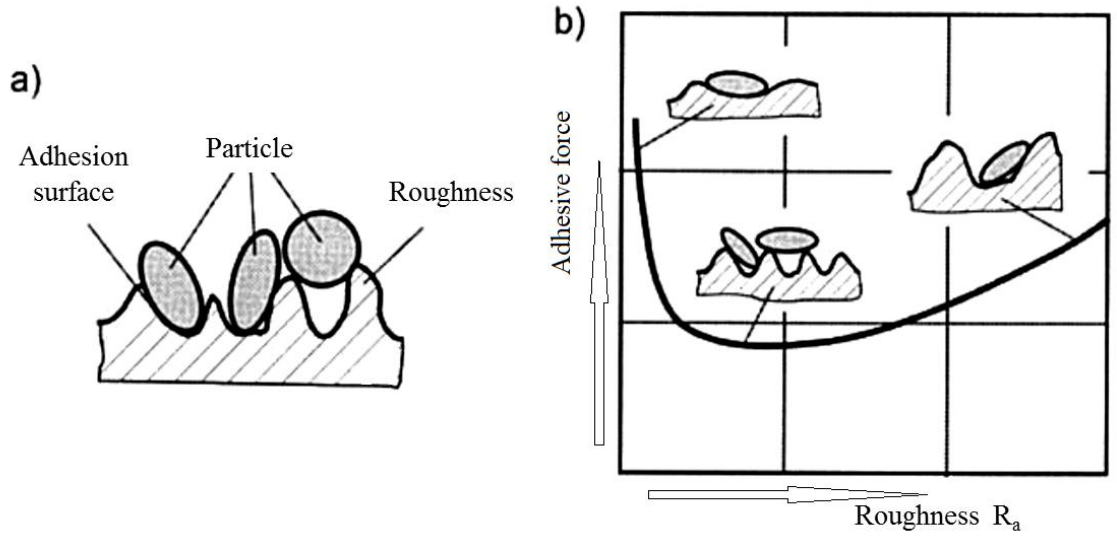

Figure 2 The influence of the adhesion surface on adhesive force: a) contact types between particles and adhesion surface; b) the change of the adhesive force depending on the adhesion surface and the surface roughness (adapted from Hauser 2008).

The amount of contact sites for particles and microorganisms depends on the roughness profile as well as on the structure and the shape of the particle. There are different modifications how particles can be arranged on the surface, which can lead to a decrease or increase of adhesion area (Hauser 2008).

(3) Hydrodynamics and mass transport

Hydrodynamics and mass transport have been shown to have an influence on the architecture, mass, and density of biofilms (Stoodley et al. 2002; Pereira et al. 2002; O'Toole et al. 2000). The availability and distribution of nutrients is an important factor for the biofilm structure, composition and formation (Chmielewski and Frank 2003). Water channels run through the biofilm structure, which enables the distribution and exchange of nutrients and metabolites (O'Toole et al. 2000; Chmielewski and Frank 2003; Bryers 1987).

The biofilm structure can be different depending on various factors such as flow conditions, surface topology, or nutrients availability (Fig. 3). The structure of matured biofilms can be divided in three general types: (a) Dense biofilm, (b) Mushroom-like biofilm, (c) Ciliate-like biofilm.

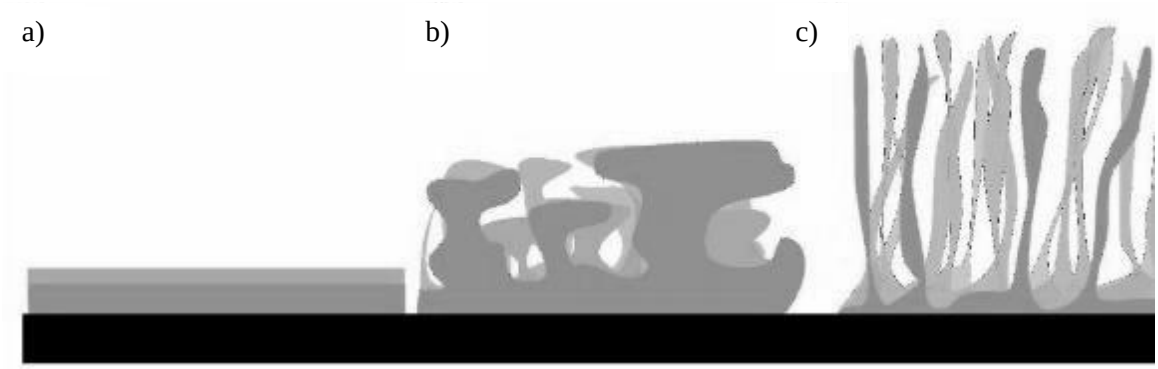

Figure 3 Types of biofilm structure: (a) Dense biofilm, (b) Mushroom-like biofilm, (c) Ciliate-like biofilm (adapted from Roßteuscher 2009).

According to Fig. 3, a dense biofilm (a) is stratified and compact. Dense biofilms are usually formed under high shear stress conditions. Roßteuscher 2009 described the dense biofilm structure for nutrient-rich environments with high shear stress. Biofilms grown under turbulent conditions also exhibit streamlined and oscillating ripples (Stoodley et al. 2002). Mushroom- like biofilms (b) are formed in areas of moderate nutrient supply and hydrodynamic conditions. In regions with restricted nutrient supply and low shear stress, biofilms exhibits ciliates-like biofilm structure (c) to increase the surface area for optimized nutrient uptake. Laminar flow conditions induce biofilm formation with a patchy structure, consisting of round shaped cell aggregates (Roßteuscher 2009).

(4) Bacterial species

The differences in the ability of biofilm formation can be observed for different types of bacterial species. The presence of cell appendages like fimbriae, pili and flagella can increase the cell attachment and adherence to the surface by overcoming electrostatic repulsion forces (Parizzi et al. 2004; Bonsaglia et al. 2014; Barnes et al. 1999). Species which are relevant in concern of biofilm formation in food processing equipment and which have the ability to attach on food contact surfaces are for example *Listeria monocytogenes, Salmonella* spp., *Escherichia coli, Pseudomonas* spp., *Paenibacillus* spp., *Bacillus* spp. (Djordjevic et al. 2002; Doijad et al. 2015; Drenkard and Ausubel 2002; Marchand et al. 2012; Gopal et al. 2015). Psychrotrophic bacteria, *Pseudomonas* spp., decrease the shelf life of dairy products due to the ability to form biofilms below 10 °C (Hood and Zottola 1997; Sørhaug and Stepaniak 1997). *Pseudomonas* spp. can produce a large amount of EPS and have shown the ability to attach to stainless steel in various studies as well as to produce attachment fimbriae at different temperatures (Stone and Zottola 1985; Barnes et al. 1999). Furthermore, *Pseudomonas* spp.

can coexist in a biofilm with *Listeria, Salmonella,* and other pathogenic microorganisms (Chmielewski and Frank 2003).

(5) Properties of product

Product properties as pH, salt concentration, and organic compounds can affect the biofilm formation as these factors determine the growth of the microorganisms in the media (Parizzi et al. 2004). Furthermore, the different components of the manufactured product can influence the initial attachment of the microorganisms by the formation of a conditioning layer on the food contact surface. Some products promote the bacterial adherence on surfaces as for example skim milk, butter milk, and butter serum (Dat et al. 2010; Barnes et al. 1999). For example, it was reported that casein in dairy products decreases the attachment of microorganisms while whey protein increases the attachment (Fletcher 1976; Speers and Gilmour 1985; Barnes et al. 1999).

1.2 Fouling control and detection

1.2.1 CIP cleaning and enzymatic cleaning

It is necessary to perform proper cleaning procedures to ensure that processing equipment retains its original functionality and maintains quality and safety of the food products (Kelly 2004). A typical cleaning method for industrial food processing is called Cleaning-in-Place (CIP). According to the IUPAC definition, CIP is defined as "*cleaning of complete items of plant or pipeline circuits without dismantling or opening of the equipment and with little or no manual involvement on the part of the operator. The process involves the jetting or spraying of surfaces or circulation of cleaning solutions through the plant under conditions of increased turbulence and flow velocity*" (Romney 1990). The CIP cleaning of dairy processing equipment includes the following steps (Table 2).

Table 2

An example of Cleaning-in-Place (CIP) program in dairy processing equipment (adapted from Bylund 1995).

CIP cleaning steps for circuits with pasteurizers and other equipment with heated surfaces	
1	Rinsing with warm water about 10 min
2	Circulation of alkaline detergent solution (0.5 − 1.0 %) for about 30 min at T = 75 ºC
3	Rinsing out alkaline detergent with warm water for about 5 min
4	Circulation of acid detergent (0.5 − 1.0 %) for about 20 min at T = 70 ºC
5	Postrinsing with cold water
6	Gradual cooling with cold water for about 8 min

The CIP cleaning is performed with alkaline/acid detergent in combination with several steam and heating phases depending on the produced food products. The choice of chemicals for the cleaning depends on the equipment, material, including the elastomers used as seals and gaskets as well as it depends on the type of fouling. The main purpose of CIP systems is to accomplish a reproducible cleaning performance while minimizing the cleaning time, effort, and costs. Hygienic design requirements of processing equipment support the cleaning efficiency and shall avoid the accumulation of deposits. The efficiency of a CIP procedure is defined by the combination of the following factors: cleaning time, temperature, detergent type, mechanical

force (degree of turbulence), and surface characteristics (Fratamico et al. 2009). In addition, depending on structure and composition of the fouling, the CIP cleaning program may differ to achieve the highest cleaning effectiveness.

A biofilm control strategy is to clean and to disinfect before bacteria irreversibly attach to the food contact surfaces (Simões et al. 2010). Due to the fact that traditional CIP procedures are ineffective against the maturation of biofilms, there is a growing demand on more effective CIP procedures against biofilms (Liu et al. 2014). One of the strategies to solve this problem is an implementation of an additional cleaning step in the CIP cleaning process, using proteases and other enzymes to actively degrade the EPS and to improve the removal of biofilms during the CIP procedure. This step is called enzymatic cleaning (Simões et al. 2010; Srey et al. 2013). A right combination of enzymes targeting several components of EPS could be a good alternative to chemical cleaning agents (Marchand et al. 2012). However, the structural composition of EPS can also vary among bacteria of the same species. Therefore, the enzyme combination for the biofilm degradation should be adapted to the specific composition of biofilms (Srey et al. 2013).

1.2.2 State of the art for fouling detection and strategies for fouling control

It is important to monitor the fouling formation and to evaluate the cleaning success in real-time in order to improve the effectiveness of strategies for better hygiene control. The reported monitoring methods for fouling control are based on the time-dependent changes of process performance, product quality and quantity (Flemming 2011).

According to Flemming 2011, monitoring devices for the detection of fouling-relevant parameters can be classified into three levels by information provided by these devices. Level 1 monitoring methods provide information about the kinetics of deposition formation and changes of thickness, but cannot differentiate between microorganisms and abiotic deposit components. The advantages of such devices are an online, in situ and continuous monitoring of deposit formation. Level 2 monitoring methods can distinguish between biotic and abiotic components of a deposit. Level 3 monitoring methods provide detailed information about the chemical composition of the deposit. Table 3 gives a short overview of selected Level 1, Level 2, and Level 3 monitoring methods.

Table 3

Selected methods of Level 1, Level 2 and Level 3 monitoring methods (adapted from Flemming 2011).

Method		Principle
Level 1	**Friction resistance measurement**	Determination of pressure drop due to deposit roughness
	Heat transfer resistance measurement	Measurement of heat transfer coefficient and thermal resistance due to deposit formation
	Acoustic fouling detection	Acoustic backscattering parameters by deposit, frequency change and energy dissipation are measured
	Quartz crystal microbalance (QCM)	Quenching frequency of quartz crystals by deposited material
	Surface acoustic waves	Determination of difference between speed of acoustic waves with and without deposit
	Differential turbidity measurement (DTM)	Determination of difference between two turbidity measurement devices caused by surface deposit
Level 2	**Autofluorescence**	Use of autofluorescence of biomolecules such as amino acids, for example, tryptophane or other biomolecules
	FTIR-ATR-spectroscopy	Use of FTIR-ATR-spectroscopy specific for amide bands
	Microscopical observation	Microscopical observation of biofilm formation in a bypass flow chamber and morphological identification of microorganisms
Level 3	**FTIR-ATR-spectroscopy in a flow-through cell**	Use of FTIR-ATR-spectroscopy not only for the specific amide bands but also for the entire spectrum of medium.
	NMR imaging of deposits in pipes or porous media	Use of NMR imaging to provide information about the extent and spatial distribution of the deposit and information about the chemical nature of certain components.

In contrast to Level 1, Level 2 and Level 3 monitoring devices are able to differentiate between biotic and abiotic substances as well as give an information about the chemical composition of fouling or adherent microorganisms, respectively (Flemming 2011). It is important to note that in real industrial processes only a few monitoring techniques listed in Table 3 are implemented

in daily operations. Most used Level 1 monitoring techniques for industrial purposes are heat transfer and pressure drop monitoring.

In case of heat transfer monitoring, if the fouling is present on the surface, the heat transfer resistance is rising due to the fact that the fouling layers have a similar effect as an insulation. If the heat flux, the wall temperatures and the fluid temperatures are known, the additional resistance can be assessed and thus it is possible to assess the deposit thickness (Janknecht and Melo 2003).

In case of friction resistance measurement, the detection is based on an increased roughness of the surface that is caused by the build-up of a fouling layer. By connecting a differential pressure sensor to the inlet and outlet of the equipment, the rise of the pressure drop can be monitored. A rising pressure drop over time indicates the build-up of a fouling.

However, a major drawback of both methods is a lack of information on the extent and location of fouling. Hence, the common analytical techniques for on-line process monitoring optimization are challenging due to several limitations. These techniques cannot differentiate between fouling and biofouling. This is a major issue since these two different types of deposit require different treatments. Although these techniques provide fast information on biofouling formation without sampling, these methods are not suitable for the detection of biofouling at the early stages of formation. According to Characklis et al. 1990, there are only significant changes in the friction factor when the biofouling reaches a critical thickness of about 35 μm.

To overcome the limitations of friction resistance and heat transfer resistance monitoring methods, the development of other methods for detection of fouling and biofouling formation in food processing equipment is needed.

Different strategies for the fouling control using sensors and CIP cleaning monitoring have been reported in the last decades. For example, Meyer 2003 proposed three different strategies to control the biofilms in processing equipment: (1) disinfection “in time”, before biofilm develops, (2) disinfection of biofilms using disinfectants, after the biofilm develops, and (3) reduce of attachment of bacteria by modification of surface materials. However, these strategies do not propose that a right combination of sensors can monitor both the biofilm formation and the CIP cleaning process. Biofilm prevention is particularly important in respect of the increased mechanical resistance of matured biofilms. The extent of cleaning procedures is often based on the experience because of the lack of industrial monitoring systems that are able to detect and to differentiate between fouling and biofouling, particularly at early stages of its development.

1.3 Nuclear magnetic resonance (NMR)

1.3.1 Short physical background of NMR

According to the literature, *Nuclear Magnetic Resonance (NMR) is a physical phenomenon based on the principle of exciting nuclear spins with radiofrequency pulses, the frequency of which matches the Larmor frequency of the nuclear spins* (Oligschläger et al. 2014). NMR can be used in different fields, e.g., medicine, material science, and structure analysis (Oligschläger et al. 2014). Various applications of NMR in food research and manufacturing have also been proven. Recent applications of NMR include chemical analysis and structural identification of components, detection of food authentication and optimization of food processing (Todt et al. 2006; Marcone et al. 2013).

A full treatment of the physical background of this method is beyond the scope of this chapter. A short physical background of NMR can be given as follows. The angular momentum or spin is a property of all atomic nuclei having an uneven number of protons or neutrons. As atomic nuclei are charged, the spinning motion causes a magnetic dipole in the direction of the spin axis. The intrinsic magnitude of the dipole is a nuclear magnetic moment, μ (Wolter and Krus 2005).

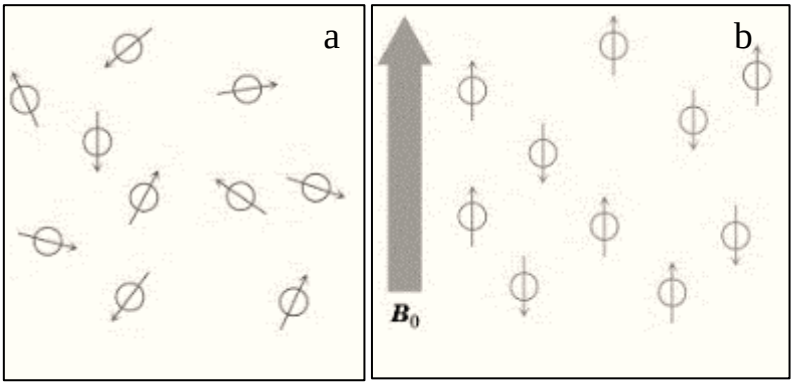

Figure 4 Alignment of protons due to an external magnetic field: a) randomly oriented nuclear magnetic fields; b) when placed in an external magnetic field, B_0, the alignment of nuclear magnetic field along or oppose the external magnetic field.

Fig. 4(a) shows that normally the nuclear magnetic fields are randomly oriented. However, when placed in an external magnetic field, B_0, the nuclear magnetic field can either be aligned with the external magnetic or oppose the external magnetic field (Fig. 4(b)).

When placed in a static magnetic field of strength B_0, a particle with a net spin can absorb a photon from an additionally applied electromagnetic field, preferably at a resonance frequency

called the Larmor frequency ω_0. The frequency ω_0 depends on the gyromagnetic ratio γ of NMR active nuclei (Equation 1).

$$\omega_0 = \gamma B_0 \quad \textbf{(1)}$$

The proportional constant γ is called the gyromagnetic ratio (42.58 MHz/T for ^{1}H) (Table 4).

Table 4

Gyromagnetic ratio of NMR active nuclei (adapted from Foster 1984).

Nuclei	Unpaired proton	Unpaired neutrons	Abundance [%]	Net spin	γ [MHz/T]
^{1}H	1	0	99.98	1/2	42.58
^{2}H	1	1	0.016	1	6.54
^{13}C	0	1	1.1	1/2	10.71
^{31}P	1	0	100	1/2	17.25
^{14}N	1	1	99.63	1	3.08

Hydrogen nuclei (^{1}H) possess the strongest magnetic moment and they are in high abundance in moist material resulting in a high NMR sensitivity. ^{1}H nuclei are present in almost all biological molecules (Wolter and Krus 2005).

1.3.2 Low-field NMR

The development of on-line techniques has increased the value of NMR as a non-invasive method for the process development applications. Small low-field NMR systems equipped with permanent magnets are available for the quantitative analysis in quality control as well as for online instruments in production environments. The advantage of low-field NMR compared to high resolution NMR is based on lower requirements regarding environment parameters, staff, maintenance, and investment costs (Dalitz 2012).

Chemical and physical changes in a sample of interest can lead to changes in NMR frequency shifts, spin-lattice (T_1) relaxation time, spin-spin (T_2) relaxation time. Spin-lattice (T_1) relaxation and spin-spin (T_2) relaxation both provide information about the local physical and chemical environment. Both NMR relaxation times can be affected by pore size distributions, fluid viscosity, and chemical properties of the bulk fluid (Callaghan 1991).

The spin-lattice (T_1) relaxation time can be explained as follows. At equilibrium, the net magnetization vector lies along the direction of the applied magnetic field B_o. This state is the

equilibrium magnetization M_o. The Z component of magnetization M_Z equals M_o in this configuration. M_Z is referred to as the longitudinal magnetization (Kotwaliwale et al. 2010).

By exposing the nuclear spin system to an energy of a frequency equal to the energy difference between the spin states, the net magnetization will be changed. The spin-lattice relaxation time (T_1) characterises the time it takes the system to reach thermal equilibrium, i.e. for the net magnetisation vector (M_Z) to reach $M_{Z,0}$ after the sample is placed within a magnetic field B_0 (Foster 1984; Pendlebury 1979).

After changing the external magnetic field, the bulk magnetization of the sample varies with time according to the following equation (Equation 2):

$$M_Z = M_{Z,0}\left(1 - e^{-t/T_1}\right) \quad \textbf{(2)}$$

where M_Z is the magnitude of the magnetization along the direction (Z) of the net magnetic field vector, $M_{Z,0}$ is the magnetization at time zero, T_1 is spin-lattice relaxation time and t is time.

The spin-spin (T_2) relaxation time can be explained as follows. The spin–spin relaxation time (T_2) characterises the loss of signal phase coherence, the time it takes the NMR signal in the transverse plane (X–Y) to decay towards zero, following radio frequency excitation (Kotwaliwale et al. 2010). It is described by the equation (Equation 3):

$$M_{x,y} = M_{x,y,0}e^{-t/T_2} \quad \textbf{(3)}$$

where $M_{x,y}$ is the magnitude of the magnetization along the transverse plane (X–Y) relative to the longitudinal direction (Z) of the net magnetic field vector, $M_{x,y,0}$ is the magnetization at time zero, T_2 is spin-spin relaxation time and t is time. The spin-spin (T_2) relaxation is based on the dipolar spin-spin interactions and provides information about the rotational mobility of the NMR-active nuclei in fluid-pore environments (Fridjonsson et al. 2015).

1.3.3 The use of low-field NMR for fouling detection and dairy research

As reported in literature, low-field NMR technique provides a cost-efficient and small size alternative for non-invasive real-time monitoring of biofilm formation in natural unconsolidated porous media (Sanderlin et al. 2013; Kirkland et al. 2015; Kirkland and Codd 2018). The longitudinal (T_1) and transverse (T_2) NMR relaxation time values of proximal water hydrogen atoms can be affected by the fouling formation. The physicochemical properties of the sample influence the amplitude and the duration of the signal response (Fridjonsson et al. 2015). Hoskins et al. 1999 recorded T_1 and T_2 weighted images

of a biofilm formed by *Escherichia coli* on a large glass plate and showed that biofilm distributions by NMR and optical imaging generally agree.

In addition, a number of NMR applications in food technology have also been reported owing to the fact that many foods are proton-rich, with protons originating from fat, carbohydrates, proteins, and water (Marcone et al. 2003). NMR studies report various applications from investigations focused on specific molecules to study the physical properties of dairy products. More specifically, low-field NMR was used for the study of dairy products (Maher and Rochfort 2014) and compounds to characterize fat and water in cheese (Mariette 2018), as well as to investigate the solid fat content in anhydrous milk fat blends (Marcone et al. 2003). Also, the application of low-field NMR in the detection of fouling was successfully shown in the literature (Vogt et al. 2000; Fridjonsson et al. 2015; Kirkland et at. 2015).

1.4 Electrochemistry

1.4.1 Fundamental principles of electrochemistry

According to literature, *electrochemistry is a part of physical chemistry that deals with the study of chemical changes caused by the passage of an electric current and the production of electrical energy by chemical reactions* (Bard and Faulkner 2001). The field of electrochemistry is concerned with electron transfer at the solution/electrode interface. A general form of a redox reaction occurring at the electrode surface is given as follows:

$$O + ne^- \underset{k_b}{\overset{k_f}{\rightleftarrows}} R \qquad \textbf{(4)}$$

in which *O* represents the oxidized component, *R* the reduced component, *n* is the number of electrons *e* exchanged between *O* and *R*, k_f and k_b are the forward and backward heterogeneous rate constants (Bagotsky 2005).

In order to obtain information about the target analyte and its concentration, controlled-potential electroanalytical experiments can be used. The current *I* is equal to the change in charge *Q* with time *t* (Wang 2006; Zoski 2007) and is defined as follows:

$$I = \frac{dQ}{dt} \qquad \textbf{(5)}$$

The correspondence of a current to the reduction and oxidation of chemical substances is called *faradaic current* (Wang 2006; Zoski 2007). Furthermore, the reaction rate and the resulting current are influenced by four major factors:

• mass transfer to the electrode surface,
• kinetics of electron transfer,
• preceding and ensuing reactions,
• surface reactions (adsorption).

The processes involved in an electron transfer are depicted in Fig. 5.

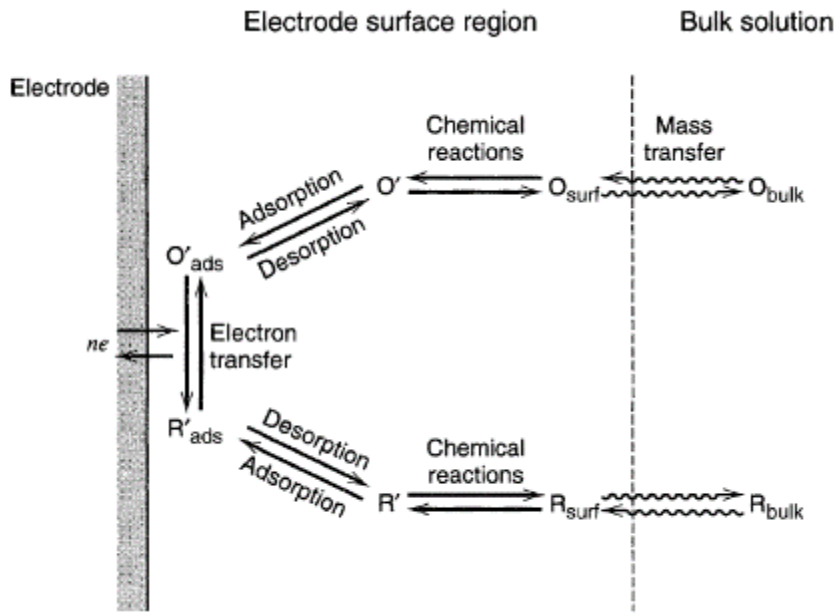

Figure 5 Pathway of an electron transfer at an electrode surface. *O* represents the oxidized form and *R* the reduced form of a redox couple (adapted from Bard and Faulkner 2001).

In Fig. 5, the sequence of steps is depicted in which the reactant migrates to the electrode surface region, reactions that occur at the electrode surface and the final products migrate from the electrode surface into the bulk solution (Bard and Faulkner 2001).

1.4.2 Electrochemical activity of biofouling

Electron transfer is an important process for the cell metabolism (Xiao and Zhao 2017). Electron transfer reactions are performed between a living cell and an extracellular electron donor or acceptor (Pinck 2017). Some microorganisms can enable efficient electron transfer between microorganisms and extracellular solid materials, as part of their metabolism. It is called extracellular electron transfer (EET). Extracellular electron transfer processes are used by microorganisms for the communication with other cells or for interaction with the external environment (Xiao and Zhao 2017). Redox molecules, proteins, or substances are able to act as electron shuttles between the bacteria and the terminal electron donor or acceptor (Pinck 2017). Although a commonly accepted mechanism of EET does not exist, it is evident that microorganisms are able to accelerate the rate of electron transfer (Faimali et al. 2010). The EET pathways are generally classified as direct EET and indirect (mediated) EET. The EET pathways of electroactive microorganism are depicted in Fig. 6.

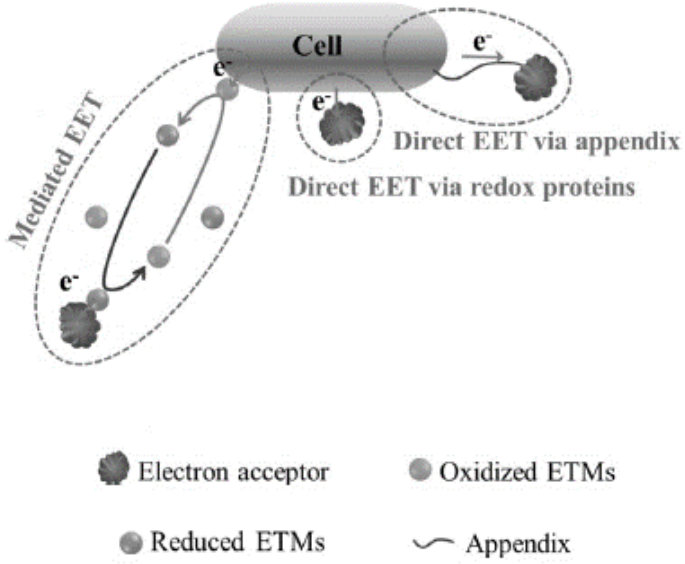

Figure 6 Direct and indirect EET mechanisms of microorganisms. ETM – electron transfer mediators (adapted from Xiao and Zhao 2017).

In the direct EET pathway, microorganisms usually use redox proteins in the outer membrane or nanowires to transport electrons directly to extracellular acceptors. In the indirect EET pathway, microorganisms usually transport electrons indirectly to the external acceptors using self-secreted or exogenetic electron shuttles (Xiao and Zhao 2017; Pinck 2017). Redox molecules such as flavin, riboflavin, and phenazine were reported to conduct EET according to the indirect EET pathway. Membrane-bound cytochrome *c* is a group of redox proteins that also contributes to the electron transfer and plays a key role in the EET processes (Pinck 2017). In addition, Xiao and Zhao 2017 have also highlighted that extracellular polymeric substances (EPS) are important for the EET mechanisms. An EPS layer is not a solid layer separating cells and external electron donors/acceptors. The redox molecules can diffuse in the EPS and contribute to the electron transfer between cells and electron donors/acceptors (Xiao and Zhao 2017).

1.4.3 Classification of electrochemical sensors

According to the IUPAC classification, electrochemical devices belong to the second group of chemical sensors. A chemical sensor is defined as follows, "*a chemical sensor is a device that transforms chemical information, ranging from the concentration of a specific sample component to total composition analysis, into an analytically useful signal. The chemical information [...] may originate from a chemical reaction of the analyte or from a physical property of the system investigated.*" (Hulanicki et al. 1991).

The chemical sensor is part of an analyser, which has the tasks of sampling a signal, sample transport, signal processing, and data processing. The chemical sensor comprises a receptor- and transducer-part as two basic functional units. Chemical information is transformed into a form of energy in the receptor-part of the chemical sensor. The transducer-part measures this energy and transforms it into an appropriate analytical signal (Hulanicki et al. 1991).
According to IUPAC classification (Hulanicki et al. 1991), electrochemical devices transform the effect of an electrochemical interaction between analyte and electrode into a signal, which can be subdivided into following categories:

a) voltammetric sensors (including amperometric devices) measuring the current,
b) potentiometric sensors measuring the potential of the indicator electrode,
c) chemically sensitized field effect transistor (CHEMFET),
d) potentiometric solid electrolyte gas sensors,
e) impedance sensors.

The electrochemical part of this work is focused on (a) voltammetric sensors. In most electrochemical experiments, a three-electrode configuration of voltammetric sensors is chosen (Fig. 7).

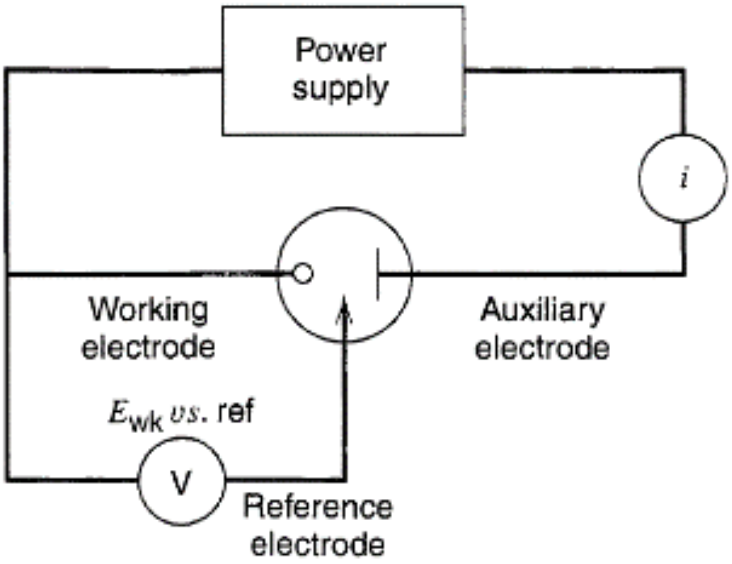

Figure 7 Three-electrode system (adapted from Bard and Faulkner 2001).

In this configuration, the electrochemical cell comprises a *working* electrode, coupled with an electrode of known potential (*reference* electrode) and a *counter* or *auxiliary* electrode (Fig. 7). Current passes through the working and counter electrodes. The electrochemical properties of the counter electrode do not affect the behaviour of the working electrode (Bard and Faulkner 2001).

1.4.4 Voltammetry

Voltammetric techniques involve the variation of the potential at a working electrode via a reference electrode while measuring the corresponding current (Armstrong et al. 2000). The electrode, where the oxidation takes place is called *anode* while the *cathode* is the electrode, where the reduction takes place. *Anodic* reactions generate electrons, while in *cathodic* reactions, electrons are received (Bagotsky 2005; Zoski 2007). In a voltammogram, the current is depicted over the potential, in which the potential is varied either continuously or stepwise (Gründler 2007). Most used voltammetric techniques that were reported for biofouling detection are linear sweep voltammetry, cyclic voltammetry, square wave voltammetry, and differential pulse voltammetry (Giao et al. 2003; Harnisch and Freguia 2012; Kang et al. 2012; Becerro et al. 2016; Molina et al. 2009).

1.4.4.1 Linear sweep voltammetry (LSV) and cyclic voltammetry (CV)

Linear sweep voltammetry (LSV) and cyclic voltammetry (CV) are potential sweep methods that were first described in 1948 by Randles and Sevcik (Randles 1948; Ševcík 1948). LSV and CV methods have become the most used voltammetric methods to obtain the information about electrochemical reactions (Bard and Faulkner 2001; Ozkan et al. 2015; Wang 2006).

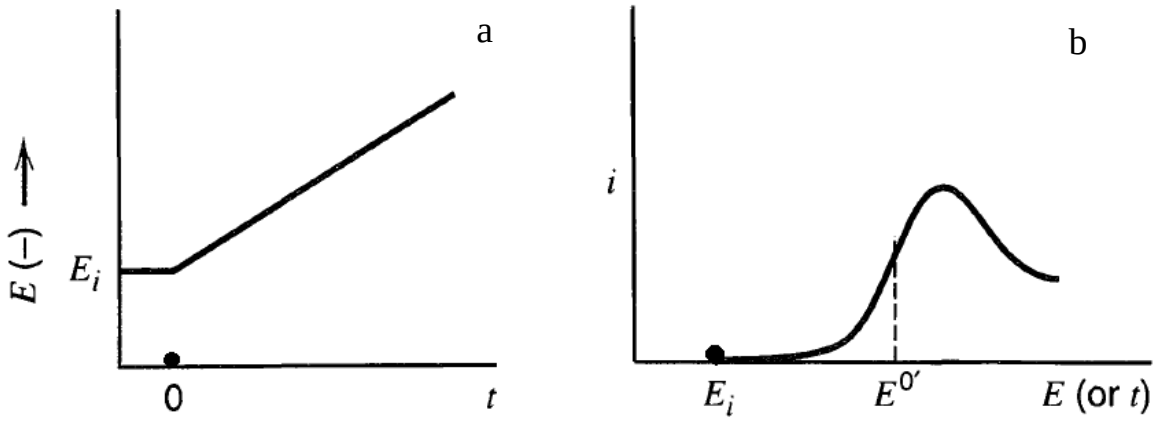

Figure 8 Linear potential sweep (a) and the resulting current-potential curve (b) (adapted from Bard and Faulkner 2001).

A typical potential sweep in linear sweep voltammetry and the resulting current-potential curve are shown in Figs. 8(a) and 8(b). When the electrode potential reaches the vicinity of $E^{0'}$ the reduction begins and current starts to flow (Fig. 8(b)).

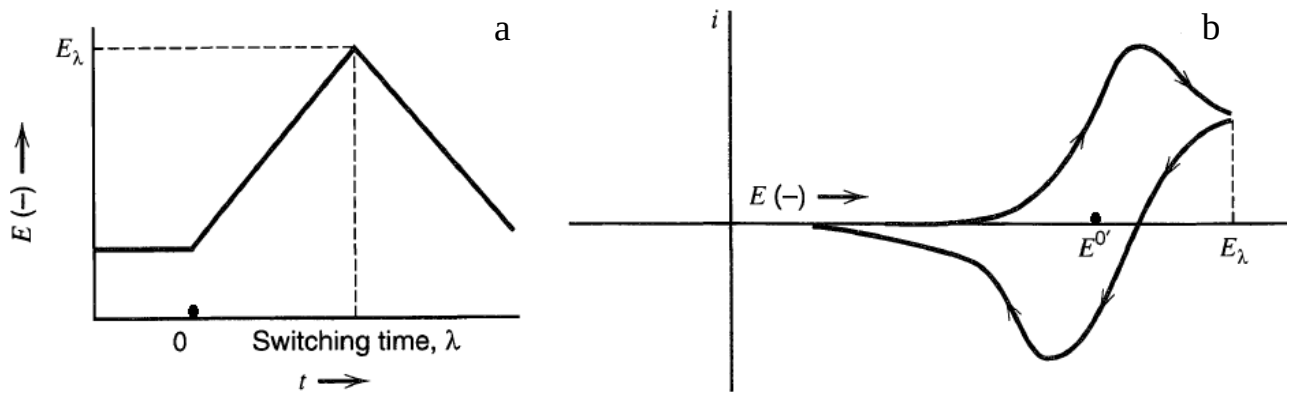

Figure 9 Cyclic potential sweep (a) and the resulting current-potential curve (b) (adapted from Bard and Faulkner 2001).

Fig. 9(a) shows a typical potential-time diagram in cyclic voltammetry with a triangularly shaped waveform. The difference between linear sweep voltammetry and cyclic voltammetry methods is that in linear sweep voltammetry a single potential sweep is applied, while in cyclic voltammetry the potential sweep is cycled over time. The potential cycling enables the visualization of the forward and backward reactions. A potential sweep starts at an initial potential and then the potential varies linearly with time, at a certain scan rate (Fig. 9(b)). A faster scan rate gives a higher peak current, because the diffusion layer has less time to develop at fast scan rates. Thus, the flux to the electrode is higher compared to slow scan rates. Initial potential is selected at a level, which does not initially oxidize or reduce the chemical species under investigation (Ozkan et al. 2015).

1.4.4.2 Square wave voltammetry (SWV)

Square wave voltammetry (SWV) was invented by Ramaley and Krause (Krause and Ramaley 1969; Ramaley and Krause 1969; Ramaley and Surette 1977) and has been mostly developed by the Osteryoungs and their coworkers (Christie et al. 1977; Wong and Osteryoung 1987; Yarnitzky et al.1980; Feder and Yarnitzky 1984; Osteryoung and Osteryoung 2012). SWV is a pulse technique in which symmetrical square pulses of progressively increasing potentials are applied to an electrochemical system. A square wave is superimposed on a staircase ramp (Bard and Faulkner 2001; Ozkan et al. 2015). A typical potential time progression with its major parameters is illustrated in Fig. 10. SWV begins at an initial potential E_i, which is applied for a delay time t_0. A typical parameter is the pulse height ΔE_p with a corresponding pulse width t_p.

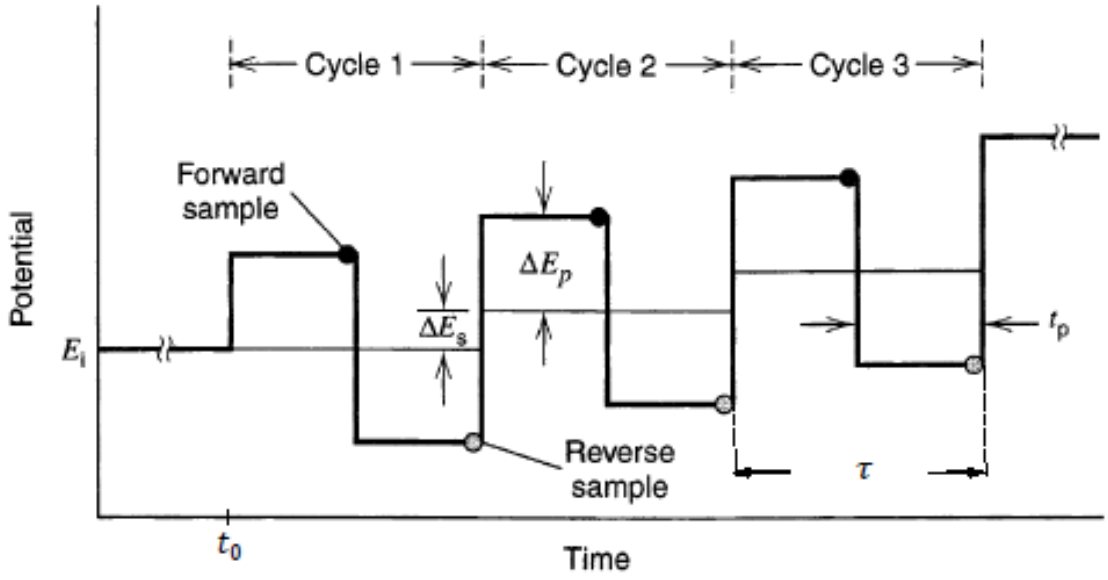

Figure 10 Potential waveform of square wave voltammetry (adapted from Bard and Faulkner 2001).

A forward and reverse scan is completed in one cycle. The staircase shift at the beginning of each cycle is denoted as ΔEs (Bard and Faulkner 2001). The current is sampled twice to suppress the residual currents and to achieve a high sensitivity to surface-confined electrode reactions (Moretto and Kalcher 2014; Scholz et al. 2010; Mirceski et al. 2013).

1.4.5 Electrochemical microelectrodes and techniques for biofouling detection

The general principle of biofouling detection using electrochemical sensors is based on a comparison of electrochemical reactions before and after adhesion of microorganisms on a conductive surface (Ahmed et al. 2016). As opposed to other methods, electrochemical detection in combination with electrochemical microelectrodes has several advantages: data can be processed rapidly, relatively simple, and inexpensive instrumentation may be used (Kang et al. 2012; Ahmed et al. 2014).

During the first steps of adhesion, microorganisms can exchange electrons with conductive surfaces like electrodes, resulting in a change of electrochemical reactions. Several articles have been published that describe the use of voltammetric methods for biofouling characterization. Table 5 summarizes the studies on biofouling using voltammetric techniques, cyclic voltammetry and square wave voltammetry.

Table 5 Biofilm detection by means of voltammetric measurements.

Method	Bacteria	References
Cyclic Voltammetry	*Geobacter sulfurreducens*	Katuri et al. 2010; Marsili et al. 2008
	Pseudomonas aeruginosa	Kang et al. 2012
	Pseudomonas fluorescens	Giao et al. 2003; Vieira et al. 2003
	Saccharomyces cerevisiae	Matsunaga and Namba 1984
	Shewanella loihica	Jain et al. 2013
	Staphylococcus epidermidis	Becerro et al. 2016
Square Wave Voltammetry	*Pseudomonas aeruginosa*	Webster et al. 2014
	Shewanella oneidensis MR-1	Nguyen et al. 2012
	Marine biofilm	Xu et al. 1998

Reduction in size of electrodes is a current trend in electrochemistry. An example for miniaturized electrodes are thin film microelectrodes (Becerro et al. 2016). Thin film microelectrodes provide a minimal invasive technique to study biofilm- relevant parameters (Babauta et al. 2012). Thin film microelectrodes can be designed in various shapes, e.g., interdigitated or stiletto shaped arrays. The microelectrodes are produced by depositing a thin film of inorganic material onto a supporting body by vacuum or by sputter deposition. A thin film pattern can be an interdigitated design (Fig. 11(a)).

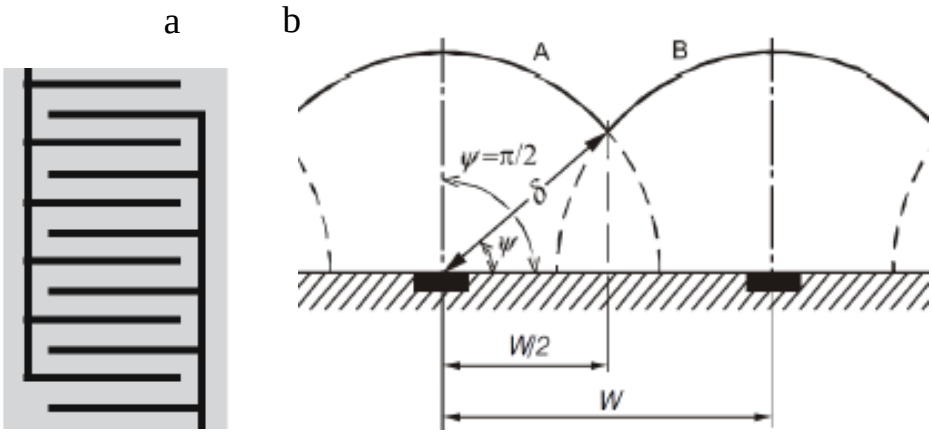

Figure 11 (a) Example of an interdigitated structure of a microelectrode (adapted from Gründler 2007); (b) Diffusion layer overlapping at closely spaced interdigitated microelectrodes (δ is the diffusion layer thickness; W is the total width; ψ is the angle that represents the degree of overlap) (adapted from Stulik et al. 2000).

The response time of microelectrodes is much shorter compared to the classical electrodes. Microelectrodes are not sensitive to convection from external sources and only need a low supporting electrolyte content (Gründler 2007). An overlapping of diffusion layers of thin film interdigitated microelectrodes is shown in Fig. 11(b). According to IUPAC (Stulik et al. 2000), three scenarios have to be distinguished with interdigitated microelectrodes:

• $\delta < W/2$: The gaps between the electrodes are wider than the diffusion layer thickness. The diffusion layers of the electodes will not overlap. Thus, the electrodes cannot affect other electrodes. Therefore, the total current is the sum of the currents passing through the individual electrodes.

• $\delta > W/2$: Partial overlapping of the individual electrodes A and B. The total current is smaller than the sum of the currents passing through the electrodes.

• $\delta >> W/2$: Total overlapping of diffusion layers of electrodes A and B, the array behaves like a continuous electrode. The surface area equals that of the whole array. The signal-to-noise ratio of interdigitated microelectrodes is improved because the signal is proportional to the surface area of the whole array and the noise is proportional only to the area of the electrodes (Stulik et al. 2000).

1.5 Motivation and objective of the thesis

The formation of fouling deposits on the food contact surfaces of food processing equipment leads to the high risk of the contamination of food products. The composition and structure of fouling are often associated with the type of food processing and the industrial environment. The fouling deposits that are associated with the food processing industry can be classified as either microbiologically-induced deposit, e.g., biofilm and biofouling, or non- microbiologically-induced deposit, e.g., mineral fouling, particle fouling, and organic fouling (Kessler 2006; Srey et al. 2013; Lewandowski and Beyenal 2014; Epstein 1981; Marchand et al. 2012; Cappitelli et al. 2014).

Several techniques for detecting of fouling deposits have been reported (Chapter 1.2.2) (Kim et al. 2012; Reyes-Romero et al. 2014; Kwak et al. 2014; Crattelet et al. 2013; Janknecht and Melo 2003; Wallhäußer et al. 2012). Some sensors have been already invented to monitor the biofouling development on surfaces and to enable the control of biofouling at early stages of development (Denkhaus et al. 2007). Although available industrial techniques for fouling detection provide information on fouling formation without sampling, these methods are not suitable for the detection of fouling at the early stage of formation. Moreover, these approaches still fail to provide a detailed and fast information about complex deposits by non-invasive measurements. Also, available sensors for fouling detection cannot distinguish between microbiologically-induced and non-microbiologically-induced deposits.

Real-time detection and monitoring of different types of fouling in dairy industry would ensure better quality control of food products during processing. In addition to this, the monitoring of the cleaning processes of processing equipment would be advantageous for the development of intelligent and effective cleaning processes on demand.

Thus, the objective of this work was to explore two techniques for the real-time detection of the microbiologically-induced and non-microbiologically-induced dairy fouling and to systematically analyse factors influencing fouling formation. The main subgoals of the work are given as follows:

1. Development of microbiologically-induced and non-microbiologically-induced dairy fouling models, analysis of factors for dairy fouling formation and evaluation of methods for fouling characterization under laboratory conditions (Section 1 in Chapter 2. Results, Publications 1 and 2);

2. Detection of microbiologically-induced and non-microbiologically-induced fouling and of cleaning media using low-field NMR (Section 2 in Chapter 2. Results, Publications 3 and 4);

3. Detection of microbiologically-induced and non-microbiologically-induced fouling and of cleaning media using electrochemical techniques, cyclic voltammetry and square wave voltammetry in combination with microelectrodes (Section 3 in Chapter 2. Results, Publications 5, 6 and 7).

In the Section 1 in Chapter 2. Results, microbiologically-induced and non-microbiologically-induced dairy fouling models that were used for the evaluation of low-field NMR and electrochemistry to detect the fouling models are described. Also, the results of the study on properties of different food-related fouling depositions and on factors that affect the fouling formation are described. In addition, different characterization techniques (microbiological, biochemical, physical and visual methods) are compared and discussed.

In the Section 2 in Chapter 2. Results, the low-field ^{1}H NMR applicability as a non-destructive technique for the fouling and CIP cleaning media detection is described and discussed. The results of transverse relaxation time determination give an insight into relaxation behaviour of microbiologically-induced and non-microbiologically-induced fouling models. Discussions and recommendations on practical implication of low-field NMR sensor in food processing equipment are also given.

In the Section 3 in Chapter 2. Results, the studies on electrochemical interdigitated platinum microelectrodes in combination with electrochemical techniques are presented and discussed. The usability of electrochemical techniques, namely cyclic voltammetry and square wave voltammetry, to detect and to distinguish between microbiologically-induced and non-microbiologically-induced fouling models as well as CIP cleaning media is described. Discussions and recommendations on practical implication of thin-film electrochemical sensor in food processing equipment are also given.

2 Results

2.1 Section 1 Fouling in food processing environments

2.1.1 Publication 1 Formation of dairy fouling deposits on food contact surfaces

This article deals with microbiological, biochemical, and physical methods to characterize different types of dairy fouling deposits. The background of the study is that literature about formation of different dairy fouling deposits on food contact surfaces at low temperatures remains lacking. Regarding these aspects, the aim of this study was to investigate the influence of temperature and type of contact material for microbiologically- and non- microbiologically- induced dairy fouling on food contact surfaces. The selected microorganism was *Pseudomonas fragi*, which can cause spoilage of dairy products and is often present in dairy processing equipment. Different types of fouling were cultivated on material sheets (PTFE and stainless steel 1.4404), with incubation temperatures (4 °C and 20 °C) and inoculation periods (24 h, 48 h and 72 h). Also, the correlation between microbiological (viable cell count), biochemical (ATP-bioluminescence assay), and physical (dry matter) methods was conducted in order prove any correlations for microbiologically- and non-microbiologically-induced dairy fouling.

The results published in the article show that non-microbiologically-induced dairy fouling and microbiological dairy fouling exhibit different adhesion behaviour on selected food contact surfaces. The highest positive correlation coefficient is found between biochemical and microbiological methods (0.932) obtained at the incubation temperatures after 24 h and 48 h. The results of the dry matter measurements show no correlations to ATP-bioluminescence assays and viable cell counts. Based on the results of this study, it can be conducted that by knowing the type of deposit expected according to the product being processed, suitable methods for detection of the dairy equipment should be applied. In addition, this study provides a good knowledge basis on microbiologically- and non-microbiologically-induced dairy fouling models and methods for the dairy fouling characterization that were used in further studies within the scope of this work.

Author contributions

Fysun, O., Wilke, B., Langowski, H.-C. devised the project, the main conceptual ideas and proof outline. Fysun, O., Kern, H. worked out the experiments and technical details, collected the data and performed the analysis for the suggested experiments. Fysun, O. wrote the manuscript. All authors discussed the results and commented on the manuscript. Langowski, H.-C. contributed to the final version of the manuscript.

International Journal of Dairy Technology

SDT Society of Dairy Technology

doi: 10.1111/1471-0307.12580

ORIGINAL RESEARCH

Formation of dairy fouling deposits on food contact surfaces

OLGA FYSUN,[1,2]* HEIKE KERN,[2,3,†] BERND WILKE[2,‡] and HORST-CHRISTIAN LANGOWSKI[1,4]

[1]*TUM School of Life Sciences Weihenstephan, Technical University of Munich, Freising,* [2]*Robert Bosch Packaging Technology GmbH, Waiblingen,* [3]*Institute of Food Science and Biotechnology, University of Hohenheim, Stuttgart, and* [4]*Fraunhofer Institute for Process Engineering and Packaging IVV, Freising, Germany*

This study aimed to compare microbiological, biochemical and physical methods to quantify dairy fouling deposits. The influence of factors affecting dairy fouling formation is investigated by selected methods with respect to material type (polytetrafluoroethylene and stainless steel) and temperature (4 and 20 °C) for a defined time. The factors were investigated using nonmicrobiologically caused and microbiologically caused dairy deposits formed by UHT and pasteurised milk inoculated with Pseudomonas fragi. *Both deposit types exhibited different adhesion behaviours. The highest positive correlation coefficient was found between biochemical and microbiological methods (0.932) obtained at both incubation temperatures after 24 and 48 h.*

Keywords Biofilm, Dairy processing, Fouling, *Pseudomonas fragi*.

INTRODUCTION

The formation of unwanted deposits on the contact surfaces of food processing equipment is a problem for the food industry constituting significant economic losses. Development of deposits can be found on many parts of food processing equipment (Brooks and Flint 2008; van Houdt and Michiels 2010). Within dairy processing plants, storage tanks, milk silos, pump exteriors, walls, milk pipelines, heat exchangers and sealing machines all have a high risk for deposit formation. Moreover, deposits can be found on industrial materials such as stainless steel, aluminium, glass, Buna-N and Teflon seals. The composition and structure of these deposits most often are associated with the type of food processing and the industrial environment (Marchand *et al.* 2012; Cappitelli *et al.* 2014).

In fact, according to several studies, deposits associated with the food processing industry can be classified as either microbiologically caused deposit (Srey *et al.* 2013) or nonmicrobiologically caused deposit (Kessler 2006). Many different terms (e.g. biofilms, bacterial deposition, biofouling, formation of slime by microorganisms) are associated with microbiological deposits (Lewandowski and Beyenal 2014). In contrast, nonmicrobiological deposits are formed by the coagulation of proteins, minerals and/or fibres due to temperature, pressure, surface properties (Kessler 2006). Attachment to surfaces is considered a physicochemical process determined by van der Waals, electrostatic and steric forces acting between the cells or particles and the attachment surface. Particularly, a wide variety of dairy processing conditions might favour deposit development due to surface properties, temperatures, relative humidity, pH, media and in case of microbiological food biofilms, type and heterogeneity of bacteria, as well as the inoculum of the raw materials (Cappitelli *et al.* 2014). Thus, microbiological and nonmicrobiological deposits can be associated strongly with dairy processing machines in industrial environments compared to other processing units. Deposits are problematic in aqueous systems, leading to manufacturing equipment malfunctions (Srey *et al.* 2013).

Microbiologically caused deposits have a heterogeneous structure including water, extracellular polymeric substances (EPS), cells, embedded particles and both polar and nonpolar

*Author for correspondence. E-mail: olga.fysun@bosch.com
†Present address: Rübezahl Schokoladen GmbH, Dettingen/Teck, Germany.
‡Present address: Leutenbach, Germany.

Vol 72, No 2 May 2019

organic molecules (Simões *et al.* 2010; Lewandowski and Beyenal 2014). They can accumulate in pipelines, storage tanks, the cooling section of heat exchangers as well as in waste water pipes (Marchand *et al.* 2012). The attachment of microorganisms to food contact surfaces can negatively contribute to the quality and safety of processed foods because of spoilage (Bower *et al.* 1996; Parizzi *et al.* 2004). Moreover, when a microbiologically caused deposit detaches from a processing surface, individual microorganism can spread easily. Inappropriate cleaning procedures may also lead to microbiological deposit formation and increase the risk of spoilage (Simões *et al.* 2010). Also, it was reported that *Pseudomonas* biofilms, which can be present in storage tanks and filling units in dairy factories, can produce enzymes. The enzymes can be released from the biofilms directly into the milk without bacterial detachment so that contamination is unnoticed until the processes product is contaminated (Marchand *et al.* 2012). The attachment of *Pseudomonas* subsp. biofilms to stainless steel at different temperatures has been shown in various studies (Stone and Zottola 1985; Barnes *et al.* 1999). Moreover, *Pseudomonas* subsp. produce large amounts of EPS (Chmielewski and Frank 2003) and can deteriorate milk quality (Hood and Zottola 1997; Sørhaug and Stepaniak 1997).

Nonmicrobiologically caused deposits can be also found in food processing equipment. In the heating process, the main fraction of the deposit is the nonmicrobiological fraction because most of the microorganisms are deactivated due to high temperatures. In the dairy industry, the milk components, such as whey proteins and calcium phosphate, are involved in the fouling process through interacting mechanisms (Kessler 2006). On the one hand, fouling starts with whey protein adhesion due to interactions occurring between the protein, the surface and other solutes, for example, minerals, even at room temperatures. On the other hand, calcium and phosphate ions precipitate as a calcium phosphate salt with increasing temperature. Moreover, these deposits increase pipeline clogs in processing plants, as well as reduce heat transfer efficiency, resulting in increased operational costs (Seth Yang-En Tan *et al.* 2014). In addition, fouling causes problems by cleaning the processing equipment (Kessler 2006).

Further, many studies on microbiological biofilms prepared in laboratory conditions have been reported (Mafu *et al.* 1990; Norwood and Gilmour 2001; Bonsaglia *et al.* 2014). However, these biofilms are not comparable to those found in industrial conditions because they are produced using defined bacterial strains in defined media. While the methods for laboratory use are well studied, industrial methods for deposit detection are rare (Brooks and Flint 2008). Previous studies have demonstrated that there is no reliable standard method for detecting deposits under industrial conditions (Marchand *et al.* 2012; Srey *et al.* 2013). The primary limitation of many of these studies is that the analytical methods, which can detect and differentiate different types of deposits under industrial conditions, were not systematically tested before. A traditional and well-established method is to count the number of viable microorganisms in samples taken at places with high risk in the production line. This method is time-consuming and can be used for detection of viable cells. Microbial contamination on accessible surfaces can be evaluated using swab methods, such as the ATP swab test. Adenosine triphosphate bioluminescence is a common biochemical method for detecting bacterial and nonbacterial contamination and rapidly assessing hygienic quality in the dairy industry in small areas; however, ATP swab tests are not useful when large areas need inspection (Bell *et al.* 1996; Turner *et al.* 2010). Also, there are a few simple commercial methods available for fast deposit detection, for example the visual biomass detection tests. In the biomass detection method, test strips of different materials can be inserted into a running system for a defined period of time and then coloured by the Safranin O solution. Any biomass available on the surface can be quantified comparing the colour intensity of the sample with the colour intensity of a reference scale. This method does not give information about bacterial counts (Morgenroth and Milferstedt 2009).

Literature about formation of structurally different dairy fouling deposit on food contact surfaces at low temperatures is still scarce. Also, critical to the previous studies is that the analytical method chosen does not distinguish between the composition and structure of the deposits among the various processes and industrial environments of the dairy industry. Regarding these aspects, the objective of this study was to investigate the influence of temperature and contact material for microbiological and nonmicrobiological dairy deposit formation on food contact surfaces in processing equipment. Therefore, sheets of materials [polytetrafluoroethylene (PTFE) and stainless steel 1.4404], different incubation temperatures (4 and 20 °C) and inoculation periods (24, 48 and 72 h) were tested. The selected bacterial species was *Pseudomonas fragi*, which is responsible for dairy spoilage and is often present in dairy processing equipment. The temperatures of 4 and 20 °C are typical minimum and maximum filling temperatures of milk in industrial processing equipment. The correlation between microbiological methods (viable cell count), biochemical methods (ATP-bioluminescence assay) and physical methods (dry matter) for deposit detection was examined in order to evaluate the methods to detect any possible correlations for nonmicrobiological and microbiological fouling deposit types.

MATERIALS AND METHODS

Chemicals

Commercial UHT and pasteurised milk (3.5% of fat) were obtained from dairy plant Weihenstephan GmbH & Co. KG

Vol 72, No 2 May 2019

(Freising, Germany). Plate count agar and rhodamine B were purchased from Merck (Darmstadt, Germany). Meat extract and yeast extract were supplied by VWR (Darmstadt, Germany). Peptone was obtained from Applichem Panreac (Barcelona, Spain). Tryptone and PBS buffer were purchased from Amresco (Solon, USA). All the reagents and chemicals used were of analytical grade.

Bacterial strain and culture conditions

The freeze-dried culture of *P. fragi* (Art. No. 3456, DSMZ, Braunschweig, Germany) was reactivated according to the instructions of the manufacturer. For each suspension, one colony of *P. fragi* was taken from the nutrient agar plate with an inoculation loop and suspended in 100 mL of nutrient medium (DSMZ GmbH 2007). The suspension was incubated at 26 °C while shaking at 100 rpm. The exponential phase of the growth curve was calculated by measuring the per cent transmission and counting the colony-forming units using plate count method. A bacterial suspension of *P. fragi* was prepared for the experiments with UHT milk in order to obtain a monoculture bacterial composition.

Preparation of the deposit samples

Three dairy deposit models were prepared: nonmicrobiological, sterile milk deposits (SMD), microbiological pasteurised milk deposits (PMD) and microbiological deposits of sterile milk inoculated with *P. fragi* (SMD-Ps). The material test sheets of PTFE (Beichler + Grünenwald GmbH, Löchgau, Germany) and stainless steel 1.4404 (Robert Bosch Packaging Technology GmbH in-house production, Waiblingen, Germany) were cleaned and autoclaved. The test sheets were put into sterile 6-well plates (Art. No. 657160, Greiner Bio one GmbH, Frickenhausen, Germany). The 6-well plates were filled with 5 mL of sterile milk for SMD and for SMD-Ps and with 5 mL of pasteurised milk for PMD using a sterile syringe (10 mL, sterile EO, BD Discardit) under laminar flow cabinet. The pasteurised milk was stored 5 days at room temperature before sample preparation. The mean value of the initial viable cell count of pasteurised milk has been determined as $6.1 \times 10^4 \pm 5.9 \times 10^4$ cfu/mL ($n = 5$) after storage of 5 days at room temperature. Large standard deviations are caused by different microbiological loads in different charges of pasteurised milk. For SMD-Ps, the *P. fragi* suspension was added to sterile milk. The *P. fragi* suspension was obtained by growth in nutrient medium at 26 °C in 50-mL flasks at 100 rpm to the early log phase. The log phase was detected by measuring the transmission. The early log phase had the transmission values at about 85–90%. Fifty microlitres of *P. fragi* suspension containing about 10^6 cfu/mL was added with a sterile pipette into 6-well plates in order to achieve a ratio of 1:100 and then vortexed at 360 rpm for 1 min. The 6-well plates with samples were stored in the climate chamber (ICH 110; Memmert, Schwabach, Germany) according to the defined experimental conditions (24, 48 and 72 h at 60% of relative humidity without stirring).

Characterisation of the material surfaces

Surface roughness measurements (R_a and R_{max}) were carried out with the 3D measuring system, Zeiss UMC 850S. The measurement was performed at 20 °C with a resolution of 0.2 µm and measuring forces of 0.1–1.0 N. The roughness of the test material sheets was measured in triplicate and the mean value calculated. The roughness measurement demonstrated that R_a and R_{max} of PTFE were 0.742 ± 0.220 and 3.110 ± 0.873 µm, respectively. R_a and R_{max} of stainless steel 1.4404 were 0.186 ± 0.050 and 8.396 ± 2.477 µm, respectively. The values of R_a of these materials were smaller than the maximum R_a benchmark recommended for hygienic design of food contact surfaces (0.8 µm; EHEDG 2004). This indicates that the roughness of the material surfaces does not affect significantly the results obtained within this study. The surface energy of PTFE was 21.4 mN/m (Jańczuk 1990), in line with the known hydrophobic nature of the material. The surface energy of stainless steel coupons was using test pens containing fluids of defined surface tension (Arcotest GmbH, Mönsheim, Germany). The surface energy of stainless steel 1.4404 coupons was determined as 41 mN/m using test pens, indicating the hydrophilic nature of stainless steel.

Investigation of the responses

Reference values of the ATP-bioluminescence assay and the dry matter measurements were carried out for UHT milk and pasteurised milk. The results are shown in the supplementary material (Table S1).

Colony-forming units

The test sheets were taken from each well of the 6-well plate with sterile tweezer and transferred into 10 mL of 0.1% sterile peptone water. The deposit was removed from the surface by vortexing the solution containing the material test sheet for 5 min at 1800 rpm. Serial log dilutions were prepared by delivering 100 µL of the stock solution in 900 µL of peptone water and mixed again; this was repeated two times to form the dilutions 10^{-1}–10^{-4}. Ten microlitres of each dilution was plated on an agar plate with a sterile spreader and incubated overnight at 30 °C. According to Lewandowski and Beyenal (2014), the colony-forming units per unit area were determined for the surface area of the test sheets by applying the following relationship: $\mathrm{CFU}/cm^2 = N \times \frac{1}{\mathrm{Dilution}} \times 1/\mathrm{Coupen\ surface\ area} \times \mathrm{Scraped\ volume}$, where N is the number of colonies growing on agar plate, Coupon surface area refers to the surface area of the test strip, and Scraped volume refers to the volume of the scraped and diluted deposit in 0.1% sterile peptone water.

Vol 72, No 2 May 2019

ATP-bioluminescence assay

The ATP-bioluminescence assay was carried out with the ATP + AMP hygiene monitoring test kit, containing the Lumitester™ PD-30 & LuciPac™Pen (Kikkoman Corporation, Japan). The material test sheets were taken from the well of the 6-well plate with a sterile tweezer and immersed in PBS buffer for 30 s. The swab stick of the LuciPac™ Pen was wiped with constant pressure over the test sheet surface of 1 cm^2, and, then the swab stick was pushed into its container allowing the releasing reagent to dissolve the luminescent reagent. The test stick was inserted into the Lumitester™ PD-30 and the measurement was carried out within 10 s. The result of ATP-bioluminescence assay was expressed in relative light units (RLU/cm^2).

Gravimetric determination of dry matter

For the determination of the dry matter of the deposits, each material test sheet was weighed before being placed in the 6-well plate (m_1) with milk. After incubation, test sheets were removed from the wells of the 6-well plate, washed with PBS buffer, dried at 104 °C for 24 h and weighed again (m_2). The differences in the weights were calculated ($DM = m_2 - m_1$) and normalised to the surface area of the test strips (mg/cm^2).

Confocal laser scanning microscopy

The confocal laser scanning microscopy (CLSM) images of test sheets with deposits were taken using the Nikon Eclipse-C1. The material test sheets were removed from each well of the 6-well plate and rinsed with PBS buffer. 20 µL of the respective dye solution (rhodamine B 0.01%) was added to the material test sheets. After 30 min of staining, samples were observed at magnifications of 40× without oil and 60× with oil. Microscope settings were controlled with the software Nikon-ECZ1 (Nikon GmbH, Düsseldorf, Germany). The temperature of the samples was kept constant at 10 °C by a water-cooled tempering unit.

Statistics

The statistical analysis was carried out using the software Cornerstone 5.3.05 (CamLine, Dresden, Germany). The results of biofilm detection are averages of three independent experiments performed for each combination of factors (temperature, fat content and material type). Mean value, standard error, normal distribution (Shapiro–Wilk test, $P < 0.05$) and an outliers test (Dixon's test, $P < 0.05$) were calculated for the responses. Pearson correlation coefficients were obtained to demonstrate correlations between the analytical methods for detecting deposits ($P < 0.05$). Significant differences between samples were determined by Student's *t*-test at $P < 0.05$. Data reported are expressed as mean ± standard error ($n = 9$).

RESULTS AND DISCUSSION

Characterisation of SMD

Sterile milk deposit was chosen as a model for sterile non-microbiological dairy deposits. Figure 1a and b shows the results of the ATP-bioluminescence assay and the dry matter measurement for the SMD after 24, 48 and 72 h.

Figure 1a shows that temperature of incubation has a significant influence on the ATP-bioluminescence results for both materials, particularly after 24 and 48 h. It can be noted that with increasing temperature, RLU values of SMD on PTFE surface increase accordingly. However, RLU values of SMD on steel surface after a 72 h do not increase significantly at 20 °C compared to 4 °C. The ATP values of investigated samples after a 72 h of incubation at 4 °C range from 113 ± 6 to 120 ± 5 RLU/cm^2. At 20 °C, the values range from 115 ± 25 to 236 ± 64 RLU/cm^2. Significant differences regarding incubation time are found for stainless steel incubated at 4 °C. Also, for PTFE samples there are significant differences between 24 and 72 h of incubation. Figure 1b illustrates that for dry matter of SMD, the material type and temperature show weak influence on the deposit formation. The values for the dry matter range from 0.81 ± 0.24 to 1.64 ± 0.40 mg/cm^2 after a 24 h of incubation. The highest values of dry matter, observed at 20 °C after 72 h of incubation for all samples, are from 3.21 ± 2.38 to 5.01 ± 3.10. The dry matter of SMD tends to increase significantly for both materials with more extended incubation time (72 h). However, it should be considered that the dry matter results after 72 h demonstrate high standard errors, which can be attributed to the formation of larger clustered fouling deposits that were nonhomogeneously distributed on the test sheet.

Characterisation of PMD

Pasteurised milk deposit was chosen as a model for microbiological dairy deposits. Figure 2a and b shows the results of the ATP-bioluminescence assay and the dry matter measurements for the PMD after 24, 48 and 72 h.

Figure 2a shows that RLU results from the ATP-bioluminescence assays at 4 °C differ significantly from the values obtained at 20 °C for both materials after 48 and 72 h. The ATP values after a 72 h of incubation at 4 °C range from 470 ± 190 to 536 ± 24 RLU/cm^2. At 20 °C, the values range from 2480 ± 1196 to 5019 ± 1225 RLU/cm^2. Significant differences influenced by incubation time are found for PTFE incubated at 20 °C. Differences in RLU concerning the material are more pronounced after 72 h of incubation; PMD on PTFE surface shows higher ATP-bioluminescence results that on stainless steel surface. For dry matter measurements (Figure 2b), however, no significant differences can be obtained with increased temperature for stainless steel and PTFE. Also, it should be noted that the time-dependent increase is not well marked for dry matter values

Vol 72, No 2 May 2019

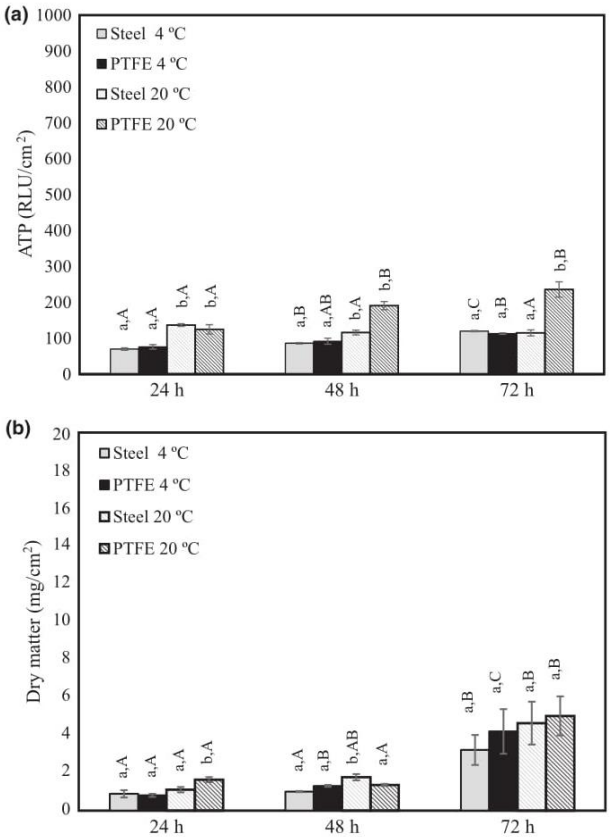

Figure 1 Experimental conditions and results of ATP-bioluminescence assay (a) and dry matter (b) for sterile milk deposit (SMD) obtained after 24, 48 and 72 h of incubation. Values shown as mean ± SE (standard error). **a**–b – the different small letters within the same incubation time and material indicate significant differences influenced by temperature (4 and 20 °C) at $P < 0.05$. A–C – the different capital letters within the same material and temperature indicate significant differences influenced by incubation time (24, 48, 72 h) at $P < 0.05$.

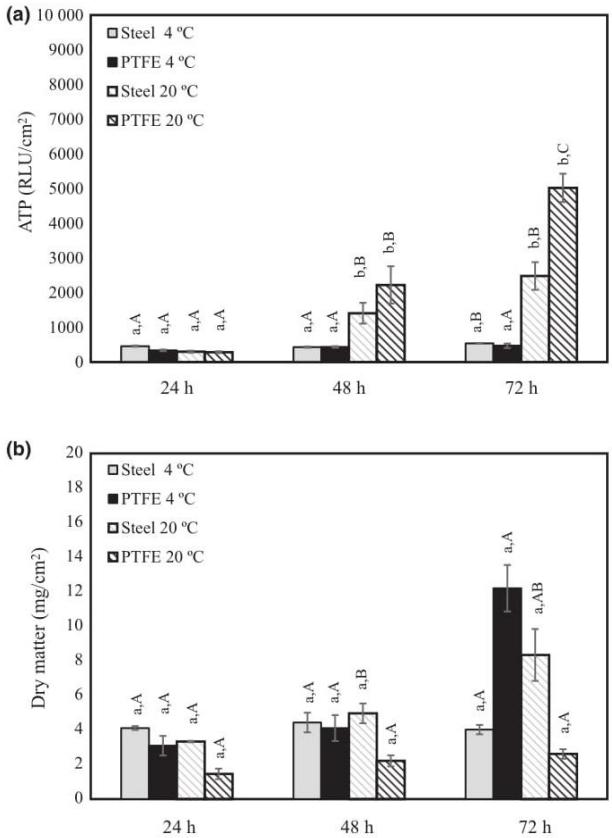

Figure 2 Experimental conditions and results of ATP-bioluminescence assay (a) and dry matter (b) for pasteurised milk deposit (PMD) obtained after 24, 48 and 72 h of incubation. Values shown as mean ± SE (standard error). a–b – the different small letters within the same incubation time and material indicate significant differences influenced by temperature (4 and 20 °C) at $P < 0.05$. A–C – the different capital letters within the same material and temperature indicate significant differences influenced by incubation time (24, 48, 72 h) at $P < 0.05$.

(except for significant difference between 24 and 48 h of incubation at 20 °C for stainless steel), particularly due to the high standard errors of obtained results.

Characterisation of the microbiological deposit (UHT milk inoculated with *P. fragi*)

Figure 3a and b shows the results of the ATP-bioluminescence assays, and the dry matter values for the microbiological deposit formed by UHT milk inoculated with *P. fragi* after 24, 48 and 72 h of incubation.

Figure 3a illustrates that results from the ATP-bioluminescence assays at 4 °C differ significantly from the values obtained at 20 °C for both materials and all incubation times. The RLU values increase at 20 °C and extended incubation times. The differences concerning the material are more pronounced after 48 and 72 h of incubation. The results obtained after 48 and 72 h of incubation are significantly different from results obtained after 24 h. However, it should be considered that the ATP results after 48 and 72 h show high standard errors, which can be caused by the formation of larger clustered fouling deposits (Figure 4b). These results are also in accordance with results obtained for PMD (Figure 2a), but different from SMD where the temperature had less pronounced influence for steel surface. Except for PTFE, no significant differences of temperature can be found for dry matter of sterile milk deposit inoculated with *P. fragi* (SMD-*Ps*) (Figure 3b). Also, influence of incubation time is significant only for some samples incubated at 20 °C. For example, after 72 h of incubation an increase in dry matter is observed for SMD-*Ps* on PTFE surface at 20 °C compared to the same sample after 24 and 48 h of incubation.

Vol 72, No 2 May 2019

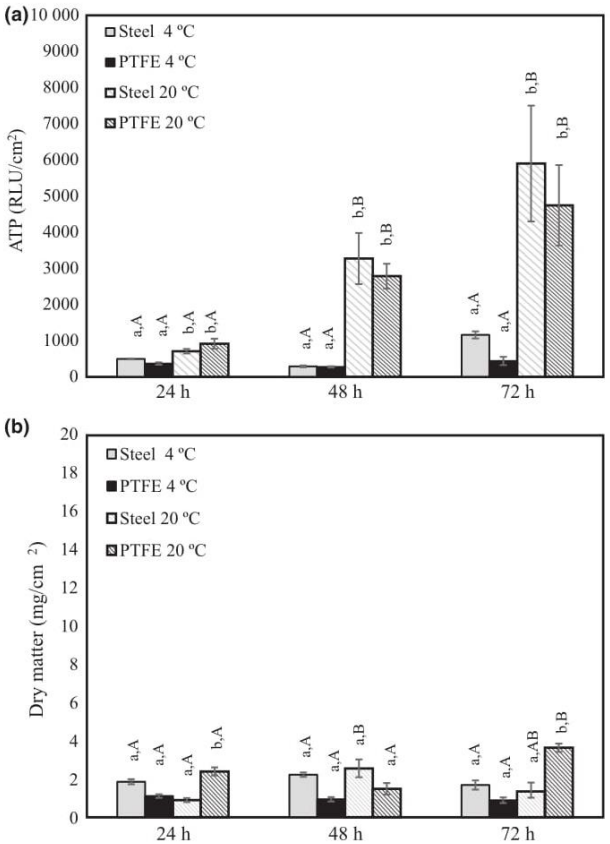

Figure 3 Experimental conditions and results of ATP-bioluminescence assay (a) and dry matter (b) for sterile milk deposit inoculated with ***Pseudomonas*** *fragi* (SMD-*Ps*) measured after 24, 48 and 72 h of incubation. Values shown as mean ± SE (standard error). **a**–b – the different small letters within the same incubation time and material indicate significant differences influenced by temperature (4 and 20 **°C**) at $P < 0.05$. A–C – the different capital letters within the same material and temperature indicate significant differences influenced by incubation time (24, 48, 72 h) at $P < 0.05$.

Table 1 demonstrates the results of viable cell counts (cfu/cm^2) for PMD and sterile milk deposit inoculated with *P. fragi* (SMD-*Ps*) measured after 24, 48 and 72 h of incubation.

Table 1 shows that as expected results from viable cell counts for PMD at 4 °C differ distinctly from the values obtained at 20 °C. In PMD with polyculture bacterial composition, the number of viable cells attached to the surface at 20 °C is found of 2.4×10^1 cfu/cm^2 for PTFE and 3.9×10^1 cfu/cm^2 for stainless steel after 24 h of incubation and of 1.0×10^3 cfu/cm^2 for PTFE and 4.4×10^3 cfu/cm^2 for stainless steel after 72 h of incubation. The number of attached viable cells at 4 °C is obtained of 1–2 log decades lower compared to the incubation at 20 °C. For PMD, the temperature affects more the attachment of viable cells, while the type of material has a less remarkable effect. The number of viable *P. fragi* cells attached to the surface at 20 °C is found between 3.2×10^2 cfu/cm^2 for PTFE and 5.2×10^2 cfu/cm^2 for stainless steel after 24 h of incubation and between 6.8×10^4 cfu/cm^2 for PTFE and 1.0×10^5 cfu/cm^2 for stainless steel after 72 h of incubation. Similar to PMD, the number of attached viable cells at 4 °C is determined to be of 1–2 log decades lower compared to the attached viable cells at 20 °C. In addition, it can be noted that *P. fragi* as the monoculture tends to attach to PTFE surface more than to stainless steel surface at 4 °C when comparing with the polyculture (PMD).

CLSM images

Surfaces and deposit images can be obtained using CLSM. Figure 4 illustrates the CLSM images of a clean steel surface (a), a sterile milk deposit inoculated with *P. fragi* (SMD-*Ps*) (b) and a *P. fragi* biofilm formed without milk (c).

Figure 4a illustrates CLSM images of the clean stainless steel surface, which can be identified by characteristic surface roughness. The microbiological dairy deposit, also on stainless steel, was formed by UHT milk inoculated with *P. fragi* (SMD-*Ps*) after 2 days of incubation (Figure 4b). Figure 4b shows a patchy heterogeneous structure of the deposit on stainless steel surface. In order to compare a microbiologically caused dairy deposit and a biofilm, Figure 4c shows the *P. fragi* biofilm after a 2-day incubation at 20 °C with nutrient broth. This biofilm is characterised by an accumulation of small clusters of *P. fragi* cells on the stainless steel surface. No patchy structure as on Figure 4b is observed for *P. fragi* biofilm on the stainless steel surface.

Correlation of the measurement methods

The methods for deposit measurement have been compared. The Pearson correlation of the results of the ATP-bioluminescence assay, number of viable cells, dry matter has been determined for all samples ($P < 0.05$). The correlation values for the results of the ATP-bioluminescence assay (RLU/cm^2) and viable cell counts (cfu/cm^2) for samples were determined after 24, 48 and 72 h at the incubation temperatures of 4 and 20 °C. A positive correlation between the viable cell counts and ATP assays of 0.499 ($n = 24$) was obtained. A small negative correlation was found between dry matter measurements and viable cell counts (−0.264) ($n = 24$), as well as between dry matter measurements and ATP-bioluminescence assays (−0.042) ($n = 36$). As shown in the results (Figures 1–3), the results of measurements after 72 h have the largest standard errors; therefore, the correlation between results of the ATP assays, numbers of viable cells and dry matter was determined by removing data measured after 72 h of incubation.

Vol 72, No 2 May 2019

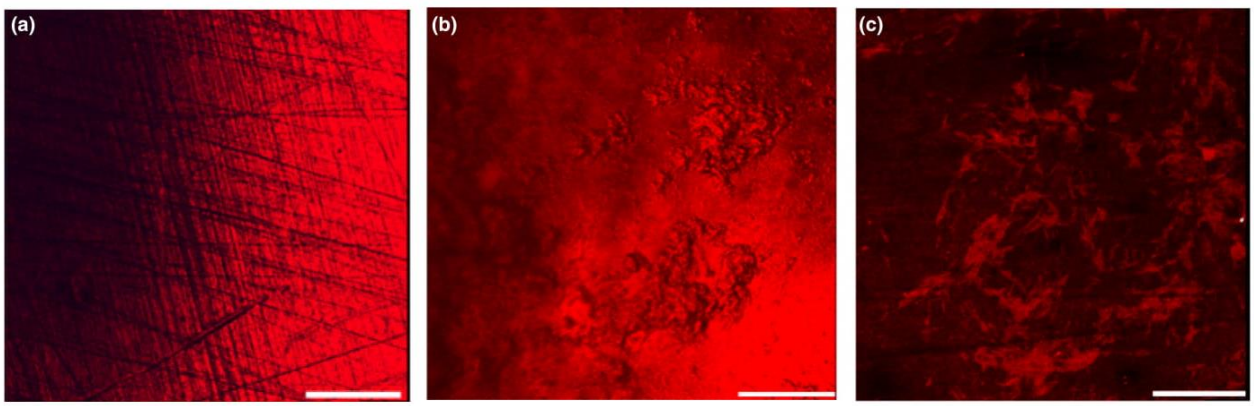

Figure 4 Confocal laser scanning microscopy (CLSM) images of stainless steel (a), SMD-*Ps* on stainless steel incubated for 2 days at 20 °C and stained with rhodamine B (b), *Pseudomonas fragi* biofilm on the stainless steel surface incubated for 2 days at 20 °C and stained with rhodamine B (c). The magnification of (a) and (b) is with a 20× objective (scale equals 150 μm), while (c) is at 60× magnification with oil (scale equals 20 μm). [Colour figure can be viewed at wileyonlinelibrary.com]

The obtained positive Pearson correlation coefficient between the viable cell counts and ATP-bioluminescence assays then increased to 0.932 (n = 12). The correlation coefficient between the dry matter measurements and the viable cell counts (n = 12), as well as between dry matter measurements and ATP assays (n = 24), for samples after 24 and 48 h at incubation temperatures of 4 and 20 °C slightly changed to −0.239 and 0.088, respectively. However, the values of dry matter determination did not correlate with microbiological and biochemical methods. It should be considered that in real industrial conditions no results regarding bacterial contamination can be obtained by determining the dry matter content of the deposit on food contact surfaces.

Formation and determination of dairy fouling deposits

Dairy fouling control in dairy manufacturing plants is important to ensure safety of manufactured food products. In this study, dairy deposit models were investigated. The results obtained in this study showed that nonmicrobiological dairy deposit and microbiological dairy deposits exhibited different adhesion behaviours on food contact surfaces (PTFE and stainless steel). Generally, it was found that different temperature (4 and 20 °C) had a different influence on the results of the ATP-bioluminescence assay (Figures 2a and 3a) and of the viable cell counts (Table 1) for the microbiological dairy deposit, while the nonmicrobiological dairy deposit was affected slightly by the increase of temperature at longer incubation times (Figure 1a). Incubation times showed a strong influence on the ATP bioluminescence (Figures 2a and 3a) and the viable cell counts (Table 1) for the microbiological dairy deposit, but a weak influence on the dry matter (Figures 2b and 3b). Conversely, the nonmicrobiological deposit formation was affected more by the incubation time regarding dry matter (Figure 1b). More specifically, the ATP-bioluminescence values for microbiological deposits (Figures 2a and 3a) were greater than for the nonmicrobiological deposit (Figure 1a) under the same preparation conditions, whereas dry matter did not show pronounces differences (Figures 1b and 3b), except for the PMD (Figure 2b). In comparison with PMD containing a polyculture of bacterial strains, dairy deposits formed from UHT milk inoculated with *P. fragi* (SMD-*Ps*) demonstrated higher ATP bioluminescence (Figures 2a and 3a) and colony-forming unit (cfu/cm^2) values (Table 1). It has been reported that several strains appear to adhere in monocultures rather than in multispecies biofilms (Norwood and Gilmour 2001). Also, it can be noted that the attachment of monoculture *P. fragi* was more pronounced on stainless steel surfaces at 20 °C while higher attachment of *P. fragi* at 4 °C was observed on PTFE surfaces (Table 1). *P. fragi* is known for having the ability to form biofilms and possesses several properties that influence cell attachment, as *P. fragi* is motile by polar flagellum (Fuerst and Hayward 1969). Although nonmicrobiological deposits do not microbiologically contaminate the processed product, food processing equipment should be regularly cleaned (Srey *et al.* 2013). The nonmicrobiological deposit increases in size over time, leading to the lower efficiency of heat transfer, which can cause the postformation of microbiological deposits (Marchand *et al.* 2012).

Also, the effect of the hydrophobicity of different materials plays an important role in the processing of liquid products and the cleaning procedures for the apparatus (McEldowney and Fletcher 1987; Chmielewski and Frank 2003). Some studies have found that higher numbers of bacteria attach to hydrophobic surfaces, such as PTFE, than to hydrophilic surfaces, like metals (Teixeira *et al.* 2005; Pasmore *et al.* 2010). However, there are conflicting views, as only small parts of microbial cells (i.e. pili, fimbriae and

Vol 72, No 2 May 2019

Table 1 Experimental conditions and results of viable cell counts (cfu/cm^2) for pasteurised milk deposit (PMD) and sterile milk deposit inoculated with *Pseudomonas fragi* (SMD-*Ps*) measured after 24, 48 and 72 h of incubation

Factors		*PMD*			*SMD*-Ps		
		24 h	*48 h*	*72 h*	*24 h*	*48 h*	*72 h*
Material	*Temperature (°C)*	*cfu/cm^2*			*cfu/cm^2*		
Steel	20	3.9×10^1	1.2×10^2	4.4×10^3	5.2×10^2	6.6×10^3	1.0×10^5
PTFE	20	2.4×10^1	1.3×10^2	1.0×10^3	3.2×10^2	2.0×10^3	6.8×10^4
Steel	4	2.6×10^0	2.6×10^0	4.5×10^2	4.3×10^1	4.0×10^1	4.0×10^3
PTFE	4	1.6×10^0	5.3×10^0	1.4×10^2	6.2×10^1	1.8×10^2	1.1×10^4

PTFE, polytetrafluoroethylene.

flagella) are hydrophobic (Lewandowski and Beyenal 2014). Nevertheless, it has also been reported that hydrophilic surfaces allow for more rapid microbiological formation and cell attachment than hydrophobic materials (Mafu *et al.* 1990; Hyde *et al.* 1997; Bonsaglia *et al.* 2014). Despite many studies on the relation among hydrophobicity, surface energy and the initial attachment of bacteria, the relation remains unclear: bacteria can colonise both hydrophobic and hydrophilic surfaces (Lewandowski and Beyenal 2014). Further, it was shown that the conditioning layer can change the hydrophobicity of the contact surface (Barnes *et al.* 1999; Dat *et al.* 2010).

Detection and differentiation of differently structured deposits in food processing equipment are important. However, when choosing the most suitable methods to determine the deposit formation, structure and composition of the deposit should be considered. The ATP-bioluminescence assay detects all organic matter on food contact surfaces and thus may give important information regarding microbiological deposit formation, as bacterial adherence may be supported by nutrients on the food contact surface (Sherlock *et al.* 2009; Turner *et al.* 2010). The linear relationship of ATP assays and the viable cell counts has been reported by Bottari *et al.* (2015). Nevertheless, it does not always apply since the ratio of microbial cells to food deposits is not constant. A relatively high amount of ATP can be also detected in UHT milk despite the fact that UHT milk does not contain viable microorganisms (Costa *et al.* 2006). As previously discussed, it has been reported that ATP assays provide a relatively poor detection of Gram-negative bacteria because of incomplete cell lysis. Furthermore, differences in metabolic status can lead to scattered results, especially when investigating thick organic deposits (Turner *et al.* 2010).

CONCLUSION

This study investigated the influence of the selected temperatures and incubation times affecting nonmicrobiological dairy deposit and two microbiological dairy deposits formed on PTFE and stainless steel surfaces. The results showed that nonmicrobiological dairy deposit and microbiological dairy deposits exhibited different adhesion behaviour. Comparing the correlation of methods, the highest positive Pearson correlation coefficient was found between ATP-bioluminescence assays and the viable cell counts (0.932) for samples obtained after 24 and 48 h at incubation temperatures of 4 and 20 °C. Dry matter measurement showed no correlations to ATP-bioluminescence assays and the viable cell counts. From the results obtained in this study, it can be concluded that by knowing the type of deposit expected according to the product being processed, suitable methods for detection of the dairy equipment can be applied. Further, this study must be supplemented with further investigation of the parameters that influence dairy fouling formation, such as surface energy and roughness of the contact material and higher temperatures simulating thermal processing of dairy products. In addition, further research will be needed to validate the influence of different factors on viable cells in fouling deposits. Also, development of new deposit detection methods in dairy processing equipment would be of great interest.

ACKNOWLEDGEMENTS

This research did not receive any specific grant from funding agencies in the public, commercial or not-for-profit sectors. The authors thank Dr. Holger Brehm for proofreading and Dr. Johannes Rauschnabel for beneficial discussions.

REFERENCES

Barnes L M, Lo M F, Adams M R and Chamberlain A H L (1999) Effect of milk proteins on adhesion of bacteria to stainless steel surfaces. *Applied and Environmental Microbiology* **65** 4543–4548.

Bell C, Bowles C D, Toszeghy M J K and Neaves P (1996) Development of a hygiene standard for raw milk based on the Lumac ATP-bioluminescence method. *International Dairy Journal* **6** 709–713.

Bonsaglia E C R, Silva N C C, Fernades Júnior A, Araújo Júnior J P, Tsunemi M H and Rall V L M (2014) Production of biofilm by *Listeria monocytogenes* in different materials and temperatures. *Food Control* **35** 386–391.

Vol 72, No 2 May 2019

Bottari B, Santarelli M and Neviani E (2015) Determination of microbial load for different beverages and foodstuff by assessment of intracellular ATP. *Trends in Food Science & Technology* **44** 36–48.

Bower C K, McGuire J and Daeschel M A (1996) The adhesion and detachment of bacteria and spores on food-contact surfaces. *Trends in Food Science & Technology* **7** 152–157.

Brooks J D and Flint S H (2008) Biofilms in the food industry: problems and potential solutions. *International Journal of Food Science & Technology* **43** 2163–2176.

Cappitelli F, Polo A and Villa F (2014) Biofilm formation in food processing environments is still poorly understood and controlled. *Food Engineering Reviews* **6** 29–42.

Chmielewski R and Frank J F (2003) Biofilm formation and control in food processing facilities. *Comprehensive Reviews in Food Science and Food Safety* **2** 22–32.

Costa P D, Andrade N J, Soares N F F, Passos F J V and Brandão S C C (2006) ATP-bioluminescence assay as an alternative for hygiene-monitoring procedures of stainless steel milk contact surfaces. *Brazilian Journal of Microbiology* **37** 345–349.

Dat N M, Hamanaka D, Tanaka F and Uchino T (2010) Surface conditioning of stainless steel coupons with skim milk solutions at different pH values and its effect on bacterial adherence. *Food Control* **21** 1769–1773.

DSMZ GmbH (2007) *1. Nutrient Agar* [Internet document] URL https://www.dsmz.de/microorganisms/medium/pdf/DSMZ_Medium1.pdf. Accessed 20/06/2016.

EHEDG (2004) EHEDG guidelines: doc 8 hygienic equipment design criteria. 2nd edn [Internet document] URL www.ehedg.org. Accessed 09/03/2017.

Fuerst J A and Hayward A C (1969) Surface appendages similar to fimbriae (Pili) on Pseudomonas species. *Journal of General Microbiology* **58** 227–237.

Hood S K and Zottola E A (1997) Adherence to stainless steel by foodborne microorganisms during growth in model food systems. *International Journal of Food Microbiology* **37** 145–153.

van Houdt R and Michiels C W (2010) Biofilm formation and the food industry, a focus on the bacterial outer surface. *Journal of Applied Microbiology* **109** 1117–1123.

Hyde F W, Alberg M and Smith K (1997) Comparison of fluorinated polymers against stainless steel, glass and polypropylene in microbial biofilm adherence and removal. *Journal of Industrial Microbiology & Biotechnology* **19** 142–149.

Jańczuk T B (1990) The total surface free energy and the contact angle in the case of low energetic solids. *Journal of Colloid and Interface Science* **140** 362–372.

Kessler H G (2006) *Lebensmittel- und Bioverfahrenstechnik: Molkereitechnologie*, 4th edn. München: Verl. A. Kessler.

Lewandowski Z and Beyenal H (2014) *Fundamentals of Biofilm Research*, 2nd edn. Boca Raton, FL: CRC Press/Taylor & Francis Group.

Mafu A A, Roy D, Goulet J and Magny P (1990) Attachment of *Listeria monocytogenes* to stainless steel, glass, polypropylene, and rubber surfaces after short contact times. *Journal of Food Protection* **53** 742–746.

Marchand S, De Block J, De Jonghe V, Coorevits A, Heyndrickx M and Herman L (2012) Biofilm formation in milk production and processing environments: influence on milk quality and safety. *Comprehensive Reviews in Food Science and Food Safety* **11** 133–147.

McEldowney S and Fletcher M (1987) Adhesion of bacteria from mixed cell suspension to solid surfaces. *Archives of Microbiology* **148** 57–62.

Morgenroth E and Milferstedt K (2009) Biofilm engineering: linking biofilm development at different length and time scales. *Reviews in Environmental Science & Biotechnology* **8** 203–208.

Norwood D E and Gilmour A (2001) The differential adherence capabilities of two *Listeria monocytogenes* strains in monoculture and multispecies biofilms as a function of temperature. *Letters in Applied Microbiology* **33** 320–324.

Parizzi S Q F, de Andrade N J, de S Silva C A, de FF Soares N and da Silva E A M (2004) Bacterial adherence to different inert surfaces evaluated by epifluorescence microscopy and plate count method. *Brazilian Archives of Biology and Technology* **47** 77–83.

Pasmore M, Todd P, Pfiefer B, Rhodes M and Bowman C N (2010) Effect of polymer surface properties on the reversibility of attachment of *Pseudomonas aeruginosa* in the early stages of biofilm development. *Biofouling* **18** 65–71.

Sherlock O, O'Connell N, Creamer E and Humphreys H (2009) Is it really clean? An evaluation of the efficacy of four methods for determining hospital cleanliness. *The Journal of Hospital Infection* **72** 140–146.

Simões M, Simões L C and Vieira M J (2010) A review of current and emergent biofilm control strategies. *LWT – Food Science and Technology* **43** 573–583.

Sørhaug T and Stepaniak L (1997) Psychrotrophs and their enzymes in milk and dairy products: quality aspects. *Trends in Food Science & Technology* **8** 35–41.

Srey S, Jahid I K and Ha S D (2013) Biofilm formation in food industries: a food safety concern. *Food Control* **31** 572–585.

Stone L S and Zottola E A (1985) Effect of cleaning and sanitizing on the attachment of *Pseudomonas fragi* to stainless steel. *Journal of Food Science* **50** 951–956.

Tan S Y-E, Chew S C, Tan S Y-Y, Givskov M and Yang L (2014) Emerging frontiers in detection and control of bacterial biofilms. *Current Opinion in Biotechnology* **26** 1–6.

Teixeira P, Lopes Z, Azeredo J, Oliveira R and Vieira M J (2005) Physico-chemical surface characterization of a bacterial population isolated from a milking machine. *Food Microbiology* **22** 247–251.

Turner D E, Daugherity E K, Altier C and Maurer K J (2010) Efficacy and limitations of an ATP-based monitoring system. *Journal of the American Association for Laboratory Animal Science* **49** 190–195.

SUPPORTING INFORMATION

The following supporting information is available for this article:

Table S1 Results of normalized reference measurements of ATP test and dry matter for UHT milk and pasteurized milk at 20.0 °C.

2.1.2 Publication 2 Evaluation of factors influencing dairy biofilm formation in filling hoses of food-processing equipment

In different literature sources it was reported that biofilms could be found in various parts of dairy-processing equipment. Particularly, filling units are often a source of contamination of dairy products during manufacturing processes. Considering this fact, this article reports the influence of factors that can affect biofilm formation in a dairy-filling hose as well as it shows a comparison between selected characterization methods. Several factors were evaluated at a constant temperature of 5.5 ± 0.5 ºC. Bacterial composition (monoculture *P. fragi* and polyculture), fat content of milk (1.5% and 3.5%), flow (laminar and turbulent), and food contact material (PTFE, stainless steel 1.4404) were considered as possible factors influencing biofilm formation in dairy processing equipment. Also, correlation coefficients between microbiological (viable-cell counting), biochemical (ATP-bioluminescence testing), and visual (biomass quantification) methods for biofilm characterization in dairy filling hoses were examined. Furthermore, enzymatic cleaning was applied after each experimental run and results of ATP-bioluminescence testing were recorded.

The obtained results show that bacterial composition, material type, and fat content significantly affect the number of viable cells. Flow and material type, both have significant impacts upon biomass quantification. For ATP-bioluminescence, however, no clear influence of the selected factors could be observed, particularly due to the wide distribution of the interquartile ranges. The highest positive Pearson correlation is found between the ATP-bioluminescence and biomass methods (0.550), while the lowest correlation is obtained between viable-cell counting and biomass quantification (0.345). When comparing data obtained from the experiments conducted in this study, the results of data analysis confirm that a biofilm development is of concern in filling units of dairy-processing equipment also at low temperature of 5.5 ± 0.5 ºC. In addition, the enzymatic treatment showed a good result for the cleaning of the PTFE-hose liner in the dairy-filling hose. In addition, this study provides a knowledge basis on methods for the dairy fouling used in further studies on sensors within the scope of this work.

Author contributions

Fysun, O. designed the study. Wilke, B., Langowski, H.-C. were involved in planning and supervised the work. Fysun, O., Kern, H. carried out the experiments, collected the data and

performed the analysis for the data. Fysun, O. wrote the manuscript. All authors discussed the results and commented on the manuscript. Langowski, H.-C. contributed to the final version of the manuscript.

Permission for the re-use of the article granted by Elsevier B.V..

Food and Bioproducts Processing 113 (2019) 39–48

Contents lists available at ScienceDirect

Food and Bioproducts Processing

journal homepage: www.elsevier.com/locate/fbp

Evaluation of factors influencing dairy biofilm formation in filling hoses of food-processing equipment

Olga Fysun[a,b,*], *Heike Kern*[b,c,1], *Bernd Wilke*[b,2], *Horst-Christian Langowski*[a,d]

[a] TUM School of Life Sciences Weihenstephan, Technical University of Munich, Freising, Germany
[b] Robert Bosch Packaging Technology GmbH, Waiblingen, Germany
[c] Institute of Food Science and Biotechnology, University of Hohenheim, Stuttgart, Germany
[d] Fraunhofer Institute for Process Engineering and Packaging IVV, Freising, Germany

ARTICLE INFO

Article history:
Received 8 August 2018
Received in revised form 9 October 2018
Accepted 16 October 2018
Available online 24 October 2018

Keywords:
Biofilm
Dairy products
Pseudomonas fragi
Dairy processing equipment
Enzymatic cleaning

ABSTRACT

Biofilms in dairy-processing environments lead to increased opportunities for microbial contamination of processed products. The aim of this work is to investigate the influence of factors that can affect biofilm onset in a dairy-filling test hose. Bacterial composition (monoculture *Pseudomonas fragi*, polyculture), fat content of milk (1.5%, 3.5%), flow condition (laminar, turbulent), and contact material (PTFE, stainless steel 1.4404) were considered as factors at a constant low temperature of 5.5 ± 0.5 °C. Biofilms were visualized by microscopy (CLSM) and analysed by counting viable cells, ATP-bioluminescence assay, and staining method for biomass quantification. The correlation between these methods was evaluated, since the chosen methods detect different characteristics of biofilms. Furthermore, enzymatic cleaning was applied after each experimental run. The results showed that the bacterial composition, material type, and fat content significantly affect the results of viable-cell counting ($p \leq 0.05$). Flow conditions and material type both have significant influence upon biomass-quantification results ($p \leq 0.001$). The highest positive Pearson correlation was estimated between the ATP-bioluminescence and biomass methods (0.550), while the lowest correlation was found between viable-cell counting and biomass quantification (0.345). Enzymatic treatment showed a good result for the cleaning of the PTFE-hose liner in the dairy-filling hose.

1. Introduction

The attachment of microorganisms to the surfaces of food-processing equipment can lead to biofilm formation. This can affect the quality and safety of foods by means of spoilage. Biofilms are considered to be microbial aggregations attached to and growing on a surface (Chmielewski and Frank, 2003). Structure and composition of biofilms depend on the environmental conditions, the surface, the bacterial genome and the components embedded in the biofilm matrix (Marchand et al., 2012). Generally, biofilms have a heterogeneous structure including water (up to 90%), extracellular polymeric substance (EPS) (up to 90% of organic matter), cells, and embedded particles with thicknesses ranging between several μm and several mm. The compositions and morphologies of different biofilms can diverge as even one bacterium can create different types of biofilms when exposed to different conditions (Marchand et al., 2012). The development of biofilms can be divided into the following different stages: reversible attachment, irreversible attachment, maturation, and dispersion (Lewandowski and Beyenal, 2014).

* *Corresponding author.*
E-mail address: olga.fysun@bosch.com (O. Fysun).
[1] Present address: Rübezahl Schokoladen GmbH, Dettingen/Teck, Germany.
[2] Present address: Consultancy in Packaging, Leutenbach, Germany.

https://doi.org/10.1016/j.fbp.2018.10.009
0960-3085/

Reversible attachment is caused by van der Waals forces, steric, electrostatic, and hydrophilic interactions. The bacteria exhibit a large variety of motility mechanisms and can easily be removed. Irreversible attachment involves short-range forces between the cell appendages and the surface, dipole–dipole interactions, hydrogen bonds, and hydrophobic and ionic covalent bonding (Chmielewski and Frank, 2003; Bower et al., 1996). Biofilm formation can be influenced by several factors, including bacterial strain, surface characteristics (such as hydrophobicity, wettability, and roughness), temperature, relative humidity, pH, media composition, the presence of other microorganisms (Cappitelli et al., 2014). Hydrodynamics and mass-transport characteristics have also been shown to have an influence on the morphology, mass, and density of biofilms in several studies (Stoodley et al., 1998; Pereira et al., 2002). Flow condition (laminar or turbulent) also significantly impacts biofilm development on a hose's interior walls (Lewandowski and Beyenal, 2014). Thus, the region near the wall can be of special interest for biofilm formation. Focusing on the food-manufacturing process, a variety of favourable conditions in dairy-processing equipment might induce the formation of biofilm, including the presence of moisture, favourable temperature ranges for bacteria growth, and rich nutrient contents (Marchand et al., 2012; Bower et al., 1996).

Biofilm formation in dairy-processing equipment can lead to product spoilage, and economic losses for manufacturers. It was found that biofilms can develop in dairy-processing equipment within a few hours (Latorre et al., 2010). Milk is an optimal medium for the growth of microorganisms because of its neutral pH and the high nutrient content (Mogha, 2014).

Previous studies indicate that biofilms can be found in different parts of dairy-processing equipment. Storage tanks, milk silos, pump exteriors, walls, milk pipelines, heat exchangers, and filling units are ranked as high-risk parts for biofilm formation (Marchand et al., 2012; Storgårds et al., 1999; Eneroth et al., 1998). Biofilms have been detected on industrial surfaces such as stainless steel, aluminum, glass, PTFE, Buna-N, and Teflon seals (Cappitelli et al., 2014). Biofilms in dairy-processing equipment are a potential source of food contamination that may lead to spoilage or transmission of foodborne pathogens. Bacteria that survive the heat treatment or enter the product by recontamination can have a negative influence on the shelf life and quality of the product. Moreover, when a biofilm detaches from the surface, individual microorganisms can easily spread, increasing opportunity for microbial contamination of the processed product (Chmielewski and Frank, 2003). In addition, bacterial colonization of food-processing equipment is the main concern with damage to metal surfaces through pitting or corrosion. Also, inappropriate cleaning procedures may contribute to biofilm development and increase the risk of spoilage. Previous studies have demonstrated that the major sources of contaminated milk and milk products are usually considered to come from improperly cleaned and sanitized equipment (Marchand et al., 2012; Srey et al., 2013).

Dairy products are exposed to a broad range of different temperatures during their production and transportation processes. The temperature can range from 5 °C to 140 °C (Kessler, 2006). In pasteurized-milk manufacturing, raw milk can be in contact with surface temperatures ranging from 5 °C to 72 °C during heating in the pasteurizer and cooling afterwards in the heat exchanger before entering the filling unit (Milchverordnung, 2000). Therefore, pasteurized milk can be spoiled by thermoduric and thermophilic microorganisms, which can adhere to processing equipment depending on the process-step conditions (Fratamico et al., 2009). Pasteurized milk can also be spoiled by Gram-positive spore-forming bacteria that survive the pasteurization or by Gram-negative psychrotrophic bacteria, which are killed during the pasteurization but can enter the dairy-processing equipment by recontamination (Eneroth et al., 2000; Cousin, 1982) . As reported, filling units are often a source of recontamination of dairy products. Recontamination of pasteurized milk with Gram-negative psychrotrophic bacteria is associated with rinsing water in and around the filling machine during the filling operation (Eneroth et al., 1998). This indicates that psychrotrophic bacteria could have formed biofilms in the rinse water system. Also, biofilms that can develop on the sides of gaskets in filling units may also be a possible source of post-pasteurization contamination. Also, an important source of recontamination due to biofilms is the filling equipment as the bacteria penetrates the filler of the vacuum or bulk tanks. Furthermore, spores that survive the pasteurization after germination can stick to dead ends, pockets, and traps and lead to biofilm formation in the filling line. Another reason for recontamination by bacteria may be a lack of cleaning and sanitation procedures in the processing equipment or malfunction of the equipment (Cousin, 1982).

A remarkable feature of biofilms is that they can become 10–1000 times more resistant to the effects of antimicrobial agents due to the production of an extracellular polymeric substance (EPS) (Cappitelli et al., 2014). Biofilms are difficult to remove from food-processing surfaces due to the complexity of processing equipment (Chmielewski and Frank, 2003). Biofilm control in dairy-manufacturing plants generally involves a process called cleaning-in-place (CIP) (Marchand et al., 2012). Cleaning-in-place (CIP) procedures are usually employed in milk-processing lines. However, conventional cleaning does not always allow the full removal of the bacteria from surfaces. If the cleaning process is insufficient, the bacteria can attach and produce EPS, making biofilm difficult to remove. Likewise, because biofilms exhibit increased resistance to cleaning and sanitation procedures, they can lead to increased corrosion and material deterioration (Flint et al., 1997). Hence, the dairy industry is constrained to prevent product contamination and biofilm formation by increasing the frequency of cleaning and longer cleaning time. Due to the current trend toward longer production runs, the use of complex equipment, and the automation of plants, the issue of bacterial contamination by biofilms are gaining increasing importance for dairy manufacturers (Bremer et al., 2006). An alternative to traditional CIP procedures is to apply enzymes for the degradation and cleaning of biofilms. The use of enzymatic cleaning agents against bacterial biofilms in dairy processing equipment have been reported (Austin and Bergeron, 1995).

Psychrotrophic bacteria groups, e.g., *Pseudomonas* spp., play a particularly important role in quality concern and shelf life due to their ability to form biofilms below 10 °C (Sørhaug and Stepaniak, 1997; Hood and Zottola, 1997). *Pseudomonas* spp. can produce a lot of EPS and have shown to attach themselves to stainless steel in various studies and produce attachment fimbriae at different temperatures (Barnes et al., 1999; Stone and Zottola, 1985). Furthermore *Pseudomonas* spp. can coexist in a biofilm with *Listeria, Salmonella* and other pathogenic microorganisms (Chmielewski and Frank, 2003). It has also been reported that *Pseudomonas* biofilms, which are present in

storage tanks in dairy factories, can produce enzymes. Many of them produce heat-stable extracellular lipases, proteases, and lecithinases. The enzymes might be released from the biofilms into the milk without bacterial detachment, such that the contamination might go unnoticed until microbiological problems arise (Sørhaug and Stepaniak, 1997; Teh et al., 2014). *Pseudomonas fragi* and *Pseudomonas lundensis* have an influence upon the shelf life milk even at low temperatures (5–10 °C) (De Jonghe et al., 2011; Marchand et al., 2009). *P. fragi* has been shown to enhance the attachment of *Listeria monocytogenes* to glass surfaces, which has been attributed to EPS production by *P. fragi* (Sasahara and Zottola, 1993).

Various industrial-detection methods for deposits have been used in recent decades (Denkhaus et al., 2007). A traditional and well-established method is viable-cell counting in samples taken manually from high-risk locations on the production line. Also, contamination on accessible surfaces can be evaluated by swabbing methods such as the ATP-swab test. Adenosine triphosphate (ATP) bioluminescence-assay is a common biochemical method to detect bacterial and non-bacterial contamination to rapidly assess hygienic quality in the dairy industry (Bell et al., 1996; Turner et al., 2010). Furthermore, there are several visual biomass-detection methods. For biomass quantification in food-processing equipment, test strips of different materials are inserted into a running system for a defined time and then colored by Safranin O solution. Any biomass available on the surface can be quantified by comparing the color intensity of the sample with the color intensity of a reference scale (Breves et al., 2004). However, most previous methods on biofilms detection in food processing equipment have not taken into account that the biofilms consist of many components and therefore a few detection methods are required to characterize the biofilm.

Regarding these concerns, the aim of this work is to investigate the influence of different factors upon biofilm formation in dairy-processing equipment with special attention to the filling process. Several factors were tested at a constant temperature of 5.5 ± 0.5 °C, which is the lowest filling temperature of milk. According to the previous studies, bacterial composition (monoculture *P. fragi* and polyculture), fat content of milk (1.5% and 3.5%), flow condition (laminar and turbulent), and contact material (PTFE, stainless steel 1.4404) were considered as possible factors influencing biofilm formation in dairy processing. Furthermore, the success of enzymatic cleaning was investigated by applying the procedure after each experimental run. Finally, the correlation coefficients between microbiological methods (viable-cell counting), biochemical methods (ATP-bioluminescence testing), and visual methods (biomass quantification) for biofilm detection in dairy filling hoses were examined. CLSM images complement the understanding of *P. fragi* biofilms on PTFE and stainless steel 1.4404 contact materials.

2. Materials and methods

2.1. Chemicals

Both commercial UHT and pasteurized milk (1.5% of fat, 3.5% of protein, 4.9% of carbohydrates and 3.5% of fat, 3.4% of protein, 4.7% of carbohydrates) were obtained from Molkerei Weihenstephan GmbH & Co. KG (Freising, Germany). Agar agar, plate-count agar, and Safranin O were purchased from Merck (Darmstadt, Germany). Meat extract and yeast extract were supplied by VWR (Darmstadt, Germany). Peptone was obtained from Applichem Panreac (Barcelona, Spain). Tryptone and PBS Buffer were purchased from Amresco (Solon, USA). Hoechst 33342 was provided by the Cayman chemical company (Ann Arbor, USA). Enzy-CIP was obtained from iTram Hygiene (Barcelona, Spain). All the reagents and chemicals used were of analytical grade.

2.2. Experimental set-up

Biofilm formation was investigated on stainless steel 1.4404 (Hernandez Edelstahl GmbH, Germany) and PTFE (Beichler + Grünenwald GmbH, Germany) coupons in a dairy-filling test hose (Aflex Hose Ltd., West Yorkshire, UK). The average roughness and the largest single roughness depth within the evaluation length, R_a and R_{max}, of PTFE were 0.211 μm and 3.110 μm, respectively; those of stainless steel 1.4404 were 0.269 μm and 3.459 μm, respectively. The values of roughness were smaller than the benchmark of hygienic design for food-contact surfaces ($R_a \leq 0.8$ μm) (EHEDG, 2004). The surface tension of PTFE (hydrophobic nature) was 21.4 mN m^{-1} (Bronislaw Jańczuk, 1990). The surface tension of stainless steel (hydrophilic nature) 1.4404 coupons was determined as 34 mN m^{-1} using test pens containing fluids of defined surface tension (arcotest GmbH, Mönsheim, Germany). Pasteurized milk (polyculture bacterial compositions) and UHT inoculated with *P. fragi* (No. 3456, DSMZ, Braunschweig, Germany) (monoculture bacterial composition) were chosen as dairy-product models. The initial number of viable cells in pasteurized milk was determined as 6.1×10^4 CFU mL^{-1} after storage for 5 days at room temperature. Pasteurized milk had a typical species of thermophilic bacteria that can survive industrial pasteurization process (*Streptococcus* spp., *Bacillus* spp., *Micrococcus* spp.). UHT milk was inoculated with monoculture psychrotrophic Gram-negative bacteria (*P. fragi*) to obtain a comparable number of viable cells of 4.1×10^4 CFU mL^{-1}. The bacterial adhesion was tested with two milk-fat contents of 1.5% and of 3.5%. Dairy-filling test hose type GP/SS/RC NW 3/4″ have a PTFE liner inside the hose, with stainless steel braid 1.4301 and EPDM liner outside the hose. The inlet hose connector was manufactured of stainless steel 1.4404 according to DIN 11864-1 Form A. For laminar flow, a peristaltic pump (Multifix, Germany) was selected. An impeller pump (Zuwa, Germany) was chosen for turbulent flow. The flow conditions in the dairy-filling test hose were selected as laminar (Re = 229 ± 8) and turbulent (Re = 7276 ± 251) with volumetric flow rates of 472 cm^3 min^{-1} and 1500 cm^3 min^{-1}, respectively. Wall-shear stress for laminar and turbulent flow were determined as 0.084 ± 0.002 Pa and 12.9 ± 0.2 Pa. The hoses and connecting elements were autoclaved before each run. The experimental set up was assembled under sterile conditions. The sterile-material test sheets were inserted manually with sterile tweezers into the autoclaved filling hose. 2000 mL of prepared milk representing a dairy-product model were used to fill the laboratory bottle (Schott, Germany). The prepared milk was pumped in a closed loop for 6 h at 5.5 ± 0.5 °C. After the experiment, the biofilm formation was evaluated using three test methods. In addition, an enzymatic-cleaning method was applied to the test filling hose after the experimental run. According to the manufacturer (iTram, Spain), the cleaning agent that was used for enzymatic treatment of CIP systems consisted of a concentrated blend of enzymes (containing 1 < 2.5% Subtilisin, 1 < 2.5% α-amylase) and a non-

foaming detergent. Each experiment was replicated three times.

2.3. Bacterial-suspension preparation for dairy-product model with monocultural bacterial composition

For each suspension, one colony of *P. fragi* was taken from the agar plate (plate count agar) with an inoculation loop and suspended in 100 mL of nutrient medium. The suspension was incubated at 26 °C under shaking at 100 rpm. The growth curve was evaluated using the correlation between the transmission and the number of colony-forming units (CFUs) (Pepper and Gerba, 2005). Samples for the plate-count method for CFU counting were taken every 30 minutes, together with transmission measurement (LLG—uni SPEC Primelab 1.0, Klettgau, Germany) of the samples. For the plate-count method, dilutions of suspensions up to 10^{-4} were prepared. 100 μL of each dilution were plated on agar nutrient plates and incubated at 26 °C for 3 days. After 3 days of incubation, the number of colonies was counted and expressed in CFU mL^{-1}. The transmission of the suspension was measured at 570 nm and expressed as an optical density (OD). The relationship between transmission and optical density is described as $OD = -\log T = \log\left(\frac{1}{T}\right)$, where *OD* is optical density and *T* represents the transmission. The relation between the optical density and the cell count is expressed as $N = k \times OD$, where *N* is number of viable cells and *k* is a coefficient determined from the correlation between the transmission, *T*, and the viable cell count, CFU (mL^{-1}), of the exponential-growth phase. A bacterial suspension of *P. fragi* was prepared for the experiments with UHT milk in order to obtain a monoculture bacterial composition. A bacterial suspension from the exponential phase with OD at about 0.05–0.07 was added at a ratio of 1:100 to UHT milk and mixed for 1 min.

2.4. Characterization methods

2.4.1. Counting of colony-forming units

The test sheets were taken from the test hose with a sterile tweezer and put in 10 mL of 0.1% sterile peptone water. The biofilm was removed from the surface by vortexing of the solution with the material test sheet for 5 min. Serial log dilutions were prepared by delivering 100 μL of the stock solution into 900 μL of peptone water and mixing again. This was repeated two times with the prepared dilution, such that dilution factors of 10^{-1}–10^{-4} were constituted. 10 μL of each dilution were spread on an agar count plate with a sterile inoculation loop incubated over night at 30 °C. The colony-forming units were measured in relation to the surface area of the test sheets and calculated by applying the following relationship: $^{CFU}/_{cm^2} = N \times \frac{1}{Dilution} \times 1/Couponsurfacearea \times Scrapedvolume$, where *N* is the number of colonies growing on the agar plate, *Coupon surface area* is the investigated coupon surface area, and *Scraped volume* refers to the first volume of the scraped and diluted deposit in 0.1% sterile peptone water, before serial log dilutions (Lewandowski and Beyenal, 2014).

2.4.2. ATP-bioluminescence assay

An ATP-bioluminescence test was carried out using an ATP + AMP hygiene-monitoring test kit. The test kit was purchased from the Kikkoman Corporation, and comprises a Lumitester™ PD-30 and a LuciPac™ Pen. The material test sheets were taken from the hose with a sterile tweezer and immersed in PBS buffer solution for a few seconds. The swab stick of the LuciPac™ Pen then was wiped with constant pressure over the coupons surface of 1 cm^2. The swab stick was pushed into the container to release the reagent to dissolve the luminescent reagent. The test stick was put in the Lumitester™ PD-30 and the measurement was carried out within 10 s. The result of ATP-bioluminescence assay was expressed in relative light units (RLU/cm^2).

2.4.3. Quantification of biomass by staining

Biomass on the material test sheets was detected visually using aqueous washing and dye solutions. After 6 h, the material test sheets were removed from the hose and immersed with an aqueous washing solution (0.726 g L^{-1} sodium hydrogen phosphate, 9.0 g L^{-1} NaCl, 0.21 g L^{-1} potassium hydrogen phosphate) for two minutes. Then, the sheets were placed in a dye solution (0.01% Safranin O aqueous solution) for 15 min to stain the biofilm and washed with aqueous solution again. The intensity of staining and the amount of the corresponding biomass was detected by comparison with a reference scale obtained according to the manufacturer (Breves et al., 2004).

2.4.4. Confocal-laser scanning microscopy

Confocal-laser scanning microscopy (CLSM) of test sheet with the deposit was carried out using a Nikon Eclipse-C1. The material test sheets (stainless steel 1.4404 and PTFE) were removed from the test hose and rinsed with PBS buffer solution. 10 μL of Hoechst 33342 dye solution (Roldán et al., 2004; Flemming et al., 2000) were added to the material test sheets. 10 min after staining, the samples were observed at magnifications of 60× with oil. Microscope settings were controlled with Nikon-ECZ1 software (Nikon GmbH, Düsseldorf, Germany). The temperature of the samples was kept constant at 10 °C by a water-cooled tempering unit.

2.5. Statistical analysis

The statistical analysis was carried out using the software Cornerstone 5.3.05 (CamLine, Dresden, Germany). The results of biofilm detection are averages of three independent experiments performed for each combination of factors (bacterial composition, fat content, flow conditions, and material type). Mean value, standard deviation, normal distribution (Shapiro–Wilk test, $p \leq 0.05$), and outlier testing (Dixon's test, $p \leq 0.05$) were calculated for all responses. A paired-sample *t*-test was used to evaluate significant differences between factor groups at different significance levels ($p \leq 0.1$). In addition, Pearson-correlation coefficients were obtained to demonstrate the correlation of the analytical methods for biofilm detection ($p < 0.05$).

3. Results and discussion

3.1. Evaluation of biofilm formation in a dairy-filling test hose

In this work, investigation of biofilms in dairy-filling test hose was performed under different experimental conditions in terms of bacterial composition, food-contact-surface materials, fat content of the milk, and flow conditions. Each factor was studied at 2 levels, which correspond the selected boundary conditions for the dairy filling process. Table 1 shows the results for various response-detection methods (viable-cell counting, ATP-bioluminescence testing, and biomass mea-

Table 1 – Results of biofilm formation on the material-test-sheet surface (PTFE and stainless steel 1.4404) in a dairy-filling hose under different conditions using viable-cell counting, ATP-bioluminescence testing, and biomass quantification (i = 3; n = 9).

Bacterial composition (–)	Material (–)	Fat content (%)	Flow (–)	Viable cells counting (log CFU cm^{-2})		ATP-bioluminescence (log RLU cm^{-2})		Biomass (mg cm^{-2})	
				Mean	SD	Mean	SD	Mean	SD
Monoculture	PTFE	3.5	L	6.9e+1	1.8e+1	9.5e+2	3.0e+2	2.33	0.58
Monoculture	Steel	3.5	L	2.3e+1	2.0e+1	5.2e+2	2.2e+2	2.00	0.00
Monoculture	PTFE	1.5	L	1.0e+2	7.0e+1	1.0e+3	7.7e+1	2.50	0.50
Monoculture	Steel	1.5	L	2.7e+1	1.8e+1	6.1e+2	9.7e+1	1.17	0.29
Monoculture	PTFE	1.5	T	1.0e+2	3.6e+1	9.3e+2	3.0e+2	1.50	0.50
Monoculture	Steel	1.5	T	2.3e+1	2.1e+1	7.4e+2	3.3e+2	0.50	0.00
Monoculture	PTFE	3.5	T	9.0e+1	3.8e+1	6.4e+2	7.6e+0	1.83	0.29
Monoculture	Steel	3.5	T	1.2e+1	1.8e+1	7.2e+2	1.6e+1	0.67	0.29
Polyculture	PTFE	3.5	L	2.3e+1	1.6e+1	8.8e+2	1.7e+2	3.67	0.76
Polyculture	Steel	3.5	L	2.4e+1	9.5e+0	6.8e+2	8.2e+1	1.83	0.29
Polyculture	PTFE	1.5	L	4.9e+1	3.7e+1	1.0e+3	1.1e+2	3.00	0.50
Polyculture	Steel	1.5	L	2.4e+1	1.1e+1	8.1e+2	3.1e+2	1.17	0.29
Polyculture	PTFE	1.5	T	3.8e+1	2.3e+1	5.1e+2	2.1e+2	1.67	0.29
Polyculture	Steel	1.5	T	2.0e+1	1.6e+1	4.9e+2	9.2e+1	1.00	0.00
Polyculture	PTFE	3.5	T	3.3e+1	5.3e+1	4.8e+2	1.1e+2	1.33	0.29
Polyculture	Steel	3.5	T	1.6e+1	1.5e+1	5.7e+2	1.6e+2	0.67	0.29

Values shown as mean ± SD (standard deviation); i indicates the number of sample preparations, n indicates total number of measurements; monoculture indicates UHT milk (ultra-high temperature processed milk) with *P. fragi*, polyculture indicates pasteurized milk; steel indicates stainless steel 1.4404; T corresponds to turbulent flow condition (Re > 4000), L corresponds to laminar flow condition (Re < 2300).

surement) for biofilm formation under various experimental conditions.

According to Table 1, the mean values of the viable-cell count range from 12 CFU cm^{-2} (stainless-steel surface under turbulent-flow conditions for 3.5% fat monoculture) to 103 CFU cm^{-2} (PTFE surface under turbulent-flow conditions for 1.5% fat monoculture). The mean values of the ATP-bioluminescence test are distributed between 491 RLU cm^{-2} (stainless-steel surface under turbulent-flow conditions for 3.5% fat polyculture) and 1032 RLU cm^{-2} (PTFE surface under laminar-flow conditions for 1.5% fat polyculture). The results of visual biomass detection range from 0.5 mg cm^{-2} (stainless-steel surface under turbulent-flow conditions for 1.5% fat monoculture) to 3.67 mg cm^{-2} (PTFE surface under laminar-flow conditions for 3.5% fat polyculture). As follows from results shown in Table 1, clear dependences between the experimental parameters and the results cannot be easily found by simply comparing the data. However, analysing the results, there are some trends showing distinct biofilm formation of monoculture (*P. fragi*) and polyculture bacteria on stainless steel and PTFE. For better overview of the result, the reader is referred to Figs. 1 and 2.

Fig. 1 shows the number of colony forming units of eight samples with polyculture or monoculture bacterial composition. It can been seen that bacterial compositions of milk affect the number of viable cells on a surface, showing higher adhesion for monoculture-bacterial composition (*P. fragi*) on PTFE surfaces compared to stainless steel surfaces.

For ATP-bioluminescence, no clear influence of the selected factors can be seen, due to the wide distribution of the interquartile ranges. In addition, the influence of flow conditions and material type on biomass formation is plotted on Fig. 2A and B.

Fig. 2A and B show the biomass of eight samples obtained under turbulent and laminar flow as well as on stainless steel and PTFE test sheets, respectively. Turbulent flow conditions lead to the decrease in biomass compared to laminar flow for all samples. Conversely, laminar flow contributed to greater biomass formation (Fig. 2A). Also, the type of material affects the biomass, with greater biomass formation on PTFE that on stainless steel for all samples (Fig. 2B).

To find significant differences between groups of experimental parameters (bacterial composition, material type fat content, and flow conditions), a paired-sample *t*-test was conducted. The differences between PTFE and stainless steel 1.4404 estimated with the viable-cell-counting method are significant ($p \leq 0.01$). The differences between monoculture and polyculture, and at fat contents of 1.5% and 3.5% are also significant at $p \leq 0.05$. The results obtained using the ATP-bioluminescence test do not show differences between polyculture and monoculture. However, groups of other factors (fat content, flow condition, and material type) differ with $p \leq 0.1$. The results of biomass quantification are significantly influenced by flow condition and material type ($p \leq 0.001$).

Summarizing the results of biofilm formation (Table 1) and the paired-sample *t*-test, the number of viable cells in the dairy-filling hose of the processing equipment after 6 h run can be significantly influenced by material type, bacterial composition, and fat content of milk. ATP-bioluminescence seems to be influenced by material type; fat content, and flow condition, however, further evaluation is required, because parameters only have a significance level of $p \leq 0.1$. Biomass formation differs between materials – PTFE and stainless steel 1.4404, and also between flow conditions – laminar and turbulent.

The effect of the material hydrophobicity on the bacteria attachment has been discussed in previous work (Lewandowski and Beyenal, 2014). The studies showed higher bacterial adhesion on hydrophobic surfaces than on hydrophilic ones. The small hydrophobic areas present on the surfaces of bacterial cells are responsible for the adherence of bacteria to hydrophobic surfaces. However, here are conflicting views, as only small parts of microbial cells (i.e., pili, fimbriae, and flagella) are hydrophobic (Bonsaglia et al., 2014). Despite many studies on the relation among hydrophobicity,

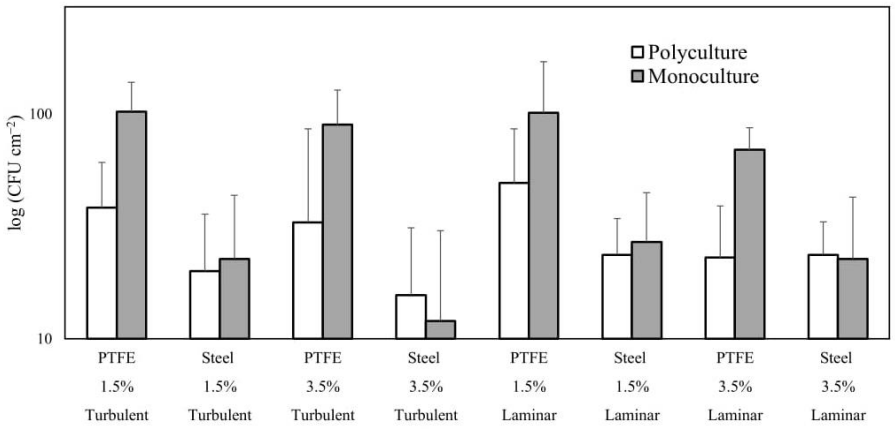

Fig. 1 – Number of colony forming units of eight samples obtained with polyculture (white bars) and monoculture (grey bars) bacterial composition under three different experimental parameters: material type — PTFE and stainless steel; fat content — 1.5% and 3.5%; flow conditions — laminar and turbulent.

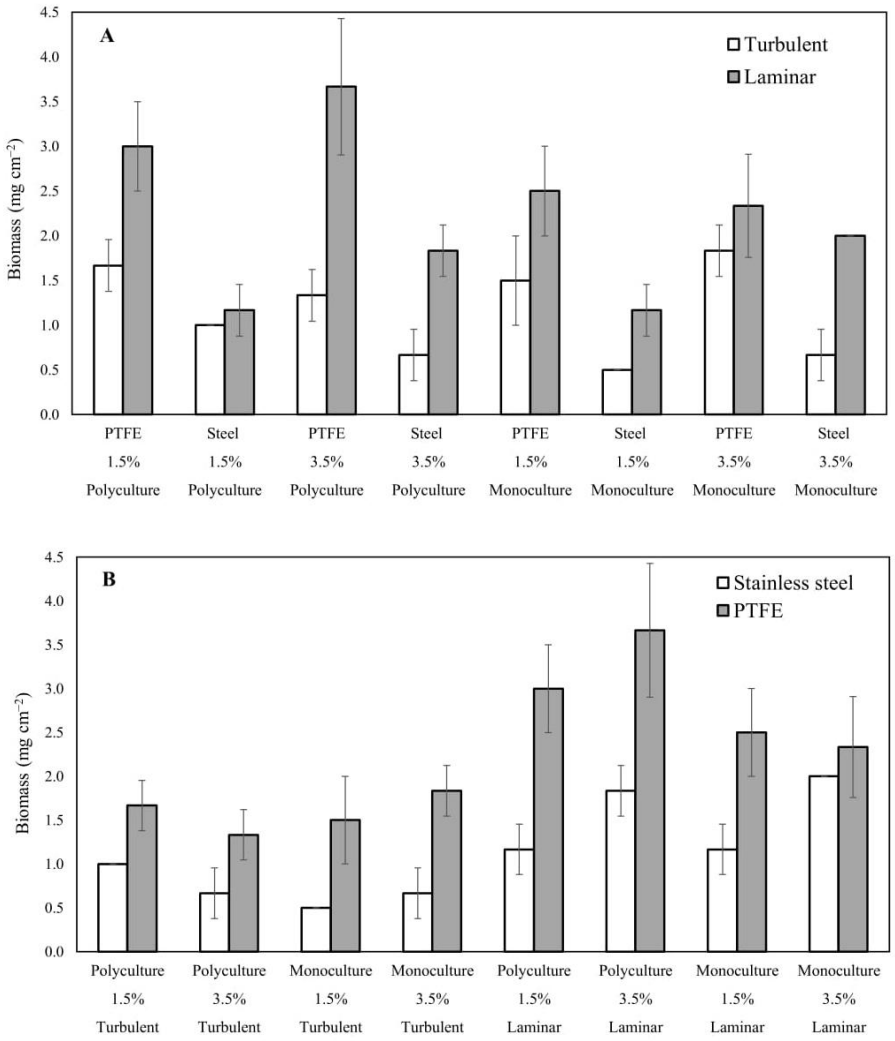

Fig. 2 – Biomass quantification of eight samples obtained (A) under turbulent and laminar flow with three different experimental parameters: material type — PTFE and stainless steel; fat content — 1.5% and 3.5%; bacterial composition — monoculture and polyculture; (B) for stainless steel and PTFE test sheets under three different experimental parameters: bacterial composition — monoculture and polyculture; fat content — 1.5% and 3.5%; flow conditions — laminar and turbulent.

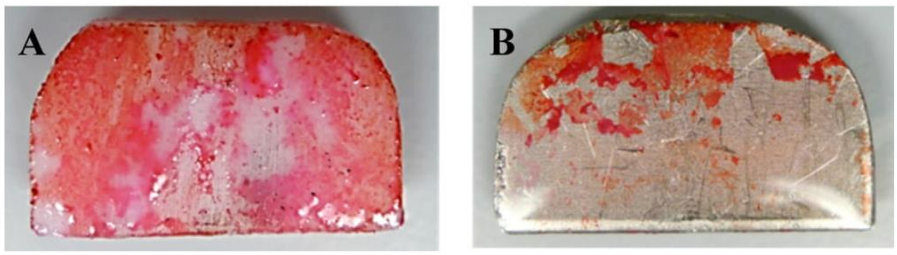

Fig. 3 – Images of PTFE (A) and stainless-steel-1.4404 (B) test sheets inserted into the experimental setup for 28 h and stained by 0.01% Safranin O solution for biomass quantification.

surface energy, and the initial attachment of bacteria, the relation remains unclear: bacteria can colonize both hydrophobic and hydrophilic surfaces (Lewandowski and Beyenal, 2014). Biofilm formation can be affected by bacterial composition. Biofilms with more than one species (polyculture) can lead to changing results, as it has been reported that several strains appear to adhere in monocultures rather than in polyculture biofilms (Norwood and Gilmour, 2001). As reported in the literature, the fat content does not significantly influence biofilm formation (Gaspar-Rolle, 1991). Nevertheless, it has also been suggested that higher fat contents might cause increased microorganism adherence (Speers and Gilmour, 1985).

Flow conditions have been reported to significantly affect the biofilm formation, with lower rates shown under turbulent flow (Marchand et al., 2012; Srey et al., 2013). It was described that biofilm thickness reach a maximum in the transition zone from laminar flow to turbulent flow (Lewandowski and Beyenal, 2014). It can be explained that biofilm development was limited in the laminar flow zone by the mass transport of the growth-limiting nutrients and in the turbulent flow zone by the shear stress. Moreover, the relations between factors and biofilm formation may depend on time and temperature (Latorre et al., 2010). In this study, these factors were kept constant.

3.2. *Visualization of the biofilm*

Fig. 3 shows the PTFE and the stainless-steel-1.4404 test sheets, which were inserted into the experimental set up to elucidate the difference between the materials.

On both coupons, the stained biomass is clearly visible. However, the color intensity and distribution of the biofilm on the stainless-steel test sheet are less remarkable than that on the PTFE test sheet. This result agrees with (Fig. 2B), where biofilm formation on the PTFE surface is more pronounced than on the stainless-steel surface. Also, both PTFE and stainless steel were investigated using images obtained by confocal-laser scanning microscopy.

CLSM images were taken of material test sheets incubated in nutrient medium and *P. fragi* at 20 °C for 2 days. Samples were treated with Hoechst 33342, which stains the DNA of cells (Roldán et al., 2004). Considering Fig. 4A and B, the biofilm formed on the PTFE test sheet shows a higher number of bacterial cell clusters than that on the stainless-steel sheet. On the steel surface, cell clusters were not well formed, but many individual cells were observed. Some studies have found that higher numbers of bacteria attach to hydrophobic surfaces, such as PTFE, than to hydrophilic surfaces, such as stainless steel or glass (Hyde et al., 1997; Teixeira et al., 2005; Pasmore et al., 2010). Bacteria that attach to hydrophobic materials tend to form clusters (McEldowney and Fletcher, 1987). Therefore, the hydrophobicity and surface energy of different materials plays an important role in the processing of liquid products and the cleaning procedures for the apparatus (Chmielewski and Frank, 2003).

3.3. *Correlation of the measurement methods*

In different studies, viable-cell counting, ATP-bioluminescence testing, and biomass measurement have been applied to investigate biofilm formation in dairy-industry filling processes (Denkhaus et al., 2007). In this work, these methods for biofilm measurement are compared. The correlations of the results of the various methods have been determined in all cases (i = 16). All methods showed weak positive correlation. The highest positive Pearson correlation was obtained between the ATP-bioluminescence and biomass results (0.550). The correlation between the ATP-bioluminescence and viable-cell-counting results was 0.539, while the lowest correlation was found between viable-cell counting and biomass detection (0.345). The highest correlation between the ATP-bioluminescence and biomass-measurement methods can be explained in that both methods can detect the food residuals, also called deposits, whereas viable-cell counting, by definition, only detects viable cells.

These results show that each chosen method characterizes specific properties of the biofilm (e.g., counting viable cells can estimate only the number of CFUs). Thus, depending upon the chosen method, different characteristics of the biofilms can be detected. However, literature studies describing the correlation between ATP-bioluminescence and visual biomass detection have not been found. As has been reported, ATP-bioluminescence testing can detects all organic matter on food-contact surfaces and can thus be used to obtain important information concerning biofilm formation, as bacterial adherence might be supported by nutrients on the food-contact surface (Bell et al., 1996; Costa et al., 2006). The correlation between the measurement results obtained by viable-cell counting and ATP-bioluminescence testing in this study is in accordance with the literature (Costa et al., 2006). The linear relationship between ATP testing and viable-cell counting has been reported by several studies (Bell et al., 1996; Bottari et al., 2015). Nevertheless, since the ratio of microbial cells to food debris is not constant, these methods are not well coordinated. For example, a high amount of ATP and a low microbial count can be detected in UHT milk (Costa et al., 2006). Similar restrictions and constraints on the sensitivity of ATP-bioluminescence testing have been found in the literature due to relatively poor detection of Gram-negative bacteria because of incomplete cell lysis by an ATP test (Bell et al., 1996; Ninios et al., 2014). Further limitations on the viable-

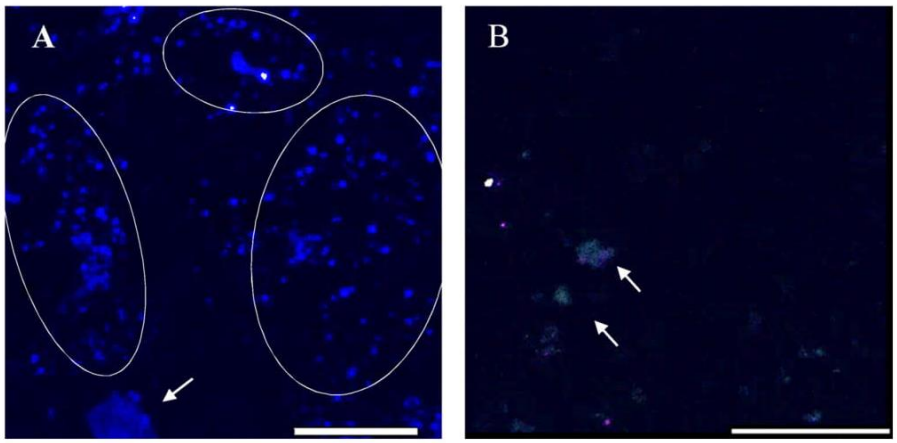

Fig. 4 – Confocal-laser scanning microscopy (CLSM) images of *P. fragi* biofilm in a nutrient medium on PTFE (A) and stainless-steel (B) surfaces incubated for 2 days at 20 °C and stained with Hoechst 33342. The magnification is 60× with an oil objective (the white bar is equivalent to 20 μm).

Table 2 – Results of ATP-bioluminescence testing before and after enzymatic-cleaning treatment of the PTFE-hose liner in the dairy-filling hose (i = 3; n = 9).

Bacterial composition (–)	Fat content (%)	Flow (–)	ATP-bioluminescence (RLU cm^{-2})				Log reduction of ATP-bioluminescence	
			Before cleaning		After cleaning			
			Mean	SD	Mean	SD	Mean	SD
UHT + *P. fragi*	1.5	T	929.3	241.9	21.1	11.3	1.697	0.19
UHT + *P. fragi*	3.5	T	639.5	6.4	15.7	10.6	1.722	0.33
UHT + *P. fragi*	1.5	L	1013.2	62.8	11.7	5.1	1.975	0.16
UHT + *P. fragi*	3.5	L	948.3	243.6	25.1	17.8	1.705	0.28
Pasteurized milk	1.5	T	514.0	174.8	18.8	10.8	1.470	0.2
Pasteurized milk	3.5	T	484.1	91.4	14.3	7.7	1.621	0.2
Pasteurized milk	3.5	L	876.2	136.0	12.3	12.0	2.073	0.4
Pasteurized milk	1.5	L	1031.7	92.0	22.8	20.7	1.841	0.4

Values shown as mean ± SD (standard deviation); i indicates the number of sample preparations, n indicates total number of measurements; steel refers to stainless steel 1.4404; T corresponds to turbulent flow, L corresponds to laminar flow.

cell-count method include time delay due to incubation and several constraints that underestimate the actual population inside the biofilm (Bell et al., 1996). It must also be mentioned that the comparison with a reference scale for the biomass-detection method can lead in some cases to subjective results. Nevertheless, the staining method leads to fast results that can suggest the biofilm-formation behaviour in relation to the surface material and other parameters.

3.4. *Enzymatic cleaning of the PTFE-hose liner*

The PTFE-hose liner in the dairy-filling hose was cleaned using enzymatic treatment. After each experiment, the cleaning success was investigated using ATP-bioluminescence testing. ATP-bioluminescence results before and after cleaning are presented in Table 2.

Table 2 shows the ATP-bioluminescence results in RLU cm^{-2} measured on the PTFE liner of the dairy-filling-hose hose before and after 6 h of the experimental run. For all results, significant decreases of ATP bioluminescence before and after enzymatic cleaning are observed ($p \leq 0.05$). The results of all runs after cleaning do not significantly differ. The benchmark for resin surface of 500 RLU after cleaning was not exceeded while the ATP values before cleaning were higher than the benchmark recommended by manufacturer. According to the recommendations of the ATP-bioluminescence-test manufacturer, measurements of resin surfaces lower than 500 RLU are considered clean, those from 500 to 1000 RLU are considered suspect, and those higher than 1000 RLU are considered inadequate for hygiene. To summarize the results, enzymatic-cleaning agent containing enzymes protease and α-amylase in combination with non-foaming detergents showed a sufficient cleaning effect for dairy processing equipment.

Several studies have reported good cleaning results using of enzymatic agents (Marchand et al., 2012; Austin and Bergeron, 1995). The efficiency of enzymatic cleaning depends upon the biofilm composition and on the enzymes applied, because the mechanism of enzymatic cleaning is based on destruction of the EPS structure by weakening the proteins, carbohydrates, and lipids (Molobela et al., 2010). Because of the diversity of the biofilm composition and the specificity in the enzymes' mode of action, a mixture of several enzymes, particularly different proteases and polysaccharide-hydrolysing enzymes, could lead to successful degradation of a biofilm (Simões et al., 2010).

4. Conclusion

Biofilms on processing equipment can cause serious problems in the dairy industry. This study investigated the influence of factors affecting biofilm formation on dairy-filling test hose.

Bacterial composition (monoculture *P. fragi* and polyculture), fat content of milk (1.5% and 3.5%), flow condition (laminar and turbulent), and contact material (PTFE and stainless steel 1.4404) were investigated as possible factors. It was found that bacterial composition, material type, and fat content significantly affected the results of viable-cell counting. Flow conditions and material type both had significant impacts upon biomass quantification. For ATP-bioluminescence, no clear influence of the selected factors can be seen, due to the wide distribution of the interquartile ranges. The results suggest that bacterial biofilm is of concern in filling units of dairy-processing equipment at low temperature. In addition, investigated methods showed weak Pearson positive correlation. From the results obtained in this study, it can be concluded that by knowing the type of deposit expected according to the product being processed, suitable methods for biofilm detection in dairy equipment should be chosen. Nevertheless, this study must be supplemented with further investigation of other parameters, such as higher temperatures being used to simulate thermal processing of dairy products. Further investigation of the effects of cleaning agents containing enzymes for specific biofilms is also needed.

Acknowledgments

This research did not receive any specific grant from funding agencies in the public, commercial, or not-for-profit sectors. The authors thank Dr. Holger Brehm for proof reading and Dr. Johannes Rauschnabel for beneficial discussion.

References

Austin, J.W., Bergeron, G., 1995. Development of bacterial biofilms in dairy processing lines. J. Dairy Res. 62 (3), 509–519.

Barnes, L.M., Lo, M.F., Adams, M.R., Chamberlain, A.H., 1999. Effect of milk proteins on adhesion of bacteria to stainless steel surfaces. Appl. Environ. Microbiol. 65 (10), 4543–4548.

Bell, C., Bowles, C.D., Toszeghy, M.J.K., Neaves, P., 1996. Development of a hygiene standard for raw milk based on the Lumac ATP-bioluminescence method. Int. Dairy J. 6 (7), 709–713, http://dx.doi.org/10.1016/0958-6946(96)00007-6.

Bonsaglia, E.C.R., Silva, N.C.C., Fernades Júnior, A., Araújo Júnior, J.P., Tsunemi, M.H., Rall, V.L.M., 2014. Production of biofilm by *Listeria monocytogenes* in different materials and temperatures. Food Control 35 (1), 386–391, http://dx.doi.org/10.1016/j.foodcont.2013.07.023.

Bottari, B., Santarelli, M., Neviani, E., 2015. Determination of microbial load for different beverages and foodstuff by assessment of intracellular ATP. Trends Food Sci. Technol. 44 (1), 36–48, http://dx.doi.org/10.1016/j.tifs.2015.02.012.

Bower, C.K., McGuire, J., Daeschel, M.A., 1996. The adhesion and detachment of bacteria and spores on food-contact surfaces. Trends Food Sci. Technol. 7 (5), 152–157, http://dx.doi.org/10.1016/0924-2244(96)81255-6.

Bremer, P.J., Fillery, S., McQuillan, A.J., 2006. Laboratory scale Clean-In-Place (CIP) studies on the effectiveness of different caustic and acid wash steps on the removal of dairy biofilms. Int. J. Food Microbiol. 106 (3), 254–262, http://dx.doi.org/10.1016/j.ijfoodmicro.2005.07.004.

Breves, R., Janssen, F., Hater, W., Gomes, M.P.J., 2004. Method of measuring and controlling the formation of biofilms in a watersystem. Applied for by Henkel Kommanditgesellschaft auf Aktien. Patent no. EP1491505 A1.

Jańczuk, T.B., 1990. The total surface free energy and the contact angle in the case of low energetic solids. J. Colloid Interface Sci. 140 (2), 362–372.

Cappitelli, F., Polo, A., Villa, F., 2014. Biofilm formation in food processing environments is still poorly understood and controlled. Food Eng. Rev. 6 (1–2), 29–42, http://dx.doi.org/10.1007/s12393-014-9077-8.

Chmielewski, R.A.N., Frank, J.F., 2003. Biofilm formation and control in food processing facilities. Comp. Rev. Food Sci. Food Safety 2, 22–32, http://dx.doi.org/10.1111/j.1541-4337.2003.tb00012.x.

Costa, P.D., Andrade, N.J., Soares, N.F.F., Passos, F.J.V., Brandão, S.C.C., 2006. ATP-bioluminescence assay as an alternative for hygiene-monitoring procedures of stainless steel milk contact surfaces. Braz. J. Microbiol. 37 (3), 345–349, http://dx.doi.org/10.1590/S1517-83822006000300026.

Cousin, M.A., 1982. Presence and activity of psychroptrophic microorganisms in milk ansd dairy products: a review. J. Food Prot. 45 (2), 172–207.

De Jonghe, V., Coorevits, A., Van Hoorde, K., Messens, W., Van Landschoot, A., De Vos, P., Heyndrickx, M., 2011. Influence of storage conditions on the growth of *pseudomonas* species in refrigerated raw milk. Appl. Environ. Microbiol. 77 (2), 460–470.

Denkhaus, E., Meisen, S., Telgheder, U., Wingender, J., 2007. Chemical and physical methods for characterisation of biofilms. Microchim. Acta 158, 1–27.

EHEDG, 2004. EHEDG Guidlines: Doc 8 Hygienic Equipment Design Criteria. With assistance of N. S.F. 3-A, 2nd ed.

Eneroth, Å, Christiansson, A., Brendehaug, J., Molin, G., 1998. Critical contamination sites in the production line of pasteurised milk, with reference to the psychrotrophic spoilage flora. Int. Dairy J. 8 (9), 829–834, http://dx.doi.org/10.1016/S0958-6946(98)00123-X.

Eneroth, Å, Ahrné, S., Molin, G., 2000. Contamination of milk with Gram-negative spoilage bacteria during filling of retail containers. Int. J. Food Microbiol. 57 (1–2), 99–106, http://dx.doi.org/10.1016/S0168-1605(00)00239-7.

Flemming, H.-C., Szewzyk, U., Griebe, T., 2000. In: Flemming, Hans-Curt, Szewzyk, Ulrich, Griebe, Thomas (Eds.), Biofilms: Investigative Methods & Applications. Technomic Pub. Co., Lancaster, PA.

Flint, S.H., Bremer, P.J., Brooks, J.D., 1997. Biofilms in dairy manufacturing plant-description, current concerns and methods of control. Biofouling 11 (1), 81–97, http://dx.doi.org/10.1080/08927019709378321.

Fratamico, P.M., Annous, B.A., Gunther, N.W., 2009. Biofilms in the Food and Beverage Industries. CRC Press (Woodhead publishing in food science, technology, and nutrition), Boca Raton.

Gaspar-Rolle, M. N. Pinto, 1991. Attachment of Bacteria to Teflon and Buna-n-rubber Gasket Materials. Doctoral Dissertation. Virginia Tech.

Hood, S.K., Zottola, E.A., 1997. Adherence to stainless steel by foodborne microorganisms during growth in model food systems. Int. J. Food Microbiol. 37 (2–3), 145–153, http://dx.doi.org/10.1016/S0168-1605(97)00071-8.

Hyde, F.W., Alberg, M., Smith, K., 1997. Comparison of fluorinated polymers against stainless steel, glass and polypropylene in microbial biofilm adherence and removal. J. Ind. Microbiol. Biotechnol. 19 (2), 142–149.

Kessler H.G. (2006) *Lebensmittel- und Bioverfahrenstechnik: Molkereitechnologie, 4th edn*. München: Verl. A. Kessler.

Latorre, A.A., Van Kessel, J.S., Karns, J.S., Zurakowski, M.J., Pradhan, A.K., Boor, K.J., Jayarao, B.M., Houser, B.A., Daugherty, C.S., Schukken, Y.H., 2010. Biofilm in milking equipment on a dairy farm as a potential source of bulk tank milk contamination with *Listeria monocytogenes*. J. Dairy Sci. 93 (6), 2792–2802, http://dx.doi.org/10.3168/jds.2009-2717.

Lewandowski, Z., Beyenal, H., 2014. Fundamentals of Biofilm Research, 2nd ed. CRC Press Taylor & Francis Group, Boca Raton.

Marchand, S., De Block, J., De Jonghe, V., Coorevits, A., Heyndrickx, M., Herman, L., 2012. Biofilm formation in milk production and processing environments; influence on milk quality and safety. Compr. Rev. Food Sci. Food Saf. 11 (2), 133–147, http://dx.doi.org/10.1111/j.1541-4337.2011.00183.x.

Marchand, S., Heylen, K., Messens, W., Coudijzer, K., De Vos, P., Dewettinck, K., Herman, L., 2009. *Pseudomonas lundensis* and

Pseudomonas fragi, Seasonal influence on heat-resistant proteolytic capacity of Pseudomonas lundensis and Pseudomonas fragi, predominant milk spoilers isolated from Belgian raw milk samples. Environ. Microbiol. 11 (2), 467–482, http://dx.doi.org/10.1111/j.1462-2920.2008.01785.x.

McEldowney, S., Fletcher, M., 1987. Adhesion of bacteria from mixed cell suspension to solid surfaces. Arch. Microbiol. 148 (1), 57–62.

Verordnung über Hygiene- und Qualitätanforderungen an Milch und Erzeugnisse auf Milchbasis (Milchverordnung: Bundesgesetzblatt Jahrgang 2000 Teil 1 Nr. 39, S. 1178 vom 31. Juli 2000, Bonn, 2000.).

Mogha, K.V., 2014. Biofilm — a threat to dairy industry. Review article. Indian J. Dairy Sci. 67 (6).

Molobela, P., Cloete, T.E., Beukes, M., 2010. Protease and amylase enzymes for biofilm removal and degradation of extracellular polymeric substances (EPS) produced by *Pseudomonas fluorescens* bacteria. Afr. J. Microbiol. Res. 4 (14), 1515–1524.

Ninios, T., Lundén, J., Korkeala, H., Fredriksson-Ahomaa, M., 2014. Meat Inspection and Control in the Slaughterhouse. John Wiley & Sons Inc., Chichester, West Sussex, UK.

Norwood, D.E., Gilmour, A., 2001. The differential adherence capabilities of two *Listeria monocytogenes* strains in monoculture and multispecies biofilms as a function of temperature. Lett. Appl. Microbiol. 33 (4), 320–324, http://dx.doi.org/10.1046/j.1472-765X.2001.01004.x.

Pasmore, M., Todd, P., Pfiefer, B., Rhodes, M., Bowman, C.N., 2010. Effect of polymer surface properties on the reversibility of attachment of *Pseudomonas aeruginosa* in the early stages of biofilm development. Biofouling 18 (1), 65–71, http://dx.doi.org/10.1080/08927010290017743.

Pepper, I.L., Gerba, C.P., 2005. Environmental Microbiology. A laboratory manual, 2nd ed. Elsevier Academic Press, Amsterdam, Boston.

Pereira, M.O., Kuehn, M., Wuertz, S., Neu, T., Melo, L.F., 2002. Effect of flow regime on the architecture of a *Pseudomonas fluorescens* biofilm. Biotechnol. Bioeng. 78 (2), 164–171, http://dx.doi.org/10.1002/bit.10189.

Roldán, M., Clavero, E., Castel, S., Hernández-Mariné, M., 2004. Biofilms fluorescence and image analysis in hypogean monuments research. Algol. Stud. 111 (1), 127–143, http://dx.doi.org/10.1127/1864-1318/2004/0111-0127.

Sørhaug, T., Stepaniak, L., 1997. Psychrotrophs and their enzymes in milk and dairy products. Quality aspects. Trends Food Sci. Technol. 8 (2), 35–41, http://dx.doi.org/10.1016/S0924-2244(97)01006-6.

Sasahara, K., Zottola, E., 1993. Biofilm formation by *Listeria monocytogenes* utilizes a primary colonizing microorganism in flowing systems. J. Food Prot. 56 (12), 1022–1028.

Simões, M., Simões, L.C., Vieira, M.J., 2010. A review of current and emergent biofilm control strategies. LWT – Food Sci. Technol. 43 (4), 573–583, http://dx.doi.org/10.1016/j.lwt.2009.12.008.

Srey, S., Jahid, I.K., Ha, S.D., 2013. Biofilm formation in food industries. A food safety concern. Food Control 31 (2), 572–585, http://dx.doi.org/10.1016/j.foodcont.2012.12.001.

Speers, J.G.S., Gilmour, A., 1985. The influence of milk and milk components on the attachment of bacteria to farm dairy equipment surfaces. J. Appl. Bacteriol. 59 (4), 325–332, http://dx.doi.org/10.1111/j.1365-2672.1985.tb03326.x.

Stone, L.S., Zottola, E.A., 1985. Effect of cleaning and sanitizing on the attachment of *Pseudomonas fragi* to stainnless steel. J. Food Sci. 50, 951–956.

Stoodley, P., Dodds, I., Boyle, J.D., Lappin-Scott, H.M., 1998. Influence of hydrodynamics and nutrients on biofilm structure. J. Appl. Microbiol. 85 (Suppl 1), 19S–28S, http://dx.doi.org/10.1111/j.1365-2672.1998.tb05279.x.

Storgårds, E., Simola, H., Sjöberg, A.-M., Wirtanen, G., 1999. Hygiene of gasket materials used in food processing equipment Part 2. Food Bioprod. Process. 77, 146–155, http://dx.doi.org/10.1205/096030899532295.

Teh, K.H., Flint, S., Palmer, J., Andrewes, P., Bremer, P., Lindsay, D., 2014. Biofilm — an unrecognised source of spoilage enzymes in dairy products? Int. Dairy J. 34 (1), 32–40, http://dx.doi.org/10.1016/j.idairyj.2013.07.002.

Teixeira, P., Lopes, Z., Azeredo, J., Oliveira, R., Vieira, M.J., 2005. Physico-chemical surface characterization of a bacterial population isolated from a milking machine. Food Microbiol. 22 (2–3), 247–251, http://dx.doi.org/10.1016/j.fm.2004.03.010.

Turner, D.E., Daugherity, E.K., Altier, C., Maurer, K.J., 2010. Efficacy and limitations of an ATP-based monitoring system. J. Am. Assoc. Lab. Anim. Sci. 49 (2), 190–195.

2.2 Section 2 Fouling detection using low-field NMR

2.2.1 Publication 3 Biofilm and dairy fouling detection in flexible tubing using low-field NMR

The control of production processes in dairy industry is challenged by fouling formation. It is known that it is difficult to detect fouling deposits in closed systems non-invasively such as flexible tubing in food processing equipment. One of the established non-invasive techniques for the process monitoring is low-field NMR. However, despite extensive low-field NMR studies on process monitoring, the detection of dairy biofouling and fouling in flexible tubing by low-field NMR has not been reported before.

This article describes the use of low-field ^{1}H NMR for the detection of differently structured deposits inside a flexible silicone tubing. The transverse relaxation time of biofilms formed using *Paenibacillus polymyxa*, dairy biofouling, and dairy fouling was obtained and analysed. The results demonstrate that low-field ^{1}H NMR can be used to distinguish between biofilm, dairy biofouling and dairy fouling due to the differences in the relaxation behaviour. In addition, low-field ^{1}H NMR offers the possibility of non-invasive detection of these deposits on inner surface inside the tubing. The comparison between the tested deposits, tubing, and liquid phase in the tubing showed characteristic relaxation behaviour of each component. Based on the results, low-field ^{1}H NMR can be recommended for the monitoring of food related deposit formation *in situ* and in real time. In addition, this article gives an insight into practical implication of low-field ^{1}H NMR in food processing equipment and gives some recommendations for further studies.

Author contributions

Fysun, O., Anzmann, T., Gschwind, P. designed the study. Rauschnabel, J., Kohlus, R. were involved in planning and supervised the work. Fysun, O. contributed to sample preparation and performed the analysis for the NMR data. Anzmann, T. carried out the experiments, collected the data and performed the analysis for the NMR data. Fysun, O. wrote the manuscript. All authors discussed the results and commented on the manuscript. Langowski, H.-C. contributed to the final version of the manuscript.

European Food Research and Technology
https://doi.org/10.1007/s00217-019-03371-4

ORIGINAL PAPER

Biofilm and dairy fouling detection in flexible tubing using low-field NMR

Olga Fysun[1,2,5] · Theresa Anzmann[3] · Peter Gschwind[3] · Johannes Rauschnabel[2] · Reinhard Kohlus[3] · Horst-Christian Langowski[1,4]

Received: 14 May 2019 / Accepted: 14 September 2019

Abstract
Biofilm and dairy fouling formation is difficult to study non-invasively in closed systems such as flexible tubing. Nuclear magnetic resonance (NMR) is considered as a promising non-invasive detection method for different deposits. This study aimed to investigate three deposit models: (1) *Paenibacillus polymyxa* biofilm, (2) dairy biofouling, and (3) dairy fouling, in different experimental set-ups by low-field ^{1}H NMR. The transverse relaxation time T_2 of each component in samples of experimental set-ups was studied. The results show that low-field NMR offers the possibility of qualitatively measuring the selected deposit models and differentiating non-destructively between the tubing and each deposit. The samples in each experimental set-up showed characteristic relaxation behavior of flexible tubing, deposit, and liquid. For the *P. polymyxa* biofilm, longer relaxation times T_2 of about 100 ms were detected, while relaxation times T_2 for dairy biofouling and dairy fouling were in range of 50–60 ms. It was thus concluded that low-field NMR has a great potential for non-invasive detection of deposit formation at practical industrial scales.

Keywords Low-field NMR · *Paenibacillus polymyxa* biofilm · Dairy biofouling · Dairy fouling · Transverse relaxation time

Introduction

In the food industry, there is widespread concern over bacterial biofilm, fouling, and biofouling, which involve the formation of deposits on surfaces of processing equipment [1]. Such deposits formed in different food industry settings are a source of food contamination [2]. Bacterial biofilms are complex multicellular bacterial communities embedded in an extracellular polymeric substance (EPS) matrix, which is produced by bacteria. The EPS matrix confers protection against environmental stress and shear flow, and enhances bacterial resistance to antibiotics and cleaning media. EPS matrix can contain up to 90% bound water, and include polysaccharides, proteins, or extracellular DNA. Biofilm has a heterogeneous structure including bound water, extracellular polymeric substance (EPS) (up to 90% of organic matter), cells, and embedded particles [3, 4]. The biofilm matrix is stabilized by weak intermolecular interactions such as (1) electrostatic interactions, (2) van der Waals forces, and (3) hydrogen bonds to form a stable molecular network [5].

Dairy processing equipment is highly challenged by fouling, which is the deposition of organic substances (e.g., proteins) and biofouling, which is caused by the adhesion of microorganisms to surfaces [6, 7]. The components, which are mainly responsible for fouling in dairy processing equipment, are calcium phosphate and proteins, particularly whey protein. According to the literature [7], there are two types of dairy fouling: Type A—fouling formation caused by thermally unstable proteins. This is dominant at lower temperatures (70–90 °C) and consists of about 60% protein and 40% minerals. Type B—fouling due to calcium phosphate

Olga Fysun and Theresa Anzmann have contributed equally to this work.

✉ Olga Fysun
olga.fysun@bosch.com

1 TUM School of Life Sciences Weihenstephan, Technical University of Munich, Freising, Germany

2 Robert Bosch Packaging Technology GmbH, Waiblingen, Germany

3 Institute of Food Science and Biotechnology, University of Hohenheim, Stuttgart, Germany

4 Fraunhofer Institute for Process Engineering and Packaging IVV, Freising, Germany

5 Present Address: Robert Bosch GmbH, Reutlingen, Germany

Published online: 01 October 2019

deposition. This is dominant at high temperatures (> 110 °C) and consists of less than 20% protein and up to 80% minerals, of which more than 80% is calcium phosphate. In fact, the fouling formation has a strong impact on biofouling development in dairy processing equipment. Prior to bacterial adhesion, organic and inorganic molecules from milk can adsorb to the surface and form a fouling layer. Thus, the concentration of nutrients closer to the surface is higher than that of the liquid phase. Moreover, fouling layers can change physical properties of the food contact surface, leading to the increase of the bacterial attachment [2]. Since milk is a good substrate for bacterial growth, dairy processing equipment has a higher risk of bacterial attachment on surfaces and, as a consequence, biofouling formation. Biofouling formation in food processing equipment is undesirable for food quality and safety of processed foods due to food spoilage. In addition, biofouling may contain pathogenic bacteria, which can lead to the transmission of foodborne illnesses [4]. For example, psychrotolerant sporeformers, specifically *Paenibacillus* spp., are important spoilage bacteria for pasteurized, refrigerated foods, such as liquid milk, due to biofilm formation in production lines. Moreover, *Paenibacillus polymyxa* has been isolated from a number of environments such as farms, raw milk processing equipment, and pasteurized liquid milk plants. *P. polymyxa* bacteria produce a variety of hydrolytic extracellular enzymes such as proteases, lipases, and lecithinases that can cause spoilage of pasteurized milk [8]. Lecithinase activity of *P. polymyxa* in particular is responsible for "bitty cream" defects in milk due to the aggregation of fat globules [9].

Several techniques for detecting deposits in different types of industrial equipment have been reported. Commonly used industrial techniques are heat transfer and pressure drop monitoring. In addition, several research approaches for the real-time detection of biofilms and fouling, such as surface acoustic wave (SAW) [10], electrochemical [11], and thermal pulse sensors [12], have been reported. However, these approaches still fail to provide a complete picture of complex deposits by non-invasive measurements [5].

Nuclear magnetic resonance (NMR) is a technique, in which the magnetic moment of NMR-active nuclei (e.g., ^{1}H) can be analyzed using electromagnetic pulses and applied magnetic fields [13]. The most sensitive NMR nucleus is the proton. Since in biological systems many molecules contain NMR-active protons, these are the most favorable NMR probes for diffusion studies in biofilms [14]. It was reported in previous studies that low-field NMR, a low-cost alternative to high-field NMR, can also be employed as a non-invasive technique to study biofilms [13–15]. Biofilms have been shown to reduce NMR relaxation times of proximal water hydrogens due to intracellular and extracellular water hydrogens associated with the biofilm structure [16].

Owing to the fact that many foods are proton-rich, with protons originating from water, fat, carbohydrates, and proteins for example, a number of NMR applications in food technology have also been reported [17]. The described NMR studies range from investigations focused on specific molecules to studying the physical properties of dairy products. Low-field NMR was used for the study of dairy products and compounds to characterize fat and water in cheese, as well as to investigate the solid fat content in anhydrous milk fat blends [18].

Detection of biofilms by low-field NMR has shown promising results [13, 14, 19, 20]. However, NMR detection of biofilm formation in production lines, such as biofilm caused the psychrotolerant spore former *P. polymyxa*, is still lacking. Moreover, despite many NMR studies of dairy products, the detection of dairy biofouling and fouling in flexible tubing by low-field NMR has not been reported. In addition, the sensitivity of deposit detection using NMR still requires detailed exploration. For instance, it was reported that biofilm was detected at film thicknesses of about 300 µm; however, for actual conditions in the dairy industry, biofilms should be detectable at an earlier and thinner stage [21].

Therefore, the aim of this study is to investigate the use of low-field nuclear magnetic resonance for detecting differently structured deposits inside flexible silicone tubing. The transverse relaxation times T_2 of (1) biofilms formed from *P. polymyxa*, (2) dairy biofouling, and (3) dairy fouling will be presented and compared. It will be shown that the method is capable of discriminating between dairy biofouling and dairy fouling. Biofilm and fouling identification is also validated by microscope images and microbiological methods, deepening the understanding of their formation in flexible silicone tubing.

Materials and methods

Chemicals and other materials

Commercial UHT and pasteurized milk (3.5% fat) was obtained from the dairy Weihenstephan GmbH & Co. KG (Freising, Germany). Meat extract and plate count agar dip slides were obtained from VWR (Darmstadt, Germany). Soy peptone was obtained from Applichem Panreac (Barcelona, Spain), while Rhodamine B and Crystal Violet solutions were purchased from Merck (Darmstadt, Germany). The freeze-dried culture of *P. polymyxa* (DSM 36) was obtained from DSMZ (Braunschweig, Germany). All reagents and chemicals used were of analytical grade.

Experimental set-up and sample preparation

In this study, three deposit models were prepared: (1) a monoculture biofilm from *P. polymyxa*, (2) dairy biofouling with mixed bacteria, and (3) dairy fouling without bacteria. For the experimental set-up, a peristaltic pump with adjustable speed (Multifix, Germany) was selected. Peroxide-cured silicone tubing with 6-mm inner and 9-mm outer diameters (Deutsch & Neumann, Germany) and at lengths of 0.5 or 1.0 m was chosen for the experimental set-up. Silicone tubing is used in the food and beverage industry in a wide range of applications, for example as milk transfer tubes for vessels to processing facility transfers, pulsation tubing for automatic rotary milking machines, tubes for transferring yogurts, and sauces with fruit or other solids. The roughness parameters R_a (the arithmetical mean roughness of a surface, following ISO 4287) and R_z (the maximum height of the assessed profile, following ISO 4287, the sum of height of the largest profile peak height and the lowest profile valley depth) of silicone tubing were assessed as 3.36 ± 0.44 µm and 14.70 ± 2.59 µm, respectively. The deposits formed at the inner surface of these tubes were investigated later via low-field NMR. The tubing and connecting elements were autoclaved before each experiment. All three experimental set-ups were assembled under sterile conditions. In total, 1.5 L of prepared liquid for the respective deposit model was dispensed in two 1.0-L laboratory bottles (Schott, Germany) and pumped at the set temperature, flow conditions, and time.

Nutrient medium (3-g L^{-1} meat extract, 5-g L^{-1} soy peptone, pH 7) was used for the *P. polymyxa* biofilm (experimental set-up I). For the preparation of a first bacterial suspension, 150 mL of sterile nutrient medium was inoculated with *P. polymyxa* taken from an agar plate with an inoculation loop. The suspension was incubated at 30 °C with shaking at 100 rpm for about 3 h to reach the exponential phase. The transmission at 570 nm of the bacterial suspension at early exponential phase that was used for inoculation was $90.9 \pm 0.6\%$ ($n = 3$). The number of bacteria in the early exponential phase corresponded to about 1.2×10^6 CFU mL^{-1}. Then, 1425 mL of sterile nutrient medium were inoculated with 75 mL of bacterial suspension. After inoculation, the pump was turned on and the inoculated medium was pumped in a closed loop for a total of 4 days at 30 °C. The flow conditions in the silicone tubing were predominantly laminar ($Re = 1400$–2100). A total of 1000 mL of nutrient medium were exchanged four times to provide the nutrition for bacterial growth. The pump was turned off overnight and the temperature was kept constant at 30 °C to provide the biofilm with the optimal conditions for growth. The measurements of samples (1) clean silicone tubing, (1.2) sterile nutrient medium, (1.3) clean tubing filled with sterile nutrient medium, (1.4) *P. polymyxa* biofilm, (1.5) silicone tubing with *P. polymyxa* biofilm on the inner surface, and (1.6) silicone tubing with *P. polymyxa* and nutrient medium were performed after experimental run.

For dairy biofouling (experimental set-up II), commercial pasteurized milk with 3.5% fat was used. Pasteurized milk still contains heterogeneous groups of bacteria, typically Gram-positive spore-forming bacteria that survive the pasteurization. Pasteurized milk was pumped for a total of 4 days at 30 °C at Reynolds numbers from 1000 to 2000 (predominantly laminar flow). A total of 1000 mL of pasteurized milk were exchanged four times. 36 h after the begin of the experiment, pasteurized milk was inoculated once with 50 µL of *P. polymyxa* bacterial suspension, prepared as for experimental set-up I (*P. polymyxa* biofilm). The pump was also turned off overnight, while the temperature was kept constant at 30 °C to promote bacterial adhesion. The measurements of following samples were performed after experimental run: (1) clean silicone tubing, (2.2) 3.5% pasteurized milk as purchased and used for biofouling formation, (2.3) 3.5% contaminated milk obtained after the experimental run, (2.4) silicone tubing with 3.5% pasteurized milk as purchased, (2.5) dairy biofouling, which was directly picked from the inner surface of the silicone tubing after the experimental run, (2.6) silicone tubing with dairy biofouling, (2.7) silicone tubing with dairy biofouling such as sample (2.6) and with additionally applied dairy biofouling in the tubing opening, and (2.8) silicone tubing with dairy biofouling and 3.5% contaminated milk.

For dairy fouling (experimental set-up III), commercial UHT milk with 3.5% fat was used, which is manufactured under aseptic conditions and does not contain bacteria. A total of 1500 mL of the milk as purchased were pumped at temperatures of 70–80 °C at $Re = 1500$–2200 for 4 days in total. During the pumping phase, the UHT milk was exchanged completely four times. The pump was turned off overnight, while the temperature was kept constant at 30 °C. The measurements of following samples were performed after experimental run: (1) clean silicone tubing, (3.2) 3.5% UHT milk as purchased, (3.3) dairy fouling, which was directly picked from the inner surface of the silicone tubing after the experimental run, (3.4) silicone tubing with 3.5% UHT milk, (3.5) silicone tubing with dairy fouling, (3.6) silicone tubing with manually added dairy fouling like sample (3.5) and with additionally applied dairy fouling in the tubing opening, and (3.7) silicone tubing with dairy fouling and 3.5% UHT milk.

NMR methods employed

Measurement of transverse relaxation time T_2

A Bruker minispec mq 20 NMR Analyzer (Bruker, Rheinstetten) operating at 20 MHz was used to measure transverse

relaxation times T_2 for the three deposit models. The NMR probehead H20-10-25-RV was used for measurement of the samples. Before using the relaxation time application for measurement, the instrument was calibrated using a suitable test sample [standard solution E1405295 from Bruker (Bruker, Rheinstetten)] to set the correct 90° and 180° pulse lengths. The instrument operated with a probe dead time of approximately 7 µs, magnet temperature of 40 °C, 90° pulse length of 2.96 µs, and 180° pulse length of 5.78 µs. All measurements were performed at 20 °C. The samples were put in standard NMR glass tubes (Bruker, Rheinstetten) with a length of 180 mm and diameter of 10 mm. To ease the placement of the biofilm (1.4), biofouling (2.5), and fouling (3.3) samples in the standard NMR glass tubes, glass inserts with a length of 45 mm and a diameter of 8 mm were used. The biofilm, biofouling, and fouling samples, which were obtained after the experimental run, were taken from the inner surface of the silicone tubing with a microdouble spatula and placed into the glass inserts. A Carr–Purcell–Meiboom–Gill pulse sequence (CPMG) was applied to determine transverse relaxation times T_2. Data were acquired using the software application "T_2_cp_mb" provided by Bruker. In this method, the first 90° pulse excites the spin system and the following 180° pulses produce the echoes (multiple echo sequence). The gain is chosen to obtain an initial intensity of about 70–80% signal intensity. Other selected method parameters were: scans—8; recycle delay—5 s; 90°–180° pulse separation (tau)—1 ms; and data points—4000. The NMR measurements were controlled with Minispec Software V2.59 Rev.06/NT/XP (Bruker, Rheinstetten). The determination of transverse relaxation time T_2 was conducted for the clean silicone tubing, the liquid, and the deposits as references, as well as the combination of tubing with liquid or with deposits.

Microbiological investigation

The ATP-bioluminescence test (RLU) and the determination of colony-forming units (CFU mL^{-1}) of the nutrient medium, pasteurized, and UHT milk were performed after each exchange. ATP-bioluminescence test of the silicone tubing was conducted after the experiment.

ATP-bioluminescence assay

The ATP-bioluminescence test was carried out using the ATP + AMP Hygiene Monitoring test kit (swab test). The test kit comprises the Lumitester™ PD-30 and LuciPac™ Pen (Kikkoman Biochemifa Company). For liquid samples such as milk and bacterial suspension, the swab stick was removed from its casing and soaked in the liquid sample. When the swab stick was saturated, it was returned into the casing, which contains the releasing and luminescent reagents. Pushing the stick firmly into the casing, the tested reagent was released into the luminescent reagent. The test tubing was shaken until the powdery luminescent reagent completely dissolved. Then, the swab stick was inserted into the Lumitester™ PD-30 and the measurement was carried out within 10 s. The result was given in relative light units (RLU). For the silicone tubing surface, the swab stick was removed from the casing and wetted with sterile water. Then the swab stick was wiped with constant pressure over an inner surface of 1 cm^2 and entered into its casing, and RLU was measured as described above.

Determination of colony-forming units

Dip slides with plate count agar were used to determine the colony-forming units (CFU mL^{-1}) of nutrient medium, and of pasteurized milk. A volume of 25 µL of sample was pipetted on the plate count agar under sterile conditions. A dip slide was returned into the container and incubated at 30 °C for 48 h. The evaluation was carried out in accordance with the instruction manual provided by the manufacturer. The number of colony-forming units was determined a total of six times for each sample.

Microscopic investigation

Microscopy images were obtained using an Olympus IX83 Inverted Microscope (Olympus, Japan) and Kern OBN 135 Microscope (Kern & Sohn GmbH, Balingen, Germany). The deposits were observed after drying for 1 h at room temperature of 22.5 °C. Prior to the microscopy, the silicone tubing was carefully cut to obtain images from the inside of the tubing. To improve the visibility of deposits on the tubing silicone surface, 10 µL of Rhodamine B (0.01 g 100 mL^{-1}) or 10 µL of Crystal Violet (0.01 g 100 mL^{-1}) were used for staining. The samples were observed in a bright field at magnifications of 10× and 20× without oil after 10 min of staining at room temperature.

Data analysis and statistics

Three different NMR tubes with the same kind of sample were provided for the relaxation time measurements. For each NMR tube, three measurements of the CPMG pulse sequence were performed. The obtained data were adjusted by inverse Laplace transform, which was performed one time for each sample. Inverse Laplace transform was applied to transverse relaxation times T_2 for the evaluation of raw NMR data using MatlabR2015b (MathWorks, Inc., USA). For the transformation of the NMR signal drop, the Matlab application (*rilt*) Regularized Inverse Laplace Transform [*g, yfit, cfg*] = *rilt* (*t, y, s,* g_0, *alpha*) was used [22]. Array $g(s)$ is the inverse Laplace Transform of the array $y(t)$, which is

calculated by a regularized least-squares method. *y* is data array, a function of the array time *t*. *yfit* is the Laplace transform of *g* and is fitted against *y* at each step of calculation. *cfg* is a structure containing the parameters of the calculation. *s* is the time-array over which the resulting *g* will be defined. g_0 is the array containing the guessed distribution. *alpha* is the regularization parameter. The fitting parameters for the inverse Laplace transform were kept constant and were defined as follows: $s - linspace$ (1250), (1500), (1, 1000) and (1, 2500); $g_0 - ones$ (*lengths*,1); $alpha - 0.1$. The quality of the inverse Laplace transform was judged on the basis of the sum of the error squares (SSE) and the coefficient of determination (r^2) for each fitting. The distributions obtained by inverse Laplace transform contained detailed information about relaxation behavior of the samples. The area under each curve depends on the signal intensity of the first data point collected (60–90%). The obtained data of the inverse Laplace transform were normalized, so that the area under each curve is the same and equal to 1.

Results and discussion

Transverse relaxation times of (1) *P. polymyxa* biofilm, (2) dairy biofouling, and (3) dairy fouling

Table 1 shows the transverse relaxation times of samples in experimental set-up I (*P. polymyxa* biofilm). For visual representation of the NMR signal distribution of T_2 relaxation times obtained by the inverse Laplace transform, the reader is referred to Fig. 1.

The relaxation time T_2 of the clean silicone tubing was determined to be 5.15 ms. The relaxation time T_2 of (1.4) *P. polymyxa* biofilm was determined to be 101 ms. The high sum of the error squares of 100.7 and the lowest r^2 of 0.938 may have been caused by different thicknesses of biofilm, because this sample was manually placed in the standard glass tubes for NMR measurement. The sterile nutrient medium revealed a longer T_2 relaxation time of 2070 ms. Remarkably, for the sample (1.3) clean silicone

Table 1 T_2 relaxation times determined by inverse Laplace transform of the NMR signal decay and statistics of the NMR evaluation for *P. polymyxa* biofilm (experimental set-up I)

Sample	T_2(1) (ms)	T_2(2) (ms)	SSE	r^2
(1) Clean silicone tubing	5.15	–	96.4	0.988
(1.2) Sterile nutrient medium	2070	–	3.81	1.000
(1.3) Clean tubing with sterile nutrient medium	25.4	1920	15.9	0.997
(1.4) *P. polymyxa* biofilm	101	–	100.7	0.938
(1.5) Tubing with *P. polymyxa* biofilm on the inner surface	5.15	25.4	4.74	0.994
(1.6) Tubing with *P. polymyxa* biofilm and nutrient medium	25.4	732	15.9	0.996

The T_2 distribution of the samples is shown in Fig. 1

SSE the sum of the error squares, r^2 the coefficient of determination

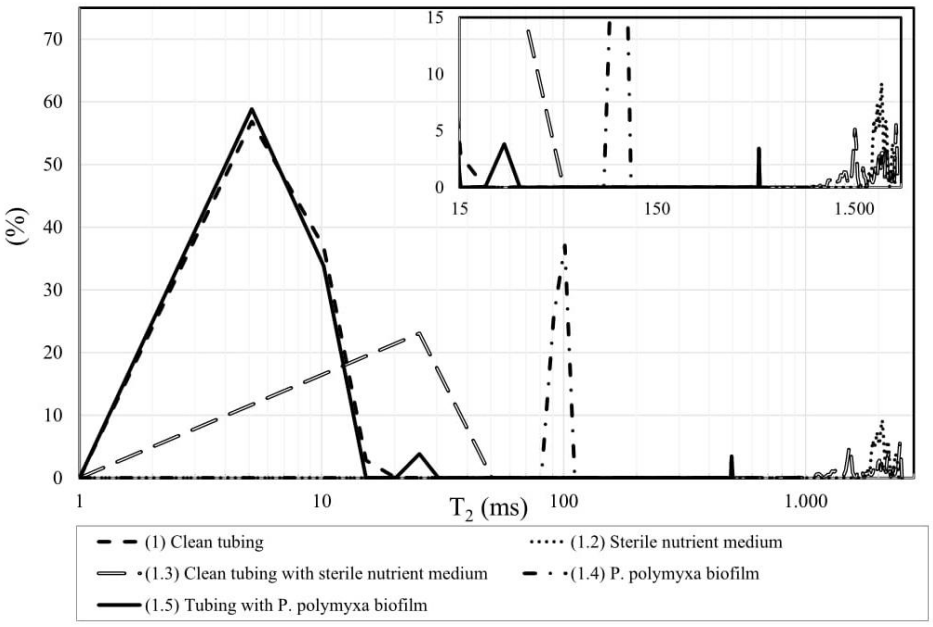

Fig. 1 Distribution of transverse relaxation time T_2 obtained for experimental set-up I using low-field NMR: (1) clean silicone tubing, (1.2) sterile nutrient medium, (1.3) clean tubing filled with sterile nutrient medium, (1.4) *P. polymyxa* biofilm, and (1.5) silicone tubing with *P. polymyxa* biofilm on the inner surface

tubing filled with sterile nutrient medium, the relaxation time of the nutrient medium decreased by 150 ms when compared to the sample (1.2) nutrient medium without silicone tubing. Conversely, $T_2(1)$ of the tubing increased by a factor of 5–25.4 ms compared with T_2 of 5.15 ms for clean tubing. The NMR signal of sample (1.5), silicone tubing with *P. polymyxa* biofilm, was separated into the signal of the silicone tubing (5.15 ms) and the signal of the biofilm (25.4 ms). The coefficient of determination r^2 was generally close to 1.0, showing a good fit.

The T_2 distribution of (1.4) *P. polymyxa* biofilm showed a narrower peak centered at approximately 100 ms (Fig. 1). The peaks of T_2 of the silicon tubing were recorded for samples (1) and (1.3) at fast relaxation rates. Remarkably, T_2 of tubing in sample (1.3) showed a shifted peak to slower relaxation rates. It can be assumed that interactions between the protons in the liquid phase and the protons in the silicone tubing may occur. It may lead to the averaging of relaxation between the silicone tubing and in this case, nutrient medium. In sample (1.5) silicone tubing with *P. polymyxa* biofilm, however, a weak peak was noted at approximately 30 ms, which may indicate the *P. polymyxa* biofilm. Samples (1.2) and (1.3) demonstrated a typical relaxation behavior of liquid phase at longer relaxation times. Sample (1.6) tubing with *P. polymyxa* biofilm and nutrient medium is not shown in Fig. 1 due to the overlap with the T_2 distribution of other samples. The T_2 distribution of his sample is shown in Fig. 4.

Table 2 shows the relaxation time T_2 for samples of experimental set-up II (dairy biofouling). Also, Fig. 2 illustrates the distribution of relaxation times T_2 of samples in experimental set-up II dairy biofouling.

A shorter relaxation time T_2 of 55.6 ms was obtained for the dairy biofouling (2.5) than T_2 of (1.4) microbiological *P. polymyxa* biofilm (101 ms) (Table 1). It can be explained by the fact that in dairy biofouling formation, both processes are involved: protein aggregation and microbial activity. The presence of protein fraction may lead to denser gel-like biofouling. Sample (2.2) 3.5% pasteurized homogenized milk

Table 2 T_2 relaxation times determined by inverse Laplace transform of the NMR signal decay and statistics of the NMR evaluation for dairy biofouling (experimental set-up II)

Sample	$T_2(1)$ (ms)	$T_2(2)$ (ms)	SSE	r^2
(1) Clean silicone tubing	5.15	–	96.4	0.988
(2.2) 3.5% Pasteurized homogenized milk	152	–	1.41	0.999
(2.3) 3.5% Contaminated milk after experimental run	192	–	1.91	0.999
(2.4) Tubing with 3.5% pasteurized milk	20.3	152	8.86	0.999
(2.5) Dairy biofouling	55.6	–	271	0.869
(2.6) Tubing with dairy biofouling	5.15	17.8	242	0.990
(2.7) Tubing with manually added dairy biofouling[a]	7.67	22.8	197	0.985
(2.8) Tubing with dairy biofouling and 3.5% milk	40.5	192	1.31	0.999

The T_2 distribution of the samples is shown in Fig. 2

SSE the sum of the error squares, r^2 the coefficient of determination

[a](2.7) Tubing with manually added dairy biofouling means double the amount of dairy biofouling manually added on the tubing surface

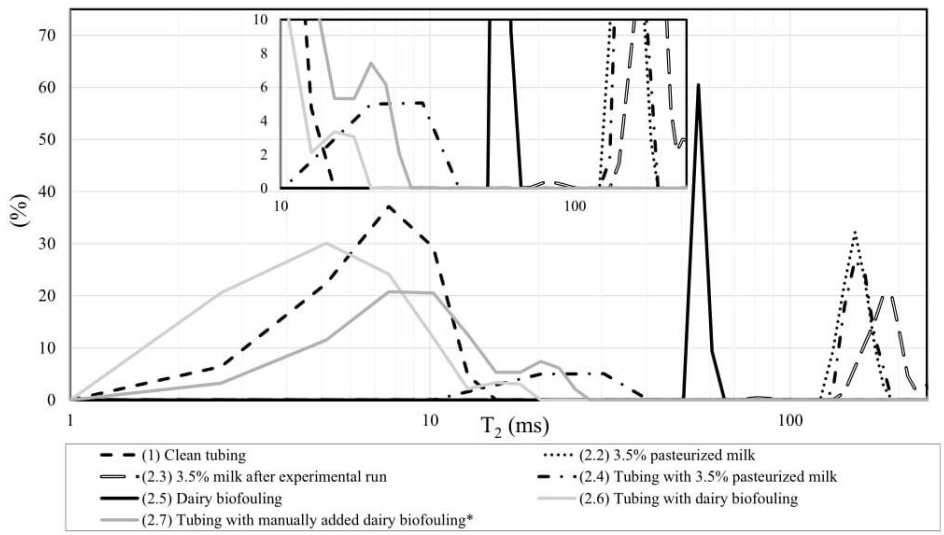

Fig. 2 Distribution of transverse relaxation time T_2 obtained for experimental set-up II: (1) clean silicone tubing, (2.2) 3.5% pasteurized milk as purchased and used for biofouling formation, (2.3) 3.5% contaminated milk obtained after the experimental run, (2.4) silicone tubing with 3.5% pasteurized milk as purchased, (2.5) dairy biofouling, (2.6) silicone tubing with dairy biofouling, and (2.7) silicone tubing with additionally manually added dairy biofouling

had a relaxation time T_2 of 152 ms, while contaminated milk after experimental run (2.3) revealed an longer T_2 of 192 ms. Contaminated milk after experimental run visibly changed its appearance. The separation of liquid whey due to microbial activity was observed. This can explain the longer relaxation time of the sample (2.3). Similarly to the measurements of the silicone tubing with sterile nutrient medium (Table 1), the presence of milk in the silicone tubing, sample (2.4), led to a longer relaxation time $T_2(1)$ of the tubing (20.3 ms) compared to the relaxation time T_2 of (1) clean tubing (5.15 ms). When dairy biofouling was present on the surface of the tubing, sample (2.6), the transverse relaxation time of dairy biofouling decreases by 37.8 ms when compared to the sample (2.5) dairy biofouling without silicone tubing. However, in sample (2.8), which represents three-component system, no directly corresponding relaxation time for dairy biofouling could be obtained. The lowest coefficient of determination r^2 was 0.869 for sample (2.5) dairy biofouling, corresponding to the highest SSE of 271 for this sample. The high sum of the error squares may have been caused by non-homogeneous distribution and thicknesses of dairy biofouling, which was manually placed in the glass tubing for NMR measurement. A similar response was also detected for the sample (1.4) *P. polymyxa* biofilm (Table 1). Other samples showed relatively high coefficients of determination of $r^2 > 0.985$.

The T_2 distribution of (2.5) dairy biofouling showed a single narrow peak centered at approximately 55 ms (Fig. 2). The significant shift of tubing T_2 to slower relaxation rates was observed for the samples with biofouling in the tubing, sample (2.6), and with milk in the tubing, sample (2.4). Measurement of silicone tubing with dairy biofouling (2.6) and with manually added dairy biofouling (2.7) showed a shift in the T_2 distribution for biofouling to faster relaxation rates and decreased intensity of the NMR signal when comparing with (2.5) dairy biofouling. This indicates that the relaxation behavior was changed by the presence of biofouling on the inner surface of tubing. A comparison of sample (2.6) and sample (2.7) also illustrates an increase in the proportion of protons experiencing slower relaxation rates, as would be expected due to an increased amount of biofouling. T_2 of pasteurized milk was shorter than T_2 of nutrient medium (Table 1) most likely due to the presence of fat and proteins in milk as well as lower content of water in milk. Sample (2.8) tubing with dairy biofouling and 3.5% contaminated milk is shown in Fig. 4 due to the overlap with the T_2 distribution of other samples.

Table 3 shows the relaxation time T_2 of samples for experimental set-up III (dairy fouling). Figure 3 illustrates the distribution of relaxation times T_2 of samples in experimental set-up III for dairy fouling.

Sample (3.3) dairy fouling had two shorter relaxation times T_2 of 51.4 and 61.5 ms compared to the sample (3.2) 3.5% UHT milk with three relaxation times T_2 of 137, 157, and 172 ms. It can be explained by the structural changes due to the formation of gel-like structure of dairy fouling. Once the silicone tubing was measured with 3.5% UHT milk, sample (3.4), the relaxation time $T_2(1)$ of the tubing shifted from 5.15 ms to 16.1 ms. Separation of NMR signals for the silicon tubing (6.04 ms) and fouling (31.2 and 41.3 ms) could be observed for sample (3.5) tubing with dairy fouling. Moreover, the fouling relaxation times $T_2(2)$ and $T_2(3)$ in sample (3.5) differed slightly in comparison with those of sample (3.3) with dairy fouling. Similar behavior was also observed in experimental set-ups I and II (Tables 1 and 2). With increased amount of fouling on the tubing surface, a shift towards longer relaxation time $T_2(2)$ of 46.4 ms for dairy fouling could be observed for sample (3.6). In sample (3.7) tubing with dairy fouling and 3.5% UHT milk, however, no clear peak separation for dairy fouling was detected. The coefficients of determination of all samples were > 0.988, which indicates sufficient goodness of fit.

Table 3 T_2 relaxation times determined by inverse Laplace transform of the NMR signal decay and statistics of the NMR evaluation for dairy fouling (experimental set-up III)

Sample	$T_2(1)$ (ms)	$T_2(2)$ (ms)	$T_2(3)$ (ms)	$T_2(4)$ (ms)	SSE	r^2
(1) Clean silicone tubing	5.15		–	–	96.4	0.988
(3.2) 3.5% UHT milk	137	157	172	–	1.91	0.999
(3.3) Dairy fouling	51.4	61.5	–	–	85.2	0.994
(3.4) Tubing with 3.5% UHT milk	16.1	116	157	167	1.25	0.999
(3.5) Tubing with dairy fouling	6.04	31.2	41.3		61.8	0.994
(3.6) Tubing with manually added dairy fouling[a]	6.04	46.4	–	–	55.3	0.995
(3.7) Tubing with dairy fouling and 3.5% UHT milk	16.1	137	172	–	3.30	0.999

The T_2 distribution of the samples is shown in Fig. 3

SSE the sum of the error squares, r^2 the coefficient of determination

[a](3.6) Tubing with manually added dairy fouling means double the amount of manually added dairy biofouling on the tubing surface

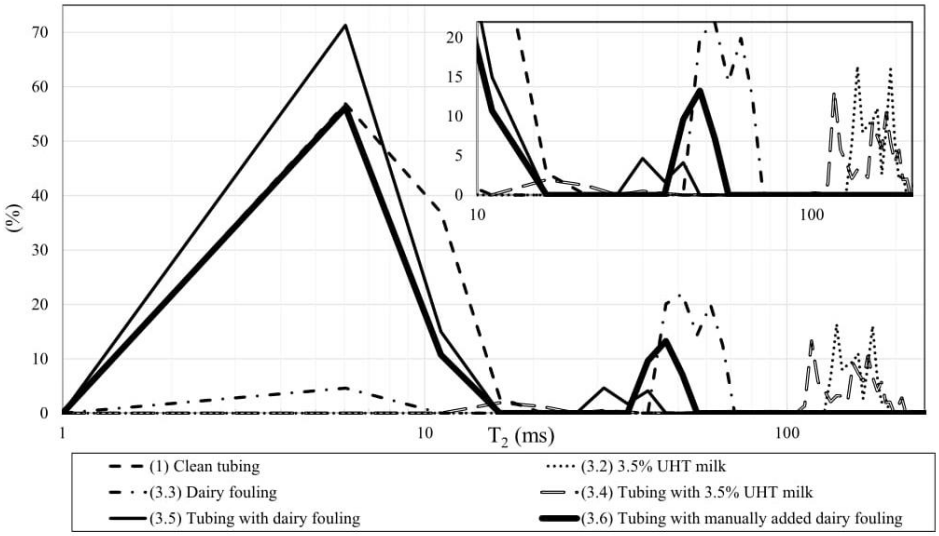

Fig. 3 Distribution of transverse relaxation time T_2 obtained for experimental set-up III: (1) clean silicone tubing, (3.2) 3.5% UHT milk as purchased, (3.3) dairy fouling, (3.4) silicone tubing with 3.5% UHT milk, (3.5) silicone tubing with dairy fouling, and (3.6) silicone tubing with manually added dairy fouling

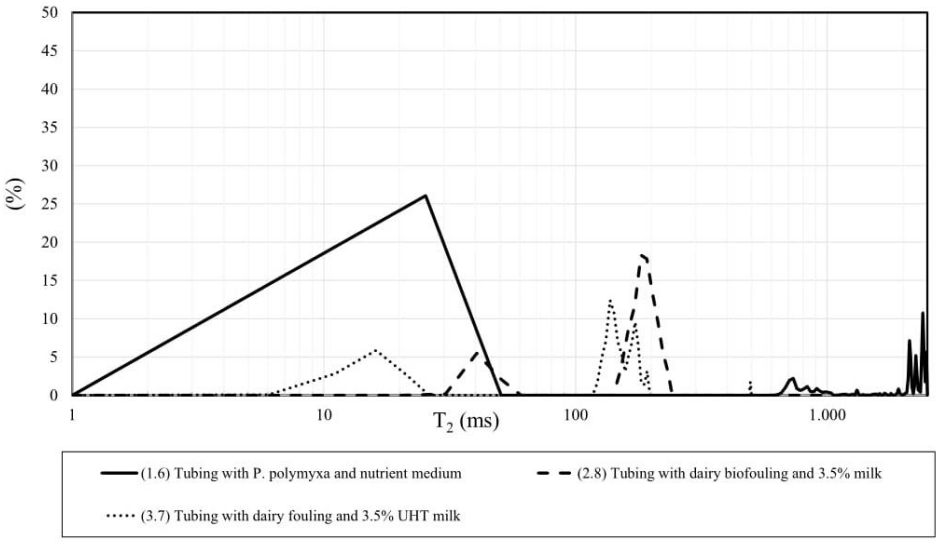

Fig. 4 Distribution of relaxation time T_2 obtained for three-component systems using low-field NMR: (1.6) silicone tubing with *P. polymyxa* and nutrient medium, (2.8) silicone tubing with dairy biofouling and 3.5% milk, and (3.7) silicone tubing with dairy fouling and 3.5% UHT milk

The T_2 distribution of sample (3.3) dairy fouling showed a double peak at around 50–60 ms. In addition, a broad signal at faster relaxation rates was detected from 2 to 10 ms (Fig. 3). The double-peak formation and a broad signal at faster relaxation rates can be attributed to the temperature of the fouling formation during 4 days, as the milk was pumped at temperatures of 70–80 °C. Fouling formation at lower temperatures is usually caused by thermally unstable whey proteins, and consists of about 60% protein and 40% minerals [7]. In addition, a slight shift in the T_2 of the silicone tubing to slower relaxation rates can be observed. Measurement of silicone tubing with dairy fouling (3.5) and with additionally added dairy fouling (3.6) showed a shift in the T_2 distribution for biofouling to longer relaxation times. Similar to the case for experimental set-up II with dairy biofouling, experimental set-up III revealed clear separation of tubing, fouling, and milk. Sample (3.7) tubing with dairy fouling and 3.5% UHT milk is shown in Fig. 4 due to the overlap with the T_2 distribution of other samples.

Figure 4 shows distribution of relaxation time T_2 of three deposits models: (1) a monoculture biofilm from *P. polymyxa*, (2) dairy biofouling with mixed bacteria, and (3) dairy fouling without bacteria, which were obtained for three-component samples. The T_2 distribution shows that for samples, which represents three-component system (silicone tubing, deposit, and liquid), no directly corresponding relaxation time for deposit could be obtained, while transverse relaxation times of silicone tubing and liquid phase (nutrient medium and milk) were clearly shown. It is possible that a real-time measurement of three-component samples with flowing liquid phase would be better to separate relaxation times of all components.

The results of the three experimental set-ups demonstrate the typical relaxation behavior of solid, gel-like, and liquid phases [16, 23]. The data indicate the shortest relaxation time T_2 at around 5–10 ms for silicone tubing. Longer T_2 was detected for biofilm and fouling at around 50–150 ms, while the longest T_2 was found for liquid phases (nutrient medium and milk) due to the high mobility of water. Typically, the faster relaxation rates can be found in solid-like materials and gels [23]. Solid materials and gels have shorter relaxation times than liquids due to low rotational mobility enhancing dipolar coupling [19, 20]. Shorter relaxation time is attributed to the water protons and macromolecule exchangeable protons trapped in the gel [23]. Based on the obtained results, it can be supposed that interactions occur between solid-like material and liquid as well as between solid and gel-like phases. For example, the presence of a liquid phase or gel-like phase in solid phase (silicone tubing) leads to a slightly longer relaxation time T_2 of the silicone tubing, while the relaxation time T_2 of the liquid phase becomes shorter. In addition, it was observed that, with increasing biofouling and fouling amount, the relaxation time $T_2(2)$ shifted towards longer relaxation times. It may be explained by the assumption that with the increasing amount of deposit in tubing, the interactions between silicone tubing wall and deposit decrease, what leads to the shift in relaxation time.

Microbiological evaluation and microscopy

Experimental set-up I (*P. polymyxa* biofilm), experimental set-up II (dairy biofouling), and experimental set-up III (dairy fouling) were performed over a period of 4 days. Nutrient medium and milk were exchanged during the experimental run four times to provide the nutrients for biofilm, biofouling, and fouling development. After each of these exchanges, ATP-bioluminescence in RLU and CFU values was recorded as described in "ATP-bioluminescence assay" and "Determination of colony forming units". The ATP-bioluminescence of clean silicone tubing was $5.8 \times 10^1 \pm 1.0 \times 10^1$ RLU cm^{-2} ($n = 9$).

In experimental set-up I (*P. polymyxa* biofilm), the number of viable cells before each exchange of nutrient medium was from 10^7 to 10^8 CFU mL^{-1} for all samples, while for ATP-bioluminescence, the value was $3.0 \times 10^4 \pm 8.9 \times 10^3$ RLU. The reference value of ATP-bioluminescence for the nutrient medium was $2.6 \times 10^4 \pm 2.2 \times 10^3$ RLU ($n = 9$). This indicates high bacterial activity, which is a precursor to biofilm formation. After 4 days, the ATP-bioluminescence value of the silicone surface with *P. polymyxa* was determined to be $3.8 \times 10^5 \pm 5.8 \times 10^4$ RLU cm^{-2}.

The reference value of ATP-bioluminescence for 3.5% pasteurized milk was $4.8 \times 10^2 \pm 1.0 \times 10^2$ RLU ($n = 9$). Figure 5 shows the ATP-bioluminescence values in RLU over the 4 days for experimental set-up II (dairy biofouling).

Figure 5 illustrates that after 6 h and 27 h, milk showed slightly higher ATP-bioluminescence values. Moreover, after inoculation with 50 µL of *P. polymyxa* bacterial suspension (1.2×10^6 CFU mL^{-1}), the ATP-bioluminescence increased rapidly to 2.6×10^3–3.5×10^3 RLU. In addition, the number of viable cells increased to more than 10^8 CFU mL^{-1}, while the number of viable cells present in pasteurized milk was determined to be 6.1×10^4 CFU mL^{-1} ($n = 5$). After the experimental run, the ATP-bioluminescence value of the silicone surface with dairy biofouling was determined to be $2.7 \times 10^5 \pm 1.5 \times 10^4$ RLU cm^{-2}.

The reference value of ATP-bioluminescence of 3.5% UHT milk in experimental set-up III was $4.7 \times 10^2 \pm 3.4 \times 10^1$ RLU ($n = 9$). This value does not differ significantly from that of 3.5% pasteurized milk. However, ATP-bioluminescence values increased slightly after heating of milk up to $1.2 \times 10^4 \pm 5.5 \times 10^3$ RLU, while viable

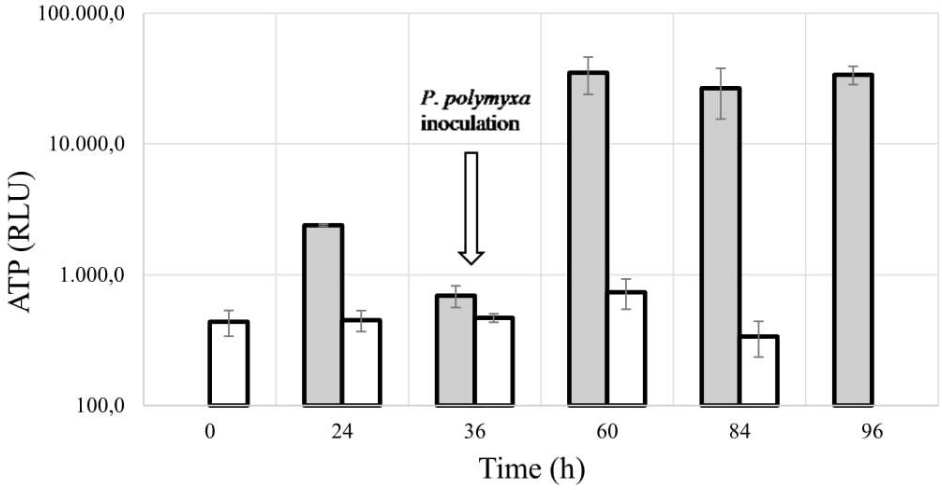

Fig. 5 ATP-bioluminescence values of 3.5% pasteurized milk before milk exchange (reference white data bars) and after milk exchange (gray data bars) in experimental set-up II (dairy biofouling). Pasteurized milk was inoculated with *P. polymyxa* bacterial suspension after 36 h of experimental run. Error bars correspond to the standard deviations

cells were not present. The ATP-bioluminescence value of the silicone surface with dairy fouling was determined to be $2.5 \times 10^5 \pm 1.3 \times 10^4$ RLU cm^{-2}.

According to recommendations of the ATP-bioluminescence test manufacturer, values of plastic surface higher than 500 RLU can be considered as inadequate hygienic conditions, being associated with a high level of deposit formation on a surface. In this work, ATP values of the silicone surface for each experimental set-up are much larger than the recommendations on deposit formation inside the tubing. This indicated high bacterial activity and deposit formation of the silicone inner surface.

Figure 6 shows images of clean silicone tubing (A), tubing with dried non-stained dairy fouling (B), tubing with dried dairy fouling stained with Rhodamine B (0.01 g 100 mL^{-1}) (C), and tubing stained with Crystal Violet (0.01 g 100 mL^{-1}) and *P. polymyxa* biofilm (D).

The image of the clean silicone tubing surface (A) showed a clean surface without a deposit. After the experimental run, clear visible clusters of fouling without staining on the tubing surface could be observed (B). Images of dairy fouling stained with Rhodamine B (0.01 g 100 mL^{-1}) solution (C) illustrated the structure of the fouling. Moreover, the biofouling structure and distribution on a silicone pipe were similar to the dairy fouling depicted in Fig. 6b, c. In addition, Fig. 6d depicts the *P. polymyxa* biofilm, which was stained with crystal violet (0.01 g 100 mL^{-1}) solution. Numerous single microbial communities could be found along the inner tubing surface. When comparing Fig. 6c, d, it can be observed that the biofilm is distributed less homogeneously on the silicone tubing.

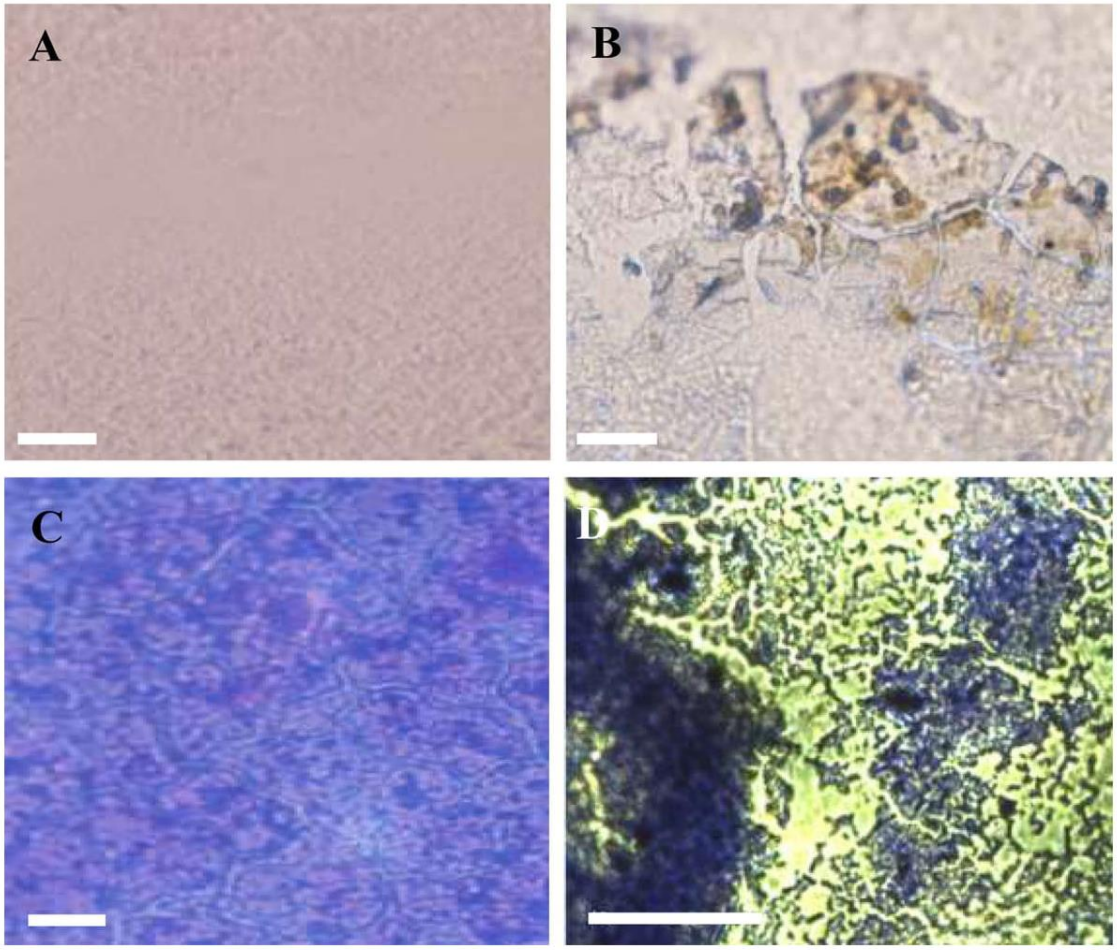

Fig. 6 Microscopic images of clean silicone tubing (**a**), tubing with dried non-stained dairy fouling (**b**), tubing with dried Rhodamine B (0.01 g 100 mL^{-1})-stained dairy fouling (**c**), and tubing stained with crystal violet (0.001 g 100 mL^{-1}) and *P. polymyxa* biofilm (**d**). The magnification of images **a** and **c** was from a×10 objective without oil (scale bars 100 µm), while the magnification of image **b** was from a×20 objective without oil (scale bar 50 µm) and the magnification of image **d** was from a 40×objective without oil (scale bar 50 µm)

Practical implications of ^{1}H NMR detection and further studies

The low-field ^{1}H NMR results obtained in this study and analyzed by inverse Laplace transform show characteristic relaxation behavior for *P. polymyxa* biofilm, dairy biofouling, and dairy fouling. The analysis of the NMR signal with inverse Laplace transform produces a statistical distribution of T_2 relaxation times. The *P. polymyxa* biofilm shows longer transverse relaxation times at about 100 ms than dairy biofouling and dairy fouling (50–60 ms). The comparison between clean tubing and tubing with corresponding deposit indicates different relaxation behaviors resulting in longer relaxation times $T_2(1)$ for tubing and in shorter relaxation times $T_2(2)$ of deposit if the respective deposit is present.

Several studies have explained the detection of biofilms using low-field NMR. The relaxation time T_2 of water contained in the biofilm is shorter than of free water. This can be explained by the fact that a biofilm is composed of bacterial cells in a hydrated gel matrix (EPS) and contributes a polymer gel-like phase [19, 20, 24]. As reported in the literature, shorter relaxation times compared to relaxation time of free water can be assigned to the biofilm, since the biofilm consists of bound water and is located near the tubing walls [16, 21]. It has been observed that the relaxation times from water in a biofilm matrix are up to an order of magnitude shorter than those of the free water phase [13]. Manz et al. [21] found that high-density biofilms consist of two components with mean T_2 values of around 150 and 700 ms. The shorter T_2 component can be identified as an area where the mobility of the water molecules is particularly restricted due to high biofilm density and/or an area with enriched ionic density. The component with the longer T_2 value is located between high-density biofilm and free water.

Besides the experimental approach, in actual process conditions, three-component systems should be considered: tubing, flowing liquid, and corresponding deposit that can grow over time. Based on the results of this study, it is likely that each component has a different relaxation behavior. For example, the silicone tubing would have the shortest relaxation time T_2, followed by the transverse relaxation times of deposit and liquid, respectively. Interactions between these components can occur, which may influence the relaxation time of each component. In future measurements, shorter 90°–180° pulse separation (tau) times and longer recycle delay values should be considered to allow detection of each component in three-component systems with different relaxation rates. Moreover, to obtain significant results for samples with a very low amount of biofilm or fouling, the sensitivity of the method has to be investigated. In addition, further measurements should be performed with different food-grade tubing to understand the interaction between deposits and tubing in more detail [25]. From a food technology perspective, it is necessary to prove the possibility of fast NMR detection at different temperatures related to dairy processing equipment, such as filling temperature (5–20 °C) or cleaning temperature (60–90 °C). As additional steps, deposit detection under flow conditions is necessary to evaluate the suitability of low-field NMR to real-time monitoring of dairy processing. Real-time measurement would be advantageous, in which the conveying liquid is not stationary but flowing, since the transient protons in the conveying liquid, moved out of the measurement region, do not interfere with the characteristic NMR signal drop due to the stationary deposit formation on the tubing wall.

Conclusion

The results obtained in this study show that low-field NMR can be used to detect bacterial biofilm, dairy biofouling, and fouling. In addition, low-field NMR offers the possibility of detection food-related deposits on tubing surfaces. The comparison of the tested deposits in this study showed characteristic relaxation behavior. Therefore, low-field ^{1}H NMR can be recommended for the better understanding of food-related deposit formation in situ and in real time.

Funding This research did not receive any specific grant from funding agencies in the public, commercial, or not-for-profit sectors.

Compliance with ethical standards

Conflict of interest The authors declare that they have no conflict of interest.

Compliance with ethics requirements This article does not contain any studies with human or animal subjects.

References

1. Cappitelli F, Polo A, Villa F (2014) Biofilm formation in food processing environments is still poorly understood and controlled. Food Eng Rev 6(1–2):29–42
2. Srey S, Jahid IK, Ha S-D (2013) Biofilm formation in food industries: a food safety concern. Food Control 31(2):572–585
3. Derlon N, Gruetter A, Brandenberger F, Sutter A, Kuhlicke U, Neu TR, Morgenroth E (2016) The composition and compression of biofilms developed on ultrafiltration membranes determine hydraulic biofilm resistance. Water Res 102:63–72
4. Marchand S, De Block J, De Jonghe V, Coorevits A, Heyndrickx M, Herman L (2012) Biofilm formation in milk production and processing environments: influence on milk quality and safety. Compr Rev Food Sci Food Saf 11(2):133–147
5. Lewandowski Z, Beyenal H (2013) Fundamentals of biofilm research, 2nd edn
6. Flemming H-C (2002) Biofouling in water systems—cases, causes and countermeasures. Appl Microbiol Biotechnol 59(6):629–640

7. Kessler HG (2006) Lebensmittel- und Bioverfahrenstechnik: Molkereitechnologie, 4th edn
8. Grady EN, MacDonald J, Liu L, Richman A, Yuan Z-C (2016) Current knowledge and perspectives of Paenibacillus: a review. Microb Cell Fact 15:203
9. De Jonghe V, Coorevits A, De Block J, Van Coillie E, Grijspeerdt K, Herman L, De Vos P, Heyndrickx M (2010) Toxinogenic and spoilage potential of aerobic spore-formers isolated from raw milk. Int J Food Microbiol 136(3):318–325
10. Kim YW, Sardari SE, Meyer MT, Iliadis AA, Wu HC, Bentley WE, Ghodssi R (2012) An ALD aluminum oxide passivated Surface Acoustic Wave sensor for early biofilm detection. Sens Actuators B Chem 163(1):136–145
11. Kang J, Kim T, Tak Y, Lee J-H, Yoon J (2012) Cyclic voltammetry for monitoring bacterial attachment and biofilm formation. J Ind Eng Chem 18(2):800–807
12. Crattelet J, Ghnimi S, Debreyne P, Zaid I, Boukabache A, Esteve D, Auret L, Fillaudeau L (2013) On-line local thermal pulse analysis sensor to monitor fouling and cleaning: application to dairy product pasteurisation with an ohmic cell jet heater. J Food Eng 119(1):72–83
13. Fridjonsson EO, Vogt SJ, Vrouwenvelder JS, Johns ML (2015) Early non-destructive biofouling detection in spiral wound RO membranes using a mobile earth's field NMR. J Membr Sci 489:227–236
14. Vogt M, Flemming H-C, Veeman WS (2000) Diffusion in *Pseudomonas aeruginosa* biofilms: a pulsed field gradient NMR study. J Biotechnol 77(1):137–146
15. Sanderlin AB, Vogt SJ, Grunewald E, Bergin BA, Codd SL (2013) Biofilm detection in natural unconsolidated porous media using a low-field magnetic resonance system. Environ Sci Technol 47(2):987–992
16. Hoskins BC, Fevang L, Majors PD, Sharma MM, Georgiou G (1999) Selective imaging of biofilms in porous media by NMR relaxation. J Magn Reson 139(1):67–73
17. Marcone MF, Wang S, Albabish W, Nie S, Somnarain D, Hill A (2003) Diverse food-based applications of nuclear magnetic resonance (NMR) technology. Food Res Int 51(2):729–747
18. Belloque J, Ramos M (1999) Application of NMR spectroscopy to milk and dairy products. Trends Food Sci Technol 10(10):313–320
19. Kirkland CM, Herrling MP, Hiebert R, Bender AT, Grunewald E, Walsh DO, Codd SL (2015) In situ detection of subsurface biofilm using low-field NMR: a field study. Environ Sci Technol 49(18):11045–11052
20. Kirkland CM, Hiebert R, Phillips A, Grunewald E, Walsh DO, Seymour JD, Codd SL (2015) Biofilm detection in a model wellbore environment using low-field NMR. Groundw Monit Remediat 35(4):36–44
21. Manz B, Volke F, Goll D, Horn H (2003) Measuring local flow velocities and biofilm structure in biofilm systems with magnetic resonance imaging (MRI). Biotechnol Bioeng 84(4):424–432
22. rilt Regularized Inverse Laplace Transform (2007) 1.0.0.0 (4.39 KB) by Iari-Gabriel Marino, in. https://de.mathworks.com/matlabcentral/fileexchange/6523-rilt
23. Belton PS (1997) NMR and the mobility of water in polysaccharide gels. Int J Biol Macromol 21(1–2):81–88
24. Garny K, Neu TR, Horn H, Volke F, Manz B (2010) Combined application of ^{13}C NMR spectroscopy and confocal laser scanning microscopy—investigation on biofilm structure and physicochemical properties. Chem Eng Sci 65(16):4691–4700
25. Simões M, Simões LC, Vieira MJ (2010) A review of current and emergent biofilm control strategies. LWT Food Sci Technol 43(4):573–583

2.2.2 Publication 4 Detection of *P. polymyxa* biofilm, dairy biofouling and CIP-cleaning agents using low-field NMR

Biofouling in food-processing equipment may cause significant production downtime, food contamination and can as well add to expenses for cleaning agents. The standard CIP procedure is limited due to the insufficient cleaning of biofouling in food processing equipment. Thus, to ensure better quality control, the implementation of advanced techniques for process monitoring is required. Low-field NMR can be proposed as a non-invasive technique for the manufacturing process and cleaning process monitoring in food processing equipment. Non-invasive detection of biofouling in flexible tubing as a multi-component system and CIP-cleaning agents would be beneficial for the better process control.

This study demonstrates the results for the detection of biofilm and biofouling inside a flexible silicone tubing as well as for the detection of CIP-cleaning agents using low-field ^{1}H NMR. The transverse relaxation time and diffusion coefficients of the samples were obtained and compared. The obtained results showed characteristic relaxation behaviour of flexible tubing, differently structured deposits, and liquid phases. The results revealed that biofouling on the inner tubing surface by assigning a specific relaxation time of each component could be also detected. Moreover, with increasing biofouling thickness, transverse relaxation time shifts toward slower relaxation rates. In addition, significant differences in the diffusion behaviour of water were obtained for both the deposit models and the CIP-cleaning agents. The diffusion coefficient of water in dairy biofouling and in microbial biofilm matrix corresponded to approximately 65% and 75% of the value in pure water, respectively. This article shows that low-field ^{1}H NMR can be used to enhance the understanding of biofouling accumulation and its cleaning. The obtained results could be applied for the development of non-invasive real-time monitoring systems based on low-field ^{1}H NMR.

Author contributions

Fysun, O., Anzmann, T., Gschwind, P. designed the study. Rauschnabel, J., Kohlus, R. were involved in planning and supervised the work. Kleesattel, A. contributed to sample preparation carried out the experiments, collected the NMR data. Fysun, O. performed the analysis for the NMR data and wrote the manuscript. All authors discussed the results and commented on the manuscript. Langowski, H.-C. contributed to the final version of the manuscript.

European Food Research and Technology (2019) 245:1719–1731
https://doi.org/10.1007/s00217-019-03288-y

ORIGINAL PAPER

Detection of *P. polymyxa* biofilm, dairy biofouling and CIP-cleaning agents using low-field NMR

Olga Fysun[1,2] · Theresa Anzmann[3] · Alexander Kleesattel[2,3,5] · Peter Gschwind[3] · Johannes Rauschnabel[2] · Reinhard Kohlus[3] · Horst-Christian Langowski[1,4]

Received: 18 December 2018 / Revised: 3 April 2019 / Accepted: 27 April 2019 / Published online: 7 May 2019

Abstract
The accumulation of unwanted deposits in food-processing equipment may cause significant production downtime, add to expenses for cleaning agents and wastewater disposal, as well as food contamination. Nuclear magnetic resonance (NMR) is considered as a promising non-invasive tool for the monitoring of processes in food industry. In this work, two deposit models and cleaning agents are investigated by low-field ^{1}H NMR: (1) *Paenibacillus polymyxa* biofilm, (2) dairy biofouling and (3) clean-in-place (CIP) cleaning agents. The transverse relaxation times T_2 obtained by inverse Laplace transform as well as diffusion coefficients D_S of the samples are studied. The obtained results reveal that low-field NMR can be used for the detection and identification of selected deposit models and CIP-cleaning agents. Transverse relaxation times T_2 demonstrate characteristic relaxation behavior of flexible tubing, differently structured deposits, and liquid phases. Moreover, with increasing biofouling thickness (up to 406.2 mg/cm^2), transverse relaxation times T_2 shift toward slower relaxation rates up to T_2 111.9 ms. In addition, significant differences in the diffusion behavior of water are noted in each sample group of the deposit models and CIP-cleaning agents. The diffusion coefficient of water in dairy biofouling and in microbial biofilm matrix corresponds to approximately 65% and 75% of the value in pure water, respectively. In addition to the NMR results, the biofilm and biofouling identification is validated through microbiological methods and by microscope images.

Keywords Low-field ^{1}H NMR · Transverse relaxation time · Diffusion coefficient · *Paenibacillus polymyxa* biofilm · Dairy biofouling · CIP-cleaning agent

Introduction

Bacterial adhesion on surfaces of food-processing environments is a concern for the food industry because it constitutes significant economic losses [1, 2]. Formation of deposits by bacterial adhesion can lead to a significant decrease in the quality and safety of processed foods due to bacteria-caused spoilage [3, 4]. The development of bacteria-caused deposits, known as biofilm or biofouling [5], can be found on surfaces in several units of food-processing equipment, for example, storage tanks, filling units and pipelines [2, 6, 7].

According to the IUPAC definition, "biofilms are an aggregate of microorganisms in which cells that are frequently embedded within a self-produced matrix of extracellular polymeric substances (EPS) adhere to each other and/or to a surface" [8]. The formation of biofilms is a dynamic process that involves (1) reversible, (2) irreversible attachment of bacterial cells, (3) maturation, and (4) dispersion [1]. The irreversible attachment of bacterial cells to a surface is induced by EPS production of bacteria. EPS formation protects the bacterial communities against environmental stresses and shear flow, and enhances the bacterial resistance to antibiotics and cleaning media [9]. Biofilm matrices have a heterogeneous structure, comprising mainly of water (up to 97% of matrix), cells (2–5% of

✉ Olga Fysun
olga.fysun@bosch.com

1 TUM School of Life Sciences Weihenstephan, Technical University of Munich, Freising, Germany

2 Robert Bosch Packaging Technology GmbH, Waiblingen, Germany

3 Institute of Food Science and Biotechnology, University of Hohenheim, Stuttgart, Germany

4 Fraunhofer Institute for Process Engineering and Packaging IVV, Freising, Germany

5 Present Address: Festo AG & Co. KG, 73734 Esslingen, Germany

matrix), polysaccharides (1–2% of matrix), protein (1–2% of matrix), and DNA and RNA (1–2% of matrix). EPS is produced by bacteria and can contain up to 90% bound water and include polysaccharides, proteins, or extracellular DNA [10]. In addition, the architecture and composition of biofilms are strongly influenced by the environmental and contact surface properties as well as the presence of other bacteria embedded in the biofilm matrix [2].

Particularly, dairy-processing equipment is highly challenged by the adhesion of bacteria to the food-contact surfaces. Since milk is a good substrate for bacteria growth, the bacterial attachment in dairy-processing environments can lead to increased opportunity for biofilm formation and, consequently, microbial contamination of the processed dairy products [2, 11]. Biofilm in a dairy-processing equipment is often known as biofouling, because not only bacteria but also milk residues (e.g., proteins and minerals) are involved in the deposit formation. The discussion about the controversial definition of different deposit types has been published elsewhere [5].

Psychrotolerant sporeformers, specifically *Paenibacillus* spp., are spoilage bacteria for pasteurized milk, particularly due to biofouling formation in the production lines. For example, *Paenibacillus polymyxa* has been isolated from farms, raw milk-processing equipment, and pasteurized liquid milk plants. *P. polymyxa* bacteria produce a variety of hydrolytic extracellular enzymes such as proteases and lipases that cause spoilage of pasteurized milk [12, 13].

Biofilm or biofouling control in dairy-manufacturing plants generally involves a cleaning process known as clean-in-place (CIP) [9]. CIP cleaning is defined as "cleaning of complete items of plant or pipeline circuits without dismantling or opening of the equipment, with little or no manual involvement by the operator. This process involves the jetting or spraying of the surfaces or the circulation of cleaning solutions through the plant under the conditions of increased turbulence and flow velocity" [14]. The aim of CIP procedures in food-processing equipment is to remove all types of deposits (e.g., protein, minerals, and/or microorganisms) and thereby preserve the plant performance and hygiene. Alkali- and acid-cleaning agents are used in combination with several steam and heating phases, depending on the produced goods. Alkali-soluble deposits are fats and proteins, whereas acid-soluble deposits are mineral scaling (mainly calcium phosphate in dairy industry) [15]. However, the CIP procedures are limited in that insufficient cleaning can increase the risk of biofilm or biofouling development and, consequently, lead to bacterial contamination of processed products [16, 17].

In the last decade, several techniques for bacteria-caused deposit detection and CIP-cleaning monitoring have been reported [18–23]. However, these approaches fail to provide a quantitative and qualitative understanding of complex deposits and their cleaning by non-invasive measurements.

The angular momentum or spin is a property of all atomic nuclei having an uneven number of protons or neutrons. As atomic nuclei are charged, the spinning motion causes a magnetic dipole in the direction of the spin axis [30]. Low-field nuclear magnetic resonance (NMR) is a non-invasive technique based on the relaxation behavior of active nuclei (i.e., ^{1}H, ^{13}C) in a magnetic field [24]. The NMR active nuclei can be oriented in a magnetic field and excited by an impulse of radiofrequency radiation. The strength of the free-induction decay (FID) signal is related to the density of protons in the sample volume. The process of returning to the equilibrium is called relaxation, and it is characterized by two parameters: T_1, the longitudinal relaxation time, which reflects the time needed for the nuclei to return to the equilibrium state, and T_2, the transverse relaxation time, which reflects the time needed for the FID pulse to decay [24]. Chemical and physical changes in a sample can affect the characteristic relaxation behavior that leads to change in the relaxation times T_1 and T_2 [24, 25]. In case of T_1, the longitudinal relaxation time, the bulk magnetisation (M) of the sample containing NMR active nuclei that is placed in a static magnetic field (B_0) varies with time according to the following equation:

$$M_Z = M_{Z,0}(1 - e^{-t/T_1}), \quad (1)$$

where M_Z reflects the magnitude of the magnetisation along the direction Z of the net magnetic field vector, $M_{Z,0}$ reflects the magnetisation at time zero, and t is time. In case of T_2, the transverse relaxation time, the bulk magnetisation (M) is described by the following equation:

$$M_{x,y} = M_{x,y,0}e^{-t/T_2}, \quad (2)$$

where $M_{x,y}$ is the magnitude of the magnetisation along the transverse plane (X–Y) relative to the longitudinal direction (Z) of the net magnetic field vector and $M_{x,y,0}$ is the magnetisation at time zero [24, 30].

^{1}H NMR measures the response of hydrogen-bearing molecules, typically water, to perturbations in a magnetic field. Thus, ^{1}H NMR is applicable in the investigation of materials containing water or organic matter [26–28]. Diverse applications of low-field ^{1}H NMR in food research and processing have been proved, which include chemical analysis and structural identification of functional components, the detection of food authentication, and optimization of food processing [27, 29–31]. Moreover, low-field NMR has been reported to be employed as a non-invasive technique in the study of biofilms due to changes in the relaxation behavior during biofilm formation [31–34].

In addition, diffusion behavior of water determined by pulsed-field gradient NMR (PFG-NMR) at low field

enables the possibility of studying composition of a biofilm matrices, which reveals a viscoelastic behavior due to bonded water [33]. The ^{1}H proton is the most sensitive NMR nucleus and is commonly applied for diffusion studies in biofilms [33]. In addition, dairy products were studied by determining the diffusion behavior of water in dairy gels [35, 36].

Generally, the application of low-field NMR in the characterization of non-food-related biofilms [33, 37] and fouling [34] has shown promising results. However, the low-field ^{1}H NMR detection of bacteria-caused deposition in dairy-processing machines, such as biofilm and biofouling in flexible tubing as multi-component samples, remains lacking. In addition, NMR studies on CIP-cleaning agents used in food industry, such as acid and alkali solutions, have not been published. Despite numerous NMR studies on diffusion coefficients, the estimation of diffusion behavior of water in dairy fouling and in CIP-cleaning agents has not been reported before.

Therefore, the present study investigated the use of low-field ^{1}H NMR for the detection of biofilm and biofouling inside a flexible silicone tubing, as well as for the detection of CIP-cleaning agents. The transverse relaxation times T_2 and diffusion coefficients D_S of sample groups (1) *P. polymyxa* biofilm, (2) dairy biofouling, and (3) CIP-cleaning agents were estimated and compared. The obtained data were analyzed by exponential curve fitting and by inverse Laplace transform. Biochemical and microbiological methods, including ATP-bioluminescence assay, and the determination of colony forming units (CFU), respectively, were used for the validation of chosen deposit models—(1) *P. polymyxa* biofilm and (2) dairy biofouling. Furthermore, *P. polymyxa* biofilm and dairy biofouling identification were visualized by microscopy.

Materials and methods

Chemicals

Commercial UHT milk (3.5% fat) was obtained from the dairy factory Molkerei Weihenstephan GmbH & Co. KG (Freising, Germany). Meat extract, 60% (v/v) nitric acid, and 70% (v/v) ethanol were acquired from VWR (Darmstadt, Germany). Soy peptone was bought from Applichem Panreac (Barcelona, Spain). Plate count agar, 30% (v/v) sodium hydroxide, and 0.01 g/mL crystal violet aqueous solution were purchased from Merck (Darmstadt, Germany). The freeze-dried culture of *P. polymyxa* (DSM 36) was obtained from DSMZ (Braunschweig, Germany). All the reagents and chemicals used were of analytical grade.

Experimental set-up and sample preparation

Experimental set-ups were prepared for two deposit models: (1) *P. polymyxa* biofilm and (2) dairy biofouling. A multichannel peristaltic pump Ismatec® MS-CA 4/640 (Cole-Parmer GmbH, Wertheim, Germany) with a constant rotational speed, pumping capacity, and three tubing connections was used for each experimental set-up. Three silicone tubings of 3 mm inner and 5 mm outer diameters (Deutsch & Neumann, Germany), and of length 2.0 m were used. Silicon tubing, bottle tops, and the connecting elements were pretreated with the following procedure: (I) pre-rinsing with demineralized water, (II) rinsing with ethanol 70% (v/v), and (III) final rinsing with demineralized water. After pretreating, silicon tubing, bottle tops, and connecting elements were autoclaved. The experimental set-up for each deposit model was assembled under the laminar flow cabinet.

Deposit model I—biofilm

For the cultivation of *P. polymyxa* biofilm, a nutrient medium consisting of 3 g/L meat extract and 5 g/L soy peptone was prepared at a pH of 7.0. Before each experiment, 4.250 L of sterile nutrient medium was inoculated with 0.250 L of *P. polymyxa* bacterial suspension at the early exponential phase. To reach the exponential phase of the *P. polymyxa* bacterial suspension, 0.300 L of the nutrient medium was inoculated with a colony of *P. polymyxa* picked from an agar plate using an inoculation loop. The suspension was incubated at 30.0 °C under constant shaking condition at 140 rpm for approximately 3 h. The optical transmission of the bacterial suspension at the early exponential phase measured at 570 nm was $92.2 \pm 0.6\%$. The number of bacteria in the early exponential phase corresponded to 1.14×10^6 CFU/mL.

After the inoculation of a sterile nutrient medium with *P. polymyxa* bacterial suspension, 4.500 L of the prepared liquid was dispensed in two 5.0-L laboratory bottles (Schott, Mainz, Germany). Then, the peristaltic pump was turned on and the inoculated medium was pumped in a closed loop for 4 days at a constant temperature of 30.0 °C and at flow rate of 1.170 L/h. The flow in the silicone tubing was in the laminar range ($Re = 170 - 180$). The pump was turned off overnight, and the temperature was maintained at 30.0 °C. The nutrient medium volume of 4.250 L was exchanged twice during the 4 days to provide an optimal nutritional environment for bacterial growth. NMR data collection of samples (1) clean silicone tubing, (1.2) sterile nutrient medium, (1.3) nutrient medium inoculated with *P. polymyxa* after 4 days of the experimental run, (1.4) *P. polymyxa* biofilm, (1.5) silicone tubing with *P. polymyxa* biofilm on the inner surface, and (1.6) tubing with *P. polymyxa* biofilm on

the inner surface and nutrient medium was performed after the experimental run.

Deposit model II—biofouling

For the dairy biofouling preparation, 4.350 L of commercial UHT milk 3.5% fat was inoculated with 0.150 L of *P. polymyxa* bacterial suspension. The bacterial suspension was prepared in the same way as for *P. polymyxa* biofilm. In total, 4.500 L of the inoculated commercial UHT milk was dispensed in two 5.0-L laboratory bottles and pumped in a closed loop for 4 days at 30 °C at Reynolds number of 130–140, which corresponded to the laminar flow. The pump was turned off overnight, while the temperature was kept constant at 30 °C. NMR data collection of samples (1) clean silicone tubing, (2.2) UHT milk 3.5%, (2.3) UHT milk 3.5% after experimental run, (2.4) dairy biofouling, (2.5) tubing with dairy biofouling, and (2.6) tubing with dairy biofouling and UHT milk 3.5% after experimental run was performed after the experimental run.

To simulate the deposition of a continuous layer, silicone tubing samples were cut to have an access to inner surface of tubing. Afterwards, the viscous dairy biofouling mass (up to 488 mg/cm^2) was spread over the inner surface of the tube. Before each NMR measurement, the silicone tubing with dairy biofouling was placed in a standard NMR sample tube and closed with a resin cap to avoid sample drying.

CIP-cleaning agents

To prepare the samples of CIP-cleaning agents, 30% (v/v) sodium hydroxide and 60% (v/v) nitric acid were diluted to a volume of 1% (v/v), which corresponded to a typical cleaning agent concentration for CIP-cleaning processes. The pH values of 1% (v/v) NaOH and 1% (v/v) HNO_3 were determined as 12.7 ± 0.3 and 1.9 ± 0.2, respectively.

NMR method

Measurement of transverse relaxation time T_2

A Bruker minispec mq 20 NMR Analyzer (Bruker, Rheinstetten, Germany) operating at 20 MHz was used to obtain the transverse relaxation times T_2 for samples of both the deposit models, (1) *P. polymyxa* biofilm, (2) dairy biofouling, and CIP-cleaning agents. The absolute NMR probehead (H20-10-25-A1) was used for the measurements (Bruker, Rheinstetten, Germany). The samples as described in "Experimental set-up and sample preparation" were inserted in standard NMR sample tubes of length 180 mm and diameter 18 mm. To fix the sample in the generated magnet field, a glass insert with an inner diameter of 10 mm and a length of 45 mm with sample was placed into the glass tube. Samples were preconditioned to 40 °C in a tempered water bath for at least 40 min to equilibrate to the operating temperature. The NMR measurements were controlled with Minispec Software V2.59 Rev.06/NT/XP (Bruker, Rheinstetten, Germany). A Carr–Purcell–Meiboom–Gill pulse sequence (CPMG) was applied to determine the transverse relaxation times T_2. The NMR instrument was calibrated using a standard solution E1405295 (Bruker, Rheinstetten) to set the correct 90° and 180° pulse lengths. The instrument operated with a probe dead time of approximately 7 µs, magnet temperature of 40 °C, 90° pulse length of 2.96 µs and 180° pulse length of 5.78 µs. Data were acquired using the software application "t2_cp_mb" provided by the manufacturer. The first 90° pulse excites the spin system, and the following 180° pulse induces multiple gradient-echo sequences. The signal amplification was selected on the basis of a signal intensity of 70–80% for the initial intensity of the sequence echoes. Other measurement parameters included: eight scans; 5-s (for biofilm and biofouling samples) and 10-s (for CIP-cleaning agent samples) recycle delay; 1 ms of 90°–180° pulse separation (tau); 21 dB of pulse attenuation; 60 dB gain; and 4000–6000 data points.

Measurement of diffusion coefficient D_S

Measurements of diffusion coefficient D_S were performed with the Bruker minispec mq 20 NMR Analyzer operating at 20 MHz and equipped with a controlled pulsed gradient unit. The gradient pluses are applied between the two RF pulses (90° and 180° pulses), and between the second RF pulse and the spin-echo. The length of a gradient pulse is described by δ, their separation by the diffusion time Δ and their amplitude by $G(t)$. The variable temperature probe head H20-10-25-AVXG (Bruker, Rheinstetten, Germany) was suitable for 10-mm sample tubes and was operated at 20 °C. The samples were placed in standard glass tubes of length 180 mm and an inner diameter of 10 mm (Bruker, Rheinstetten, Germany). Samples were preconditioned to 20 °C in a tempered water bath for at least 40 min to equilibrate to the operating temperature. The samples were measured with a software application "*diffusio*" for the determination of the diffusion coefficients D_S. Before measurement, the gradient pulse G was calibrated for a number of different amplitude settings using a standard solution 1.25 g/L $CuSO_4 \times 5\ H_2O$ with known diffusion coefficient. The measurements were repeated nine times for each sample, with the following measurement settings: 16 scans, 2 s of recycle delay, 59 dB gain, gradient pulse width $\delta = 0.5$ ms, diffusion time $\Delta = 7.5$ ms (separation of the gradient pulses) and the range of gradient amplitude $G(t) = 2.5$ T/m.

Microbiological investigation

ATP-bioluminescence assay

The ATP + AMP Hygiene Monitoring test kit consisting of the Lumitester™ PD-30 and LuciPac™ Pen (Kikkoman Biochemifa Company, Japan) was used to perform the ATP-bioluminescence assay. For liquid samples such as milk and bacterial suspension, the swab stick was removed from the main body and soaked in the liquid sample. For the silicone tubing surface, the swab stick was removed from the main body and wetted with sterile demineralized water. Then, the swab stick was wiped with a constant pressure over a surface of 1 cm^2. When the swab stick was saturated, it was returned into the main body. Pushing the stick firmly into the container of the main body, the tested reagent was released into the luminescent reagent. The test tubing was shaken until the powdery luminescent reagent was completely dissolved. Then, the swab stick was inserted into the optical luminescence device and the measurement was performed within 10 s. The result is given in relative light units (RLU).

Determination of colony forming units (CFU)

The determination of colony forming units (CFU) was performed for the verification of bacteria adhesion to the inner surface of silicone tubing. For the CFU determination of *P. polymyxa* biofilms and dairy biofouling, three tube samples of length 5.0 cm were carefully cut from three different positions of the tubing after the experimental run, which was prepared as described in "Experimental set-up and sample preparation". The silicon tube samples were bisected and inserted into glass tubes filled with 4.5 mL of sterile nutrient medium. To remove the deposit of the inner surface, the samples were vortexed for 5 min. Serial log dilutions were prepared by mixing 0.5 mL of the stock solution with 4.5 mL of sterile nutrient medium. Subsequently, the dilution factors from 10^{-1} to 10^{-6} were prepared. Each dilution (0.1 mL) was plated on the plate count agar plates and incubated for 24 h at 30 °C. After the incubation, the CFU number on the agar plate was counted. The CFU values were expressed in CFU/cm^2 and calculated according to the relation described previously [5].

Microscopy

Microscopic images of the clean silicone tubing were obtained with a digital microscope (Keyence VHX-1000, Japan) with the objectives ZS200 at a magnification of 1000× and ZS20 at a magnification of 150×. Microscopic images of deposit thickness were obtained using the transmitted light microscope (Kern OBN 135, Kern & Sohn GmbH, Germany). The samples were observed at magnification of 20× without oil after 10 min of staining with 10 µL of crystal violet solution (0.01 g/100 mL) at room temperature.

Data analysis and statistics

For each sample as described in "Experimental set-up and sample preparation", three NMR tubes with a sample were prepared. Each tube was used for the relaxation time measurements. Three measurements of the CPMG pulse sequence were performed for each NMR tube. Inverse Laplace transform was applied to NMR data to obtain the distribution of transverse relaxation times T_2 (MatlabR2017b, MathWorks, Inc., USA). For inverse Laplace transform, the application (*rilt*) regularized inverse Laplace transform [*g, yfit, cfg*]=*rilt* (*t, y, s,* g_0*, alpha*) was used [38]. The quality of the inverse Laplace transform was judged on the basis of the sum of the error squares (SSE) and the coefficient of determination (R^2) for each fitting. Significant differences between diffusion coefficients in each sample group were calculated using one-way analysis of variance for independent samples at significance level of $p \leq 0.05$.

Results and discussion

T_2 of sample group (I) *P. polymyxa* biofilm

Table 1 presents the transverse relaxation times and statistics for samples in the experimental set-up of deposit model I (*P. polymyxa* biofilm) obtained by the inverse Laplace transform.

The T_2 value of the clean silicone tubing was determined to be 6.01 ms. The value was located at shorter relaxation times, which are typical for rubbery materials. T_2 values at longer relaxation times of 2243 ms were obtained for the (1.2) sterile nutrient medium and of 2849 ms for the (1.3) inoculated nutrient medium (Table 1). Slower relaxation rates indicate a large amount of free water in the samples. Two shorter and longer T_2 values were obtained for the *P. polymyxa* biofilm, sample (1.4). These data indicate a decrease in the free water content and, thus, the formation of gel-like components such as EPS in *P. polymyxa* biofilm [39]. In the sample (1.5), silicone tubing with *P. polymyxa* biofilm, the T_2 (2) of the biofilm component was shorter when compared to the single *P. polymyxa* biofilm, sample (1.4). The changes in the relaxation behavior may be attributed to the lower amount of biofilm and the high roughness of the silicone tubing (Fig. 1), which could have led to the interactions between biofilm and inner surface of the silicone tubing. The results of the sample (1.6), tubing with *P. polymyxa* biofilm and nutrient medium, which is a three-component system, exhibited characteristic

Table 1 The peaks of transverse relaxation times T_2 obtained by the inverse Laplace transform as well as statistics for the samples in the experimental set-up of deposit model I (*P. polymyxa* biofilm)

Sample	Inverse Laplace transform			
	T_2 (1) (ms)	T_2 (2) (ms)	SSE	R^2
(1) Clean tubing	6.01	–	1.99	0.999
(1.2) Sterile nutrient medium	2243	–	1.49	0.999
(1.3) Nutrient medium inoculated with *P. polymyxa* (after experimental run)	2849	–	3.69	0.999
(1.4) *P. polymyxa* biofilm	164.5	1382	63.7	0.999
(1.5) Tubing with *P. polymyxa* biofilm	6.02	46.15	148.7	0.921
(1.6) Tubing with *P. polymyxa* biofilm and nutrient medium	12.8	2558	318.9	0.997

SSE sum of the error squares, R^2 coefficient of determination

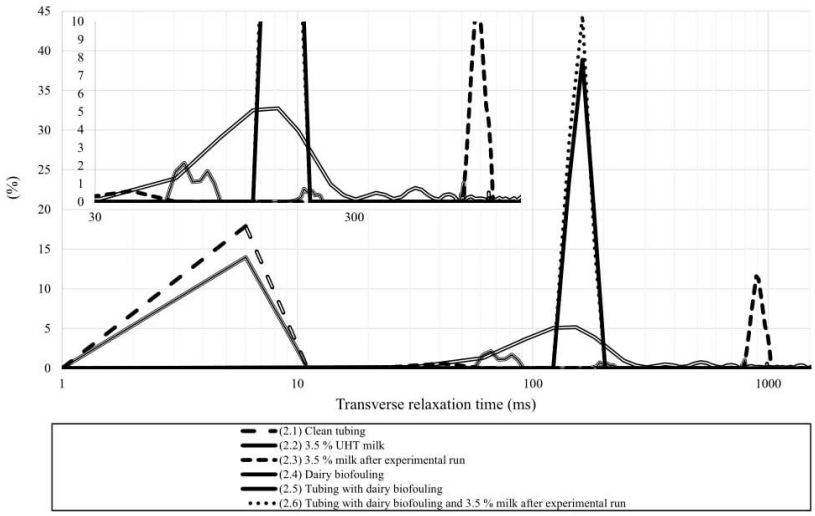

Fig. 1 Distribution of transverse relaxation time T_2 obtained for experimental set-up II (biofouling): (2.1) clean silicone tubing, (2.2) 3.5 % UHT milk as purchased and used for biofouling formation, (2.3) 3.5 % UHT milk obtained after the experimental run, (2.4) dairy biofouling, (2.5) silicone tubing with dairy biofouling, (2.6) silicone tubing with dairy biofouling and 3.5% UHT milk after the experimental run

relaxation times for a rubbery material and a liquid component. However, with selected measurement settings it was not possible to detect the characteristic T_2 values of biofilm that are usually observed at 40–400 ms. All the coefficients of determination R^2 were close to 1.0, which showed a good fit. The highest sum of the error squares (SSE) was obtained for sample (1.6), which may have been caused by different thicknesses of biofilm in the tubing ("Microscopy").

The ATP-bioluminescence of clean silicone tubing at the room temperature of 22.5 °C was $5.8\times10^1\pm1.0\times10^1$ RLU/cm^2 ($n=9$). The ATP mean of *P. polymyxa* biofilm on the surface of silicone tubing increased to $1.0\times10^4\pm0.4\times10^4$ RLU/cm^2 ($n=3$). The number of colony forming units was obtained as $9.0\times10^5\pm3.6\times10^5$ CFU/cm^2 ($n=3$). The results of the ATP-bioluminescence assay and the colony forming unit determination indicated a clear tendency for biofilm formation in the silicone tubing during the experimental run. Figure 4 shows the biofilm distribution on the inner surface of the tubing.

Several studies have shown that the transverse relaxation times T_2 of a biofilm are up to an order of magnitude lower than that of the free water phase [32, 34, 40]. A past study demonstrated that a low-field NMR sensitively detects changes in the pattern of transverse relaxation time T_2 due to biofilm accumulation in the reactor pores [39]. As reported in the literature, the component with the highest T_2 value (mean value > 1000 ms) could be defined as free water. The shorter relaxation times can be assigned to biofilm, since it consists of bound water and is located near the tubing walls [40].

T_2 of sample group (II) of dairy biofouling

The transverse relaxation time and its distribution for samples in the experimental set-up for deposit model II-dairy biofouling are presented in Table 2 and Fig. 1, respectively.

The purchased sterile UHT milk showed T_2 value (1) of 152.5 ms, as obtained by inverse Laplace transform. The inoculated UHT milk after experimental run, sample (2.3),

Table 2 The peaks of transverse relaxation times T_2 obtained by the inverse Laplace transform as well as statistics for samples in the experimental set-up of deposit model II (dairy biofouling)

Sample	Inverse Laplace transform[a]				
	T_2 (1) (ms)	T_2 (2) (ms)	T_2 (3) (ms)	SSE	R^2
(1) Clean tubing	6.01	–	–	1.99	0.999
(2.2) UHT milk 3.5%	152.5	–	–	3.86	0.999
(2.3) UHT milk 3.5% after experimental run	41.4	909.6	–	0.300	0.999
(2.4) Dairy biofouling	152.5	–	–	0.012	0.999
(2.5) Tubing with dairy biofouling	6.04	66.3	795.0	15.7	0.998
(2.6) Tubing with dairy biofouling and UHT milk 3.5% after experimental run	162.5	–	–	4.06	0.999

SSE sum of the error squares, R^2 coefficient of determination

[a]The T_2 distribution of the samples is shown in Fig. 1

exhibited two relaxation times at slower and faster relaxation rates. This can be attributed to the structural changes in milk due to increased temperature and the presence of *P. polymyxa* in milk during the experimental run. The T_2 (1) value could be assigned to gel-like components, such as denatured proteins, while the T_2 (2) value could be assigned to a milk serum that is a liquid component. The T_2 values of dairy biofouling were 152.5 ms. When dairy biofouling was present on the surface of the silicone tubing, sample (2.5), the T_2 (2) of dairy biofouling shifted towards shorter relaxation times, when compared with that of a single biofouling, sample (2.4). The T_2 (3) value of 795 ms of sample (2.5) could be assigned to the drained milk serum, which was accumulated on the bottom of the sample tube. For multi-component sample, sample (2.6), only one peak T_2 was obtained at approximately 160 ms (Fig. 1). All the coefficients of determination R^2 were close to 1.0, which showed a good fit. The lowest coefficient of determination R^2 was 0.998 for sample (2.5) tubing with dairy biofouling, and, accordingly, the highest SSE of 15.7 was noted for this sample. The high sum of the error squares may have been caused by the non-homogeneous distribution and thicknesses of dairy biofouling in the silicone tubings.

The ATP mean of dairy biofouling on the surface of silicone tubing increased to $2.93 \times 10^3 \pm 0.68 \times 10^3$ RLU/cm^2 ($n = 3$) compared to the reference value of $5.8 \times 10^1 \pm 1.0 \times 10^1$ RLU/cm^2 ($n = 9$). The mean of the CFU determination of dairy biofouling in silicone tubing was $7.0 \times 10^5 \pm 2.6 \times 10^5$ CFU/cm^2 ($n = 3$). These results confirm the biofouling formation in the silicone tubing during the experimental run. The ATP and CFU values of dairy biofouling on the surface of silicone tubes were similar when compared with the values obtained in the experimental set-up for *P. polymyxa* biofilm ("T_2 of sample group (I) *P. polymyxa* biofilm").

Figure 1 shows the distribution of transverse relaxation time for samples listed in Table 2.

From Fig. 1, it can be seen that the T_2 distributions can be divided into three different ranges of relaxation time, each reflecting the relaxation behavior of (i) solid-like, (ii) gel-like, and (iii) liquid components. The T_2 distribution of dairy biofouling, sample (2.4), showed a broad peak centered between approximately 60 and 280 ms. Comparatively, the signal of dairy biofouling, sample (2.4), was much wider than the signal peak of UHT milk before and after the experimental run (Fig. 1). The signal broadening, which indicates the changes in the relaxation behavior, could be related to the complex composition of dairy biofouling. The shorter relaxation time compared to the bulk liquid can be attributed to the water protons and macromolecule exchangeable protons trapped in the gel [36]. It can be observed that the T_2 distribution of the two component system, sample 2.5, exhibits distinct relaxation times for the silicone tubing part and the dairy biofouling part at slower and faster relaxation rates, respectively. The presence of a gel-like components from biofouling in the silicone tubing leads to a shorter relaxation time T_2 of the biofouling. The obtained results suggest that interactions occur between solid-like (rubber material) and gel-like phases (biofouling). The one-component liquid samples (2.2) and (2.3) revealed the relaxation times at slower relaxation rates, which indicated that these samples do not contain bound water. Notably, a small peak for UHT milk was detected after the experimental run at approximately 40 ms, which most likely originates from the protein aggregation during the experimental run. The T_2 relaxation time of liquid components was longer and in agreement with literature report, indicating high T_2 for liquids due to the high mobility of water [41].

NMR measurements of manually added dairy biofouling

Table 3 shows the results of the determination of T_2 for samples with manually added amount of dairy biofouling as described in "Experimental set-up and sample preparation" onto the inner surfaces of silicone tubing.

The obtained relaxation time of the silicone tubing with an increased amount of dairy biofouling (up to 406 mg/cm^2) onto

Table 3 The peaks of transverse relaxation time T_2 of samples with increasing amount of manually applied dairy biofouling (deposit model II) onto the inner surface of the silicone tubing as well as statistics obtained by the inverse Laplace transform

Sample	Biofouling (mg/cm^2)	Inverse Laplace transform					
		T_2 (1) (ms)	T_2 (2) (ms)	T_2 (3) (ms)	T_2 (4) (ms)	SSE	R^2
Clean tubing	0	6.01	–	–	–	1.99	0.999
Tubing with manually applied biofouling[a]	69.7	6.04	56.4	66.5	71.6	0.538	0.998
	169.7	6.04	66.5	76.6	86.7	0.851	0.998
	297.1	6.04	71.6	86.7	101.8	0.694	0.999
	406.2	6.04	86.7	91.7	111.9	0.611	0.999
	488.1	6.04	66.5	86.7	106.9	0.734	0.999

SSE sum of the error squares, R^2 coefficient of determination

[a]An amount of dairy biofouling manually applied onto the inner surface of the silicone tubing

the inner surface of the tubing revealed a characteristic relaxation response and can be separated into two distinctive signal groups: (1) relaxation time of the silicone tubing and (2) one or several relaxation times of biofouling. The obtained results demonstrated that with increasing amount of biofouling on the inner surface of the silicone tubing, the transverse relaxation times [T_2 (1), T_2 (2), and T_2 (3)] of biofouling shifted towards slower relaxation rates. Multiple relaxation times can be explained by the complex structure of biofouling, which can be reflected by inverse Laplace transform. Notably, the application of a larger amount of dairy biofouling, for example, 488.1 mg/cm^2, led again to faster relaxation rates of biofouling compared to the T_2 of sample with 406.2 mg/cm^2 of biofouling (Table 3).

For the better depiction of T_2 dependency on the added amount of biofouling, the reader is referred to Fig. 2a, b.

In Fig. 2, the shift in the relaxation time toward slower relaxation rates can be observed for the dairy biofouling component with an increasing amount of manually added biofouling. The logarithmic fitting of the data showed a good fit for the experimental data from Table 3, exhibiting a high coefficient of determination R^2. It can be deducted that the shift in the transverse relaxation time of biofouling onto the inner surface of a tubing is not linearly dependent on the biofouling amount.

To explain this behavior, the authors suppose that the increasing amounts of biofouling on the inner surface of the tubing shift the relaxation times toward longer T_2 values due to additional free water molecules introduced into the system. Slower relaxation rates indicate a more water-like behavior, which could be achieved with the higher amount of biofouling inside the same tubing geometry. A comparison of the samples in Table 3 confirms an increase in the proportion of protons experiencing slower relaxation rates, what can be expected due to an increased amount of biofouling.

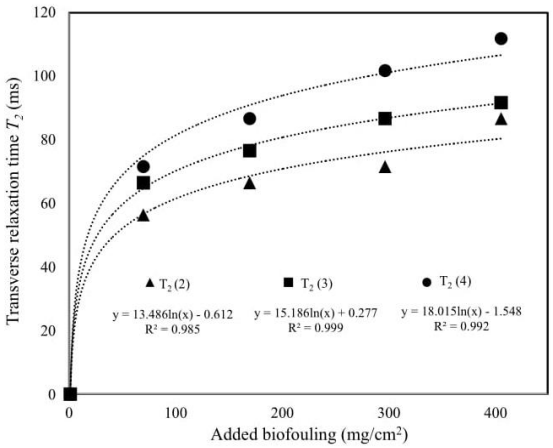

Fig. 2 The logarithmic curve fitting of the transverse relaxation times of biofouling [due to the fact that biofilm amount of 488.1 mg/cm^2 led to shorter relaxation times, these data were not considered for the fitting. The additional amount of biofouling displaced the biofouling layer partially, which led to the shorter T_2 (2), T_2 (3), and T_2 (4) values (Table 3)] as a function of the biofouling amount was determined by the inverse Laplace transform. The curves do not show the transverse relaxation time of silicone tubing

NMR measurements of CIP-cleaning agents

Table 4 presents the transverse relaxation time T_2 of CIP-cleaning agents, 1% (v/v) nitric acid, and 1% (v/v) sodium hydroxide.

Demineralized water, 1% (v/v) nitric acid, and 1% (v/v) sodium hydroxide revealed transverse relaxation times at slower relaxation rates (Table 4). From Table 4, it can be noted that demineralized water has in total shorter relaxation time compared to the CIP-cleaning media, while both 1% (v/v) nitric acid and 1% (v/v) sodium hydroxide had rather similar relaxation behavior, but slightly longer relaxation rates were observer for 1% (v/v) nitric acid.

To the best of our knowledge, to date, no studies have been reported on low-field ^{1}H NMR measurement of

Table 4 The peaks of transverse relaxation times T_2 obtained by the mono-exponential curve fitting as well as statistics for CIP-cleaning agents at 40 °C ($n=3$, $i=9$ for every type of cleaning agent)

Sample	Sample number	Mono-exponential fitting		
		T_2 (1) (ms)	SSE	R^2
H_2O	1	3010	277.3	0.999
	2	3025	292.4	0.999
	3	3050	140.5	0.999
HNO_3 1%	1	3744	124.0	0.999
	2	3780	111.5	0.999
	3	3843	53.7	0.999
NaOH 1%	1	3684	105.5	0.999
	2	3719	108.2	0.999
	3	3773	108.2	0.999

SSE sum of the error squares, R^2 coefficient of determination

Table 5 Diffusion coefficient D_S and standard deviation obtained at 20 °C ($n=18$)

Group	Sample	Diffusion coefficient D_S ($10^{-9} \times m^2/s$)
1	*P. polymyxa* biofilm	1.71 ± 0.04^{abc}
	Nutrient medium sterile	2.30 ± 0.06^{ba}
	Nutrient medium inoculated with *P. polymyxa*	2.26 ± 0.09^{ca}
2	Dairy biofouling	1.51 ± 0.03^{abc}
	UHT milk sterile	1.75 ± 0.07^{ba}
	UHT milk inoculated with *P. polymyxa*	1.86 ± 0.04^{ca}
3	Demineralized water	2.27 ± 0.04^{abc}
	Nitric acid 1% (v/v)	2.07 ± 0.00^{abc}
	Sodium hydroxide 1% (v/v)	1.94 ± 0.00^{abc}

[a,b,c]Significant difference among the samples in the groups with $p<0.05$ (one-way ANOVA, Tukey HSD test)

CIP-cleaning agents. Our results indicate that low-field NMR allows differentiation of standard CIP-cleaning agents from water at a temperature of 40 °C due to the characteristic transverse relaxation times. However, since the temperature of CIP-cleaning media during the CIP-cleaning process occurs at approximately 70–90 °C, it would be advantageous to investigate the CIP-cleaning media at these temperatures. In food-processing equipment, CIP-cleaning process is usually monitored by pH and conductivity sensors. However, the range of application of these sensors is limited, e.g., pH and conductivity sensors cannot detect the formation of any deposit on food-contact surfaces. Development of a sensor based on low-field ^{1}H NMR for real-time monitoring would enable both deposit formation and CIP process monitoring in real time. After the development of low-field ^{1}H NMR sensor, a study of the effect of CIP agents on the cleaning different deposits should be performed in real time in processing equipment.

Diffusion coefficients

Table 5 depicts the diffusion coefficients D_S of water for samples from three sample groups, (1) *P. polymyxa* biofilm, (2) dairy biofouling, and (3) CIP-cleaning agents, obtained using PFG-NMR at low field.

The results shown in Table 5 demonstrate that significant differences were found between the samples in each group. In the first sample group, (1) *P. polymyxa* biofilm, the diffusion coefficient of water in *P. polymyxa* biofilm of $1.71 \pm 0.04 \times 10^{-9}$ m^2/s was significantly lower, when compared to the nutrient medium before and after inoculation with diffusion coefficients of 2.26×10^{-9} and 2.30×10^{-9} m^2/s, respectively. In the next sample group, (2) dairy biofouling, significant differences in diffusion coefficient were found between dairy fouling of 1.51×10^{-9} m^2/s and UHT before and after inoculation with the diffusion coefficients of 1.75×10^{-9} and 1.86×10^{-9} m^2/s, respectively. In addition, it can be noticed that the diffusion coefficient of *P. polymyxa* biofilm was significantly different from that of dairy fouling. The results obtained are also in accordance with the obtained transverse relaxation time values of both the deposits (biofilm and biofouling). The T_2 was found at faster relaxation rates when compared with the corresponding bulk liquid. In the last sample group, (3) CIP-cleaning agents, the diffusion coefficients of water in demineralized water, 1% (v/v) nitric acid, and 1% (v/v) sodium hydroxide revealed significant differences between each sample. The diffusion coefficient of demineralized water was 2.27×10^{-9} m^2/s, which is similar to that of water in nutrient medium. Nitric acid 1% (v/v) and 1% (v/v) sodium hydroxide revealed diffusion coefficient of 2.07×10^{-9} and 1.94×10^{-9} m^2/s, respectively. When compared with *P. polymyxa* biofilm and dairy biofouling with demineralized water, the diffusion coefficient of water in dairy biofouling and in microbial biofilm matrix corresponded to approximately 65% and 75% of the value in pure water, respectively.

The diffusion behavior of water in biofilm can be explained by the fact that biofilm is composed of bacterial cells in a matrix of extracellular polymeric substances (EPS), which is a hydrated gel matrix. Since the EPS matrix restrains the diffusion of mobile water, the relaxation time T_2 of water contained in the biofilm is shorter than that for free water alone [33, 39]. Water mobility in dairy biofouling may be reduced due to biofouling composition and structure. The components mainly responsible for dairy biofouling on the food-contact surfaces are calcium phosphate and proteins, particularly whey protein. Dairy biofouling formed at lower temperatures is described as soft and bulky, and is composed mainly of proteins [42]. Thus, the water content of

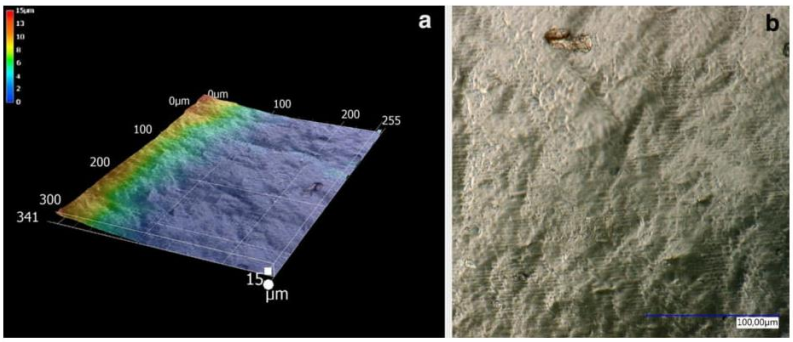

Fig. 3 Micrographs of the clean inner surface of silicone tubing. The samples were recorded **a** with the objective ZS20 at 150× magnification and **b** with the objective ZS200 at 1000× magnification without oil

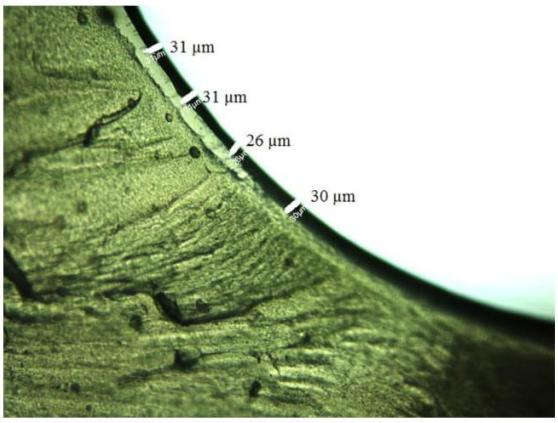

Fig. 4 The thickness of *P. polymyxa* biofilm at four different points at the cross section of the inner surface of the silicone tubing, stained with crystal violet solution (0.01 g/100 mL). The magnification of image 20× without oil

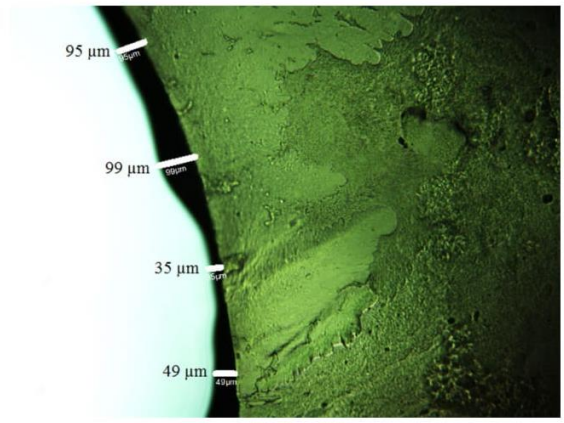

Fig. 5 The thickness of dairy biofouling at four different points at the cross section of the inner surface of the silicone tubing, stained with crystal violet (0.01 g/100 mL). The magnification of image was 20× without oil

dairy biofouling is expected to be lower than that of biofilm, which may explain the difference in the diffusion coefficient between both the deposits. Thus, NMR can be used to determine the diffusion coefficients of water in both biofilm and biofouling. Although the determination in diffusion coefficient in CIP-cleaning agents was not reported earlier, the present results demonstrate that diffusion coefficients may provide some practical significance for the detection of CIP-cleaning agents.

Microscopy

Figure 3 illustrates the images of clean silicone tubing for the experimental set-ups in this work.

Figure 4 shows the image of the cross section of inner silicone tube surface with *P. polymyxa* biofilm.

Figure 4 illustrates that the biofilm on the tubing surface had an inhomogeneous structure. According to figure, the thickness of biofilm layer ranged between 26 and 31 µm. However, it should be also considered that biofilm thickness may vary strongly along the silicone tubing since the biofilm growth and distribution on surfaces is usually non-homogenous.

Figure 5 shows the image of the cross section of inner silicone tube surface with dairy biofouling.

Figure 5 shows that the thickness of dairy biofouling layer on the silicone tube surface ranged from 35 to 100 µm, indicating non-homogenous distribution of biofouling.

Practical implications of low-field NMR and further studies

The development of on-line techniques has increased the value of NMR as a non-invasive method for process development applications. Small low-field NMR systems equipped with permanent magnets are available for quantitative analysis in quality control as on-line instruments in production environments [43].

The advantages of low-field NMR compared to high-resolution NMR relay on the lower requirements of

environmental parameters, staff, maintenance, and investment costs [43]. For these reasons, low-field NMR technique provides a cost-efficient and small size alternative for non-invasive on-line monitoring tool when comparing with high-field NMR [27].

On-line monitoring of bacteria-caused deposit formation as well as cleaning processes by NMR sensor has a great benefit for the monitoring for food-processing processes. The results obtained in this study can be used for the development of real-time monitoring systems based on low-field ^{1}H NMR. This study shows that the low-field ^{1}H NMR results revealed a characteristic relaxation behavior of one and two-component samples in the sample groups (1) *P. polymyxa* biofilm, (2) dairy biofouling, and (3) CIP-cleaning agents. The analysis of the NMR signal decay curves produced a statistical distribution of the transverse relaxation time T_2, which is related to molecular interactions occurring among excited water molecules and their interactions. Due to the restricted mobility in the biofilm, the transverse relaxation time values of the water molecules inside biofilm and biofouling are reduced compared to those of bulk liquid. In addition, the measurements of diffusion coefficient in samples implement the results of transverse relaxation times, which reflect the relaxation behavior of water. This finding can be used for the further development of a low-field ^{1}H NMR sensor.

Based on the results of this study, it is evident that each investigated component (e.g., tubing, deposit, and bulk liquid) has a different relaxation behavior. It is assumed that the interactions between differently structured components can occur, which may influence the relaxation behavior of each component. Thus, the interpretation of relaxation time parameters is difficult because relaxation involves several mechanisms, such as chemical exchange, cross-relaxation, and diffusive exchange between different water populations [36]. Furthermore, the major difficulty with the multi-component systems from an NMR perspective is the fact that the relaxation cannot be described by a single component, necessitating the use of advance a statistical analysis.

Most NMR relaxation data are characterized by a complex structure, with both compositional and spatial information [44]. The optimal extraction of information from such data structures requires the use of advanced statistical data analysis techniques. A study of Santos et al. used both exponential fitting and inverse Laplace transform to obtain T_2 values measured using NMR to detect olive oil adulteration with polyunsaturated vegetable oils in filled bottles [45]. Similar T_2 values were obtained from exponential fitting compared to inverse Laplace transform. In addition, in a study of Kim and Kim, the NMR relaxation signals were analyzed with both exponential curve fitting and inverse Laplace transform primarily obtained by a portable NMR-based system to detect food-borne pathogens. Also in the study, the calculated values by exponential curve fitting and inverse Laplace transform did not demonstrate any significant difference in the value [46].

For further measurements, the NMR sensitivity has to be improved to obtain significant results for samples with extremely low amount of deposits. From the perspective of food-processing technology, it is necessary to prove the possibility of NMR detection at different temperature ranges, such as the temperature of the filling process (10–20 °C) or temperature of the cleaning process (60–90 °C). As an additional step, the deposit detection under flow conditions is necessary to evaluate the suitability of the use of low-field NMR for real-time monitoring. Moreover, a low-field NMR sensor for process monitoring should be integrable in high-risk zones.

Conclusion

The results indicate that low-field ^{1}H NMR can be recommended to detect bacteria-caused deposits (biofilm and dairy biofouling) as well as CIP-cleaning agents. The characteristic relaxation behavior and diffusion behavior of water were shown for selected deposit types and CIP-cleaning agents. Moreover, the results revealed that NMR can detect deposition on the inner tubing surface by assigning distinct relaxation times to each component. Therefore, low-field NMR can be used to enhance the understanding of bacteria-caused deposit accumulation and their cleaning. Also, the obtained results can be used for the development of real-time monitoring systems based on low-field ^{1}H NMR.

Acknowledgements This research did not receive any specific grant from funding agencies in the public, commercial, or not-for-profit sectors. The authors thank Prof. Dr. Bernd Wilke for beneficial discussions.

Compliance with ethical standards

Conflict of interest The authors declare that they have no conflict of interest.

Compliance with ethics requirements This article does not contain any studies with human or animal subjects.

References

1. Cappitelli F, Polo A, Villa F (2014) Biofilm formation in food processing environments is still poorly understood and controlled. Food Eng Rev 6:29–42
2. Marchand S, De Block J, De Jonghe V, Coorevits A, Heyndrickx M, Herman L (2012) Biofilm formation in milk production and processing environments: influence on milk quality and safety. Compr Rev Food Sci Food Saf 11:133–147

3. Srey S, Jahid IK, Ha S-D (2013) Biofilm formation in food industries: a food safety concern. Food Control 31:572–585
4. Bower CK, McGuire J, Daeschel MA (1996) The adhesion and detachment of bacteria and spores on food-contact surfaces. Trends Food Sci Technol 7:152–157
5. Lewandowski Z, Beyenal H (2013) Fundamentals of biofilm research, 2nd edn. CRC Press, Taylor and Francis Group, Boca Raton
6. Chmielewski RAN, Frank JF (2003) Biofilm formation and control in food processing facilities. Compr Rev Food Sci Food Saf 2:22–32
7. Storgards E, Simola H, Sjoberg A-M, Wirtanen G (1999) Hygiene of gasket materials used in food processing equipment part 2. Trans IChemE. https://doi.org/10.1205/096030899532295
8. Vert M, Doi Y, Hellwich K-H, Hess M, Hodge P, Kubisa P, Rinaudo M, Schué F (2012) Terminology for biorelated polymers and applications (IUPAC Recommendations 2012). Pure Appl Chem 84:377–410
9. Simões M, Simões LC, Vieira MJ (2010) A review of current and emergent biofilm control strategies. LWT Food Sci Technol 43:573–583
10. Derlon N, Gruetter A, Brandenberger F, Sutter A, Kuhlicke U, Neu TR, Morgenroth E (2016) The composition and compression of biofilms developed on ultrafiltration membranes determine hydraulic biofilm resistance. Water Res 102:63–72
11. Teh KH, Flint S, Brooks J, Knight G (2015) Biofilms in the dairy. Wiley, London. https://doi.org/10.1002/9781118876282
12. Grady EN, MacDonald J, Liu L, Richman A, Yuan Z-C (2016) Current knowledge and perspectives of *Paenibacillus*: a review. Microb Cell Fact 15:203
13. De Jonghe V, Coorevits A, De Block J, Van Coillie E, Grijspeerdt K, Herman L, De Vos P, Heyndrickx M (2010) Toxinogenic and spoilage potential of aerobic spore-formers isolated from raw milk. Int J Food Microbiol 136:318–325
14. Romney AJD (ed) (1990) CIP: cleaning in place, 2nd edn. The Society of Dairy Technology, Huntingdon
15. van Asselt AJ, van Houwelingen G, Te Giffel MC (2002) Monitoring system for improving cleaning efficiency of cleaning-in-place processes in dairy environments. Food Bioprod Process 80:276–280
16. Bremer PJ, Fillery S, McQuillan AJ (2006) Laboratory scale Clean-In-Place (CIP) studies on the effectiveness of different caustic and acid wash steps on the removal of dairy biofilms. Int J Food Microbiol 106:254–262
17. Sharma M, Anand S (2002) Biofilms evaluation as an essential component of HACCP for food/dairy processing industry—a case. Food Control 13:469–477
18. Kim YW, Sardari SE, Meyer MT, Iliadis AA, Wu HC, Bentley WE, Ghodssi R (2012) An ALD aluminum oxide passivated surface acoustic wave sensor for early biofilm detection. Sens Actuators B Chem 163:136–145
19. Reyes-Romero DF, Behrmann O, Dame G, Urban GA (2014) Dynamic thermal sensor for biofilm monitoring. Sens Actuators A 213:43–51
20. Kwak YH, Lee J, Lee J, Kwak SH, Oh S, Paek S-H, Ha U-H, Seo S (2014) A simple and low-cost biofilm quantification method using LED and CMOS image sensor. J Microbiol Methods 107:150–156
21. Crattelet J, Ghnimi S, Debreyne P, Zaid I, Boukabache A, Esteve D, Auret L, Fillaudeau L (2013) On-line local thermal pulse analysis sensor to monitor fouling and cleaning: application to dairy product pasteurisation with an ohmic cell jet heater. J Food Eng 119:72–83
22. Janknecht P, Melo LF (2003) Online biofilm monitoring. Rev Environ Sci Biotechnol 2:269–283
23. Wallhäußer E, Hussein MA, Becker T (2012) Detection methods of fouling in heat exchangers in the food industry. Food Control 27:1–10
24. Callaghan PT (1991) Principles of nuclear magnetic resonance microscopy. Clarendon Press, Oxford
25. Marcone MF, Wang S, Albabish W, Nie S, Somnarain D, Hill A (2003) Diverse food-based applications of nuclear magnetic resonance (NMR) technology. Food Res Int 51:729–747
26. Hills BP, Manning CE, Godward J (1999) A multi state theory of water relations in biopolymer systems. In: Fourth international conference on applications of magnetic resonance. https://doi.org/10.1533/9781845698133.2.45
27. Todt H, Guthausen G, Burk W, Schmalbein D, Kamlowski A (2006) Water/moisture and fat analysis by time-domain NMR. Food Chem 96:436–440
28. Kirkland CM, Codd SL (2018) Low-field borehole NMR applications in the near-surface environment. Vadose Zone J 17:1–11
29. Kirtil E, Cikrikci S, McCarthy MJ, Oztop MH (2017) Recent advances in time domain NMR and MRI sensors and their food applications. Curr Opin Food Sci 11:9–15
30. Wolter B, Krus M (2005) In: Kupfer K (ed) Moisture measuring with nuclear magnetic resonance (NMR). Electromagnetic aquametry. Springer, Berlin
31. Maher AD, Rochfort SJ (2014) Applications of NMR in dairy research. Metabolites 4:131–141
32. Hoskins BC, Fevang L, Majors PD, Sharma MM, Georgiou G (1999) Selective imaging of biofilms in porous media by NMR relaxation. J Magn Reson 139:67–73
33. Vogt M, Flemming H-C, Veeman WS (2000) Diffusion in *Pseudomonas aeruginosa* biofilms: a pulsed field gradient NMR study. J Biotechnol 77:137–146
34. Fridjonsson EO, Vogt SJ, Vrouwenvelder JS, Johns ML (2015) Early non-destructive biofouling detection in spiral wound RO membranes using a mobile earth⁄$ field NMR. J Membr Sci 489:227–236
35. Belloque J, Ramos M (1999) Application of NMR spectroscopy to milk and dairy products. Trends Food Sci Technol 10:313–320
36. Mariette F (2001) NMR relaxation of dairy products. In: Webb GA (ed) Modern magnetic resonance, 1st edn. Springer, New York
37. Kirkland CM, Hiebert R, Phillips A, Grunewald E, Walsh DO, Seymour JD, Codd SL (2015) Biofilm detection in a model wellbore environment using low-field NMR. Groundw Monit Remediat 35:36–44
38. rilt Regularized Inverse Laplace Transform 1.0.0.0 (4.39 KB) by Iari-Gabriel Marino (2007). https://de.mathworks.com/matlabcentral/fileexchange/6523-rilt
39. Kirkland CM, Herrling MP, Hiebert R, Bender AT, Grunewald E, Walsh DO, Codd SL (2015) In situ detection of subsurface biofilm using low-field NMR: a field study. Environ Sci Technol 49:11045–11052
40. Manz B, Volke F, Goll D, Horn H (2003) Measuring local flow velocities and biofilm structure in biofilm systems with magnetic resonance imaging (MRI). Biotechnol Bioeng 84:424–432
41. Belton PS (1997) NMR and the mobility of water in polysaccharide gels. Int J Biol Macromol 21:81–88
42. Kessler HG (2006) Lebensmittel- und Bioverfahrenstechnik: Molkereitechnologie, 4th edn. Publishing House A. Kessler, Munich
43. Dalitz F, Cudaj M, Maiwald M, Guthausen G (2012) Process and reaction monitoring by low-field NMR spectroscopy. Prog Nucl Magn Reson Spectrosc 60:52–70
44. Johns ML, Fridjonsson EO, Vogt SJ, Haber A (eds) (2016) Mobile NMR and MRI: developments and applications. Royal Society of Chemistry, Cambridge

45. Santos PM, Kock FVC, Santos MS, Lobo CMS, Carvalho AS, Colnago LA (2017) Non-invasive detection of adulterated olive oil in full bottles using time-domain NMR relaxometry. J Braz Chem Soc 28:385–390
46. Kim SM, Kim MH (2014) Design of portable NMR-based *E. coli* detecting system. In: Proceedings international conference of agricultural engineering, Zurich

2.3 Section 3 Fouling detection using electrochemical methods

2.3.1 Publication 5 Electrochemical detection of food-spoiling bacteria using interdigitated platinum microelectrodes

Real-time detection of biofilms is an important issue for medicine, food safety, and public health. Therefore, the fast detection of bacterial attachment may be an effective strategy to control the biofilm formation. Electrochemical sensors have been reported for detection of bacterial attachment on the surface of microelectrodes. However, biofilm-forming bacteria *Bacillus subtilis* ssp. *subtilis, Paenibacillus polymyxa,* and *Pseudomonas fragi* that are also known to cause dairy spoilage, have not yet been studied by electrochemical methods. This article describes the study of the cyclic voltammetry method on *Bacillus subtilis* ssp. *subtilis, Paenibacillus polymyxa,* and *Pseudomonas fragi* attachment onto the surface on interdigitated platinum microelectrodes. The differences in the current responses between the uncolonized microelectrodes and the microelectrodes after bacterial attachment were determined. In addition, the surface coverage of microelectrodes was visualized using microscopy techniques. The results of this study indicate that the electrochemical detection of *Bacillus subtilis* ssp. *subtilis*, *Paenibacillus polymyxa,* and *Pseudomonas fragi* on surfaces with interdigitated ring array platinum microelectrodes is possible. All bacterial suspensions demonstrated higher current values compared to the reference medium. It might be explained by the enhanced electron transfer between the microorganisms and the electrode surface. Also, the results obtained at the scan rates of 50, 100, 250 and 350 mV s^{-1} depict that a current change is observed after bacterial attachment and biofilm formation on the microelectrode surfaces. Considering the results of this study, it can be suggested that electrochemical sensors without a biorecognition element (like enzymes, nucleic acids, aptamers, antibodies, organelles, membranes, cells) can be potentially implemented into processing equipment for the monitoring of biofilms.

Author contributions

Fysun, O., Rauschnabel, J., Langowski, H.-C. devised the project, the main conceptual ideas and proof outline. Fysun, O. worked out the experiments and technical details of the electrochemical sensors. Schmitt, A., Auernhammer, P. T. collected the data and performed the analysis for the data. Fysun, O. wrote the manuscript. All authors discussed the results and

commented on the manuscript. Langowski, H.-C. contributed to the final version of the manuscript.

Permission for the re-use of the article granted by Elsevier B.V..

Journal of Microbiological Methods 161 (2019) 63–70

Contents lists available at ScienceDirect

Journal of Microbiological Methods

journal homepage: www.elsevier.com/locate/jmicmeth

Electrochemical detection of food-spoiling bacteria using interdigitated platinum microelectrodes

Olga Fysun[a,b,*,1], Alexander Schmitt[b,c,2], Peter Thomas Auernhammer[a,b,3], Johannes Rauschnabel[b], Horst-Christian Langowski[a,d]

[a] TUM School of Life Sciences Weihenstephan, Technical University of Munich, Freising, Germany
[b] Robert Bosch Packaging Technology GmbH, Waiblingen, Germany
[c] Faculty of Applied Chemistry, Nuremberg Institute of Technology, Nuremberg, Germany
[d] Fraunhofer Institute for Process Engineering and Packaging IVV, Freising, Germany

ARTICLE INFO

Keywords:
Cyclic voltammetry
Interdigitated microelectrodes
Bacillus subtilis ssp. *subtilis*
Paenibacillus polymyxa
Pseudomonas fragi
Bacterial biofilms

ABSTRACT

The fast and non-destructive detection of bacterial attachment on food contact surfaces is important for the prevention of the unwanted formation of biofilms. Biofilms constitute a protected growth mode that allows bacteria to survive even in hostile environments. Therefore, the fast detection of bacterial attachment may be an effective strategy for biofilm control. In this study cyclic voltammetry (CV) was used to detect *Bacillus subtilis* ssp. *subtilis, Paenibacillus polymyxa, Pseudomonas fragi* attachment on interdigitated microelectrodes. The differences in current between the uncolonized sterile microelectrodes and the microelectrodes after bacterial attachment were determined. In addition, the surface coverage of microelectrodes was visualized using microscopy techniques. The results showed that the cyclic voltammetry in combination with interdigitated platinum microelectrodes can be used to detect bacterial biofilms.

1. Introduction

Fast and non-destructive biofilm detection is an important issue for medicine, food safety, and public health. The presence of bacteria can lead to problems such as infection propagation and biocorrosion of surfaces among many others (Cappitelli et al., 2014; Costerton et al., 1987; Lewandowski and Beyenal, 2013). Concerning industrial food equipment, the accumulation of unwanted biofilms can result in significant economic losses and in the decreased quality and safety of processed foods (Marchand et al., 2012). Specifically, bacterial biofilms on food contact surfaces of processing equipment may lead to the spoilage of processed products, contamination of product by spoilage bacteria, metal biocorrosion in pipelines and tanks; and reduced heat transfer efficacy in processing equipment (Cappitelli et al., 2014). Therefore, bacterial attachment in food processing environments increases the possibilities of microbial contamination of the processed product (Chmielewski and Frank, 2003).

Psychrotolerant sporeformers, *Bacillus* and *Paenibacillus* genera, are known spoilage bacteria that adhere to production lines and contaminate pasteurized refrigerated foods, e.g., milk (Marchand et al., 2012; de Jonghe et al., 2010). Additionally, it was found that *Bacillus* spp. and *Paenibacillus* spp. are responsible for spoilage of dairy products that had been contaminated by Gram-positive bacteria. Moreover, Gram-positive endospore-forming *Bacillus subtilis* and *Paenibacillus polymyxa* have been isolated from both farm and processing plant environments, and raw and pasteurized fluid milk. *B. subtilis* is not categorized as a human pathogen, however, it has been reported that *B. subtilis* was involved in food poisoning cases. *B. subtilis* induces defects in flavor and texture of yoghurt that are caused due to proteinase activities of *B. subtilis* (Gopal et al., 2015). *P. polymyxa* produces a variety of hydrolytic extracellular enzymes such as proteases, lipases, and lecithinases that can cause the spoilage of pasteurized milk even in the absence of fast bacterial growth. Particularly, the lecithinase activity of *P. polymyxa* is responsible for so-called bitty cream defects in milk due to the aggregation of fat globules (de Jonghe et al., 2010). It has been also reported that *Pseudomonas* spp. can negatively contribute to the quality and shelf life of food due to their ability to form biofilms at low temperatures (Hood and Zottola, 1997; Sørhaug and Stepaniak, 1997).

* Corresponding author at: TUM School of Life Sciences Weihenstephan, Technical University of Munich, Freising, Germany.
E-mail address: olga.fysun@bosch.com (O. Fysun).
[1] Robert Bosch GmbH, Reutlingen, Germany.
[2] Present address: Roche Diagnostics GmbH, Penzberg, Germany.
[3] Present address: Roche Diagnostics GmbH, Mannheim, Germany.

https://doi.org/10.1016/j.mimet.2019.04.015
Received 21 September 2018; Received in revised form 20 April 2019; Accepted 22 April 2019
Available online 22 April 2019

Also, the enhanced attachment of *Listeria monocytogenes* to glass surfaces was observed, which was attributed to the EPS (extracellular polymeric substance) production of *Pseudomonas fragi* (Sasahara and Zottola, 1993).

The fast detection of biofilms is of great importance for the effective prevention of contamination (Cappitelli et al., 2014). Several techniques based on biological, physical, and chemical principles have been employed for the detection of bacterial attachment (Kim et al., 2012a, 2012b; Kirkland et al., 2015; Kwak et al., 2014; Crattelet et al., 2013). However, many of the methods used in the food industry are time-consuming, costly and require trained specialists. Additionally, it has been reported that electrochemical methods can be used for real time detection at early stages of bacterial attachment (Giao et al., 2003). As opposed to the other methods, electrochemical detection has several advantages: data can be processed rapidly, relatively simple and inexpensive instrumentation may be used, and the practical analysis is flexible (Kang et al., 2012; Ahmed et al., 2014).

In electrochemical methods, the reaction under investigation would generate one of the following measurable responses: current, potential or changes in the conductive properties of a medium between electrodes (Moretto and Kalcher, 2014; Zoski, 2007). Voltammetric methods belong to the electrochemical techniques involving the change of the potential at a working electrode versus a reference electrode, while measuring the corresponding current (Armstrong et al., 2000). The reaction of interest, such as the reduction or oxidation of redox couples, occurs on the working electrode. The materials used for the electrodes should be chemically stable and must not interact with any of the species in solution, e.g. platinum or gold are preferred. Also, the miniaturization of the electrodes is a common trend in electrochemistry over the last decades (Ahmed et al., 2014). Cyclic voltammetry (CV) is one of the most used voltammetric methods. This method has been used for monitoring of bacterial attachment on electrochemical microelectrodes (Giao et al., 2003; Harnisch and Freguia, 2012; Becerro et al., 2016).

Several theories have been proposed for the mechanisms of electrochemical detection of bacteria (Nealson and Finkel, 2011; Sultana et al., 2015). According to the literature, the electron transfer can occur: (1) directly to the acceptor via outer membrane cytochromes, or through (2) electron shuttles (redox mediators), (3) conductive nanowires, or (4) other extracellular matrices. Such mechanisms may vary depending on the strain of the microorganism and environmental conditions (Nealson and Finkel, 2011). Although there is not a widely accepted explanation, it is evident that bacteria living in surface-attached biofilms must maintain electrochemical gradients to support basic cellular functions. Usually, electrons are delivered and accepted by dissolved substances. As an examples, some molecules in bacterial biofilms (exoenzymes, exopolysaccharides) adsorbed on the surface of electrodes are believed to catalyze oxygen reduction (Liengen et al., 2014; Faimali et al., 2011).

To the best of our knowledge, despite the numerous studies related to electrochemical detection of bacteria, *B. subtilis* ssp. *subtilis, P. polymyxa, P. fragi* that are known to cause food spoilage, have not yet been studied using electrochemical methods. In addition, there are a few reports only of electrochemical sensors based on interdigitated electrochemical microelectrodes for the detection of bacterial adhesion. Therefore, the aim of this work was to investigate the *B. subtilis* ssp. *subtilis, P. polymyxa, P. fragi* biofilm formation by cyclic voltammetry using interdigitated platinum microelectrodes.

2. Material and methods

2.1. Chemicals

Meat extract and ethanol 70% were supplied by VWR (Darmstadt, Germany). Peptone from casein (pancreatic digest) was obtained from Applichem Panreac (Barcelona, Spain). Plate count agar, and potassium chloride 3 mol L^{-1} were purchased from Merck (Darmstadt, Germany). Potassium ferrocyanide (1%) was obtained from Clin-Tech (Guildford, UK). Freeze-dried cultures of *Bacillus subtilis* ssp. *subtilis* (DSM 10), *Paenibacillus polymyxa* (DSM 36), *Pseudomonas fragi* (DSM 3456) were acquired from DSMZ (Braunschweig, Germany). All the reagents and chemicals were of analytical grade.

2.2. Sample preparation and experimental setup

The freeze-dried cultures of *B. subtilis* ssp. *subtilis* (DSM 10), *P. polymyxa* (DSM 36), *P. fragi* (DSM 3456) were reactivated according to the manufacturer's instructions. A glass ampoule containing the freeze-dried bacteria was cracked by flaming the end and placing three drops of water on the glass. After the cotton plug was removed, 0.5 mL of sterile nutrient medium (5.0 g L^{-1} soya peptone, 3.0 g L^{-1} meat extract) was added. The pellet of freeze-dried bacteria was allowed to rehydrate for 30 min and the contents were mixed using a sterile inoculation loop. Then, 10 µL of the content were added to agar plates, spread with a sterile glass spreader on the surface of the agar, and incubated at 30 °C (*B. subtilis* ssp. *subtilis*, *P. polymyxa*) and at 26 °C (*P. fragi*) for 24 h (DSMZ GmbH, n.d). These agar plate cultures were used for the preparation of a bacterial suspension. A colony was taken from the plate and resuspended in an Eppendorf tube filled with 1 mL of the sterile nutrient medium. The inoculated medium was then transferred into an Erlenmeyer flask with 49 mL of the sterile nutrient medium. The suspension was incubated under stirring at 130 rpm and 30 °C (*B. subtilis* ssp. *subtilis*, *P. polymyxa*) or 26 °C (*P. fragi*) for 2 h until the early log phase of growth. The log phase was detected by measuring the transmission. The optical transmittance at 570 nm of the bacterial suspension at the early log phase was 90.0 ± 3.0%. The number of bacteria in the early log phase corresponds to about 10^6 CFU mL^{-1}. To achieve the bacterial adhesion on the microelectrode surface, a microelectrode was placed into each well of the sterile 6-well plates. Then, the wells were filled with 5 mL of sterile nutrient medium and inoculated with 100 µL of the bacterial suspension at the early log phase as described above. The cleaned and activated microelectrodes were immersed in the wells filled with either sterile nutrient medium or inoculated nutrient medium. The 6-well plates with the microelectrodes were incubated at 30 °C (*B. subtilis* ssp. *subtilis*, *P. polymyxa*) or 26 °C (*P. fragi*) for 18 h.

2.3. Electrochemical methods

The experimental setup has been checked using 100 mM potassium ferrocyanide solution. Platinum interdigitated ring array (IDRA) microelectrodes (MicruX Fluidic, Spain) were cleaned and activated electrochemically before every use. First, they were immersed in ethanol 70% for 5 min. The solvent was then removed with Kimtech Science™ wipes. Secondly, they were rinsed twice with sterile deionized water. After these cleaning steps, the microelectrodes were activated electrochemically using 20 µL of 0.1 M KCl via cyclic voltammetry using a PalmSens 3 bipotentiostat (PalmSens BV, Netherlands) run by a Windows 7 based PC. The potential was cycled 10 times between −1.5 and 1.5 V at a scan rate of 0.100 V s^{-1}. Once the activation step was completed, the microelectrodes were rinsed again twice with sterile deionized water. The electrochemical cell of the microelectrode has a diameter of 2.0 mm. The working electrode has 12 ft pairs. Each foot was 10 µm wide with a 10 µm gap between each foot. The electrochemical cell had a reference electrode, an auxiliary electrode, and two working electrodes. The software PSTrace 4.8 (PalmSens BV, Netherlands) was used to record the data and to control the bipotentiostat. The bipotentiostat was connected to a drop cell (MicruX Fluidic, Spain). For the measurements, the microelectrodes were placed into the slot of the drop cell. Then, 10 µL of either sterile nutrient medium or bacterial suspension of the corresponding well were pipetted onto the electrode surface before the cyclic voltammetry took place. In cyclic voltammetry (CV) a triangular shape potential scan is

applied to an electrode while the current is monitored. A potential scan is performed between two vertex potentials, E_{vtx1} and E_{vtx2}. The potential change is reversed once a vertex potential is reached. For each microelectrode, the cycles were done with the following parameters: $T_{equilibrium} = 15\,s$, $E_{vtx1} = -0.8\,V$, $E_{vtx2} = 0.8\,V$, $E_{step} = 0.01\,V$, scan rate = 50, 100, 250, 350 mV s^{-1}. All the experiments were carried out in ninefold. One scan was conducted for each prepared microelectrode.

2.4. Microscopy

After cyclic voltammetry measurements, the surface of the microelectrodes covered with bacteria biofilm was visualized. The transmitted light microscope (Kern OBN 135, Kern & Sohn GmbH, Germany) was used to visualize the surface of the microelectrodes covered by bacteria. The microelectrodes with biofilms were observed at magnifications of 20× without oil after 10 min of drying at room temperature.

3. Results and discussion

3.1. Electrochemical investigation of Bacillus subtilis ssp. subtilis

Fig. 1 depicts the cyclic voltammogram obtained on the platinum interdigitated microelectrodes for the sterile nutrient medium, the nutrient medium inoculated for 18 h with *B. subtilis* ssp. *subtilis*, and *B. subtilis* ssp. *subtilis* biofilm at scan rate of 250 mV s^{-1}.

As shown in Fig. 1, the presence of *B. subtilis* ssp. *subtilis* biofilm 18 h leads to the pronounced changes in cathodic and anodic current in potential window from −0.2 to −0.8 V. Compared to the *B. subtilis* ssp. *subtilis* biofilm, the difference between nutrient medium and *B. subtilis* ssp. *subtilis* bacterial suspension (planktonic state) at scan rate of 250 mV s^{-1} was not remarkable. Thus, the comparison between nutrient medium and *B. subtilis* ssp. *subtilis* bacterial suspension at different scan rates is required to obtain more details.

Fig. 2 illustrates the anodic (IpA) and cathodic (IpC) peak currents and respective peak potentials (V) obtained from the cyclic voltammogams for the sterile nutrient medium and the nutrient medium inoculated for 18 h with *B. subtilis* ssp. *subtilis,* and *B. subtilis* ssp. *subtilis* biofilm at scan rates of 50, 100, 250 and 350 mV s^{-1}.

The anodic (IpA) and cathodic (IpC) peak currents shown on Fig. 2(A and B) illustrate that the current signals of anodic (oxidation) and cathodic (reduction) curves increase with an increasing scan rate for both nutrient medium and *B. subtilis* ssp. *subtilis* suspension (planktonic state). The current values are slightly increased for *B. subtilis* ssp. *subtilis* suspension when comparing with nutrient medium at the same scan rate. The potential of the anodic peaks (Fig. 2C) does not change with the increasing scan rate. The potential of the cathodic peaks (Fig. 2D) for the *B. subtilis* ssp. *subtilis* suspension slightly shifts towards positive potentials with the increasing scan rate.

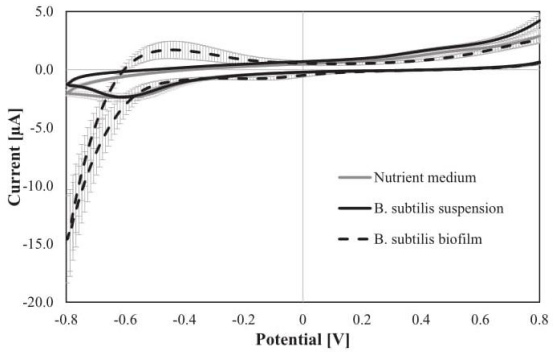

Fig. 1. Cyclic voltammogams obtained for (1) sterile nutrient medium, (2) *B. subtilis* ssp. *subtilis* bacterial suspension 18 h, and (3) *B. subtilis* ssp. *subtilis* biofilm 18 h covering the microelectrode and *B. subtilis* ssp. *subtilis* bacterial suspension 18 h at scan rate of 250 mV s^{-1}. Error bars correspond to the standard errors ($i = 3$, $n = 9$).

3.2. Electrochemical investigation of Paenibacillus polymyxa

Fig. 3 depicts the cyclic voltammogram obtained on the platinum interdigitated microelectrodes for the sterile nutrient medium, the nutrient medium inoculated for 18 h with *P. polymyxa,* and *P. polymyxa* biofilm at scan rate of 250 mV s^{-1}, respectively.

Similarly to Fig. 1, *P. polymyxa* biofilm leads to the pronounced changes in cathodic and anodic current in negative potential window from −0.4 to −0.8 V. Moreover, differences in shape of cyclic voltammorgam are also observed in positive potential window. As shown in Fig. 3, the standard errors of the measurements of the sterile nutrient medium and *P. polymyxa* bacterial suspension 18 h is smaller than that of the measurements of microelectrodes covered with biofilm. Similar behavior can be also observed for *B. subtilis* ssp. *subtilis* (Fig. 1).

Some studies reported large variations in the peak current after bacteria attachment to the surface (Xu et al., 2012; Strycharz et al., 2011; Becerro et al., 2015). The inhomogeneous surface coverage depicted in Fig. 7C may explain the large standard errors.

Fig. 4 illustrate the anodic (IpA) and cathodic (IpC) peak currents and respective peak potentials (V) obtained from the cyclic voltammogams for the sterile nutrient medium and the nutrient medium inoculated for 18 h with *P. polymyxa,* and *P. polymyxa* biofilm at scan rates of 50, 100, 250 and 350 mV s^{-1}.

The anodic (IpA) and cathodic (IpC) peak currents shown on Fig. 4(A and B) illustrate that the current signals of anodic (oxidation) and cathodic (reduction) curves increase with an increasing scan rate for both nutrient medium and *P. polymyxa* suspension 18 h (planktonic state). No remarkable differences have been observed between nutrient medium and *P. polymyxa* suspension 18 h at each scan rate. Similarly to results for *B. subtilis* ssp. *subtilis* suspension (Fig. 2D), cathodic peak slightly shifted towards negative potentials with increasing scan rate for *P. polymyxa* suspension (Fig. 4D). For the anodic peak currents (Fig. 4C), the differences were less pronounced than for the cathodic peaks and no potential shift was observed.

3.3. Electrochemical investigation of Pseudomonas fragi

Fig. 5 depicts the cyclic voltammogram obtained on the platinum interdigitated microelectrodes for the sterile nutrient medium, the nutrient medium inoculated for 18 h with *P. fragi,* and *P. fragi* biofilm 18 h at scan rate of 250 mV s^{-1}, respectively.

Similarly to Figs. 1 and 3, *P. fragi* biofilm formation leads to the pronounced changes in cathodic and anodic current in negative potential window from −0.4 to −0.8 V. Moreover, remarkable differences in shape of cyclic voltammorgam for *P. fragi* suspension (planktonic state) can be observed in positive potential window for the anodic curve. In contrast to Fig. 1 (*B. subtilis* ssp. *subtilis*) and Fig. 3 (*P. polymyxa*), the differences between nutrient medium and bacterial suspension are evident showing higher current values at IpC for *P. fragi* suspension.

The anodic (IpA) and cathodic (IpC) peak currents shown on Fig. 6(A and B) illustrate that the current in anodic (oxidation) and cathodic (reduction) curves increase with an increasing scan rate for both nutrient medium and *P. fragi* suspension 18 h (planktonic state). Moreover, pronounced differences in current at both anodic (IpA) and cathodic (IpC) peak have been observed between nutrient medium and *P. fragi* suspension at each scan rate. *P. fragi* suspension demonstrates higher current values compared to the nutrient medium. It might be contributed to the enhanced electrochemical activity of *P. fragi.* Cathodic peak slightly shifts towards negative potentials with increasing scan rate for the *P. fragi* suspension (Fig. 6C), while potentials

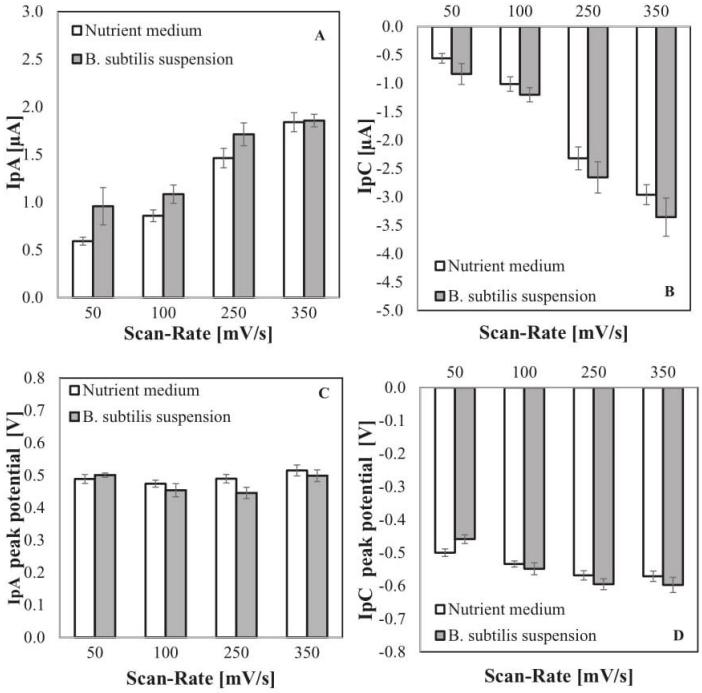

Fig. 2. Anodic (IpA) (A) and cathodic (IpC) (B) peak currents and respective peak potentials (V) (C and D, respectively) for nutrient medium and *B. subtilis* ssp. *subtilis* suspension 18 h obtained at scan rates of 50, 100, 250 and 350 mV s^{-1}. Error bars correspond to the standard errors (i = 3, n = 9).

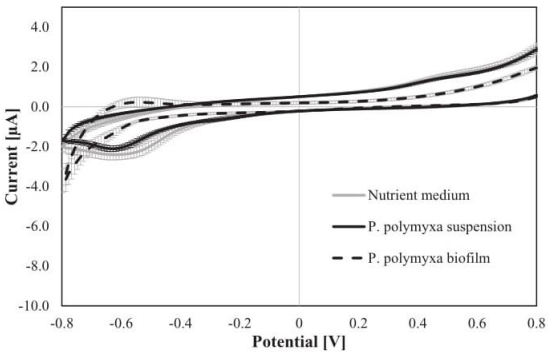

Fig. 3. Cyclic voltammogams obtained for (1) sterile nutrient medium, (2) *P. polymyxa* bacterial suspension 18 h, and (3) *P. polymyxa* biofilm 18 h covering the microelectrode and *P. polymyxa* bacterial suspension 18 h at scan rate of 250 mV s^{-1}. Error bars correspond to the standard errors (i = 3, n = 9).

at anodic peaks do not shifted notably (Fig. 6D).

3.4. Microscopy

A detailed visualization of the *B. subtilis* ssp. *subtilis, P. polymyxa, P. fragi* adhesion on the surface of microelectrodes was obtained using transmitted light microscopy (Fig. 7).

Fig. 7A shows the clean interdigitated microelectrode with pairs of feet of the IDRA structure. Fig. 7B–D depict the attachment of bacteria to the working electrode after 18 h of incubation in nutrient medium. The bacterial distribution on the surface is non-homogeneous, showing bacterial communities in clusters and single cells. Non-homogeneous bacterial biofilm formation may explain the deviations in the voltammetric measurements using microelectrodes. The partial removal of the bacteria from the working electrode surface was observed after three CV cycles. The removal of adhered bacteria may result from the formation of bubbles, which occurred at large positive and negative potentials, thus, leading to the mechanical removal of bacteria. Bacteria removal during cyclic voltammetry, especially at low scan rates of 0.150 V s^{-1}, has been observed previously by Giao et al., 2003. In the study of Giao et al., 2003 it was reported that most of the bacteria remaining on the surface were viable. At higher scan rates (0.500 V s^{-1}) the number of dead bacteria on the surface increased (Giao et al., 2003). Thus, the parameters of cyclic voltammetry must be selected carefully to prevent the removal or death of the adhered bacteria.

3.5. Electrochemical microsensors for detection of bacterial adhesion

Previous research has documented the applicability of cyclic voltammetry for the bacteria detection (Marsili et al., 2008; Giao et al., 2003; Becerro et al., 2016). In this work, cyclic voltammetry (CV) was investigated to detect the bacterial biofilms using interdigitated platinum microelectrodes.

Vieira et al., 2003 studied bacterial detection using cyclic voltammetry with platinum microelectrodes. It was reported that the shape of the cyclic voltammogram may provide information on the surface coverage. According to the authors, as the coverage of the surface increases, the peaks' intensity in the voltammograms will decrease. The author's explanation is based on the fact that as the accumulation on the surface increases, the area available for the oxidation-reduction processes decreases. Becerro and collaborators (Becerro et al., 2016) evaluated the cyclic voltammetry and differential pulse voltammetry for detection of *Staphylococcus epidermidis*. At the beginning of the

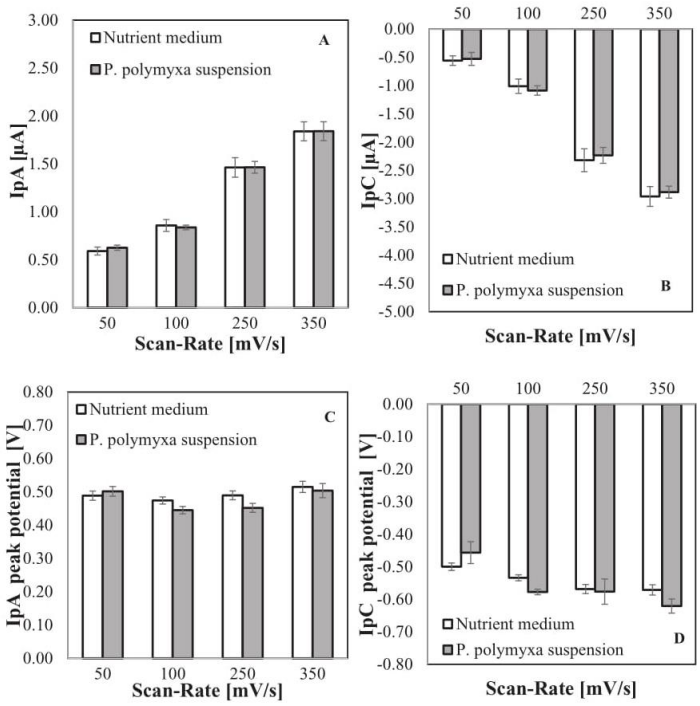

Fig. 4. Anodic (IpA) (A) and cathodic (IpC) (B) peak currents and respective peak potentials (V) (C and D, respectively) for nutrient medium and *P. polymyxa* suspension 18 h obtained at scan rates of 50, 100, 250 and 350 mV s^{-1}. Error bars correspond to the standard errors (i = 3, n = 9).

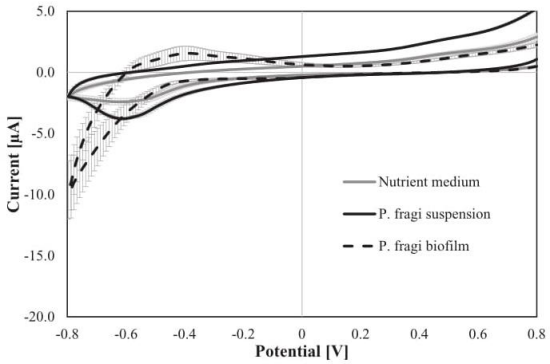

Fig. 5. Cyclic voltammogams obtained for (1) sterile nutrient medium, (2) *P. fragi* bacterial suspension 18 h, and (3) *P. fragi* biofilm 18 h covering the microelectrode and *P. fragi* bacterial suspension 18 h at scan rate of 250 mV s^{-1}. Error bars correspond to the standard errors (i = 3, n = 9).

experiment, they recorded the oxidation and reduction peaks and observed an increase in the current value. These peaks may be indicative of the bacterial growth. Once the biofilm developed completely, they observed a decrease in current that may be caused by enzymatic activity of bacteria. The voltammograms were correlated with the activity of different redox centers present on the bacterial surface that are related to the metabolic activity of bacterial cells (Becerro et al., 2016). Also in present work, it may be assumed that metabolic activity of selected bacteria contributes to the current increases which were showed in cyclic voltammograms (Figs. 1, 3, and 5). A possible explanation for the increased peak currents is an enhanced electron transfer between bacteria and the electrode surface. According to Nealson et al. (Nealson and Finkel, 2011), electrochemical reactions during cyclic voltammetry can occur for all bacterial products, e.g., secreted exoenzymes, carbohydrates, and exopolysaccharides (EPS). It can be assumed that since *B. subtilis* ssp. *subtilis*, *P. polymyxa*, *P. fragi* can produce a variety of enzymes including, proteases and lipases and produce EPS, they may interfere with electron transport.

Marsili et al., 2008 studied the effect of low scan rates on the results of cyclic voltammetry measurements to understand the main redox-active species that participate in the electron transfer processes to an electrode from *Geobacter sulfurreducens*. As the scan rate decreases, the kinetic effects of electron transfer between cell surface and the electrodes were minimized, and the enzymatic effects, which are related to bacterial activity, became primary factors. As the scan rate increased, slow reactions may not have time to occur before the potential was changed to the next step. Thus, the kinetics of interfacial electron transfer between redox proteins and electrodes strongly affects the voltammetric response and the kinetics of continuous enzymatic turnover may be masked.

According to literature, the use of microelectrode systems offers several advantages compared to macroelectrodes: higher sensitivities, enhanced mass transport, better signal-to-noise ratio and no need for supporting electrolyte (Becerro et al., 2016; Garci-A-Aljaro et al., 2010). It has also been reported that the signal measured for the attached bacteria is more significant for microelectrodes with smaller active surface area (Laczka et al., 2008). Moreover, the design and features of interdigitated microelectrode arrays eliminate the need for a reference electrode, allowing for a simpler experimental setting than in classical three or four electrode systems. In addition, IDA electrodes with small gap between microbands may provide better sensitivity for bacteria

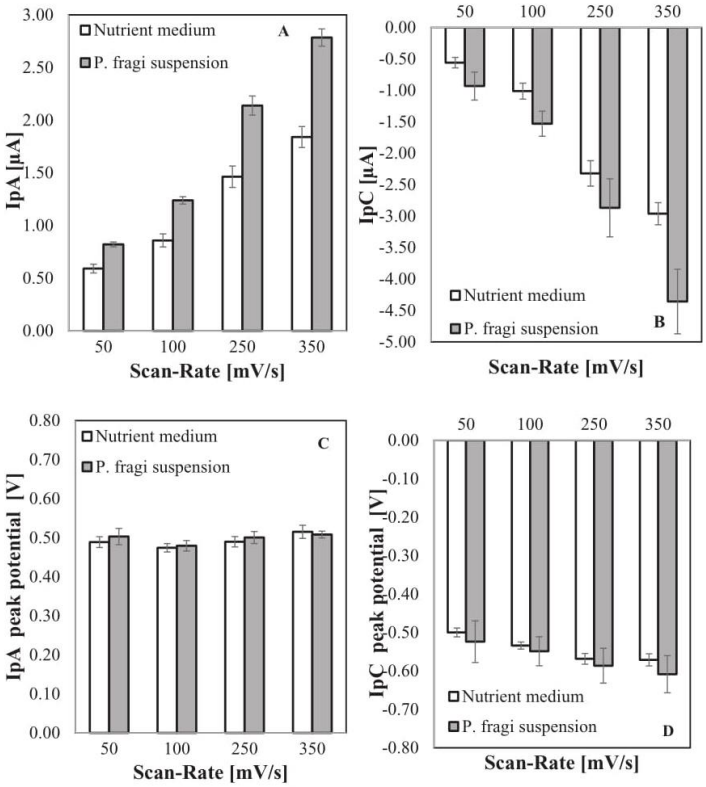

Fig. 6. Anodic (IpA) (A) and cathodic (IpC) (B) peak currents and respective peak potentials (V) (C and D, respectively) for nutrient medium and *P. fragi* suspension 18 h obtained at scan rates of 50, 100, 250 and 350 mV s^{-1}. Error bars correspond to the standard errors (i = 3, n = 9).

detection (Kim et al., 2012a, 2012b). The configuration for the interdigitated array microelectrodes is the paired electrode configuration (generation/collection scheme). The intermediate species generated on one electrode (generator), diffuses to the other electrode (collector), where it can be regenerated to the initial reactant present in bulk solution (Zoski, 2007). The interdigitated electrodes of smaller features show significantly higher perimeters and smaller surface areas than single electrodes occupying a similar pattern. It has been demonstrated that the perturbation produced by the binding of big targets, such as bacteria, is more significant for electrodes of smaller active surface area (Laczka et al., 2008).

When it comes to the processing equipment, an important aspect is the comparability between the electrode material and the material of contact surfaces in processing equipment. Platinum is a metal commonly used as an electrode material. However, platinum is not used material in industrial equipment for contact surfaces. Therefore, it is important to compare its surface properties to the most commonly used material in processing equipment, e.g., stainless steel. Important surface properties are the adhesion free energy and the hydrophobicity of both materials (Teixeira and Oliveira, 1999). From the results published in the literature, it can be seen that the difference between them is rather negligible. The adhesion free energy for platinum is 43.98 mJ m^{-2}, while for stainless steel 42.35 mJ m^{-2}. The hydrophobicity for platinum was defined as 53.02 mJ m^{-2}, while for stainless steel 45.21 mJ m^{-2} (Teixeira and Oliveira, 1999). Thus, it can assumed that the initial bacterial attachment should be nearly similar on both materials.

Accordingly, both electrochemical sensors and biosensors can be used for bacterial detection (Grieshaber et al., 2008; Ahmed et al., 2014). Sensors are devices with a receptor specific for an analyte (molecular or ionic recognition). The response detected by the receptor is converted into an electric signal by the transducer. Electrochemical biosensors are based on the same principles as electrochemical sensors are. However, electrochemical biosensors are differentiated from electrochemical sensors according to the biorecognition element used as receptor: enzymes, nucleic acids, aptamers, antibodies, organelles, membranes, cells, tissues, or even whole organisms (Moretto and Kalcher, 2014). Thus, electrochemical biosensors for bacterial detection require receptors such as enzymes, antibodies, phages, or DNA. Several publications in recent years report whole-cell bacterial detection using electrochemical biosensors (Ahmed et al., 2014; Vanegas et al., 2016). However, due to the protein nature, biorecognition elements in biosensors are not stable at high temperatures (above 80 °C) or common pressures, or in the presence of steam and under typical machine cleaning conditions (acidic and basic solutions) (Moretto and Kalcher, 2014). Thus, electrochemical biosensors cannot be implemented in industrial processing equipment for long term usage. Electrochemical biosensors can be recommended for the quality control in laboratories, while electrochemical sensors without a biorecognition element can be potentially implemented into processing equipment for the monitoring of bacterial biofilms. Nevertheless, it should be noted that the major drawback of the electrochemical sensors is that every bacteria type cannot be identified with this technique. Although the remarkable differences in cyclic voltammograms between *B. subtilis* ssp. *subtilis, P. polymyxa, P. fragi* biofilms have been shown in this study, it is assumed that only real time biofilm detection without bacteria identification

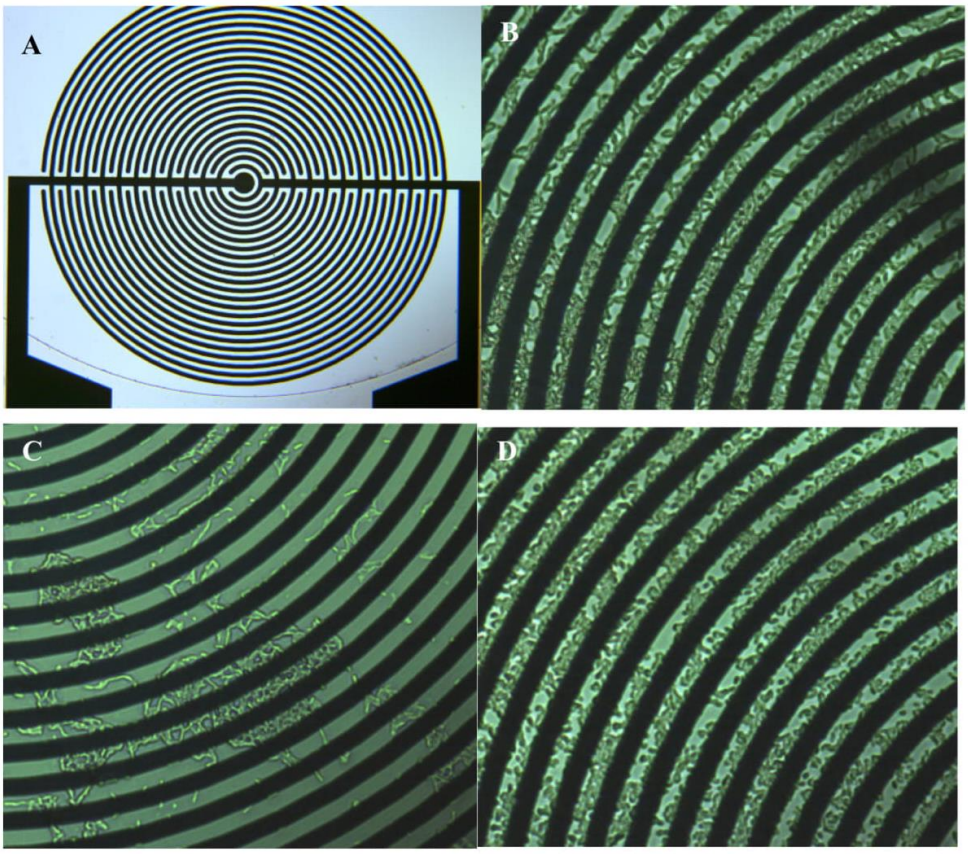

Fig. 7. Surface of clean interdigitated ring array (IDRA) microelectrode (A) and microelectrodes with (B) *B. subtilis* ssp. *subtilis* biofilm, (C) *P. polymyxa* biofilm, (D) *P. fragi* biofilm (after 18 h incubation in nutrient medium).

might be possible in processing equipment.

4. Conclusion

The results from this study indicate that the electrochemical detection of *B. subtilis* ssp. *subtilis, P. polymyxa, P. fragi* biofilms on surfaces with interdigitated ring array platinum microelectrodes is possible. The results from cyclic voltammograms obtained at scan rates of 50, 100, 250 and 350 mV s^{-1} showed that a current increase was observed after bacterial attachment to the microelectrode surfaces. Further studies are being performed to detect bacterial attachment on electrodes in flow conditions. In addition, improvement of the electrochemical microsensors for better sensitivity and their adaptation under production conditions for real time detection will be investigated in the near future.

Acknowledgments

This research did not receive any specific grant from funding agencies in the public, commercial, or not-for-profit sectors.

References

Ahmed, A., Rushworth, J.V., Hirst, N.A., Millner, P.A., 2014. Biosensors for whole-cell bacterial detection. Clin. Microbiol. Rev. 27 (3), 631–646. https://doi.org/10.1128/CMR.00120-13.

Armstrong, F.A., Camba, R., Heering, H.A., Hirst, J., Jeuken, L.J.C., Jones, A.K., Leger, C., McEvoy, J.P., 2000. Fast voltammetric studies of the kinetics and energetics of coupled electron-transfer reactions in proteins. Faraday Disc 116, 191–203. https://doi.org/10.1039/b002290j.

Becerro, S., Paredes, J., Arana, S., 2015. Multiparametric biosensor for detection and monitoring of bacterial biofilm adhesion and growth. In: Lacković, I., Vasic, D. (Eds.), 6th European Conference of the International Federation for Medical and Biological Engineering. Springer International Publishing, Cham, pp. 333–336.

Becerro, S., Paredes, J., Mujika, M., Lorenzo, E.P., Arana, S., 2016. Electrochemical real-time analysis of bacterial biofilm adhesion and development by means of thin-film biosensors. IEEE Sensors J. 16 (7), 1856–1864. https://doi.org/10.1109/JSEN.2015.2504495.

Cappitelli, F., Polo, A., Villa, F., 2014. Biofilm formation in food processing environments is still poorly understood and controlled. Food Eng. Rev. 6 (1–2), 29–42. https://doi.org/10.1007/s12393-014-9077-8.

Chmielewski, R.A.N., Frank, J.F., 2003. Biofilm formation and control in food processing facilities. Comp Rev Food Sci Food Safety 2 (1), 22–32. https://doi.org/10.1111/j.1541-4337.2003.tb00012.x.

Costerton, J.W., Cheng, K.J., Geesey, G.G., Ladd, T.I., Nickel, J.C., Dasgupta, M., Marrie, T.J., 1987. Bacterial biofilms in nature and disease. Annual Reviews in Microbiology 41 (1), 435–464. https://doi.org/10.1146/annurev.mi.41.100187.002251.

Crattelet, J., Ghnimi, S., Debreyne, P., Zaid, I., Boukabache, A., Esteve, D., Auret, L., Fillaudeau, L., 2013. On-line local thermal pulse analysis sensor to monitor fouling and cleaning: application to dairy product pasteurisation with an ohmic cell jet heater. J. Food Eng. 119 (1), 72–83.

DSMZ GmbH, catalogues - Psuedomonas fragi (Eichholz 1902) Gruber n.d: DSM No.: 3456, available at https://www.dsmz.de/catalogues/details/culture/DSM-3456.html

Faimali, M., Benedetti, A., Pavanello, G., Chelossi, E., Wrubl, F., Mollica, A., 2011. Evidence of enzymatic catalysis of oxygen reduction on stainless steels under marine biofilm. Biofouling 27 (4), 375–384. https://doi.org/10.1080/08927014.2011.576756.

Garci-A-Aljaro, C., Bangar, M.A., Baldrich, E., Munoz, F.J., Mulchandani, A., 2010. Conducting polymer nanowire-based chemiresistive biosensor for the detection of bacterial spores. Biosens. Bioelectron. 25, 2309–2312.

Giao, M.S., Montenegro, M.I., Vieira, M.J., 2003. Monitoring biofilm formation by using cyclic voltammetry-effect of the experimental conditions on biofilm removal and

activity. Water Sci. Technol. 47 (5), 51–56.
Gopal, N., Hill, C., Ross, P.R., Beresford, T.P., Fenelon, M.A., Cotter, P.D., 2015. The prevalence and control of bacillus and related spore-forming bacteria in the dairy industry. Front. Microbiol. 6, 1418. https://doi.org/10.3389/fmicb.2015.01418.
Grieshaber, D., MacKenzie, R., Vörös, J., Reimhult, E., 2008. Electrochemical Biosensors - Sensor Principles and Architectures. vol. 8 MDPI AG, Basel, Switzerland. https://doi.org/10.3390/s80314000.
Harnisch, F., Freguia, S., 2012. A basic tutorial on cyclic voltammetry for the investigation of electroactive microbial biofilms. Chem. Asian J. 7 (3), 466–475. https://doi.org/10.1002/asia.201100740.
Hood, S.K., Zottola, E.A., 1997. Adherence to stainless steel by foodborne microorganisms during growth in model food systems. Int. J. Food Microbiol. 37 (2–3), 145–153. https://doi.org/10.1016/S0168-1605(97)00071-8.
de Jonghe, V., Coorevits, A., de Block, J., van Coillie, E., Grijspeerdt, K., Herman, L., de Vos, P., Heyndrickx, M., 2010. Toxinogenic and spoilage potential of aerobic spore-formers isolated from raw milk. Int. J. Food Microbiol. 136 (3), 318–325. https://doi.org/10.1016/j.ijfoodmicro.2009.11.007.
Kang, J., Kim, T., Tak, Y., Lee, J.-H., Yoon, J., 2012. Cyclic voltammetry for monitoring bacterial attachment and biofilm formation. J. Ind. Eng. Chem. 18 (2), 800–807. https://doi.org/10.1016/j.jiec.2011.10.002.
Kim, Y.W., Sardari, S.E., Meyer, M.T., Iliadis, A.A., Wu, H.C., Bentley, W.E., Ghodssi, R., 2012a. An ALD aluminum oxide passivated surface acoustic wave sensor for early biofilm detection. Sensors Actuators B Chem. 163, 136–145.
Kim, Seonghwan, Yu, Guiduk, Kim, Taeyoung, Shin, Kyusoon, Yoon, Jeyong, 2012b. Rapid bacterial detection with an interdigitated array electrode by electrochemical impedance spectroscopy. Electrochim. Acta 82, 126–131. https://doi.org/10.1016/j.electacta.2012.05.131.
Kirkland, C.M., Herrling, M.P., Hiebert, R., Bender, A.T., Grunewald, E., 2015. In situ detection of subsurface biofilm using low-field NMR: A field study. Environ. Sci. Technol. 49, 11045–11052.
Kwak, Yeon Hwa, Lee, Junhee, Lee, Junghoon, Kwak, Soo Hwan, Oh, Sangwoo, Paek, Se-Hwan, Ha, Un-Hwan, Seo, Sungkyu, 2014. A simple and low-cost biofilm quantification method using LED and CMOS image sensor. J. Microbiol. Methods 107, 150–156. https://doi.org/10.1016/j.mimet.2014.10.004.
Laczka, O., Baldrich, E., Muñoz, F.X., del Campo, F.J., 2008. Detection of Escherichia coli and Salmonella typhimurium using interdigitated microelectrode capacitive immunosensors. The importance of transducer geometry. Anal. Chem. 80 (19), 7239–7247. https://doi.org/10.1021/ac800643k.
Lewandowski, Z., Beyenal, H., 2013. Fundamentals of Biofilm Research. CRC Press/Taylor & Francis Group, Boca Raton.
Liengen, T., Basseguy, R., Feron, D., Beech, I., Birrien, V., 2014. Understanding Biocorrosion: Fundamentals and Applications. Elsevier Reference Monographs (ISBN 978-1-78242-125-2).
Marchand, S., de Block, J., de Jonghe, V., Coorevits, A., Heyndrickx, M., Herman, L., 2012. Biofilm formation in Milk production and processing environments; influence on milk quality and safety. Compr. Rev. Food Sci. Food Saf. 11 (2), 133–147. https://doi.org/10.1111/j.1541-4337.2011.00183.x.
Marsili, E., Baron, D.B., Shikhare, I.D., Coursolle, D., Gralnick, J.A., Bond, D.R., 2008. Shewanella secretes flavins that mediate extracellular electron transfer. Proc. Natl. Acad. Sci. U. S. A. 105 (10), 3968–3973. https://doi.org/10.1073/pnas.0710525105.
Moretto, L.M., Kalcher, K., 2014. Environmental Analysis by Electrochemical Sensors and Biosensors. Springer New York, New York, NY. https://doi.org/10.1007/978-1-4939-0676-5.
Nealson, K.H., Finkel, S.E., 2011. Electron flow and biofilms. MRS Bull. 36 (5), 380–384. https://doi.org/10.1557/mrs.2011.69.
Sasahara, K., Zottola, E., 1993. Biofilm formation by listeria monocytogenes utilizes a primary colonizing microorganism in flowing systems. J. Food Prot. 56 (12), 1022–1028.
Sørhaug, T., Stepaniak, L., 1997. Psychrotrophs and their enzymes in milk and dairy products. Quality aspects. Trends Food Sci. Technol. 8 (2), 35–41. https://doi.org/10.1016/S0924-2244(97)01006-6.
Strycharz, S.M., Malanoski, A.P., Snider, R.M., Yi, H., Lovley, D.R., Tender, L.M., 2011. Application of cyclic voltammetry to investigate enhanced catalytic current generation by biofilm-modified anodes of Geobacter sulfurreducens strain DL1 vs. variant strain KN400. Energy Environ. Sci. 4 (3), 896–913. https://doi.org/10.1039/C0EE00260G.
Sultana, S.T., Babauta, J.T., Beyenal, H., 2015. Electrochemical biofilm control: A review. Biofouling 31 (9–10), 745–758. https://doi.org/10.1080/08927014.2015.1105222.
Teixeira, P., Oliveira, R., 1999. Influence of surface characteristics on the adhesion of alcaligenes denitrificans to polymeric substrates. J. Adhes. Sci. Technol. 13 (11), 1287–1294. https://doi.org/10.1163/156856199X00190.
Vanegas, D.C., Gomes, C., McLamore, E.S., 2016. Biosensors for indirect monitoring of foodborne Bacteria. Biosens J 5 (1). https://doi.org/10.4172/2090-4967.1000137.
Vieira, M.J., Pinho, I.A., Gião, S., Montenegro, M.I., 2003. The use of cyclic voltammetry to detect biofilms formed by pseudomonas fluorescens on platinum electrodes. Biofouling 19 (4), 215–222.
Xu, S., Liu, H., Fan, Y., Schaller, R., Jiao, J., Chaplen, F., 2012. Enhanced performance and mechanism study of microbial electrolysis cells using Fe nanoparticle-decorated anodes. Appl. Microbiol. Biotechnol. 93 (2), 871–880.
Zoski, C.G. (Ed.), 2007. Handbook of Electrochemistry. United Kingdom Elsevier, Oxford.

2.3.2 Publication 6 Electrochemical detection of a *P. polymyxa* biofilm and CIP cleaning solutions by voltammetric microsensors

Thin-film interdigitated electrochemical microelectrodes have gained new relevance in the real-time detection and monitoring of biofilms at early stage of its development.

This article describes the investigation of *P. polymyxa* biofilm and CIP cleaning solutions by using interdigitated microelectrodes combined with two electrochemical voltammetric methods, cyclic voltammetry and square wave voltammetry. The differences between the responses of the uncolonized sterile microelectrodes, the microelectrodes after *P. polymyxa* bacterial attachment for 18 h and of CIP cleaning solutions were reported in the article.

The results described in this article indicate that cyclic voltammetry and square wave voltammetry measurements with interdigitated microelectrodes can be used for the detection of biofilm and of CIP cleaning solutions. First, cyclic voltammetry showed the possibility to detect *P. polymyxa* biofilms at scan rates of 50, 100 and 250 mV s^{-1}. Secondly, square wave voltammetry can be recommended for the detection of the CIP cleaning solutions at lower frequencies. It was observed that for a *P. polymyxa* bacterial suspension the peak currents increased after incubation, while for a *P. polymyxa* biofilm the peak currents decreased. Therefore, it has been suggested that there may be two behaviours in opposite direction that affect the current change with the bacterial attachment. On the one hand, the current increases due to the enhanced electrochemical interaction, by the electron transfer between the bacterial surface-associated molecules and the electrode surface, and on the other hand, the current decreases due to the surface-covering by the fully developed biofilm, which diminish the available area for the electrochemical interaction.

Author contributions

Fysun, O., Rauschnabel, J., Langowski, H.-C. devised the project, the main conceptual ideas and proof outline. Fysun, O. designed the experiments and technical details. Khorshid, S. collected the data and performed the analysis for the data. Fysun, O. wrote the manuscript. All authors discussed the results and commented on the manuscript. Langowski, H.-C. contributed to the final version of the manuscript.

Engineering in Agriculture, Environment and Food 12 (2019) 232–243

Contents lists available at ScienceDirect

Engineering in Agriculture, Environment and Food

journal homepage: www.elsevier.com/locate/eaef

Electrochemical detection of a *P. polymyxa* biofilm and CIP cleaning solutions by voltammetric microsensors

Olga Fysun[a,b,*], Sara Khorshid[b,c,1], Johannes Rauschnabel[b], Horst-Christian Langowski[a,d]

[a] TUM School of Life Sciences Weihenstephan, Technical University of Munich, Freising, Germany
[b] Robert Bosch Packaging Technology GmbH, Waiblingen, Germany
[c] Department of Mechanical and Process Engineering, University of Kaiserslautern, Kaiserslautern, Germany
[d] Fraunhofer Institute for Process Engineering and Packaging IVV, Freising, Germany

ARTICLE INFO

Keywords:
Electrochemistry
Voltammetry
Microelectrodes
P. polymyxa
Biofilm
CIP cleaning

ABSTRACT

Biofilm formation in processing equipment can lead to higher costs due to more frequent cleaning events as well as the contamination of processed foods and is a concerning issue. It is necessary to establish new methods for the detection of biofilms formation on surfaces. The use of electrochemical microsensors for biofilm detection could be a strategy for real time biofilm control in processing equipment. In this study, voltammetric methods, cyclic voltammetry (CV) and square wave voltammetry (SWV), were employed to detect *P. polymyxa* biofilms and CIP cleaning solutions on platinum-based interdigitated ring array microelectrodes. The differences between the current responses of the uncovered sterile microelectrodes and the microelectrodes after *Paenibacillus polymyxa* attachment for 18 h were determined. The surface coverage of microelectrodes was visualized using microscopy techniques. The results of this study demonstrated that cyclic voltammetry revealed the most promising results for *P. polymyxa* biofilm detection, while square wave voltammetry can be recommended for the detection of CIP cleaning solutions.

1. Introduction

Food industry is highly challenged by the bacterial contamination of processing equipment and successive biofilm formation, due to extended production runs, the use of more complex processing equipment, and the further automation of processing plants (Chmielewski and Frank, 2003; Marchand et al., 2012).

Bacterial adhesion is the initial step in colonization and biofilm formation (Hori and Matsumoto, 2010). Many characteristics of the environment surrounding bacteria, e.g., pH, nutrient levels, ionic strength and temperature, have effects on the bacterial attachment (Pringle and Fletcher, 1983; Vu et al., 2012). Several physicochemical models based on the DLVO theory and a thermodynamic approach were proposed to describe the bacterial adhesion processes (Hori and Matsumoto, 2010).

According to the IUPAC definition, "biofilms are an aggregate of microorganisms in which cells that are frequently embedded within a self-produced matrix of extracellular polymeric substances (EPS) adhere to each other and/or to a surface" (Vert et al., 2012). Biofilm thickness can range between several μm to mm (Cappitelli et al., 2014). The EPS consists predominantly of polysaccharides, a wide variety of proteins, glycoproteins, glycolipids, and in some cases, amounts of extracellular DNA (e-DNA) (Flemming et al., 2007). One of the most important functions of EPS is to supply the matrix, which acts as a scaffold for the microbial structures. The biofilm formation and lifecycle can be divided into five steps: reversible attachment to a surface (1), irreversible attachment to a surface (2), formation of microcolonies (3), biofilm maturation (4) and detachment and dispersion (5) (Marchand et al., 2012).

Bacterial attachments and biofilm formation in processing equipment can cause serious problems, resulting in significant economic losses and decreased safety of processed foods. The EPS-stability and the increased tolerance of microorganisms in biofilms towards biocides, require an increased effort in the cleaning processes (Van Houdt and Michiels, 2010). Therefore, biofilm formation can limit the uptime of manufacturing plants, increasing the cleaning times and lowering the quality of products (Chmielewski and Frank, 2003). For example, in dairy industry, the contamination with non-starter bacteria due to biofilms can threaten whole batches (Somers et al., 2001). In heat exchangers, biofilm development can decrease the heat transfer, which

* Corresponding author. TUM School of Life Sciences Weihenstephan, Technical University of Munich, Freising, Germany.
E-mail address: olga.fysun@bosch.com (O. Fysun).
[1] Present address: Sanofi-Aventis Deutschland GmbH, Frankfurt, Germany.

https://doi.org/10.1016/j.eaef.2019.01.004
Received 17 August 2018; Received in revised form 10 December 2018; Accepted 18 January 2019
Available online 29 January 2019

Abbreviations

CV	Cyclic voltammetry
SWV	Square wave voltammetry
EPS	Extracellular polymeric substance
RLU	Relative light units
DLVO theory	B. Derjaguin, L. Landau, E. Verwey, T. Overbeek theory
CFU	Colony forming units
EET	Extracellular electron transfer
CIP	Cleaning-in-place

leads to higher resource consumption (Al-Haj, 2012). Moreover, most unfavorable outcomes for customers are product spoilage and food-borne illnesses (Verran, 2002).

The cleaning-in-place (CIP) process is a commonly used cleaning procedure for industrial food processing equipment. CIP cleaning is defined as: "cleaning of complete items of plant or pipeline circuits without dismantling or opening of the equipment and with little or no manual involvement on the part of the operator. The process involves the jetting or spraying of surfaces or circulation of cleaning solutions through the plant under conditions of increased turbulence and flow velocity" (Romney, 1990). The target of CIP-procedures is to remove all kinds of deposits (protein, minerals, micro-organisms) and, thus, preserving the plant performance and hygiene (Gillham et al., 1999). Depending on the goods being produced, alkali and acid cleaning solutions are used in combination with several steam and heating phases. Alkali soluble deposits are fats and proteins, whereas acid soluble deposits are calcium salts and mineral oil (Kessler, 2006).

Bacteria belonging to the *Bacillus* and *Paenibacillus* genus, are spoilage bacteria for pasteurized, refrigerated foods, e.g., milk is spoilt due to biofilm formation in the production lines (Marchand et al., 2012; De Jonghe et al., 2010). Gopal et al. (2015) reported that *Paenibacillus* spp. are a concern for the dairy industry because *Paenibacillus* spores can be found in raw and pasteurized milk. Gram-positive endospore-forming *Paenibacillus polymyxa* has been isolated from both farm and processing plant environments, and also from raw and pasteurized fluid milk. *P. polymyxa* is a rod-shaped bacterium, which is motile due to peritrichous flagella (He et al., 2007). *P. polymyxa* bacteria produce a variety of hydrolytic extracellular enzymes such as proteases, lipases and lecithinases that can cause spoilage of pasteurized milk. Lecithinase activity of *P. polymyxa* is responsible for the bitty cream defects in milk due to the aggregation of fat globules (De Jonghe et al., 2010).

Several techniques could be employed for biofilm detection (Kim et al., 2012; Kirkland et al., 2015; Reyes-Romero et al., 2014; Hwa Kwak et al., 2014). The techniques used for biofilm assessment in industrial equipment are based on heat transfer measurements or monitoring pressure drops (Janknecht and Melo, 2003). Although these techniques provide fast information on biofilm formation without sampling, these methods are not suitable for the detection of biofilms at the early stages of formation. According to Characklis et al. (1990), there are only significant changes in the friction factor when the biofilm reaches a critical thickness of about 35 μm.

Electrochemical sensors have gained new relevance in real time biofilm detection and monitoring in the last decades. Electrochemical measurements monitor the faradaic current generated by the reduction and oxidation of an electrolyte in contact with a solid electrode (Becerro et al., 2016). Several electrochemical methods have been investigated to detect biofilm formation, e.g., electrochemical impedance spectroscopy, potentiometric, and voltammetric methods. Voltammetric methods such as, cyclic voltammetry (Kang et al., 2012; Marsili et al., 2008, 2010; Vieira et al., 2003; Becerro et al., 2016), and square wave voltammetry (Webster et al., 2015; Webster and Goluch, 2012; Xu et al., 1998; Nguyen et al., 2012), are particularly useful techniques in biofilm research (Lewandowski and Beyenal, 2013).

Several theories on the mechanisms of electrochemical detection of bacteria have been reported (Babauta et al., 2012; Kato, 2016). Although a widely shared explanation does not exist, it is evident that bacteria living in surface-attached biofilms must maintain electrochemical gradients to support basic cellular functions (Nealson and Finkel, 2011; Sultana et al., 2015). Bacteria can enable efficient electron transfer between themselves and extracellular solid materials as part of their metabolism, which is called extracellular electron transfer (EET). EET can be divided into direct and indirect mechanisms. Direct EET describes electrons, which are transferred directly via the outer-membrane proteins, or through a solid conductive matrix, such as pili or outer membrane extensions. Indirect electron transfer occurs via electron mediators, e.g., enzyme complexes (Kato, 2016; Babauta et al., 2012; Reguera et al., 2005).

In the last decade, great effort has been devoted to the development of electrochemical sensor and biosensors (Ren et al., 2017; Wang et al., 2018; Becerro et al., 2015; Tarditto et al., 2016). They are produced by depositing a thin film of inorganic material onto a supporting body, e.g., by vacuum or sputter deposition. Microelectrodes can be designed in various shapes, e.g., interdigitated or stiletto shaped arrays. The response time of a microelectrode is much shorter than the response time of classical electrodes, they are not sensitive to convection from external sources, and only need a lower content of supporting electrolyte (Gründler, 2007).

Therefore, this study investigated the detection of two substance groups (*P. polymyxa* biofilm group and CIP cleaning solutions group) by using interdigitated microelectrodes and the electrochemical voltammetric methods of cyclic voltammetry and square wave voltammetry. Cyclic voltammetry was conducted at three scan rates, while square wave voltammetry was performed at three frequencies. The differences between the responses of the uncolonized sterile microelectrodes and the microelectrodes after *P. polymyxa* bacterial attachment for 18 h were determined. In addition, the bacterial surface coverage of the microelectrodes was visualized by microscopy.

2. Material and methods

2.1. Chemicals

Meat extract, nitric acid 60% (v v^{-1}), and ethanol 70% (v v^{-1}) were supplied by VWR (Darmstadt, Germany). Peptone from casein (pancreatic digest) was obtained from Applichem Panreac (Barcelona, Spain). Plate count agar, potassium chloride 3 mol L^{-1}, and sodium hydroxide 30% (v v^{-1}) were purchased from Merck (Darmstadt, Germany). Potassium ferrocyanide 1% was supplied by Clin-Tech, (Guildford, UK). The freeze-dried culture of *Paenibacillus polymyxa* (DSM 36) was acquired from DSMZ (Braunschweig, Germany). All the chemicals were of analytical grade.

2.2. Sample preparation

2.2.1. P. polymyxa biofilm preparation

Agar plate cultures *P. polymyxa* (DSM 36) were prepared from the freeze-dried culture according to the manufacturer's instructions. A colony of *P. polymyxa* was taken from a prepared agar plate and was resuspended in an Eppendorf vial filled with 1 mL of sterile nutrient medium. The inoculated medium was transferred into a 250 mL Erlenmeyer flask with 99 mL of the sterile nutrient medium. The suspension was incubated, stirred at 140 rpm, and kept at 30 °C for 2 − 3 h to reach the early exponential growth phase. To ensure the exponential growth phase of *P. polymyxa* for the experiments, the transmittance of the bacterial suspension used for the inoculation had to reach around 90.0 ± 3.0% at 570 nm. The number of bacteria in the early exponential phase corresponds to about 1.2×10^6 CFU mL^{-1}.

For the *P. polymyxa* adhesion, a cleaned and activated microelectrode was placed into each well of the sterile 6-well plates (Greiner Bio-One GmbH, Frickenhausen, Germany). Each microelectrode was immersed into

a well in such a way that the electrochemical cell of the microsensor has a direct contact with the liquid phase. The wells were filled with 5 mL of the sterile nutrient medium and inoculated with 100 µL of bacterial suspension at the early exponential phase, prepared as described above. The 6-well plates containing the microelectrodes were incubated at 30 °C for 18 h in the climate chamber. After incubation, the microelectrodes were removed gently with plastic tweezers. The electrode pads on the bottom of the microelectrode were wiped with Kimtech Science™ wipes, while the electrochemical cell of the microsensor was not touched. Then, the microelectrode was placed into the slot of a drop-cell to conduct electrochemical measurements. Three types of samples in the biofilm group were measured: (1) bacterial suspension of *P. polymyxa* after incubation in a 6-well plate, (2) *P. polymyxa* biofilm covering the microelectrode + bacterial suspension of *P. polymyxa* after incubation (sample 1), and (3) sterile nutrient medium as the reference. For each experiment, 5 µL of either sterile nutrient medium or *P. polymyxa* bacterial suspension of the corresponding well were pipetted onto the electrochemical cell of the microsensor before measurement.

2.2.2. CIP solutions preparation

CIP cleaning solutions, sodium hydroxide NaOH 30% (v v^{-1}) and nitric acid HNO_3 60% (v v^{-1}) were diluted to 1% (v v^{-1}), which corresponds to the typical cleaning solution concentration for CIP cleaning processes. The pH values of demineralized H_2O, NaOH 1% (v v^{-1}), HNO_3 1% (v v^{-1}) were determined as 5.7 ± 0.2, 12.7 ± 0.3 and 1.9 ± 0.2, respectively. The cleaned and activated microelectrode was placed into the slot of the drop-cell to conduct electrochemical measurements. Before each measurement, 5 µL of each sample from within the CIP cleaning solutions group were pipetted onto the working electrode of the electrochemical cell.

2.3. Electrochemical setup and electrodes

Voltammetric experiments were conducted using a drop-cell and a platinum interdigitated microelectrode provided by MicruX Fluidic (Oviedo, Spain). The microelectrode comprises of four electrodes: two working electrodes, one auxiliary, and one reference electrode. The electrochemical cell has a diameter of 2.0 mm. The working electrode has120 feet pairs, which are 10 µm wide, with a 10 µm gap between each foot. The drop-cell was connected to a PalmSense 3 bipotentiostat (PalmSens BV, Houten, The Netherlands) via a mini-USB cable. The measurements were performed in single-mode using one working electrode. All the measurements were conducted at room temperature, 23.5 ± 0.5 °C.

The microelectrodes were cleaned and electrochemically activated before use. First, the microelectrodes were wiped with demineralized water using Kimtech Science™ wipes, degreased with ethanol 70% (v v^{-1}) for 5 min, and then rinsed with demineralized water again. Secondly, the microelectrodes were activated electrochemically using 10 µL of 0.1 M KCl via cyclic voltammetry. During activation, the potential was cycled 12 times between −1.5 and 1.5 V at a scan rate of 100 mV s^{-1}.

2.4. Electrochemical methods employed

Voltammetric methods, cyclic voltammetry and square wave voltammetry, were used to measure the changes in current as a function of potential. In cyclic voltammetry a triangular changing potential is applied to an electrode while the current is monitored. Square-wave voltammetry uses a potential ramp consisting of large-amplitude variations in potential. In cyclic voltammetry, a potential scan is performed between two vertex potentials, E_{vtx1} and E_{vtx2}. The potential change is reversed once a vertex potential is reached. For each microelectrode, three cycles were performed with the following parameters: $T_{equilibrium}$ = 15 s, E_{begin} = −0.5 V, E_{vtx1} = −0.5 V, E_{vtx2} = 1.0 V, E_{step} = 0.01 V, scan rate = 50, 100, and 250 mV s^{-1} with overall duration of 04:15, 02:15, and 01:03 mm:ss, respectively. In square wave voltammetry, the following parameters were used: $T_{equilibrium}$ = 5 s, E_{begin} = −0.5 V, E_{end} = 0.5 V, E_{step} = 0.001 V, $E_{amplitude}$ = 0.024 V, frequency = 25, 50, and 100 Hz with overall duration of 00:54, 00:35, and 00:25 mm:ss, respectively. All the experiments were carried out in triplicate. All the samples were scanned three times during one measurement. In total, each sample was scanned nine times at each scan rate or frequency. The mean value and standard deviation were calculated from obtained measurements. In addition, the standard errors of the mean (SE), the sum of the standard errors of mean, and the sum of the variances were calculated for the whole potential window.

2.5. Microscopy analysis

Microscopic analysis of the *P. polymyxa* biofilm on the microelectrodes was conducted with a digital microscope (Keyence VHX-1000, Japan). For this, the microelectrodes were taken out of the 6-well plate and were dried for 2–3 min at room temperature. The *P. polymyxa* biofilm was not stained with dyes. Two objectives were used: ZS20 at a magnification of 150×, and ZS200 at a magnification of 1000× and 2000×.

2.6. Statistics

Excel 2013 (Microsoft Corporation, USA) was used to obtain the mean and standard deviation of the retrieved data from the electrochemical measurements. The average and standard deviations were calculated from the results of the second, third and fourth scans. MATLAB R2016b 64bit (The MathWorks, Inc., USA) was used for descriptive statistics to calculate the standard errors of the mean (SE), the sum of the standard errors of mean, and the sum of the variances for the whole potential window. The voltammograms were also plotted in MATLAB R2016b 64bit. The peak currents and peak potentials were obtained using software PSTrace (version 5.3311) (PalmSens BV, The Netherlands).

3. Results

3.1. Microscopy analysis

A detailed analysis of the early stage of biofilm formation on the surface of the electrode was performed using micrographs of the electrodes without staining (Fig. 1 A–D). The images show the microcolonies of *P. polymyxa* on the electrode surface.

Fig. 1A–D show the attachment of *P. polymyxa* bacteria to the electrode after 18 h of incubation in nutrient medium at 30 °C. The microcolony distribution on the surface was non-homogeneous, showing many bacterial microcolonies and single cells. The large standard deviations in the voltammetric measurements can be explained due to the non-homogeneous distribution of microcolonies of *P. polymyxa* on the electrode surface (Fig. 1 A). Since the diameter of the electrochemical cell is 2.0 mm, bacteria can adhere also to other non-measuring areas of the sensor surface. Fig. 1 C demonstrates the scaled up micrograph of the bacterial community. Fig. 1 D illustrates the three-dimensional micrograph of the interdigitated microelectrode with attached bacteria, and shows the microcolonies on the pairs of the microbands within the IDA structure (marked with the red circle). From Fig. 1 D it can be derived that the thickness of the microcolony is about 6 µm.

3.2. Electrochemical investigations

3.2.1. Cyclic voltammetry

The cyclic voltammograms at scan rates of 50 mV s^{-1}, 100 mV s^{-1}, and 250 mV s^{-1} from the three samples within the biofilm group were: (1) the bacterial suspension of *P. polymyxa* after 18 h incubation, (2) *P. polymyxa* biofilm covering the microelectrode + bacterial suspension of

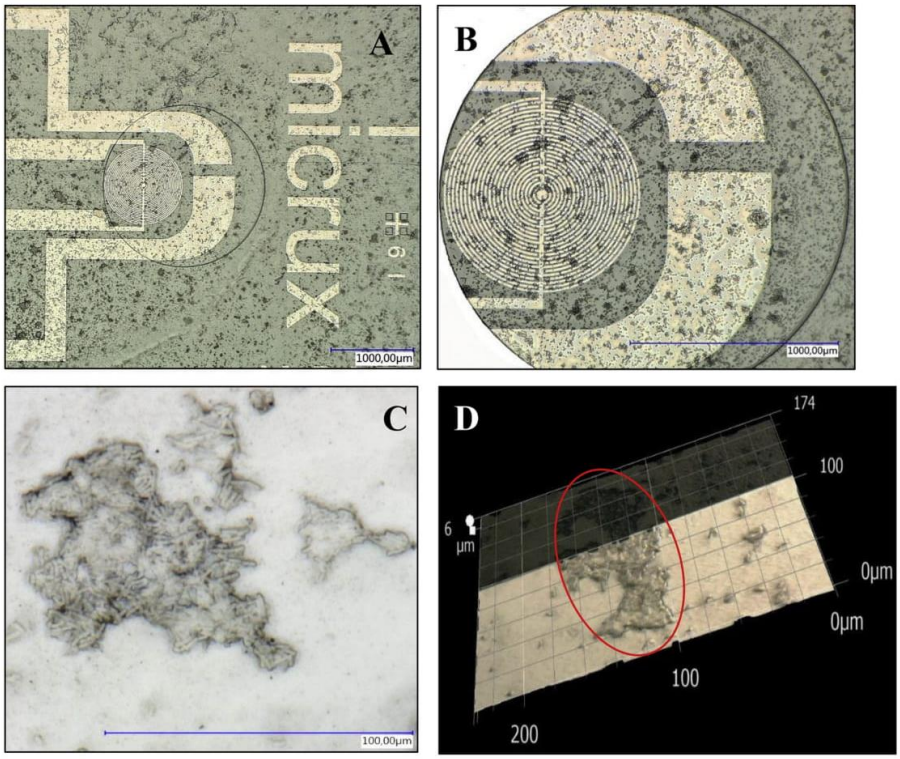

Fig. 1. Micrographs of the interdigitated microelectrode surface with attached *P. polymyxa* at early stage of biofilm formation (18 h incubation in nutrient medium at 30 °C). All the samples were recorded without an oil objective, ZS20 (A) 50× and (B) 150× magnification with the objective ZS200 (C) 2000× magnification, (D) three dimensional pictures of the attached *P. polymyxa* microcolony on the interdigitated microelectrode surface with the objective ZS200 at 1000× magnification.

P. polymyxa after18 h incubation (sample 1), and (3) the sterile nutrient medium as the reference, and are shown in Fig. 2 A, B and C, respectively.

From the CVs of the *P. polymyxa* bacterial suspension, an anodic (oxidation) peak at potentials of 0.67 V, 0.79 V and 0.88 V was observed at scan rates of 50 mV s^{-1}, 100 mV s^{-1} and 250 mV s^{-1}, respectively (Fig. 2 and Table 1). In addition, a cathodic (reduction) peak was detected for the bacterial suspension at −0.21 V at a scan rate of 250 mV s^{-1}. The peaks for *P. polymyxa* bacterial suspension were more pronounced at 250 mV s^{-1} that at the lower scan rates of 50 mV s^{-1} and 100 mV s^{-1}. No anodic peaks were found for the *P. polymyxa* biofilm at the selected scan rates. A cathodic peak for the *P. polymyxa* biofilm at a potential of −0.43 V was observed at scan rates of 50 mV s^{-1} and 100 mV s^{-1}. No oxidation or reduction peaks could be obtained from the voltammograms of the nutrient medium (Fig. 2 A, 2 B, 2 C). Notable differences between the reference (sterile nutrient medium) and *P. polymyxa* bacterial suspension as well as *P. polymyxa* biofilm were detected in the potential window from 0.7 to 1.0 V in the anodic curve at all tested scan rates as well as in the cathodic curve in the potential window from −0.3 to −0.5 V.

Analyzing, from the standard error of the mean, it can be observed that the errors from the bacterial suspension and biofilm were higher than the errors from the reference (nutrient medium), at each scan rate (Fig. 2 AI, 2 BI, 2 CI). This observation could be attributed to the movement of bacteria via peritrichous flagella (He et al., 2007) and/or the inhomogeneous distribution of bacteria on the surface of the working electrode in the electrochemical cell (Fig. 1 A and B). Notably, the highest standard error of the mean was observed at the potentials where the anodic and the cathodic peaks were obtained (Fig. 2 A, 2 B, 2 C). In addition, an increase in the standard error of the mean was detected for the biofilm in the potential window between −0.1 and 0.5 V, where no anodic or cathodic peak was present (Fig. 2 B, 2 C). This observation could be attributed to different electrode surface coverages by the biofilm.

Table 1 summarizes the anodic and cathodic peak currents and peak potentials for the *P. polymyxa* bacterial suspension and the biofilm.

The results in Table 1 show that with increasing scan rate, the current at anodic and cathodic peaks increased considerably for the bacterial suspension. According to literature, the currents at peaks may correspond to the adsorption and desorption of oxygen for the platinum electrode (Kang et al., 2012; Vieira et al., 2003). The potential of the anodic and cathodic peaks shifted towards more positive potentials with increasing scan rate. This indicated an irreversible electrochemical process. This result is in accordance with the previous study that showed that an irreversible oxidation peak appears at about 0.69 V for 2.0×10^8 CFU mL^{-1} ETEC F4 suspensions in PBS at a scan rate of 50 mV s^{-1} (Tarditto et al., 2016).

The higher standard error of the mean for the *P. polymyxa* biofilm and the bacterial suspension can be explained by the fact that the mean average was calculated from three independent measurements, which was repeated four times (four scans). To explain in more details, the cyclic voltammogram of the one independent measurement (three scans) of (1) the *P. polymyxa* bacterial suspension 18 h and (2) *P. polymyxa* biofilm covering the microelectrode + bacterial suspension of *P. polymyxa* 18 h at scan rate of 250 mV s^{-1}, are shown in Fig. 3 A and B, respectively.

From Fig. 3 A it can be seen that the current intensity of the anodic (oxidation) peak for the *P. polymyxa* bacterial suspension decreased

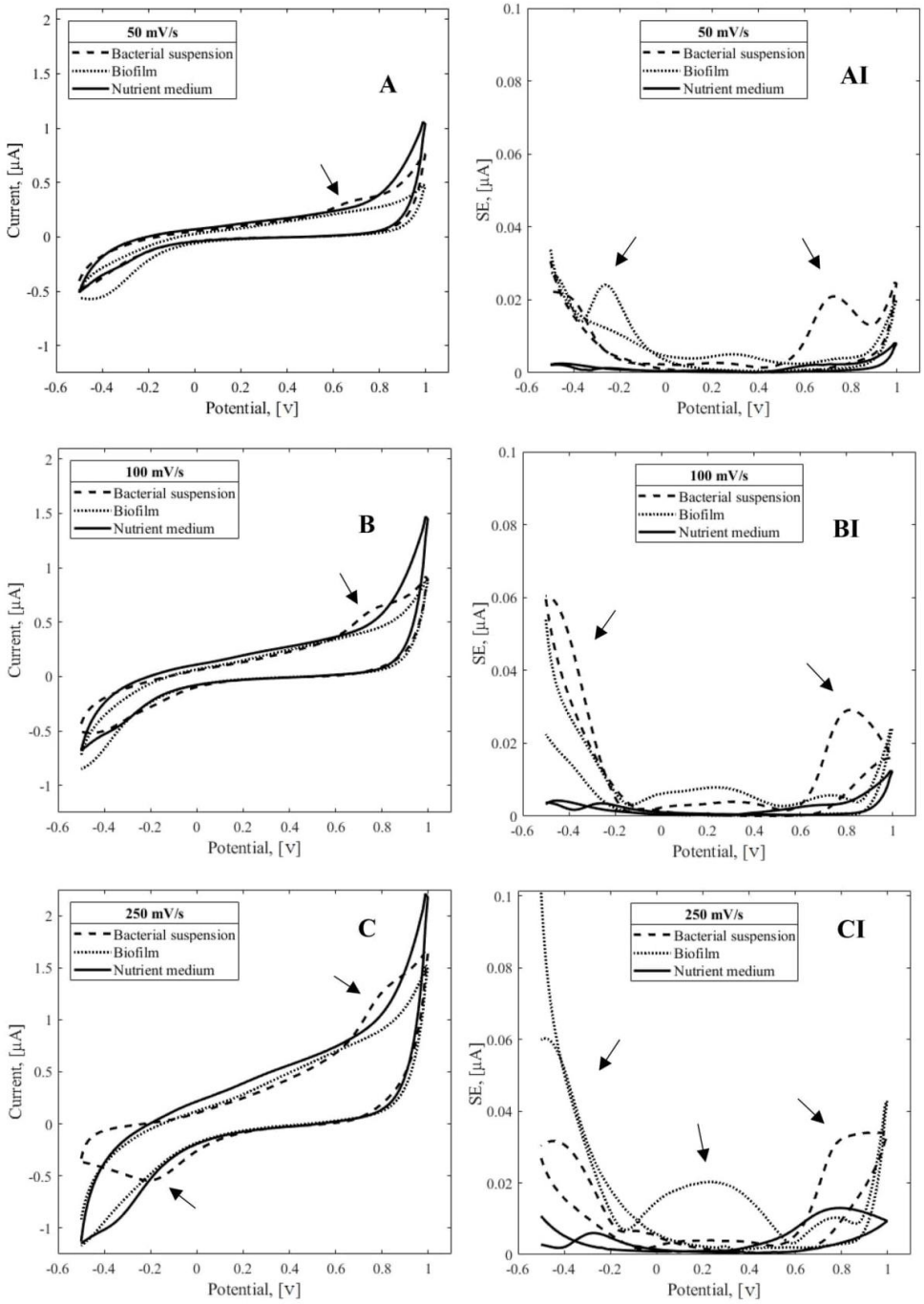

Fig. 2. Cyclic voltammograms obtained for (1) *P. polymyxa* bacterial suspension 18 h, (2) *P. polymyxa* biofilm covering the microelectrode + *P. polymyxa* bacterial suspension 18 h, and (3) sterile nutrient medium. Scan rates of (A) 50 mV s^{-1}, (B) 100 mV s^{-1} and (C) 250 mV s^{-1} with the respective standard errors of the mean (SE) (AI, BI, CI) (i = 3, n = 9).

Table 1
Anodic and cathodic peak currents (μA) and peak potentials (V) of the *P. polymyxa* bacterial suspension and the *P. polymyxa* biofilm obtained from cyclic voltammetry (i = 3, n = 9).[a]

Scan rate (mV s^{-1})	I_{pA}, I_{pC} (μA) E_{pA}, E_{pC} (V)	Bacterial suspension	Biofilm
50	I_{pA}	0.10 ± 0.00	none
	E_{pA}	0.67 ± 0.03	none
	I_{pC}	−0.21 ± 0.62	−0.45 ± 0.08
	E_{pC}	−0.48 ± 0.00	−0.43 ± 0.05
100	I_{pA}	0.20 ± 0.03	none
	E_{pA}	0.79 ± 0.06	none
	I_{pC}	−0.21 ± 0.14	−0.19 ± 0.16
	E_{pC}	−0.38 ± 0.08	−0.47 ± 0.01
250	I_{pA}	0.47 ± 0.04	none
	E_{pA}	0.88 ± 0.02	none
	I_{pC}	−0.40 ± 0.20	−0.21 ± 0.12
	E_{pC}	0.13 ± 0.01	−0.47 ± 0.03

[a] The reference (nutrient medium) did not show anodic and cathodic peaks.

after a few consecutive scans. This behaviour suggests the gradual passivation of the electrode surface, due to the possible blocking effect of electro-inactive anodic reaction products (Tarditto et al., 2016). On the contrary, Fig. 3 B shows the increase in the cathodic (reduction) peak for the *P. polymyxa* biofilm. It has been previously reported that in electrochemical measurements of a *Pseudomonac fluorescens* biofilm on platinum electrodes, the voltammograms obtained with increasing number of scans (1, 2, 5, 10 and 100 scans), approached that corresponding to an uncolonized surface (Vieira et al., 2003). According to Vieira et al. (2003), this can be explained by the fact that the distance between the adhered bacteria and the surface is very low due to an interaction on the primary minimum of energy according to DLVO theory (Hori and Matsumoto, 2010). Therefore, the oxidation-reduction reactions cannot occur on some areas of the electrodes. As the potential is applied to the platinum surface, the distance between the bacterial cells and the surface may increase and the liquid film between the bacterial cells and the surface becomes thicker. Consequently, oxidation-reduction processes may occur on the platinum surface that was previously occupied by cells, and a voltammogram similar to that of an uncolonized surface is thereby obtained. Similar behaviour was observed also in this work, as shown in Fig. 3 B.

The cyclic voltammograms at scan rates of 100 mV s^{-1}, and 250 mV s^{-1} for samples of the CIP cleaning solutions are presented in Fig. 4 for NaOH 1% (v v^{-1}) and Fig. 5 for HNO_3 1% (v v^{-1}) and H_2O).

In general, among the CIP cleaning solutions that were tested, NaOH 1% (v v^{-1}) exhibited the highest current signal. However, no clear anodic or cathodic peaks for NaOH 1% (v v^{-1}) were observed at scan rates of 100 mV s^{-1} or 250 mV s^{-1} using the same method settings that were employed in the samples from the biofilm group. Moreover, for NaOH 1% (v v^{-1}), anodic and cathodic peak currents could be present, although they seem negligible compared to the highest current response of 49.7 μA for scan rates of 100 mV s^{-1} and of 250 mV s^{-1}. One possible explanation is that the choice of the same potential window as for bacterial biofilm samples is not suitable for electrochemical measurements of NaOH 1% (v v^{-1}). As reported, aqueous solutions with different pH may have decreased the electrochemical window. Therefore, the sudden increase of current in the anodic curve can be explained by the oxidation of water in sodium hydroxide solution (Atkins and Paula, 2006).

The voltammogram shown in Fig. 5 A indicates that with an increasing scan rate the current, and the difference between the forward and backward scans for HNO_3, increases. Furthermore, the peak potential also shifts with increasing scan rate, which means that no reversible reactions were occurring (Fig. 5 A and Table 2) (Bard and Zoski, 2000). The reference, H_2O showed the lowest current signals and no peaks, due to the fact, that in this potential window no reactions are expected (Atkins and Paula, 2006).

Table 2 summarizes the cathodic peak currents and peak potentials for the nitric acid.

Table 2 shows that with increasing scan rate, the current at the cathodic peaks increased for HNO_3 1% (v v^{-1}). However, no considerable differences between the scan rates for HNO_3 1% (v v^{-1}), can be detected due to a high standard deviation. Also, the potential of the cathodic peak shifted toward positive potentials with increasing scan rate.

Table 3 summarizes the total sum of the standard error of the mean (SSE) and the sum of the variances (SV) for (1) the bacterial suspension of *P. polymyxa* after 18 h incubation, (2) *P. polymyxa* biofilm covering the microelectrode + bacterial suspension of *P. polymyxa* after18 h incubation (sample 1), (3) the sterile nutrient medium, (4) NaOH 1% (v v^{-1}), (5) HNO_3 1% (v v^{-1}), and (6) water at scan rates of 50 mV s^{-1}, 100 mV s^{-1} and 250 mV s^{-1}.

As expected, the reference samples, the water and the nutrient medium showed the lowest sum of the standard error of the mean and the sum of the variances. The highest sum of the standard error of the mean and the sum of the variances among all the samples were obtained for NaOH 1% (v v^{-1}). In the samples of the biofilm group, no clear relationship between the scan rates and the sum of the standard error of the mean or the sum of the variances were observed. For the *P. polymyxa* bacterial suspension, the lowest values were obtained at a scan rate of 50 mV s^{-1}, while the highest at a scan rate of 100 mV s^{-1}. For the *P. polymyxa* biofilm, the sum of the standard error of the mean or the sum of the variances was obtained at 250 mV s^{-1}. The lower values of the sum of the standard error of the mean and the sum of the variances for NaOH 1% (v v^{-1}) and HNO_3 1% (v v^{-1}) were obtained at a scan rate of 100 mV s^{-1}.

3.2.2. Square wave voltammetry

The square wave voltammograms at frequencies of 25 Hz, 50 Hz, and 100 Hz for the samples of the biofilm group: (1) the bacterial suspension of *P. polymyxa* after 18 h incubation, (2) *P. polymyxa* biofilm covering the microelectrode + bacterial suspension of *P. polymyxa* after18 h incubation (sample 1), and (3) the sterile nutrient medium as the reference are plotted in Fig. 6.

From Fig. 6, it can be noted that, similar to the CV results, with increasing frequency, the current responses of the samples increase. The highest current values were obtained for the nutrient medium, followed by the *P. polymyxa* bacterial suspension and finally the *P. polymyxa* biofilm. No peaks were observed for the nutrient medium or the *P. polymyxa* biofilm at all tested scan rates. Only the *P. polymyxa* bacterial suspension showed a small peak at 0.1 V at a frequency of 25 Hz (Fig. 6 A).

A decrease in the maximum current can be observed in going from the sterile nutrient medium, to the *P. polymyxa* bacterial suspension and finally to the *P. polymyxa* biofilm at all the selected frequencies (Fig. 6 A, B, C). This indicates that an additional layer on the working electrode may create a resistance, which decreases the current signal. The standard error of the mean of the *P. polymyxa* biofilm at a frequency of 100 Hz are noteworthy high (Fig. 6 CI). The standard error of the mean is much higher in comparison to the errors obtained at lower frequencies. Therefore, the measurements at 100 Hz were not reproducible compared to the measurements at the lower frequencies of 25 and 50 Hz. In addition, noticeable errors can be seen at 0.1 V for the *P. polymyxa* bacterial suspension measured at 25 Hz. At a potential of 0.1 V, where the peak was obtained (Fig. 6 A), the highest errors were obtained. When the current drops down, the high standard error of the mean disappeared on the SWV voltammogram.

The square wave voltammograms at frequencies of 25 Hz, 50 Hz, and 100 Hz for the three samples of the CIP cleaning solutions are presented in Fig. 7.

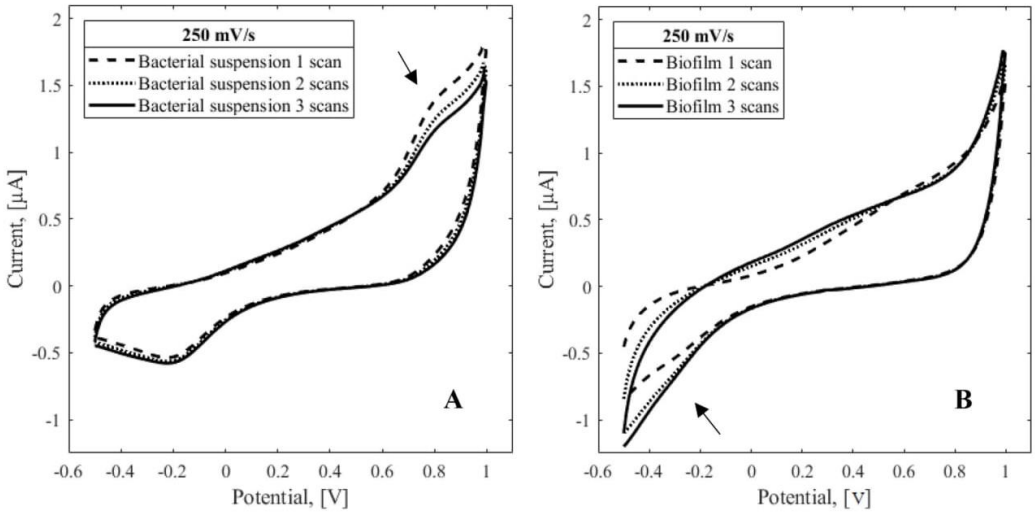

Fig. 3. Cyclic voltammograms (3 scans) obtained for (1) *P. polymyxa* bacterial suspension 18 h (A) and (2) *P. polymyxa* biofilm covering the microelectrode + *P. polymyxa* bacterial suspension 18 h (B) at scan rates of 250 mV s^{-1}.

As shown in the voltammograms (Fig. 7), H_2O showed no peaks in the potential window from −0.5 to 0.5 V. Nevertheless, the SWV results of NaOH 1% (v v^{-1}) and HNO_3 1% (v v^{-1}) demonstrated two oxidation peaks and one oxidation peak at each frequency in the forward scan, respectively. HNO_3 1% (v v^{-1}) showed in all voltammograms a lower current signal than for NaOH 1% (v v^{-1}). Remarkable results were obtained by analyzing the standard errors of the mean for NaOH 1% (v v^{-1}). At potentials of −0.1 V and −0.3 V a strong drop in the standard error of the mean was observed. From comparison to the square wave voltammograms (Fig. 7), these are the potentials where the current peaks are detected. Table 4 summarizes the peak currents and peak potentials for the CIP cleaning solutions.

Similar to the cyclic voltammetry measurements, the peak magnitude increased with the frequency for all samples (Table 4). Considering the standard deviations in peak potentials, it can be seen that potential do not differ significantly between the selected scan rates.

Table 5 shows the total sum of the standard error of the mean (SSE) and the sum of the variances (SV) for (1) the bacterial suspension of *P.*

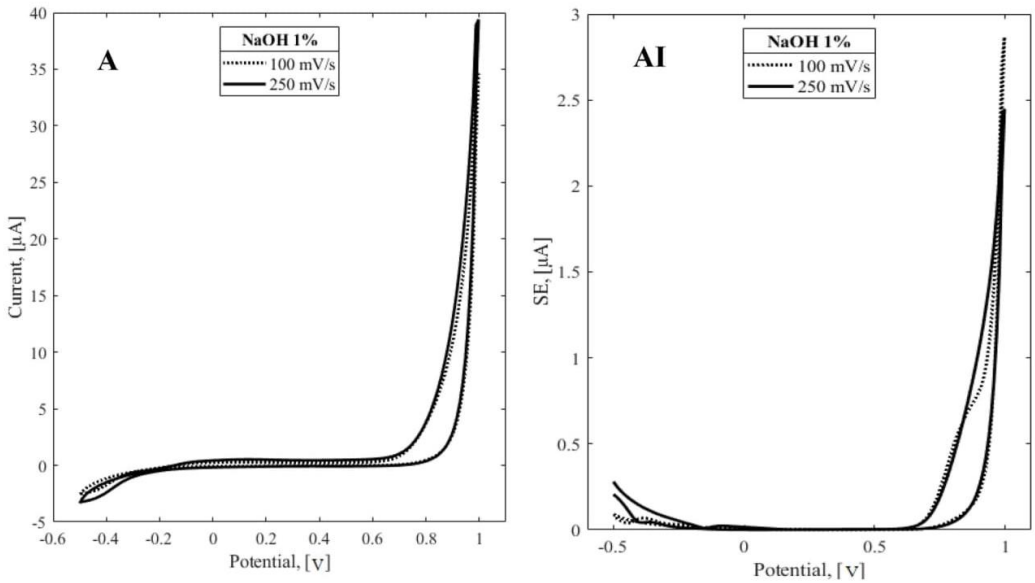

Fig. 4. Cyclic voltammograms obtained for NaOH 1% (v v^{-1}) at scan rates of 100 mV s^{-1} and of 250 mV s^{-1} (A) with respective standard errors of the mean (SE) (AI) (i = 3, n = 9).

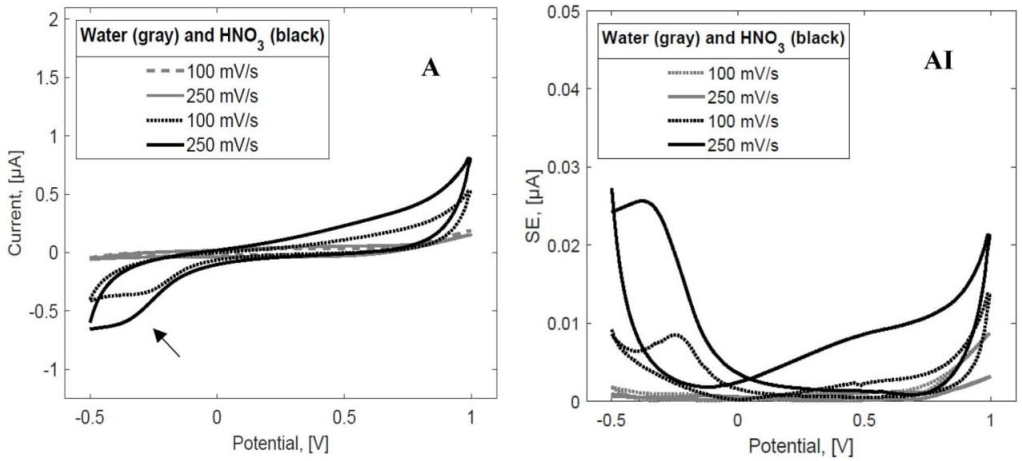

Fig. 5. Cyclic voltammograms for HNO_3 1% (v v^{-1}) and H_2O at scan rates of 100 mV s^{-1} and 250 mV s^{-1} (A) with respective standard errors of the mean (SE) (AI) (i = 3, n = 9).

Table 2
Cathodic peak currents (μA) and peak potentials (V) of HNO_3 1% (v v^{-1}) from cyclic voltammograms (i = 3, n = 9).

Scan rate (mV s^{-1})	I_{pC} (μA) E_{pC} (V)	HNO_3 1% (v v^{-1})
100	I_{pC}	−0.26 ± 0.01
	E_{pC}	−0.34 ± 0.03
250	I_{pC}	−0.37 ± 0.17
	E_{pC}	−0.42 ± 0.02

*H_2O and NaOH 1% (v v^{-1}) did not show anodic and cathodic peaks.

polymyxa after 18 h incubation, (2) *P. polymyxa* biofilm covering the microelectrode + bacterial suspension of *P. polymyxa* after18 h incubation (sample 1), (3) the sterile nutrient medium, (4) NaOH 1% (v v^{-1}), (5) HNO_3 1% (v v^{-1}), and (6) water at frequencies of 25 Hz, 50 Hz and 100 Hz.

It can be noted that with increasing frequency the sum of the standard error of the mean and the sum of the variances increased in the biofilm group. Similar results were obtained in the cyclic voltammetry measurements (except for the *P. polymyxa* bacterial suspension) (Table 3). In addition, in the biofilm group, the *P. polymyxa* biofilm showed the highest sum of the standard error of the mean and the sum of variance in comparison to the *P. polymyxa* bacterial suspension and the sterile nutrient medium. Generally, the highest values of the sum of the standard error of the mean and the sum of the variances among all the samples tested were obtained for NaOH 1% (v v^{-1}). In the CIP solutions group, the highest values for the sum of the standard error of the mean and the sum of the variances for NaOH 1% (v v^{-1}) and HNO_3 1% (v v^{-1}) were obtained at 100 Hz, while the lowest were obtained at 50 Hz.

4. Discussion

In this study, cyclic voltammetry (CV) and square wave voltammetry (SWV) were employed to detect *P. polymyxa* biofilm and CIP cleaning solutions using interdigitated microelectrodes.

Based on the results obtained in this study, cyclic voltammetry showed promising results for biofilm detection. It was observed that for *P. polymyxa* bacterial suspension after incubation the peak currents increased, while for *P. polymyxa* biofilm the peak currents decreased. Literature reports are also contradictory; on the one hand, the current response increases, and, on the other hand, the current response decreases with the presence of a biofilm on the surface of the working electrode. The results shown in Fig. 2 are in accordance with the results published in the studies of (Kang et al., 2012; Marsili et al., 2008), which explained that the observed increase in cathodic and anodic peak currents of the bacterial suspension might be an enhanced electron transfer between the *P. polymyxa* surface-associated molecules and the surface of the electrode. Furthermore, the peak currents increase and shift to more positive potentials with an increasing scan rate. This

Table 3
The sum of the standard error (SSE) of the mean and the sum of the variances (SV) for the tested samples using cyclic voltammetry at scan rates of 50 mV s^{-1}, 100 mV s^{-1} and of 250 mV s^{-1}.

Scan rate (mV s^{-1})		*P. polymyxa* bacterial suspension	*P. polymyxa* biofilm	Nutrient medium	NaOH 1% (v v^{-1})	HNO_3 1% (v v^{-1})	H_2O
50	SSE	1.967	2.172	0.364	none	none	none
	SV	0.263	0.286	0.009	none	none	none
100	SSE	3.347	1.994	0.604	38	0.907	0.411
	SV	0.935	0.316	0.023	425	0.046	0.014
250	SSE	3.168	4.859	1.109	42	2.292	0.230
	SV	0.620	1.527	0.072	428	0.292	0.003

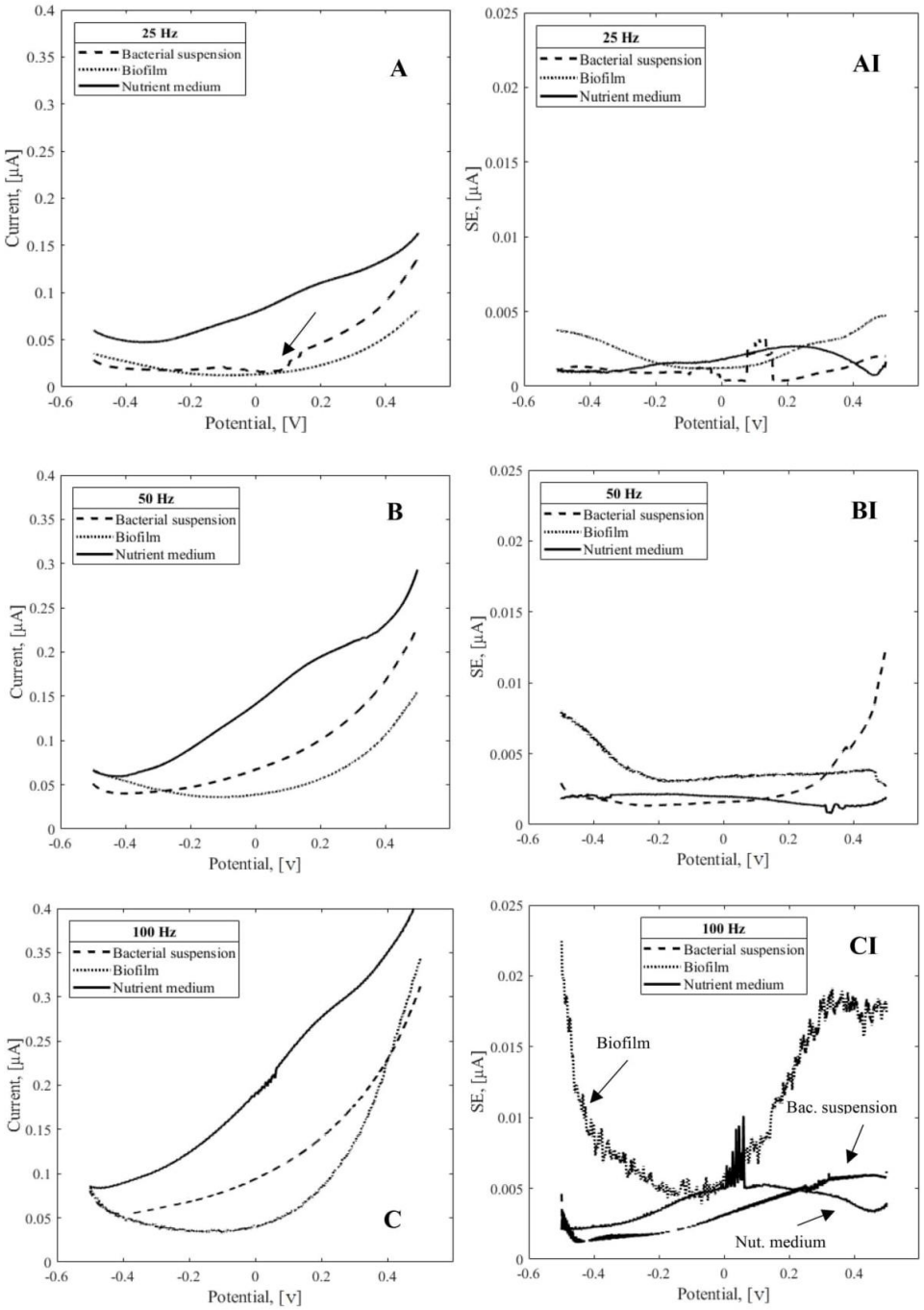

Fig. 6. Square wave voltammograms for (1) *P. polymyxa* bacterial suspension 18 h, (2) *P. polymyxa* biofilm covering the microelectrode + *P. polymyxa* bacterial suspension 18 h and (3) sterile nutrient medium at frequencies of 25 Hz (A), 50 Hz (B), and 100 Hz (C) with the respective standard errors of the mean (SE) (AI, BI, CI) (i = 3, n = 9).

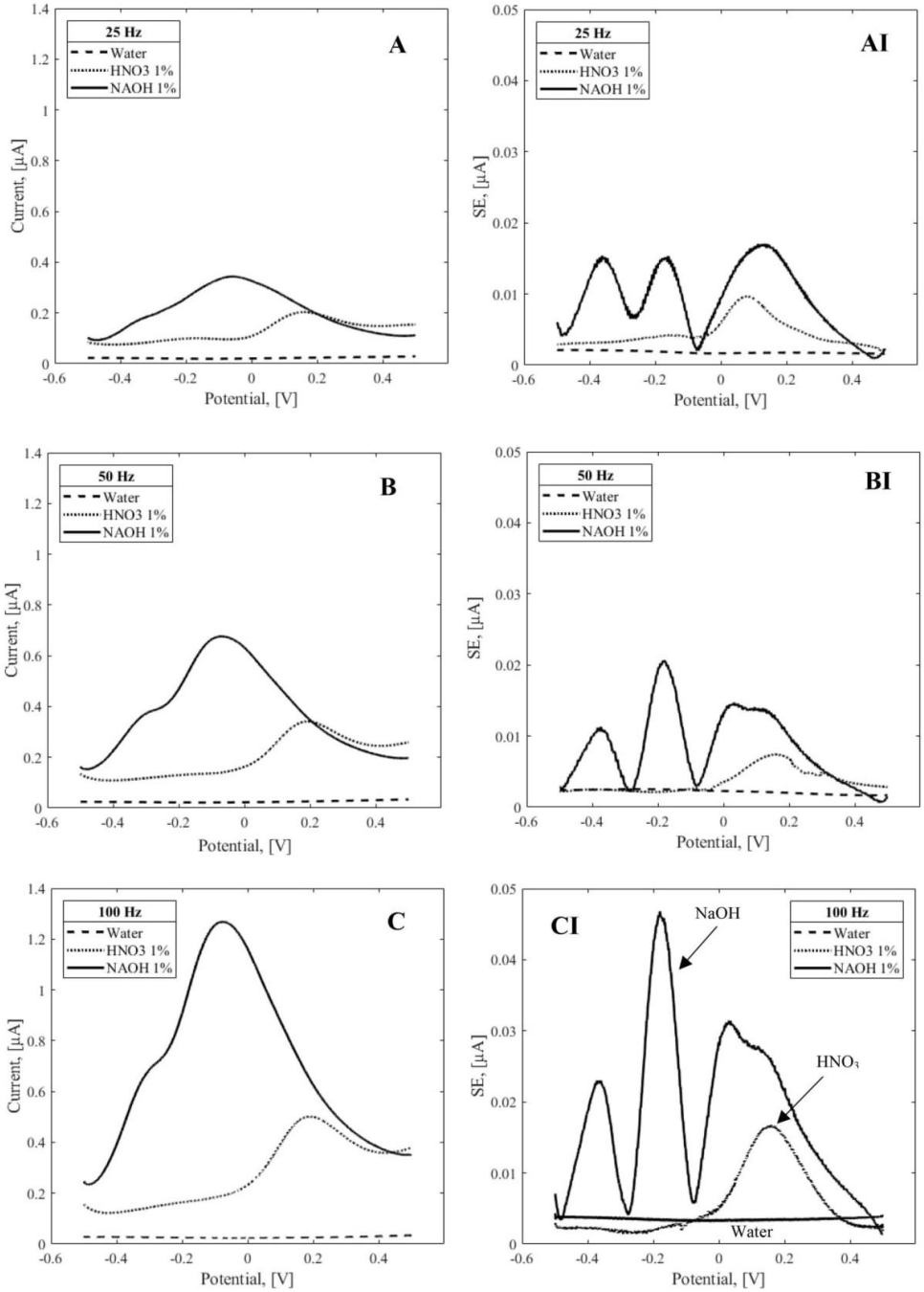

Fig. 7. Square wave voltammograms for H_2O, HNO_3 1% (v v^{-1}), and NaOH 1% (v v^{-1}) at frequencies of 25 Hz (A), 50 Hz (B) and 100 Hz (C) with the respective standard error of the mean (SE) (AI, BI, CI) (i = 3, n = 9).

Table 4
Peak currents (μA) and peak potentials (V) of NaOH 1% (v v^{-1}) and HNO_3 1% (v v^{-1}) in square wave voltammograms (i = 3, n = 9).[a]

Frequency (Hz)	I_{p1}, I_{p2} (μA) E_{p1}, E_{p2} (V)	NaOH 1% (v v^{-1})	HNO_3 1% (v v^{-1})
25	I_{p1}	0.10 ± 0.02	none
	E_{p1}	−0.29 ± 0.04	none
	I_{p2}	0.25 ± 0.01	0.11 ± 0.01
	E_{p2}	−0.04 ± 0.04	0.15 ± 0.02
50	I_{p1}	0.20 ± 0.01	none
	E_{p1}	−0.30 ± 0.02	none
	I_{p2}	0.51 ± 0.01	0.15 ± 0.01
	E_{p2}	−0.07 ± 0.02	0.18 ± 0.00

[a] H_2O did not show an anodic peak. Results at 100 Hz are not shown due to the high standard errors (Fig. 6 CI and 7 CI).

indicates that an irreversible reaction occurred during the measurement (Wang, 2006).

The results of the microelectrodes covered with a *P. polymyxa* biofilm showed lower current signals in the potential window 0.6–1.0 V, compared to the sterile nutrient medium and the bacterial suspension after incubation period. Also for *P. polymyxa* biofilm samples, the positions of the peaks shift with increasing scan rate to more positive potentials that indicates that an irreversible reaction (Wang, 2006). Moreover, the cathodic (reduction) peaks were less pronounced for the *P. polymyxa* biofilm than for the bacterial suspension (Table 1). According to the study of Becerro et al. (2016), this might result from the additional resistance that the biofilm causes, which extenuates the current. The shape of the cyclic voltammogram may constitute a means of providing information on the coverage of the surface (Vieira et. al., 2003). According to the authors, since the coverage of the surface increases, the peaks will be lower in the voltammograms (Kang et al., 2012). The authors explain this behavior by the fact that as the accumulation of the biofilm on the surface increases, the area available for the oxidation-reduction processes on the surface decreases and, therefore, the cathodic/anodic peak area in the voltammogram decreases.

Therefore, it has been suggested that there may be two behaviours in opposite directions that change the current with the bacterial attachment using cyclic voltammetry. On the one hand, the current increases due to the enhanced electrochemical interaction, electron transfer between the bacterial surface-associated molecules and the electrode surface, and on the other hand, the current decreases due to the surface-covering action to diminish the area available for the electrochemical interaction. Similar behavior was observed in a study with *P. aeruginosa* (Kang et al., 2012). Also, it is important to highlight that more research into extracellular electron transfer (EET) of *P. polymyxa* is still necessary before obtaining a definitive answer about EET pathway.

Square wave voltammetry demonstrated promising results for the differentiation between CIP cleaning solutions when measured at lower frequencies. However, at higher frequencies a stable results was not possible to obtain (Fig. 6 CI and 7 CI). According to the literature, the main advantage of square wave voltammetry is that it can detect low concentrations of electrochemically active reactants that are not easily detectable by cyclic voltammetry (Lewandowski and Beyenal, 2013). However, SWV is used more for analytical purposes, for which the frequency of 100 Hz can be too fast (Mirceski et al., 2007). In addition, the variation in biofilm thickness between different electrodes may contribute further to the inaccuracy of the measurements. This result is in accordance with the literature (Nguyen et al., 2012), where, as the frequency was increased from 1 Hz to 40 Hz. However, when the frequency was greater than 20 Hz, the noise level became significant. Therefore, the use of smaller frequencies should be advantageous. In addition, the use of smaller potential windows can be recommended. For example in study of (Tarditto et al., 2016), the potential window for SWV was 0.4–0.85 V while others used a the potential window for SWV from −0.4 to 0.05 V (Webster et al., 2015).

Finally, it should be noted that to the authors' knowledge, descriptive statistics for the whole potential window has not been reported in the previous studies on the electrochemical detection of bacteria. In the report of (Matsunaga and Namba, 1984) only an average relative error of the peak current was published. Nevertheless, from the results of this study, it is evident that the descriptive statistics of the measurement may be important to gain a deeper understanding of the electrochemical processes in biofilm and CIP cleaning solutions detection. In addition, this information may be useful for the evaluation of scan rates, in order to find the scan rate with the lowest errors.

5. Conclusion

The results of this work indicate that CV and SWV measurements with interdigitated microelectrodes without a biorecognition element can be used for the biofilm detection and the differentiation between CIP cleaning solutions. On the one hand, CV showed promising results for *P. polymyxa* biofilm detection at early stage of formation at different scan rates. On the other hand, SWV can be recommended for the detection of the CIP cleaning solutions at lower frequencies, since each cleaning solution showed a specific voltammogram shape. However, although promising results have been achieved with both methods, the methods have to be optimized for specific samples regarding the measurement settings. In addition, electrochemical measurements under dynamic conditions and for all stages of biofilm development should be conducted. Lastly, questions about location and incorporation of the microelectrode into industrial equipment have to be answered.

Table 5
The sum of the standard error of the mean (SSE) and the sum of variances (SV) for samples tested using SWV at frequencies of 25 Hz, 50 Hz and 100 Hz.

Frequency (Hz)		*P. polymyxa* bacterial suspension	*P. polymyxa* biofilm	Nutrient medium	NaOH 1% (v v^{-1})	HNO_3 1% (v v^{-1})	H_2O
25	SSE	1.051	2.240	1.563	8.707	4.171	1.690
	SV	0.014	0.057	0.027	0.922	0.199	0.028
50	SSE	2.498	3.683	1.676	7.862	3.366	2.036
	SV	0.099	0.143	0.028	0.813	0.131	0.041
100	SSE	3.172	9.643	3.720	16.784	5.160	3.277
	SV	0.120	0.747	0.146	3.745	0.444	0.104

Acknowledgments

This research did not receive any specific grant from funding agencies in the public, commercial, or not-for-profit sectors. The authors thank Prof. Bernd Wilke and Dr. Holger Brehm for beneficial discussion.

Appendix A. Supplementary data

Supplementary data to this article can be found online at https://doi.org/10.1016/j.eaef.2019.01.004.

References

Al-Haj, H., 2012. In: Ibrahim, H.A.-H. (Ed.), Fouling in heat exchangers. InTech. https://doi.org/10.5772/46462.
Atkins, P.W., Paula, J., 2006. Physical chemistry, eighth ed. Oxford University Press, Oxford.
Babauta, J., Renslow, R., Lewandowski, Z., Beyenal, H., 2012. Electrochemically active biofilms. Facts and fiction. A review. Biofouling 28, 789–812. https://doi.org/10.1080/08927014.2012.710324.
Bard, A.J., Zoski, C.G., 2000. Voltammetry retrospective. Anal. Chem. 72, 346 A–352 A. https://doi.org/10.1021/ac002791t.
Becerro, S., Paredes, J., Arana, S., 2015. Multiparametric biosensor for detection and monitoring of bacterial biofilm adhesion and growth. In: Lacković, I., Vasic, D. (Eds.), 6th European Conference of the International Federation for Medical and Biological Engineering. Springer International Publishing, Cham, pp. 333–336.
Becerro, S., Paredes, J., Mujika, M., Lorenzo, E.P., Arana, S., 2016. Electrochemical real-time analysis of bacterial biofilm adhesion and development by means of thin-film biosensors. IEEE Sensor. J. 16, 1856–1864. https://doi.org/10.1109/JSEN.2015.2504495.
Cappitelli, F., Polo, A., Villa, F., 2014. Biofilm formation in food processing environments is still poorly understood and controlled. Food Eng Rev 6, 29–42. https://doi.org/10.1007/s12393-014-9077-8.
Characklis, W.G., Turakhia, M.H., Zelver, N., 1990. Transport and interfacial transfer phenomena. In: Characklis, W.G., Marshall, K.C. (Eds.), Biofilms. John Wiley, New York, pp. 265–339.
Chmielewski, R.A.N., Frank, J.F., 2003. Biofilm formation and control in food processing facilities. Compr. Rev. Food Sci. Food Saf. 2, 22–32. https://doi.org/10.1111/j.1541-4337.2003.tb00012.x.
De Jonghe, V., Coorevits, A., Block, J., Van Coillie, E., Grijspeerdt, K., Herman, L., De Vos, P., Heyndrickx, M., 2010. Toxinogenic and spoilage potential of aerobic spore-formers isolated from raw milk. Int. J. Food Microbiol. 136, 318–325. https://doi.org/10.1016/j.ijfoodmicro.2009.11.007.
Flemming, H.-C., Neu, T.R., Wozniak, D.J., 2007. The EPS matrix. The "house of biofilm cells". J. Bacteriol. 189, 7945–7947. https://doi.org/10.1128/JB.00858-07.
Gillham, C.R., Fryer, P.J., Hasting, A.P.M., Wilson, D.I., 1999. Cleaning-in-place of whey protein fouling deposits. Food Bioprod. Process. 77, 127–136. https://doi.org/10.1205/096030899532420.
Gopal, N., Hill, C., Ross, P.R., Beresford, T.P., Fenelon, M.A., Cotter, P.D., 2015. The prevalence and control of bacillus and related spore-forming bacteria in the dairy industry. Front. Microbiol. 6, 1418. https://doi.org/10.3389/fmicb.2015.01418.
Gründler, P., 2007. Chemical Sensors. Springer Berlin Heidelberg, Berlin, Heidelberg. https://doi.org/10.1007/978-3-540-45743-5.
He, Z., Kisla, D., Zhang, L., Yuan, C., Green-Church, K.B., Yousef, Ahmed E.Y., 2007. Isolation and identification of a Paenibacillus polymyxa strain that coproduces a novel lantibiotic and polymyxin. Appl. Environ. Microbiol. 73, 168–178. https://doi.org/10.1128/AEM.02023-06.
Hori, K., Matsumoto, S., 2010. Bacterial adhesion: From mechanisms to control. Biochem. Eng. J. 48, 424–434. https://doi.org/10.1016/j.bej.2009.11.014.
Hwa Kwak, Y., Lee, J., Lee, J., Hwan Kwak, S., Oh, S., Paek, S.-H., Ha, U.-H., Seo, S., 2014. A simple and low-cost biofilm quantification method using LED and CMOS image sensor. J. Microbiol. Methods 107, 150–156. https://doi.org/10.1016/j.mimet.2014.10.004.
Janknecht, P., Melo, L.F., 2003. Online biofilm monitoring. Rev. Environ. Sci. Biotechnol. 2, 269–283. https://doi.org/10.1023/B:RESB.0000040461.69339.04.
Kang, J., Kim, T., Tak, Y., Lee, J.-H., Yoon, J., 2012. Cyclic voltammetry for monitoring bacterial attachment and biofilm formation. J. Ind. Eng. Chem. 18, 800–807. https://doi.org/10.1016/j.jiec.2011.10.002.
Kato, S., 2016. Microbial extracellular electron transfer and its relevance to iron corrosion. Microb. Biotechnol. 9, 141–148. https://doi.org/10.1111/1751-7915.12340.
Kessler, H.G., 2006. Lebensmittel- und Bioverfahrenstechnik: Molkereitechnologie, fourth ed. Verl. A. Kessler, München.
Kim, Y.W., Sardari, S.E., Meyer, M.T., Iliadis, A.A., Wu, H.C., Bentley, W.E., Ghodssi, R., 2012. An ALD aluminum oxide passivated Surface Acoustic Wave sensor for early biofilm detection. Sensor. Actuator. B Chem. 163 (1), 136–145.
Kirkland, C.M., Herrling, M.P., Hiebert, R., Bender, A.T., Grunewald, E., Walsh, D.O., Codd, S.L., 2015. In situ detection of subsurface biofilm using low-field NMR: a field study. Environ. Sci. Technol. 49, 11045–11052.
Lewandowski, Z., Beyenal, H., 2013. Fundamentals of biofilm research, second ed. CRC Press/Taylor & Francis Group, Boca Raton.
Marchand, S., De Block, J., De Jonghe, V., Coorevits, A., Heyndrickx, M., Herman, L., 2012. Biofilm formation in milk production and processing environments: influence on milk quality and safety. Compr. Rev. Food Sci. Food Saf. 11, 133–147. https://doi.org/10.1111/j.1541-4337.2011.00183.x.
Marsili, E., Rollefson, J.B., Baron, D.B., Hozalski, R.M., Bond, D.R., 2008. Microbial biofilm voltammetry: direct electrochemical characterization of catalytic electrode-attached biofilms. Appl. Environ. Microbiol. 74, 7329–7337. https://doi.org/10.1128/AEM.00177-08.
Marsili, E., Sun, J., Bond, D.R., 2010. Voltammetry and growth physiology of geobacter sulfurreducens biofilms as a function of growth stage and imposed electrode potential. Electroanalysis 22, 865–874. https://doi.org/10.1002/elan.200800007.
Matsunaga, T., Namba, Y., 1984. Detection of microbial cells by cyclic voltammetry. Anal. Chem. 56, 798–801. https://doi.org/10.1021/ac00268a047.
Mirceski, V., Komorsky-Lovric, S., Lovric, M., 2007. Square-Wave Voltammetry: Theory and Application, first ed. Springer Berlin Heidelberg, Berlin, Heidelberg. https://doi.org/10.1007/978-3-540-73740-7.
Nealson, K.H., Finkel, S.E., 2011. Electron flow and biofilms. MRS Bull. 36, 380–384. https://doi.org/10.1557/mrs.2011.69.
Nguyen, H.D., Renslow, R., Babauta, J., Ahmed, B., Beyenal, H., 2012. Sensor. Actuator. B Chem. 161, 929–937. https://doi.org/10.1016/j.snb.2011.11.066.
Pringle, J., Fletcher, M., 1983. Influence of substratum wettability on attachment of freshwater bacteria to solid surfaces. Appl. Environ. Microbiol. 45, 811–817.
Reguera, G., McCarthy, K.D., Mehta, T., Nicoll, J.S., Tuominen, M.T., Lovley, D.R., 2005. Extracellular electron transfer via microbial nanowires. Nature 435, 1098–1101. https://doi.org/10.1038/nature03661.
Ren, X., Yan, J., Wu, D., Wei, Q., Wan, Y., 2017. Nanobody-based apolipoprotein e immunosensor for point-of-care testing. ACS Sens. 2, 1267–1271. https://doi.org/10.1021/acssensors.7b00495.
Reyes-Romero, D.F., Behrmann, O., Dame, G., Urban, G.A., 2014. Dynamic thermal sensor for biofilm monitoring. Sensor Actuator Phys. 213, 43–51. https://doi.org/10.1016/j.sna.2014.03.032.
Romney, A.J.D., 1990. CIP: Cleaning in Place. In: second ed. In: Romney, A.J.D. (Ed.), International Journal of Dairy Technology, vol. 43 59-59. https://doi.org/10.1111/j.1471-0307.1990.tb02427.x.
Somers, E.B., Johnson, M.E., Wong, A.C.L., 2001. Biofilm formation and contamination of cheese by nonstarter lactic acid bacteria in the dairy environment. J. Dairy Sci. 84, 1926–1936. https://doi.org/10.3168/jds.S0022-0302(01)74634-6.
Sultana, S.T., Babauta, J.T., Beyenal, H., 2015. Electrochemical biofilm control. Biofouling 31, 745–758. https://doi.org/10.1080/08927014.2015.1105222.
Tarditto, L.V., Arévalo, F.J., Zon, M.A., Ovando, H.G., Vettorazzi, N.R., Fernández, H., 2016. Electrochemical sensor for the determination of enterotoxigenic Escherichia coli in swine feces using glassy carbon electrodes modified with multi-walled carbon nanotubes. Microchem. J. 127, 220–225. https://doi.org/10.1016/j.microc.2016.03.011.
Van Houdt, R., Michiels, C.W., 2010. Biofilm formation and the food industry, a focus on the bacterial outer surface. J. Appl. Microbiol. 109, 1117–1123. https://doi.org/10.1111/j.1365-2672.2010.04756.x.
Verran, J., 2002. Biofouling in food processing. biofilm or biotransfer potential? Food Bioprod. Process. 80, 292–298. https://doi.org/10.1205/096030802321154808.
Vert, M., Doi, Y., Hellwich, K.-H., Hess, M., Hodge, P., Kubisa, P., Rinaudo, M., Schué, F., 2012. Terminology for biorelated polymers andapplications (IUPAC Recommendations 2012)*. Pure Appl. Chem. 84, 377–410.
Vieira, M.J., Pinho, I.A., Gião, S., Montenegro, M.I., 2003. The use of cyclic voltammetry to detect biofilms formed by Pseudomonas fluorescens on platinum electrodes. Biofouling 19, 215–222.
Vu, D.L., Červenka, L., Vavřičková, J., 2012. The attachment of Staphylococcus epidermidis on the surface of a carbon paste electrode at various positive potentials: The effect of pH, incubation time, and solid-medium type. J. Biomed. Sci. Eng. 5, 699–704. https://doi.org/10.4236/jbise.2012.512087.
Wang, J., 2006. Analytical Electrochemistry. John Wiley & Sons, Inc, Hoboken, NJ, USA.
Wang, Y., Wang, Y., Wu, D., Ma, H., Zhang, Y., Fan, D., Pang, X., Du, B., Wei, Q., 2018. Label-free electrochemical immunosensor based on flower-like Ag/MoS2/rGO nanocomposites for ultrasensitive detection of carcinoembryonic antigen. Sensor. Actuator. B Chem. 255, 125–132. https://doi.org/10.1016/j.snb.2017.07.129.
Webster, T.A., Goluch, E.D., 2012. Electrochemical detection of pyocyanin in nanochannels with integrated palladium hydride reference electrodes. Lab Chip 12, 5195–5201. https://doi.org/10.1039/c2lc40650k.
Webster, T.A., Sismaet, H.J., Chan, I.J., Goluch, E.D., 2015. Electrochemically monitoring the antibiotic susceptibility of Pseudomonas aeruginosa biofilms. Analyst 140, 7195–7201. https://doi.org/10.1039/C5AN01358E.
Xu, K., Dexter, S.C., Luther, G.W., 1998. Voltammetric microelectrodes for biocorrosion studies. Corrosion 54, 814–823. https://doi.org/10.5006/1.3284801.

2.3.3 Publication 7 Electrochemical detection of dairy fouling by cyclic voltammetry and square wave voltammetry

Industrial processing equipment is challenged by fouling formation on the inner surface of dairy equipment during manufacturing processes. Fouling deposits can change the physical properties of the food contact surface, leading to the increased risk of the bacterial attachment and subsequently to the formation of biofouling.

This article describes a study about the usability of two electrochemical techniques, cyclic voltammetry and square wave voltammetry, in combination with interdigitated platinum microelectrodes to detect dairy fouling. The differences between the current responses of the clean microelectrodes and the microelectrodes after the dairy fouling formation were shown in this study. In addition, the surface coverage of the microelectrodes by the fouling attachment visualized by microscopy was also presented.

The results shown in this article demonstrated that the dairy fouling formation on the microelectrode surface leads to change of current responses compared to the clean microelectrodes. Dairy fouling led to the decrease in the current in cyclic voltammograms. This behaviour can be explained by the additional insulated layer on the microelectrodes that extenuates the current response. Both methods, cyclic voltammetry and square wave voltammetry can potentially be used for the fouling detection. Cyclic voltammetry demonstrated good results for the fouling detection and for the differentiation between the dairy emulsion and the dairy fouling at scan rates 50, 100 and 250 mV s^{-1}. Square wave voltammetry can be recommended for the fouling detection at low frequencies.

Author contributions

Fysun, O., Rauschnabel, J., Langowski, H.-C. devised the project, the main conceptual ideas and proof outline. Fysun, O. worked out the experiments and technical details of the electrochemical sensors. Khorshid S. collected the data and performed the analysis for the data. Fysun, O. wrote the manuscript. All authors discussed the results and commented on the manuscript. Langowski, H.-C. contributed to the final version of the manuscript.

Detection of dairy fouling by cyclic voltammetry and square wave voltammetry

Olga Fysun[1,2,†], Sara Khorshid[2,3, ††], Johannes Rauschnabel[2], Horst-Christian Langowski[1,4]

[1]TUM School of Life Sciences Weihenstephan, Technical University of Munich, Freising, Germany

[2]Robert Bosch Packaging Technology GmbH, Waiblingen, Germany

[3]Department of Mechanical and Process Engineering, University of Kaiserslautern, Kaiserslautern, Germany

[4]Fraunhofer Institute for Process Engineering and Packaging IVV, Freising, Germany

[†]Present address: Robert Bosch GmbH, Reutlingen, Germany

[††]Present address: Sanofi-Aventis Deutschland GmbH, Frankfurt, Germany

Abbreviations:

CV	Cyclic voltammetry
SWV	Square wave voltammetry
RLU	Relative light units
DLVO theory	Theory of adhesion from B. Derjaguin, L. Landau, E. Verwey, T. Overbeek

ABSTRACT

Fouling in food processing environment can cause the increase of production costs due to additional cleaning steps and risk of contamination of food products. There is a demand to introduce advanced techniques to detect fouling in food processing equipment. Cyclic voltammetry (CV) and square wave voltammetry (SWV) were probed in this work to detect the dairy fouling and the reconstructed dairy emulsion by platinum-based interdigitated microelectrodes. The results demonstrated that both methods can potentially be used for the fouling detection, since the attachment of fouling to the microelectrode surface leads to lower current responses compared to the clean microelectrodes.

Keywords: Dairy fouling, Electrochemistry, Cyclic voltammetry, Square wave voltammetry, Microelectrodes

1. Introduction

Industrial food processing equipment is highly challenged by fouling formation on the inner wall of equipment during operation. The presence of fouling leads to the significant decrease of the equipment's performance. In industrial processing equipment, different types of fouling can be found (Groysman 2017; Kazi 2012), which can be classified according to the type of equipment undergoing fouling; to the type of fluid causing the fouling; or to the key chemical/physical mechanism giving rise to the fouling. According to Groysman 2017, fouling types can be divided into the following categories according to the mechanisms: crystallization fouling, particulate fouling, chemical reaction fouling, corrosion fouling and biofouling. In these categories (except for biofouling), the fouling layer is formed from deposited accumulations of non-microbiological origin. In biofouling, the accumulations refer to the attachment of microorganisms to the surfaces, which can grow when nutrients are available (Bhushan 2016). In the literature, such attachments of microorganisms are also called a biofilm.

The mechanisms of fouling and biofouling attachment are different. In fact, fouling is often a precursor for biofouling due to the reduced heat transfer rate (Al-Haj 2012). Prior to bacterial adhesion, organic and inorganic molecules from milk can adsorb to surfaces and form a first fouling layer. Thus, the concentration of nutrients closer to the surface is higher than that of the liquid phase. In addition, the fouling layer can change the physical properties of the food contact surface, leading to the increase of the bacterial attachment and subsequently to the formation of biofouling (Fratamico *et al.* 2009). Biofouling increases the risk for microbial contamination and can be a reason for limiting the run length in manufacturing plants (Bhushan 2016; Brooks and Flint 2008; Chmielewski and Frank, 2003). Therefore, it is important to detect fouling on different surfaces in order to decrease the risk of microbiological contamination of processed products due to possible biofouling formation.

Fouling formation in the food processing equipment involves the deposition from liquids and suspension of liquid in liquids or solids in liquids. In the dairy processing equipment, particularly in manufacturing processes at lower temperatures, the fouling chemical reaction can be found most often. Conversely, at higher temperatures, crystallization fouling is most prevalent. Components that are mainly responsible for fouling in dairy processing equipment are calcium phosphate and whey proteins, particularly β-1actoglobulin (β-LG) (Visser and Jeurnink 1997). According to the literature (Kessler 2006), there are two types of dairy fouling: Type A and Type B. Fouling formation caused by thermally unstable proteins is dominant at lower temperatures (70–90 ºC) and consists of about 60% protein and 40% minerals (Type A). Fouling due to the precipitation of calcium phosphate is dominant at high temperatures (> 110 ºC) and consists of less than 20% protein and up to 80% minerals, of which more than 80% is calcium phosphate (Type B).

It was described that the first step in dairy fouling formation is the adsorption of a monolayer of proteins onto the surface that occurs already at room temperature. The formation of macroscopic layers of fouling follows in a next step by particle formation (whey protein aggregates and calcium phosphate) in the bulk of the liquid being processed at higher temperatures. Many studies to explore the process of fouling have been reported by many researchers. However, a complete understanding of fouling mechanisms remains elusive due to the complexity of the dairy systems (Visser and Jeurnink 1997).

Monitoring devices for the detection of fouling-relevant parameters are classified into three levels of information provided by these devices (Flemming 2011). Level 1 monitoring methods, e.g., friction resistance measurement, heat transfer resistance measurement, quartz crystal microbalance, surface acoustic waves, differential turbidity measurement, provide information about the kinetics of deposition formation and changes of thickness, but cannot differentiate between microorganisms and abiotic deposit components. Level 2 monitoring methods, e.g., FTIR-ATR-spectroscopy, microscopical observation, can distinguish between biotic and abiotic components of a deposit. Level 3 monitoring methods, e.g., FTIR-ATR-spectroscopy in a flow-through cell, NMR imaging of deposits in pipes or porous media, provide detailed information about the chemical composition of the deposit (Flemming 2011). It is important to note that in real industrial processes not all monitoring techniques are implemented in daily operations. On the one hand, there are a few commercial methods to detect fouling formation in industrial equipment. For example, heat transfer changes or increase of the frictional pressure drop can be measured (Lee *et al.* 1998; Characklis *et al.* 1990). On the other hand, a major drawback of both methods is a lack of information on the extent and location of fouling. Although these techniques provide fast information on fouling formation without sampling, these methods are not suitable for the detection of fouling at the early stages of formation. According to Characklis et al. 1990, there are only significant changes in the friction factor when the biofouling reaches a critical thickness of about 35 µm. There are also other methods that provide a higher

sensitivity of fouling detection, but they are less common in industrial equipment. For example, optical sensors analyze the relation between emission, transmission and absorption of different light sources. Fouling can be detected with optical sensors, since it can act as an additional refractor (Fischer *et al.* 2015). Also, mass sensitive sensors such as quartz crystal microbalance (QCM) devices were used in real-time biofilm monitoring and showed promising results (Olsson *et al.* 2015; Tam *et al.* 2007). The resonance frequency of the quartz depends on the adsorbed mass upon it and thus, the mass variation per unit can be measured. However, QCM devices cannot differentiate between different fouling types (mineral fouling, particle fouling, organic fouling, biofouling (Epstein 1981)).

Lastly, some studies about electrochemical devices have been published to explore the fouling detection in industrial equipment (Kang *et al.* 2012; Muthukumaran *et al.* 2016; Pavanello *et al.* 2011). According to the IUPAC definition, electrochemical devices transform the effect of an electrochemical interaction between analyte and electrode into a useful signal, which can be subdivided into voltammetric sensors, potentiometric sensors, chemically sensitized field effect transistor (CHEMFET), potentiometric solid electrolyte gas sensors and impedance sensors as well (Hulanicki *et al.* 1991). For example, voltammetric sensors are the most prevalent in biofilm detection (Ahmed *et al.* 2014). In voltammetry, information about an analyte is obtained by measuring the current as a function of the varied potential. This technique is based on the measurement of the current resulting from the electrochemical oxidation or reduction of an electroactive species. The resulting current is directly correlated to the bulk concentration of the electroactive species or its production or consumption rate within the adjacent biocatalytic layer (Thévenot *et al.* 2001). Cyclic voltammetry (CV) is a quantitative electrochemical method used to study oxidation or reduction peaks, which are proportional to the concentration of a chemical species that oxidizes or reduces the electrode. In CV, the potential sweep is cycled over time. The potential cycling enables the visualization of the forward and backward reactions (Bard and Faulkner 2001). CV can be used to identify the potentials at which active redox couples are oxidized and reduced and is an electrochemical technique capable of monitoring redox reactions (Lewandowski and Beyenal 2013). Square wave voltammetry (SWV) is a pulse technique in which symmetrical square pulses at progressively increasing potentials are applied to an electrochemical system. A square wave is superimposed on a staircase ramp (Bard and Faulkner 2001; Ozkan *et al.* 2015).

In order to conduct electrochemical measurements, the electrochemical sensor is placed in an electrochemical cell, which involves the presence of a faradaic current. The electrode where the oxidation takes place is named anode and the cathode is the electrode where the reduction takes place, respectively. Anodic reactions generate electrons, whereas electrons are accepted in cathodic reactions (Bagotsky 2005; Bard and Faulkner 2001; Bard *et al.* 2012).

A clear trend in the decrease of the size of electrochemical electrodes can be observed in recent decades. An example is the reduction of the thickness of electrochemical electrodes to the nanosize

range. The response time of such electrodes is shorter compared to classical electrodes (Gründler 2007). Electrochemical interdigitated microelectrode have been used for glucose (Huang *et al.* 2014) and biofilm detection (Becerro *et al.* 2015; Strycharz-Glaven *et al.* 2014; Tubia *et al.* 2018). Interdigitated microelectrode arrays consist of a series of parallel microband electrodes in which alternating microbands are connected together (Varshney and Li 2009). Also, interdigitated microelectrodes have an improved and increased signal-to-noise ratio (Min and Baeumner 2004). According to IUPAC, microelectrode arrays can be prepared by dispersing sufficiently small particles of a conductive material in an insulator or by photolithography (Stulik *et al.* 2000).

Many studies describe the electrochemical detection of a microbiologically cased deposit, called biofouling or biofilm, particularly due to the extracellular electron transfer of microorganisms. In the dairy industry, however, fouling of non-microbiological origin can be a precursor of microbiological contamination of the processing equipment. Thus, dairy fouling should be detected at an early stage of adhesion. However, very few publication can be found in literature that discuss the detection of dairy fouling using electrochemical techniques by interdigitated microelectrodes. Thus, this study aimed to prove the usability of electrochemical techniques, namely cyclic voltammetry (CV) and square wave voltammetry (SWV), to detect dairy fouling. The changes in current between the clean microelectrodes and the microelectrodes with attachment dairy fouling were determined. Surface of the microelectrodes after the fouling attachment was shown using microscopy.

2. Materials and methods

2.1 Chemicals

Potassium ferrocyanide 1% was obtained from Clin-Tech (Guildford, *United Kingdom).* Potassium chloride 3 mol L^{-1} and crystal violet solution 1% were supplied by Merck (Darmstadt, Germany). Ethanol 70% and meet extract were obtained from VWR (Darmstadt, Germany). Powdered skimmed milk was purchased from Nestlé Deutschland AG (Frankfurt, Germany).

2.2 Sample preparation

A reconstituted dairy emulsion was used for the formation of dairy fouling. The dairy emulsion was reconstituted by diluting 2.5 g powdered skimmed milk in 100 mL demineralized water at 22.5 ± 0.5 ºC. Water activity (a_w) of powdered skimmed milk was 0.243 ± 0.032. The dairy emulsion was stirred for 5 min at approx. 120 rpm to achieve homogeneous dilution. The prepared dairy emulsion contained 0.023 g 100 mL^{-1} of fat, 1.3 g 100 mL^{-1} of carbohydrates, 0.9 g 100 mL^{-1} of proteins, and 0.028 g 100 mL^{-1} of salt. For incubation, the 6-well plates were used (Greiner Bio-One GmbH, Frickenhausen, Germany). After cleaning and activation, the microelectrodes were immersed into wells. Than 5 mL of the prepared dairy emulsion was added to each well. The 6-well plates with microelectrodes and dairy emulsion were incubated for 18 h at 30 °C in the climate chamber. After 18 h incubation, the microelectrodes were removed from wells. Then, the microelectrode was used for electrochemical measurements. Both the dairy fouling that was formed of the microelectrode surface

and dairy emulsions were measured and compared with the reference, the non-incubated dairy emulsion. Three types of samples were measured: (1) the reconstituted dairy emulsion after 18 h of incubation, (2) the dairy fouling covering the microelectrode immersed in the reconstituted dairy emulsion after 18 h of incubation, and (3) the non-incubated reconstituted dairy emulsion as the reference. Before each measurement, 5 µL of either the non-incubated reconstituted dairy emulsion or the reconstituted dairy emulsion after 18 h of incubation were pipetted onto the surface of the microelectrodes.

2.3 Electrochemical setup

For the experiments a drop-cell and interdigitated microelectrodes (MicruX Fluidic, Oviedo, Spain) with four electrodes (one auxiliary, one reference electrode, two working electrodes) were used. The working electrode has 120 feet pairs, which are 10 µm wide, with a 10 µm gap between each foot. The diameter of the electrochemical cell is 2.0 mm. A PalmSens BV bipotentiostat (Houten, The Netherlands) was used to run measurements. The measurements were performed at temperature 22.5 ± 0.5 ºC.

Before each use, the microelectrodes were cleaned using demineralized water and ethanol 70%. Then, the microelectrodes were activated electrochemically with 10 µL of 0.1 M potassium chloride by cyclic voltammetry (12 cycles between −1.5 and 1.5 V, scan rate 100 mV s^{-1}). After activation, the microelectrodes were cleaned using sterile demineralized water.

2.4 Voltammetric methods

In this work, cyclic voltammetry and square wave voltammetry were probed. In cyclic voltammetry, three cycles were applied to each microelectrode with the following parameters: E_{begin} = −0.5 V, E_{vtx1} = −0.5 V, E_{vtx2} = 1.0 V, scan rate = 0.050, 0.100, and 0.250 V s^{-1} with overall duration of 255, 135, and 63 s, respectively. The square wave voltammetry, the following settings were selected: $E_{begin\,=}$ −0.5 V, E_{end} = 0.05 V, $E_{amplitude}$ = 0.024 V, frequency = 25, 50, and 100 Hz with overall duration of 54, 35, and 25 s, respectively. In SWV measurements, anodic current was measured. The measurements done in triplicate. Three scans were conducted during one measurement. A detailed description of the measurement methodology is shown in Supplementary material.

2.5 ATP bioluminescence

The quantitative detection of the intra- and extracellular Adenosine Triphosphates (ATP) as well as Adenosine Monophosphate (AMP) was performed using an ATP bioluminescence method. The ATP bioluminescence method is a widespread biochemical technique to detect organic residues, like bacteria or food residues on surfaces and in liquids (Bottari *et al.* 2015). The method can be used to rapidly evaluate food and microbial residues on product contact surfaces. The energy stored within the ATP molecule is released as light by splitting of ATP to AMP (Adenosine Monophosphate). The light can be measured quantitatively and corresponds with the ATP level. The reaction uses the enzyme

luciferase. The ATP bioluminescence test was carried out using the ATP + AMP Hygiene Monitoring test kit. The test kit was obtained from Kikkoman Corporation and included the Lumitester™ PD-30 & LuciPac™ Pen. For liquid samples, the swab stick was removed from its casing and soaked in reconstructed dairy emulsion. For microelectrode surfaces, the wetted swab stick of the LuciPac™ pen was wiped over the surface. Then, the stick was returned to the casing. The test tubing was shaken until the powdery luminescent reagent was dissolved completely. After this step, the swab stick was inserted in the device and the measurement was carried out within 10 s. The results are expressed in relative light units (RLU).

2.6 Microscopy

A digital microscope (VHX 100, Keyence, Japan) with bright-field illumination was used to obtain microscopy images. Before taken images, the microelectrodes were dried for 2−3 min at room temperature. To improve the visibility of dairy fouling, 5 μL of crystal violet solution (0.01 g 100 mL^{-1}) was used for staining.

3. Results

3.1 Cyclic voltammetry

The cyclic voltammograms at scan rates of 50 mV s^{-1}, 100 mV s^{-1}, and 250 mV s^{-1} of (1) the reconstituted dairy emulsion after 18 h of incubation, (2) the dairy fouling covering the microelectrode with the reconstituted dairy emulsion after 18 h of incubation, and (3) the non-incubated reconstituted dairy emulsion as the reference, are depicted in Figs. 1 A, 1 B and 1 C, respectively.

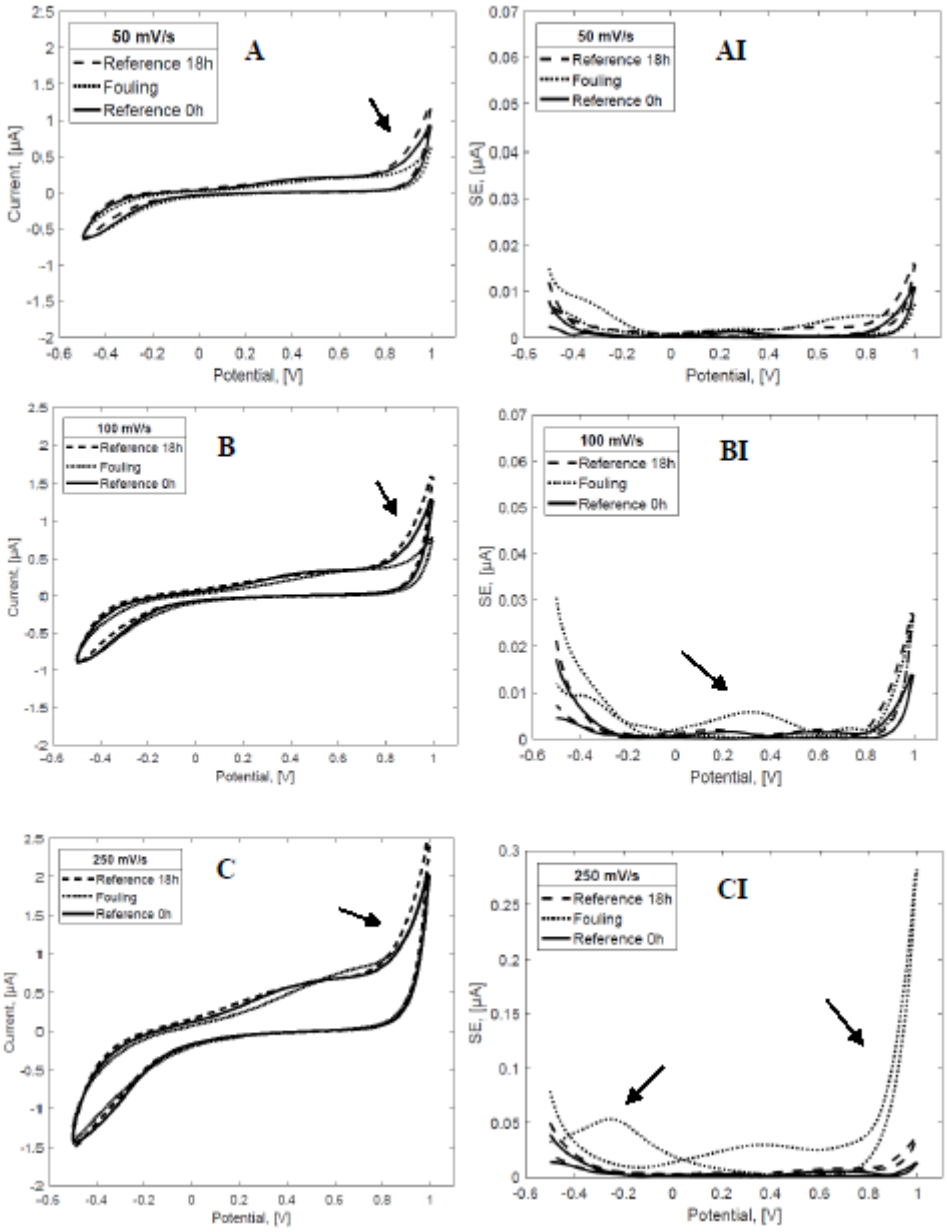

Figure 1. The changes in cyclic voltammogams obtained for (1) reconstituted dairy emulsion after incubation for 18 h (Reference 18 h), (2) dairy fouling after incubation for 18 h (Fouling) and (3) non-incubated reconstituted dairy emulsion (Reference 0 h) at scan rates of (A) 50 mV s^{-1}, (B) 100 mV s^{-1} and (C) 250 mV s^{-1} with the respective standard errors of the mean (SE) (AI, BI, CI) (i = 3, n = 9).

The cyclic voltammograms shown in the curves of Fig. 1 illustrate that the current signals of anodic (oxidation) and cathodic (reduction) curves increase with an increasing scan rate for all samples. The reconstituted dairy emulsion after 18 h of incubation illustrates the highest current response in the anodic (oxidation) curve, followed by a non-incubated reconstituted dairy emulsion, and finally by dairy fouling. This succession remains at all three scan rates. The differences between the samples are less pronounced for the cathodic curves that for the anodic curves.

It can be seen that the errors from the dairy fouling and the incubated reconstituted dairy emulsion are higher than the errors from the reference at scan rates of 100 mV s^{-1} and 250 mV s^{-1} (Figs. 1 BI, 1 CI). This behaviour can be explained by the non-homogeneous surface coverage of fouling of the working electrode (Fig. 4 B) and to the structural changes of the dairy emulsion during the incubation time. The highest standard error of the mean is found at the potentials where the anodic and the cathodic curves have a peak (Figs. 1 A, 1 B, 1 C). The highest standard error of the mean is obtained for the dairy fouling measured at the scan rate of 250 mV s^{-1}.

Table 1 summarizes the anodic and cathodic peak currents as well as the peak potentials for the investigated samples. From the dairy fouling voltammograms, an anodic peak at potentials of 0.38 V and 0.88 V is recorded at scan rates of 100 mV s^{-1} and 250 mV s^{-1}, respectively. A cathodic peak is found for the dairy fouling at –0.38 V and –0.36 V at a scan rates of 100 mV s^{-1} and 250 mV s^{-1}, respectively (Fig. 1 and Table 1). The vertical distance between forward and reverse scans increases at higher scan rates. With increasing scan rate, the curve shapes appear wider and more distinctive. Notable differences between the reconstituted dairy emulsion 18 h and dairy fouling are found in the anodic curve in the potential window 0.7-1.0 V while in the cathodic curve from –0.2 to –0.5 V (Fig. 1).

Table 1. Anodic (oxidation) and cathodic (reduction) peak currents (µA) and peak potentials (V) of the (1) reconstituted dairy emulsion after incubation for 18 h, (2) dairy fouling and (3) non-incubated reconstituted dairy emulsion obtained from the cyclic voltammetry results (i = 3, n = 9).

Scan rate (mV s^{-1})	I_{pA}, I_{pC} (µA) E_{pA}, E_{pC} (V)	Non-incubated reconstituted dairy emulsion	Dairy fouling	Reconstituted dairy emulsion 18 h
50	I_{pA}	0.10 ± 0.07	0.03 ± 0.00	none
	E_{pA}	0.45 ± 0.01	0.54 ± 0.01	none
	I_{pC}	−0.04*	none	none
	E_{pC}	−0.43*	none	none
100	I_{pA}	0.06 ± 0.00	0.06 ± 0.02	0.03 ± 0.00
	E_{pA}	0.42 ± 0.01	0.58 ± 0.04	0.38 ± 0.05
	I_{pC}	−0.18*	−0.68*	−0.21 ± 0.14
	E_{pC}	−0.43	−0.49*	−0.38 ± 0.08
250	I_{pA}	0.13 ± 0.01	0.07 ± 0.04	0.07 ± 0.01
	E_{pA}	0.44 ± 0.00	0.56 ± 0.05	0.88 ± 0.02
	I_{pC}	none	−0.13 ± 0.08	−0.07 ± 0.01
	E_{pC}	none	−0.47 ± 0.01	−0.36 ± 0.02

*Only an average of one sample could be evaluated (1 sample - 3 scans)

Table 1 illustrates that the current at anodic peaks increases for the dairy fouling with enhanced scan rate. The potential of the anodic and cathodic peaks for the dairy fouling moves towards positive potentials with enhanced scan rate. The result assumes that an irreversible process takes place in the

electrochemical cell. For both reconstituted dairy emulsions, no considerable differences in peak potential are observed with increasing scan rate.

Fig. 1 CI shows the highest values of the standard error of the mean for the dairy fouling at scan rate of 250 mV s^{-1}. It can be explained that the fouling could be detached from the surface of the microelectrode after each measurement, which could have led to the increase in fouling on the surface of the working electrode. As an example, the cyclic voltammogams with three consecutive scans, of the dairy fouling and the reconstituted dairy emulsion after 18 h of incubation at scan rate of 250 mV s^{-1}, are shown in Figs. 2 A and 2 B, respectively. The results of the dairy fouling measurements illustrate the differences between scans (Fig. 2 A). On the contrary, the measurements of the reconstituted dairy emulsion after 18 h do not show differences between three consecutive scans (Fig. 2 B).

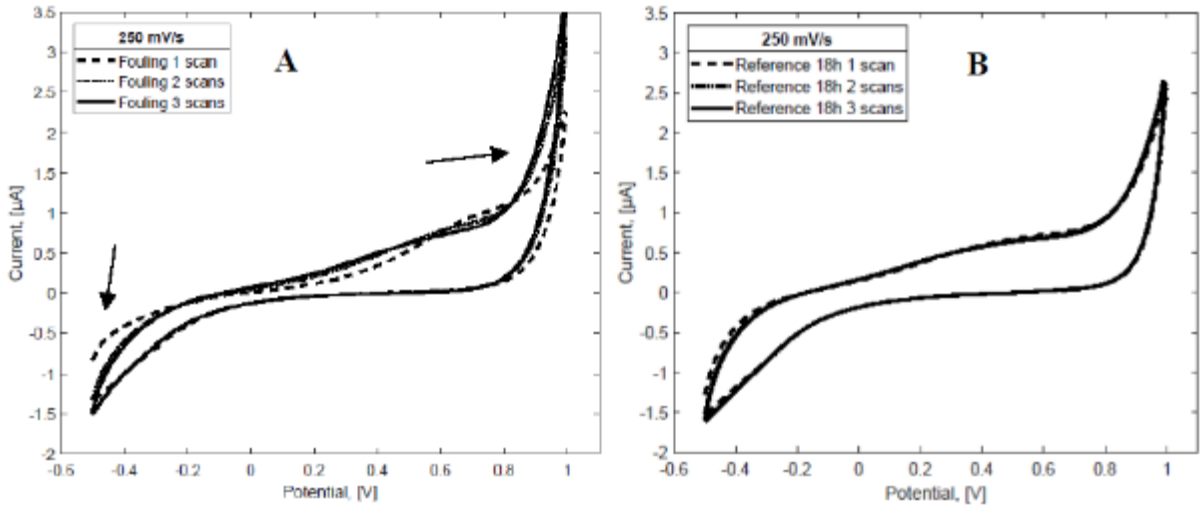

Figure 2. Cyclic voltammogams (3 scans) obtained for dairy fouling 18 h (A) and reconstituted dairy emulsion 18 h (B) at scan rates of 250 mV s^{-1}.

From Fig. 2 B shows that the current of both the anodic (oxidation) and cathodic (reduction) peaks for the incubated dairy emulsion does not change after a few consecutive scans. On the contrary, in Fig. 2 A the changes in the cathodic (reduction) and anodic (oxidation) curves for the dairy fouling are evident. It was published that for a *P. fluorescens* aggregation on electrodes, the pattern of the voltammograms obtained after 1, 2, 5, 10 and 100 scans approximated the voltammogram obtained for a surface without biofilm (Vieira *et al.* 2003). The reported finding was similar to results observed in the study of Vieira *et al.* 2003, as shown in Fig. 2 B. According to Vieira *et al.* 2003, the distance between the deposited bacteria and the surface is very short that, according to DLVO theory, is caused due to an interaction on the primary minimum of energy (Hori and Matsumoto 2010)). It means that the redox reactions cannot take place on specific places of the electrode. Once the potential is applied the distance between the bacterial aggregations and the surface may enlarge. Then, redox reactions may occur on the electrode surface that was covered by deposited bacteria. In this case, a voltammogram

similar to the voltammogram of a surface without deposit is obtained. It suggests that similar behavior may be also observed for the dairy fouling.

Table 2 shows the total sum of the standard error of the mean (SSE) and the sum of the variances (SV) for (1) the reconstituted dairy emulsion before incubation, (2) the dairy fouling, and (3) the reconstituted dairy emulsion after 18 h of incubation at scan rates of 50 mV s^{-1}, 100 mV s^{-1} and 250 mV s^{-1}.

Table 2. The sum of the standard error of the mean (SSE) and the sum of the variances (SV) for the tested samples using cyclic voltammetry at scan rates of 50 mV s^{-1}, 100 mV s^{-1} and of 250 mV s^{-1} ($p < 0.05$).

Scan rate (mV s^{-1})		Non-incubated reconstituted dairy emulsion	Dairy fouling	Reconstituted dairy emulsion 18 h
50	SSE	0.315	0.754	0.646
	SV	0.011	0.036	0.032
100	SSE	0.551	1.375	0.799
	SV	0.031	0.136	0.077
250	SSE	1.165	10.132	2.162
	SV	0.127	8.231	0.313

As expected, the reconstituted dairy emulsion before and after incubation shows the lowest sum of the standard error of the mean and the sum of the variances. On contrary, the dairy fouling has the highest sum of the standard error of the mean and the sum of the variances. It can be attributed to the non-homogeneous biofouling attachment to the surface of the microelectrodes (Fig. 4 B). For all the samples, a clear relation between the scan rates and the sum of the standard error of the mean or the sum of the variances is found. The lowest errors are obtained at a scan rate of 50 mV s^{-1}, while the highest are obtained at a scan rate of 250 mV s^{-1}.

3.2 Square wave voltammetry

The voltammograms of SWV measurements obtained at frequencies of 25 Hz, and 50 Hz for (1) the reconstituted dairy emulsion after 18 h incubation, (2) the dairy fouling covering the microelectrode with the reconstituted dairy emulsion after 18 h incubation, and (3) the non-incubated reconstituted dairy emulsion as the reference are plotted in Fig. 3.

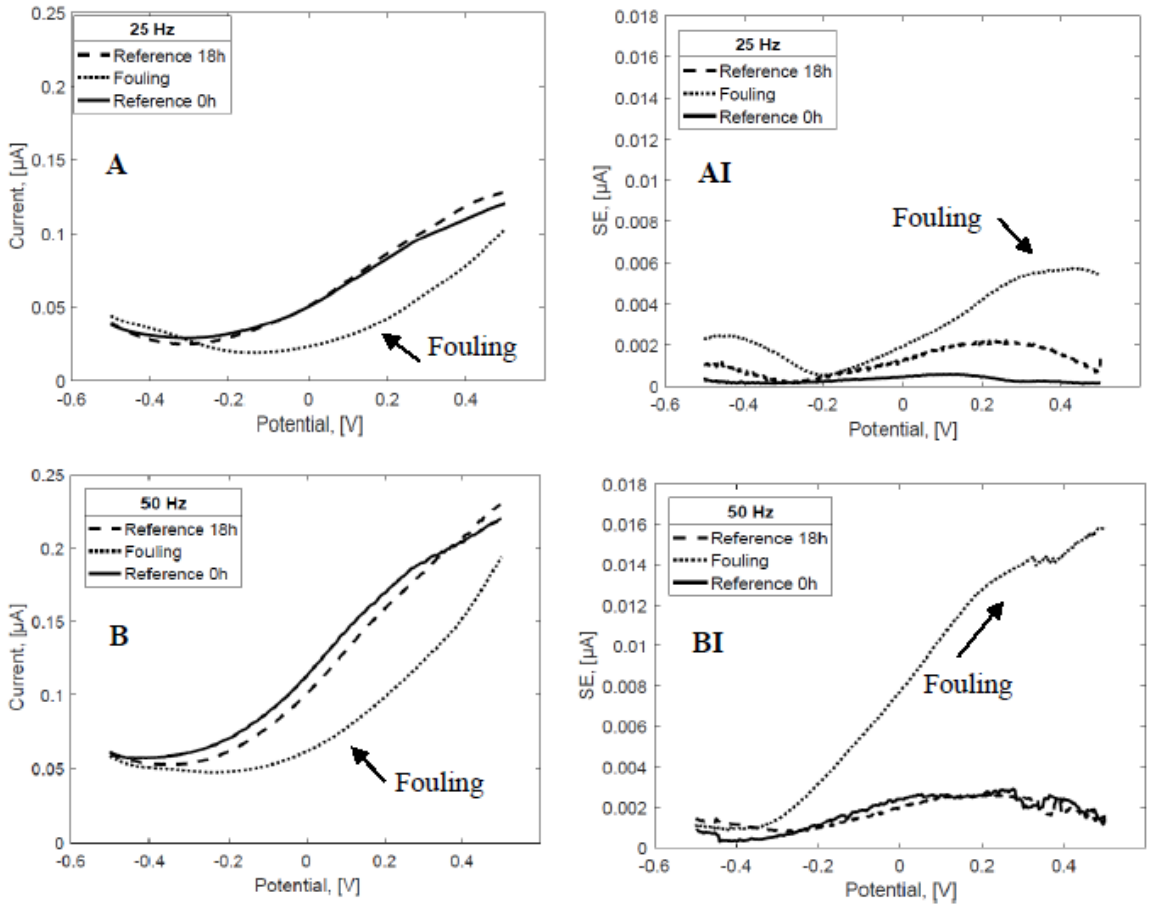

Figure 3. Square wave voltammograms (forward scan) for (1) reconstituted dairy emulsion after incubation for 18 h (Reference 18 h), (2) dairy fouling 18 h (Fouling) and (3) non-incubated reconstituted dairy emulsion (Reference 0 h) at frequencies of 25 Hz (A), and 50 Hz (B) with the respective standard errors of the mean (SE) (AI, BI) (i = 3, n = 9).

The curves in Fig. 3, show that, similarly to the results of cyclic voltammetry, the current increases with increasing frequency. The highest currents are found for the reconstituted dairy emulsions before and after incubation, followed by the dairy fouling. It can be assumed that an additional fouling layer on the working electrode may cause a resistance that lowers the current responce. The standard error of the mean for the dairy fouling is much higher compared to the errors obtained for the incubated and non-incubated dairy emulsions. Moreover, the standard errors of the dairy fouling mean increased with the increasing scan rate. The measurements were also conducted at frequency of 100 Hz. However, it was not possible to conduct the evaluation of the obtained data due to the high noise level.

Table 3 shows the total sum of the standard error for (1) the reconstituted dairy emulsion before incubation, (2) the dairy fouling covering the microelectrode with the reconstituted dairy emulsion after 18 h incubation, and (3) the reconstituted dairy emulsion after 0 h incubation at frequencies of 25 Hz, and 50 Hz.

Table 3. The sum of the standard error of the mean and the sum of variances for samples tested using SWV at frequencies of 25 Hz, and 50 Hz.

Frequency (Hz)		Non-incubated reconstituted dairy emulsion	Dairy fouling	Reconstituted dairy emulsion 18 h
25	SSE	0.310	2.742	1.131
	SV	0.001	0.100	0.016
50	SSE	1.621	7.330	1.596
	SV	0.031	0.759	0.028

Table 3 shows that the sum of the standard error of the mean and the sum of the variances increased for all samples with increasing frequency. The highest sum of the standard error of the mean and the sum of the variances among were found for the dairy fouling. Analogical results were also found for the results of cyclic voltammetry measurements (Table 2).

3.3 ATP bioluminescence measurement

The mean value of the ATP bioluminescence test for the non-incubated reconstituted dairy emulsion was 6396 ± 851 RLU (n = 9). After 18 h incubation, the RLU value slightly increased to 7386 ± 159 RLU (n = 9). The RLU value of clean electrode surface without dairy fouling was 14 ± 6 RLU (n = 9). The RLU value of the electrode surface increased to 193 ± 60 RLU after 18 h of incubation in the reconstituted dairy emulsion. In dairy industry, the method detects food/organic residues and offer proactive cleanliness management. Since the ATP bioluminescence test can detect all organic matter on food-contact surfaces (Costa *et al.* 2006), the obtained results confirm that initial whey protein adhesion to microelectrode occurred.

3.4 Microscopy

Figs. 4 A and B show the clean microelectrode and the dairy fouling on the microelectrode surface stained with crystal violet solution (0.01 g/100 mL).

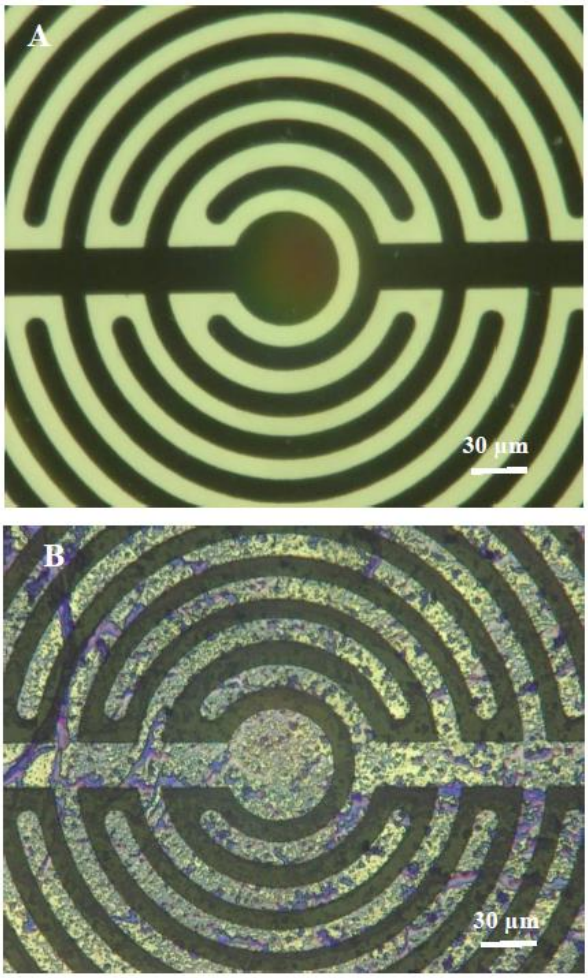

Figure 4. Micrographs of the clean interdigitated microelectrode (A), the interdigitated microelectrode surface with attached dairy fouling (18 h incubation at 30 °C) (B). All the samples were recorded with a digital microscope (VHX 100 Microscope, Keyence, Japan) at 500× magnification.

Fig. 4 B indicates that the fouling attachment on the microelectrode surface was not homogeneous with thicker and thinner clusters. It is assumed that non-homogeneous distribution of the dairy fouling (Figs. 1 and 2) may lead to the large standard deviations.

4. Discussion

Cyclic voltammetry and square wave voltammetry were used to determine dairy fouling on interdigitated ring array microelectrodes.

When discussing the attachment of fouling to the contact surfaces, the initial composition of fouling has to be considered. Since there are different components involved in fouling formation, the first question is what will attach first to the contact surface: proteins or minerals. According to literature, whey protein denaturation and aggregation as well as calcium phosphate particle formation are two

different processes and both processes follow different kinetics. Belmar-Beiny and Fryer 1993 reported that, for a solution of a whey protein concentrate, the first layer of the deposit contains mainly proteins. This indicates that the first layer adsorbed at room temperature will always be proteinaceous. The deposition of aggregates, calcium phosphate and whey protein particles, will occur at higher temperatures after the surface has been covered by a protein monolayer (Visser and Jeurnink 1997).

Indeed, β-lactoglobulin (β-LG) and α-lactalbumin (α-LA), which are responsible for initial fouling formation, are of a globular nature and both proteins are act on heat. β-lactoglobulin is the dominant protein and also more heat sensitive than α-lactalbumin. In literature it was shown that the initial binding of β-LG to a metal surface is due to a chemical linkage (Visser and Jeurnink 1997). The electrochemical study of Roscoe *et al.* 1993 showed that at pH = 7.0 and 26 °C, β-LG adsorbs onto a platinum surface as a monolayer by binding its carboxyl groups to a platinum surface OH group under decarboxylation. It was reported that the first layer of fouling can be formed at room temperature. However, the first layer formed at room temperature cannot cause a further growth of protein fouling due to the fact that bulk fouling starts at temperatures above 72 °C (Roscoe *et al.* 1993).

The cyclic voltammetry measurements of each sample showed that the current responses and the peak current magnitude increased with an increasing scan rate. Interdigitated ring array microelectrodes covered by dairy fouling showed the lowest current responses, when compared with the incubated and non-incubated dairy emulsions. This observation indicates that fouling on the working electrode represents an additional resistance, which extenuates the current response (Becerro *et al.* 2015). It was reported that the adsorption of β-lactoglobulin (β-LG) and α-lactalbumin (α-LA) to the surface enhanced the decrease of the current (Roscoe *et al.* 1993). This agrees with literature reporting that the surface coverage of the working electrode affects the current response (Bard and Zoski 2000). In the study of Rana *et al.* 2018, it was found that with increasing concentrations of Zn acetate in milk, the current decreased. The authors of the study (Rana *et al.* 2018) suggested that these metal ions can be attached to the active sites of proteins and reduce the flow of electrons onto the working surface of the electrode, thus decreasing the peak current.

The study of Rouhana *et al.* 1997, investigated the adsorption of α-lactalbumin and bovine serum albumin using cyclic voltammetry. The interfacial behavior of proteins was studied on a platinum electrode over a temperature range from 0 to 90 ºC. It was reported that both proteins adsorbed strongly on the metal surface with increasing temperature. Mixtures of the two proteins showed substantial increase in the surface charge density at the higher temperatures of 80 and 90 ºC. The authors suggested that this may be caused by intermolecular interaction which, in more concentrated solutions, provides a strong gel network. The interactions between protein and a metal surface, resulting in adsorption, can be affected by the protein properties, including other parameters such as pH, concentration, and temperature (Kiss 1993).

In square wave voltammetry, the current responses and the peak current magnitude of the voltammograms increased with the increasing frequency. As obtained in CV, microelectrodes covered by the dairy fouling showed the lowest current responses within their substance groups. Similarly to CV results, the adsorption of proteins to the surface can lead to the current's decrease. However, SWV was a less suitable method for the purpose of distinguishing dairy fouling from their corresponding substances with the chosen parametric setup. No oxidation peak currents could be detected. Only the current signal height could be used for the comparison between samples. This can be explained by the fact that SWV is better for quantitative analysis and therefore more sensitive in detecting specific analytes (Mirceski *et al.* 2013). SWV usually provides less distortion, which makes fitting of data to theoretical models more accurate. According to the literature, SWV is more suitable for the detection of low concentrations of electrochemically active species, which cannot be detectable by other voltammetric techniques. SWV can be recommended for analytical purposes, however, for which frequencies of 100 Hz might be too high (Mirceski *et al.* 2007). Similar result was also obtained in this work. At lower frequencies, the duration of the measurement is much longer and this can lead to structural changes of the tested sample. This result agrees with the study (Nguyen *et al.* 2012), where, as the frequency was increased from 1 Hz to 40 Hz, the flavin redox peak centered around −425 mV Ag/AgCl increases. Moreover, when the frequency was greater than 20 Hz, the noise level became significant, a reproducible effect across multiple flavin microelectrodes; thus, 20 Hz was chosen as the optimum frequency. Therefore, it is doubtful whether SWV is suitable for industrial implementations.

Also, emulsion, e.g., dairy emulsions as measured in this work, are of importance and cyclic voltammetry allows them to be investigated. Through electrochemical investigations, the complex structure of dairy emulsions as mixture of immiscible liquids should be considered. According to Bagotsky 2005, processes that may need to be considered in these multi-phase liquids are (1) partitioning of solutes, (2) electro-dissolution of one phase into the other, (3) the electrochemical conversion of a solute in phase to another redox level accompanied by ion exchange, and (4) processes involving material adsorbed at the interface between the two phases. In voltammetrical studies of stabilized microemulsions, processes monitored were shown to be consistent with reactions in which the reactant diffused from the emulsion droplet towards the electrode surface (Bagotsky 2005). Also, the adsorption of milk proteins at interfaces provides information on the properties of dairy emulsions (Dickinson 1989).

The presence of fouling is often assumed when poor process performance and decreased product quality are observed after production. Moreover, according to literature there is a lack of a reliable monitoring and detecting sensor system that allows to monitor both the fouling development and the cleaning processes in food processing equipment (Marchand *et al.* 2012). Real-time detection and monitoring of fouling would ensure better quality control of dairy products during processing in dairy industry. In addition, the monitoring of the cleaning processes would be advantageous for the

development of intelligent cleaning processes. The use of electrochemical interdigitated microelectrodes for the detection of biofilms and CIP cleaning solutions has been already reported in the previous study (Fysun *et al.* 2019). However, when working with electrochemical microelectrodes, it also should be taken into account that electrochemical microelectrodes require a direct contact with a target analyte, e.g., dairy products being manufactured. Therefore, an implementation of electrochemical microelectrodes into food processing equipment must be retained regarding hygienic design standards of food processing equipment.

5. Conclusion

The results showed that cyclic voltammetry and square wave voltammetry measurements combined with interdigitated microelectrodes can potentially be used for the detection of dairy fouling. Cyclic voltammetry demonstrated good results for the fouling detection and for the differentiation between the dairy emulsion and the dairy fouling at different scan rates. The attachment of dairy proteins leads to the decrease in the current in cyclic voltammograms, which can be explained by the additional insulated layer on the microelectrodes that extenuates the current response. Square wave voltammetry can be recommended for the fouling detection at low frequencies. In future, electrochemical investigations under flow conditions should be performed. Moreover, the microelectrode integration into specific high-risk parts of industrial dairy equipment have to be studied.

Founding

This work was supported by the German Research Foundation (DFG) and the Technical University of Munich (TUM) in the framework of the Open Access Publishing Program.

Acknowledgements

The authors would like to thank Prof. Dr. Bernd Wilke for beneficial discussions.

Conflict of interest

The authors declare that they have no conflict of interest.

Compliance with Ethics Requirements

This article does not contain any studies with human or animal subjects.

References

Ahmed A, Rushworth J V, Hirst N A and Millner P A (2014) Biosensors for whole-cell bacterial detection. *Clinical Microbiology Reviews* **27** 631–646.

Al-Haj H (2012) Fouling in heat exchangers. In H. A.-H. Ibrahim (Ed.), *Fouling in heat exchangers*. InTech.

Bagotsky V S (2005) *Fundamentals of electrochemistry*. Hoboken, NJ, USA: John Wiley & Sons, Inc.

Bard A J, Inzelt G, Scholz F (2012) *Electrochemical dictionary*, Springer Berlin Heidelberg, Berlin, Heidelberg.

Bard A J and Faulkner L R (2001) *Electrochemical methods: Fundamentals and applications* (2nd ed.). New York and Chichester: John Wiley.

Bard A J and Zoski C G (2000) Voltammetry Retrospective. *Analytical chemistry* **72** 346A–352A

Becerro S, Paredes J and Arana S (2015) in: Lacković, I., Vasic D. (Eds.), *6th European Conference of the International Federation for Medical and Biological Engineering (IFMBE Proceedings)*, Springer International Publishing Cham **45** 333–336.

Belmar-Beiny M T and Fryer P J (1993) Preliminary stages of fouling from whey protein solutions. *Journal of Dairy Research* **60** 467–483.

Bhushan B (2016) Bio- and inorganic fouling: in Bhushan B. (Ed.), *Biomimetics: Bioinspired hierarchical-structured surfaces for green science and technology*, Cham: Springer International Publishing 423–456.

Bottari B, Santarelli M, Neviani E (2015) Determination of microbial load for different beverages and foodstuff by assessment of intracellular ATP. *Trends in Food Science & Technology* **44** 36–48. doi: 10.1016/j.tifs.2015.02.012

Brooks J D and Flint S H (2008) Biofilms in the food industry: Problems and potential solutions. *International Journal of Food Science & Technology* **43** 2163–2176.

Characklis W G, Turakhia M H, Zelver N (1990) Transport and interfacial transfer phenomena. *Biofilms* 265–340.

Chmielewski R A N and Frank J F (2003) Biofilm formation and control in food processing facilities. *Comprehensive Reviews in Food Science and Food Safety* **2** 22–32.

Costa P D, Andrade N J, Soares N F F, Passos F J V and Brandão S C C (2006) ATP-bioluminescence assay as an alternative for hygiene-monitoring procedures of stainless steel milk contact surfaces. *Brazilian Journal of Microbiology* **37** 345–349.

Dickinson E (1989) Protein adsorption at liquid interfaces and the relationship to foam stability. In: *Foams: Physics, chemistry and structure,* Wilson A J (Ed.), Springer-Verlag, Berlin 39–53.

Epstein N (1981) Fouling in Heat Exchangers and Fouling: Technical Aspects. In: *Fouling of Heat Transfer Equipment*, Somerscales EFC & Knudsen JG, eds. 701–734.

Fischer M, Triggs G J, Krauss T F (2015) Optical Sensing of Microbial Life on Surfaces. *Applied and environmental microbiology* **82** 1362–1371.

Fysun O, Khorshid S, Rauschnabel J, Langowski H.-C (2019) Electrochemical detection of a P. polymyxa biofilm and CIP cleaning solutions by voltammetric microsensors. *Engineering in Agriculture, Environment and Food* **12** 232–243. doi: 10.1016/j.eaef.2019.01.004.

Flemming H.-C (2011) Microbial Biofouling: Unsolved Problems, Insufficient Approaches, and Possible Solutions. In: *Biofilm Highlights*, Flemming H.-C, Wingender J, Szewzyk U (Eds.), Springer International, Heidelberg, New York. doi: 10.1007/978-3-642-19940-0_5.

Fratamico P M, Annous B A, Gunther N W (2009) *Biofilms in the food and beverage industries*. Boca Raton, FL: CRC Press, Woodhead publishing.

Groysman A (2017) Corrosion Problems and Solutions at Oil Refinery and Petrochemical Units. In: *Corrosion Problems and Solutions in Oil Refining and Petrochemical Industry. Topics in Safety, Risk, Reliability and Quality* **32** Springer, Cham.

Gründler P (2007) *Chemical sensors*. Berlin, Heidelberg: Springer Berlin Heidelberg.

Hori K, Matsumoto S (2010) Bacterial adhesion: From mechanism to control. *Biochemical Engineering Journal* **48** 424–434.

Huang S.-Y, Choum C.-M, Chen T.-H, Chiou P.-C, Hsiao V K S, Ching C T.-S, Sun T.-P (2014) Enhanced Sensitivity Using Microfluidic, Interdigitated Microelectrode Based Capacitance Glucose Sensor Measured at 4 MHz. *Journal of the Electrochemical Society* **161** B102–B105.

Hulanicki A, Glab S, Ingman F (1991) Chemical sensors: Definitions and classifi cation. *Pure and Applied Chemistry* **63.**

Kang J, Kim T, Tak Y, Lee J.-H, Yoon J (2012) Cyclic voltammetry for monitoring bacterial attachment and biofilm formation. *Journal of Industrial and Engineering Chemistry* **18** 800–807.

Kazi S N (2012) Fouling and fouling mitigation on heat exchanger surfaces, in: J. Mitrovic (Ed.), *Heat Exchangers—Basics Design Applications*, InTech.

Kessler H G (2006) *Lebensmittel- und Bioverfahrenstechnik: Molkereitechnologie, 4th edn*. München: Verl. A. Kessler.

Kiss É (1993) *Colloids and Surfaces A: Physicochemical and Engineering Aspects* **76** 135–140.

Lee H J, Han D G, Lee S H, Yoo J W, Baek S H, Lee E K (1998) On-line monitoring and quantitative analysis of biofouling in low-velocity cooling water system. *Korean Journal of Chemical Engineering* **15** 71–77.

Lewandowski Z and Beyenal H (2013) *Fundamentals of biofilm research, second edn.* Boca Raton: CRC Press/Taylor & Francis Group.

Marchand S, De Block J, De Jonghe V, Coorevits A, Heyndrickx M, Herman L (2012) Biofilm formation in milk production and processing environments: influence on milk quality and safety. *Comprehensive reviews in Food Science and Food Safety* **11** 133–147. doi: 10.1111/j.1541-4337.2011.00183.x.

Min J, and Baeumner A J (2004) Characterization and Optimization of Interdigitated Ultramicroelectrode Arrays as Electrochemical Biosensor Transducers. *Electroanalysis* **16** 724–729.

Mirceski V, Guziejewski D, Lisichkov K (2013) Electrode kinetic measurements with square-wave voltammetry at a constant scan rate. *Electrochimica acta* **114** 667–673.

Mirceski V, Komorsky-Lovric S, Lovric M (2007) *Square-Wave Voltammetry: Theory and Application, first edn.*, Springer Berlin Heidelberg, Berlin, Heidelberg.

Muthukumaran S, Jagadeesh K, Srividhya V (2016) On-Line Monitoring of Biofilm Forming Pseudomonas Sp on Stainless Steel Electrodes by Repetitive Cyclic Voltammetry. *International Journal of Biotech Trends and Technology (IJBTT)* **6** 6–9.

Nguyen H D, Renslow R, Babauta J, Ahmed B, Beyenal H (2012) A voltammetric flavin microelectrode for use in biofilms. *Sensors and Actuators B: Chemical* **161** 929–937

Olsson A L, Mitzel M R, Tufenkji N (2015) Qcm-d for non-destructive realtime assessment of pseudomonas aeruginosa biofilm attachment to the substratum during biofilm growth. *Colloids and Surfaces B: Biointerfaces* **136** 928–934.

Ozkan S A, Kauffmann J.-M, Zuman P (2015) *Electroanalysis in biomedical and pharmaceutical sciences*. Berlin, Heidelberg: Springer Berlin Heidelberg.

Pavanello G, Faimali M, Pittore M, Mollica A, Mollica A, Mollica A (2011) Exploiting a new electrochemical sensor for biofilm monitoring and water treatment optimization. *Water research* **45** 1651–1658.

Rana B, Kaushik R, Kaushal K, Arora S, Kaushal A, Gupta S, Upadhyay N, Rani P, Kaushik P (2018) Physicochemical and electrochemical properties of zinc fortified milk. *Food Bioscience* **21** 117–124.

Roscoe S G, Fuller K L, Robitaille G (1993) An Electrochemical Study of the Effect of Temperature on the Adsorption Behavior of β-Lactoglobulin. *Journal of Colloid and Interface Science* **160** 243–251.

Rouhana R, Budge S M, Macdonald S M, Roscoe S G (1997) Electrochemical studies of the interfacial behaviour of α-lactalbumin and bovine serum albumin. *Food Research International* **30** 13–20.

Strycharz S M, Malanoski A P, Snider R M, Yi H, Lovley D R., Tender L M (2011) Application of cyclic voltammetry to investigate enhanced catalytic current generation by biofilm-modified anodes of Geobacter sulfurreducens strain DL1 vs. variant strain KN400. *Energy & Environmental Science* **4** 896–913.

Stulik K, Amatore C, Holub K, Marecek V, Kutner W (2000) Microelectrodes. definitions, characterization, and applications. *Pure and Applied Chemistry* **72** 1438–1492.

Tam K, Kinsinger N, Ayala P, Qi F, Shi W, Myung N V (2007) Real-time monitoring of Streptococcus mutans biofilm formation using a quartz crystal microbalance. *Caries research* **41** 474–483.

Thévenot D R, Toth K, Durst R A, Wilson G S (2001) Electrochemical biosensors: Recommended definitions and classification. *Biosensors and Bioelectronics* **16** 121–131.

Tubia I, Paredes J, Pérez-Lorenzo E, Arana S (2018) *Brettanomyces bruxellensis* growth detection using interdigitated microelectrode based sensors by means of impedance analysis. *Sensors and Actuators A: Physical* **269** 175–181.

Varshney M and Li Y (2009) Interdigitated array microelectrodes based impedance biosensors for detection of bacterial cells. *Biosensors and Bioelectronics* **24** 2951–2960.

Vieira M J, Pinho I A, Gião S, Montenegro M I (2003) The use of cyclic voltammetry to detect biofilms formed by pseudomonas fluorescens on platinum electrodes. *Biofouling* **19** 215–222.

3 DISCUSSION AND CONCLUSION

The main aim of this work was to explore new techniques for the real-time detection of the microbiologically-induced and non-microbiologically-induced dairy fouling and to systematically analyse factors influencing fouling formation. In addition, the techniques for the fouling detection that were considered in this work were used to detect alkaline and acid cleaning agents. Also, the possibility to implement these techniques in food processing equipment as a small sensor was discussed. Based on the approach presented in the Chapter 1.5 Motivation and objective of the thesis, the main subgoals of the work are given as follows:

1. Development of microbiologically-induced and non-microbiologically-induced dairy fouling models, analysis of factors for dairy fouling formation, and evaluation of methods for fouling characterization under laboratory conditions;
2. Detection of microbiologically-induced and non-microbiologically-induced fouling and of cleaning media using low-field NMR;
3. Detection of microbiologically-induced and non-microbiologically-induced fouling and of cleaning media using the two electrochemical techniques, cyclic voltammetry and square wave voltammetry in combination with microelectrodes.

3.1 Development of microbiologically-induced and non-microbiologically-induced dairy fouling models, analysis of factors for dairy fouling formation, and evaluation of methods for fouling characterization under laboratory conditions

In order to compare microbiologically and non-microbiologically-induced fouling formation in flow and in non-flow states, different experimental set-ups were constructed to investigate the selected factors (temperature, incubation time, bacterial composition, fat content of milk, food contact material, and flow) for fouling formation on food contact surfaces (Section 1 in the Chapter 2. Results).

The first study on fouling formation in non-flow state shows the evaluation of two temperatures (4 ºC and 20 ºC) and three incubation times (24 h, 48 h, 72 h) on different dairy fouling types (non-microbiologically induced dairy fouling, microbiologically-induced polyculture and monoculture (*P. fragi*) dairy fouling) formed on PTFE and stainless steel surfaces. Three methods were used for the fouling characterization: a microbiological method (viable cell count), a biochemical method (ATP-bioluminescence assay), and a physical method (dry

matter determination). The results demonstrated that non-microbiologically-induced and microbiologically-induced dairy fouling exhibited different adhesion behaviour on both food contact surfaces, namely PTFE and stainless steel. When comparing the correlation of methods ($P \leq 0.05$), the highest positive correlation coefficient is found between ATP-bioluminescence assays and viable cell count (0.932) for the fouling samples obtained after 24 h and 48 h at incubation temperatures of 4 ºC and 20 ºC. Dry matter determination shows no correlation to ATP-bioluminescence assay and no correlation to the viable cell count. Based on the results, it can be concluded that suitable detection and characterization methods should be applied for every specific fouling type, which is expected to be found in processing equipment according to the product being processed. In addition, it is confirmed that microbiologically-induced dairy fouling (monoculture *Pseudomonas fragi*) can be also formed on food contact surfaces at low temperature of 4 ºC. The results obtained in the study and the results reported in literature confirm that, although non-microbiologically-induced fouling does not necessarily microbiologically contaminate the processed product during production, food processing equipment should be regularly cleaned (Srey et al. 2013). The non-microbiological fouling can increase in size over time, what can lead to the lower efficiency of heat transfer. It can be a reason for the formation of microbiologically-induced dairy fouling (biofilm) and the recontamination of product (Marchand et al. 2012). In addition, this study documented a preparation methodology of microbiologically- and non-microbiologically-induced dairy fouling models and methods for the dairy fouling characterization that was used in the further studies on techniques for the fouling detection.

The second study on fouling formation in flow state shows the influence of factors affecting biofilm formation onset in a dairy-filling hose. Bacterial composition (monoculture *Pseudomonas fragi*, polyculture), fat content of milk (1.5%, 3.5%), flow condition (laminar, turbulent), and contact material (PTFE, stainless steel 1.4404) were evaluated as factors at a temperature of 5.5ºC. In addition, the obtained fouling models were analysed by a microbiological method (viable cell count), a biochemical method (ATP-bioluminescence assay), and a staining method for biomass quantification. The result showed that the bacterial composition, material type, and fat content significantly affect the number of viable-cell ($p \leq 0.05$). Flow conditions and material type both have significant influence upon biomass ($p \leq 0.001$). The highest positive correlation is obtained between the ATP-bioluminescence and biomass methods (0.550), followed by the ATP-bioluminescence and viable-cell-counting correlation (0.539), while the lowest correlation is found between viable-cell-counting and biomass quantification (0.345). The highest correlation between the ATP-bioluminescence and

biomass-measurement method can be explained by the fact that both methods can detect the food residuals, also called deposits, whereas viable-cell counting, by definition, only detects viable cells. Enzymatic treatment shows a good result for the cleaning of the PTFE-hose liner in the dairy-filling hose. The obtained results show that biofilm is of concern in filling units of dairy-processing equipment even at low temperature of 5.5 ºC. In addition, an experimental set-up is documented in the study that was used for the further experiments on sensors for the fouling detection. Also, a preparation methodology of different fouling models in flow state is described to achieve a good reproducibility of fouling formation for the sensor characterization.

3.2. Detection of microbiologically-induced and non-microbiologically-induced fouling and of cleaning media using low-field NMR

Within the scope of this work, different fouling types and cleaning media were investigated by low-field ^{1}H NMR to obtain a basic knowledge whether low-field ^{1}H NMR could be used as a tool for the in-line detection. In total, two studies on low-field ^{1}H NMR detection have been conducted (Section 2 in the Chapter 2. Results).

In the first study, three fouling models, (1) *Paenibacillus polymyxa* biofilm, (2) dairy biofouling, and (3) dairy fouling were investigated by low-field ^{1}H NMR. The results showed that the transverse relaxation time obtained by low-field ^{1}H NMR differs between the tubing and each deposit type. Characteristic relaxation behaviour was obtained for tubing, each deposit model, and liquid phase. The data indicates the transversal relaxation time T_2 at around 5 – 10 ms for silicone tubing. For the *P. polymyxa* biofilm, longer relaxation times T_2 of about 100 ms were detected, while relaxation times T_2 for dairy biofouling and dairy fouling were in range of 50 – 60 ms. The longest transverse relaxation time is obtained for liquid phases (nutrient medium and milk) due to the high mobility of water. The obtained results are in accordance with literature reporting that the faster relaxation rates can be found in solid-like materials and gels (Belton 1997). Solid materials and gels have shorter relaxation time than liquids due to low rotational mobility enhancing dipolar coupling (Kirkland et al. 2015). In gels, shorter relaxation time is attributed to the water protons and macromolecule exchangeable protons trapped in the gel (Belton 1997). The possibility of fouling detection by low-field ^{1}H NMR can be explained by the fact that transverse relaxation time of water contained in fouling is shorter than that of free water. Low-field NMR has been reported to be employed as a non- invasive technique in the study of biofilms due to changes in the relaxation behaviour during biofilm formation (Vogt et al. 2000; Fridjonsson et al. 2015). Biofilm is composed of bacterial cells in a hydrated gel matrix (EPS) and contributes a polymer gel-like phase

(Kirkland et al. 2015). Shorter relaxation time compared to relaxation time of free water can be assigned to the biofilm, since the biofilm consists of bound water and is located near the tubing walls (Hoskins et al. 1999; Manz et al. 2003). Based on the results, it can be concluded that low-field NMR can be used for the non-invasive detection of deposit formation in industrial processing equipment.

The second NMR study provides additional measurements for the detection of different fouling types and of CIP cleaning agents using low-field ^{1}H NMR as well as determination of diffusion coefficients. The transverse relaxation time and diffusion coefficient of sample groups (1) *P. polymyxa* biofilm, (2) dairy biofouling, and (3) CIP-cleaning agents are obtained and compared. The transverse relaxation times T_2 was obtained by inverse Laplace transform. Similar to the first NMR study, the obtained results reveal a characteristic relaxation behaviour of differently structured samples. Moreover, with increasing biofouling thickness, transverse relaxation time shifts towards slower relaxation rates. In addition, significant differences in the diffusion behaviour of water are noted for both the fouling models and for CIP-cleaning agents. The diffusion coefficient of water in dairy biofouling and in *P. polymyxa* biofilm corresponds to approximately 65% and 75% of the value of pure water, respectively. Water mobility in dairy biofouling may be reduced due to biofouling composition and structure. The components mainly responsible for dairy biofouling on the food-contact surfaces are calcium phosphate and proteins, particularly whey protein. Dairy biofouling formed at lower temperatures as studied in this study is composed mainly of proteins. The diffusion behaviour of water in biofilm can be explained by the fact that biofilm is composed of bacterial cells in a matrix of extracellular polymeric substances, which is a hydrated gel matrix. These findings are an important insight for the developments of further low-field ^{1}H NMR monitoring sensor to monitor fouling formation in processing equipment and cleaning processes.

Small low-field NMR systems equipped with permanent magnets are already available for quantitative analysis in quality control and as on-line instruments in production environments. The advantage of the low-field NMR compared to the high resolution NMR is the lower requirement regarding environment parameters, staff, maintenance and investment costs (Dalitz 2012). However, small low-field NMR systems for fouling monitoring are still lacking. Thus, the obtained results can be used for the development of real-time monitoring systems based on low-field ^{1}H NMR.

3.3 Detection of microbiologically-induced and non-microbiologically-induced fouling and of cleaning media using two electrochemical techniques, cyclic voltammetry and square wave voltammetry in combination with microelectrodes

Apart from low-field NMR methods, also electrochemical methods have been reported for real-time detection of bacterial attachment (Gião et at. 2003). Due to the electron transfer mechanisms (Nealson and Finkel 2011), electrochemical methods in combination with electrochemical microelectrodes have been investigated as a second technique for fouling detection in this work (Section 3 in the Chapter 2. Results).

In the first study on electrochemical methods, the attachment of *Bacillus subtilis* ssp. *subtilis*, *Paenibacillus polymyxa*, and *Pseudomonas fragi* to the surface on interdigitated platinum microelectrodes was investigated using the voltammetric method cyclic voltammetry (CV). The differences between the responses of the uncolonized sterile microelectrodes and the microelectrodes after the bacterial attachment were recorded and compared. The results from cyclic voltammograms obtained at scan rates of 50, 100, 250 and 350 mV s^{-1} show that the current increase is observed after bacterial attachment to the microelectrode surfaces. It can be explained by the enhanced electron transfer between the microorganisms and the electrode surface. Also, the results obtained at all scan rates depicted that the current change was observed after bacterial attachment and biofilm formation on the microelectrode surface. Therefore, it has been suggested that there may be two behaviours in opposite direction that affect the current change with the bacterial attachment. On the one hand, the current increases due to the enhanced electrochemical interaction, electron transfer between the bacterial surface-associated molecules and the electrode surface, and on the other hand, the current decreases due to the surface-covering action to diminish the area available for the electrochemical interaction. In addition, these results gave a basis for optimization of cyclic voltammetry measurement parameters for a next study to enable better detection of bacterial attachment. The interdigitated microelectrode aproach used in this work could be an alternative to the conventional electrochemical sensors due to the reduction of the thickness of electrochemical electrodes to the nanosize range. The response time of such electrodes is much shorter compared to classical electrodes (Gründler 2007).

In the second study on electrochemical methods, the results of the detection of two groups (*P. polymyxa* biofilm group and CIP cleaning solutions group) by using interdigitated platinum microelectrodes and the electrochemical voltammetric methods of cyclic

voltammetry and square wave voltammetry are reported. Cyclic voltammetry is conducted at three scan rates (50, 100 and 250 mV s^{-1}), while square wave voltammetry is performed at three frequencies (25, 50, and 100 Hz). The differences between the responses of the uncolonized sterile microelectrodes and the microelectrodes after *P. polymyxa* bacterial attachment for 18 h were determined. The results of cyclic voltammetry measurements demonstrated the possibility for the biofilm detection and for the differentiation between *P. polymyxa* in planktonic state (bacterial suspension) and *P. polymyxa* biofilm at the selected scan rates. *P. polymyxa* in planktonic state induces an increase in the current in the cyclic voltammograms. This indicates that there is an enhanced electron transfer between the bacterial surface-associated molecules and the surface of the electrodes. According to the literature, the electron transfer can occur (1) directly to the acceptor via outer membrane proteins, or via a solid conductive matrix, such as pili or outer membrane extensions or (2) indirectly through electron mediators, e.g., redox mediator. Such mechanisms may vary depending on the strain of the microorganism and environmental conditions (Nealson and Finkel 2011). The exact mechanism of the electron transfer of microorganisms selected for this work was not aimed being investigated. The microelectrodes covered with a *P. polymyxa* biofilm showed extenuated current signals, what might result from the additional resistance. The resistance is caused by the final biofilm development and deposition on the surface of the microelectrodes. Square wave voltammetry can be recommended for the detection of the CIP cleaning solutions at lower frequencies, since each investigated cleaning solution showed a specific voltammogram shape. The results indicate that cyclic voltammetry and square wave voltammetry measurements with interdigitated microelectrodes without a biorecognition element can be used for the biofilm detection and the differentiation between CIP cleaning solutions. Biorecognition elements used as receptor are usually enzymes, nucleic acids, aptamers, antibodies, organelles, membranes, cells, tissues, or even whole organisms. However, although electrochemical sensors with biorecognition elements are more sensitive, due to the protein nature, biorecognition elements in biosensors are not stable at high temperatures (above 80 °C) or common pressures, or in the presence of steam and under typical machine cleaning conditions (acidic and basic solutions).

In the last study on voltammetric methods, cyclic voltammetry and square wave voltammetry, were used to detect a non-microbiologically-induced dairy fouling and a reconstructed dairy emulsion by interdigitated platinum microelectrodes. The results obtained using cyclic voltammetry demonstrated the possiblity for the detection of non-microbiologically-induced fouling and for the differentiation between the dairy emulsion and the dairy fouling at scan

rates of 50, 100 and 250 mV s^{-1}. The attachment of dairy proteins leads to the decrease in the current in cyclic voltammograms, which can be explained by the additional insulating layer on the microelectrodes that extenuates the current response. Also, square wave voltammetry can be recommended for the fouling detection at low frequencies of 25 Hz and 50 Hz. The explanation for the current decrease by the formation of dairy fouling can be explained by the fouling composition reported in literature. For example, Belmar-Beiny and Fryer, 1993 have shown that the initial layer of the deposit in the first seconds of processing consists mainly of protein. This means that the first layer adsorbed at room temperature will always be proteinaceous. Dairy proteins, β-lactoglobulin (β-LG) and α-lactalbumin (α-LA), which are responsible for initial fouling formation, are of a globular nature and sensitive to heat. In the study of Roscoe 1993, it was published that at pH = 7.0 and 26 °C, β-LG adsorbs onto a platinum surface as a monolayer by binding its carboxyl groups to a platinum surface OH group under decarboxylation. Thus, the results of this work and literature indicate that cyclic voltammetry and square wave voltammetry measurements combined with interdigitated microelectrodes can potentially be used for the detection of dairy fouling.

4 OUTLOOK

Development of non-destructive real-time monitoring methods to detect different fouling types would be beneficial for the process control in food processing environments. Based on the results obtained within this work, the outlook for both techniques, low-field ^{1}H NMR and electrochemistry in combination with thin film microsensors, can be recommended as follows. For low-field ^{1}H NMR several questions remain to be resolved before the industrial scale introduction and production of sensor systems for food processing equipment. For further measurements, the NMR sensitivity has to be probed to obtain significant results for samples with very low amount of fouling. As additional step, the detection of fouling formation under real flow conditions is necessary to evaluate the suitability of low-field NMR for real-time fouling monitoring in dairy processing equipment. Real-time fouling detection with flowing liquid was not considered in this work and therefore, it is recommended for future studies. Real-time fouling detection in processing equipment would be advantageous for the low-field NMR sensor development, in which the conveying liquid is not stationary but flowing, as the transient protons in the conveying liquid would move out of the measurement region and would therefore not interfere with the characteristic NMR signal drop resulting from the stationary fouling formation on the tubing wall. From the perspective of food-processing technology, it is necessary to prove the possibility of NMR detection at different temperature ranges, such as the temperature of the filling process (5 – 20 ºC) or the temperature of the cleaning process (60 – 90 ºC).

In case of electrochemical thin film microsensors, good results for the detection of microbiologically-induced and non-microbiologically-induced fouling and of CIP cleaning agents have been achieved with both electrochemical methods, cyclic voltammetry and square wave voltammetry. In addition, electrochemical measurements under flow conditions should be conducted. Also, cyclic voltammetry and square wave voltammetry measurements settings should be adapted to the measurements under real industrial flow conditions. The adaptation of the electrochemical microsensors to production conditions for real-time fouling detection should be investigated. Lastly, in future research, new solutions for the implementation of electrochemical microelectrodes into food processing equipment will be needed and several questions about area of application and incorporation of electrochemical microelectrode into industrial equipment have to be answered.

5 SUMMARY

Fouling deposits on food contact surfaces in food processing equipment is a rising problem for the food industry due to more complex processing equipment and consequently due to the high risk of the cross-contamination. Thus, there is a demand on new monitoring sensor systems for the food processing equipment. The development of sensors for the real-time detection of microbiologically-induced and non-microbiologically-induced fouling as well as for the monitoring of cleaning processes would improve the process control in food processing equipment.

The main goal of this work was to explore two techniques (low-field ^{1}H NMR and electrochemistry in combination with thin film microsensors) for the real-time detection of the microbiologically-induced and non-microbiologically-induced dairy fouling as well as to systematically analyse different factors influencing fouling formation. In addition, the possibility to implement the selected techniques in food processing equipment as a small monitoring sensor system was discussed. The main results of this work are divided into three sections.

In the first section, the properties of microbiologically-induced and non-microbiologically-induced dairy fouling and factors that affect fouling formation under non-flow and flow conditions were investigated. Different experimental set-ups were constructed to investigate the selected factors (temperature, incubation time, bacterial composition, fat content of milk, food contact material, and flow) if the factors affect the fouling formation on food contact surfaces. Also, the correlation between a microbiological method (viable cell count), a biochemical method (ATP-bioluminescence assay), and a physical method (dry matter) applied to the selected fouling models was conducted. In the first study, the results obtained under non-flow state showed that non-microbiologically-induced dairy fouling and microbiologically-induced dairy fouling exhibited different adhesion behaviours. The results of the study confirmed that microbiologically-induced dairy fouling (monoculture *Pseudomonas fragi*) could be even formed on food contact surfaces at low temperature of 4 ºC. When comparing the correlation of the characterization methods, the highest positive correlation coefficient was found between ATP-bioluminescence assays and the viable cell counts for samples obtained after 24 h and 48 h at incubation temperatures of 4 ºC and 20 ºC. Dry matter measurement showed no correlations to ATP-bioluminescence assays and the viable cell counts. Also, a preparation methodology of microbiologically- and non-microbiologically-induced dairy

fouling models and methods for the dairy fouling characterization used in the further studies on techniques for the fouling detection was documented in this study.

In the second study, the influence of factors affecting fouling formation on the surface of a dairy-filling test hose under flow state at temperature of 5.5 ± 0.5 ºC showed that bacterial composition, material type, and fat content significantly affected the measured results of the number of viable-cell. Flow conditions and material type both had significant impact upon accumulated biomass weight. For ATP-bioluminescence, however, no clear influence of the selected factors could be seen. The results also show that bacterial biofilms may be formed in filling units even at low temperatures. The results suggest that microbiologically-induced fouling (biofilm) is of concern in filling units of dairy-processing equipment at low temperature. From the results obtained in both studies, it can be concluded that by knowing the type of fouling expected according to the product being processed, suitable methods for detection in dairy equipment should be applied.

In the second section, low-field ^{1}H NMR as non-destructive technique for the microbiologically-induced and non-microbiologically-induced dairy fouling and CIP cleaning agents was evaluated in two studies. The obtained results show that low-field ^{1}H NMR can potentially be used to detect and to differentiate between the different fouling types and the CIP-cleaning media. In addition, low-field ^{1}H NMR provided a possibility of non-invasive detection of fouling depositions on the inner surface of the tubing. The characteristic relaxation behaviour and diffusion behaviour of water are found and reported for the selected fouling types and CIP-cleaning agents. Therefore, low-field ^{1}H NMR can be recommended for the better understanding of food-related deposit formation and its cleaning in real time. In addition, the obtained results could be used as a basis for the development of real-time monitoring systems based on low-field ^{1}H NMR. The results provide an important insight for the developments of further low-field NMR monitoring sensors to monitor fouling formation in processing equipment and cleaning processes.

In the third section, the detection of the microbiologically-induced and non-microbiologically-induced dairy fouling and CIP cleaning agents using electrochemical interdigitated microelectrodes was evaluated. First, *Bacillus subtilis* ssp. *subtilis*, *Paenibacillus polymyxa*, and *Pseudomonas fragi* attachment to the surface on interdigitated platinum microelectrodes was detected using cyclic voltammetry. The surface coverage of microelectrodes after bacteria attachment was visualised and confirmed using microscopy techniques. The results from cyclic voltammograms obtained at scan rates of 50, 100, 250 and 350 mV s^{-1} show that the current

increase due to the extracellular electron transfer is observed after bacterial attachment to the interdigitated microelectrode surfaces.

Secondly, further results demonstrate the usage of cyclic voltammetry and square wave voltammetry measurements with interdigitated microelectrodes for the detection of *P. polymyxa* biofilm and the differentiation between CIP cleaning solutions. Cyclic voltammetry showed the possibility for *P. polymyxa* biofilm detection already at early stage of formation at different scan rates, while square wave voltammetry can be recommended for the detection of the CIP cleaning solutions at lower frequencies, since each cleaning solution showed a specific voltammogram shape.

Thirdly, the results show that cyclic voltammetry and square wave voltammetry measurements combined with interdigitated microelectrodes could potentially be used for the detection of dairy fouling. Cyclic voltammetry demonstrates the possibility for the fouling detection and for the differentiation between the dairy emulsion and the dairy fouling at different scan rates. Square wave voltammetry can be used for the non-microbiologically-induced dairy fouling detection at low frequencies of 25 Hz and 50 Hz. The attachment of dairy proteins leads to the decrease in the current, which can be explained by the additional insulating layer on the microelectrodes that extenuates the current response.

When comparing low-field ^{1}H NMR and electrochemistry, it has been demonstrated that both techniques are generally recommended for the detection of different food-related fouling types and CIP cleaning media. However, when working with NMR, it should be considered that an NMR sensor cannot detect fouling through metal surfaces. The advantage of an NMR sensor is the possibility of a non-destructive measurement. When working with electrochemical microelectrodes, it also should be taken into account that this is a technique, which requires a direct contact with a target analyte. Compared with an NMR sensor, an implementation of an electrochemical sensor into food processing equipment must be retained regarding hygienic design standards of food processing equipment. The advantage of the electrochemical microelectrodes is the small size and the possibility to incorporate the sensor into small parts of food processing equipment.

6 LITERATURE*

**The literature shown below does not include the literature cited in the seven publications that are listed in the doctoral thesis.*

Ahmed, A., Rushworth, J. V., Hirst, N. A. & Millner, P. A. (2014). Biosensors for whole-cell bacterial detection. Clinical Microbiology Reviews, 27(3), 631–646. doi: 10.1128/CMR.00120-13.

Al-Haj, H. (2012). Fouling in heat exchangers. In H. A.-H. Ibrahim (Ed.), Fouling in heat exchangers. InTech. doi: 10.5772/46462.

Armstrong, F. A., Camba, R., Heering, H. A., Hirst, J., Jeuken, L. J. C., Jones, A. K., Leger, C. & McEvoy, J. P. (2000). Fast voltammetric studies of the kinetics and energetics of coupled electron-transfer reactions in proteins. Faraday Disc. 116, 191–203. doi: 10.1039/b002290j.

Babauta, J., Renslow, R., Lewandowski, Z. & Beyenal, H. (2012). Electrochemically active biofilms: Facts and fiction. a review. Biofouling, 28(8), 789–812. doi: 10.1080/08927014.2012.710324.

Bagotsky, V. S. (2005). Fundamentals of electrochemistry. Hoboken, NJ, USA: John Wiley & Sons, Inc. doi: 10.1002/047174199X.

Bard, A. J. & Faulkner, L. R. (2001). Electrochemical methods: Fundamentals and applications (2nd ed.). New York and Chichester: John Wiley.

Bard, A. J. & Stratmann, M. (2002). Encyclopedia of electrochemistry. Weinheim and Cambridge: Wiley-VCH.

Barnes, L. M., Lo, M. F., Adams, M. R. & Chamberlain, A. H. (1999). Effect of milk proteins on adhesion of bacteria to stainless steel surfaces. Applied and Environmental Microbiology, 65(10), 4543–4548.

Becerro, S., Paredes, J. & Arana S. (2015). In: Lacković, I., Vasic D. (Eds.), 6th European Conference of the International Federation for Medical and Biological Engineering (IFMBE Proceedings), Springer International Publishing, Cham, 45, 333–336.

Becerro, S., Paredes, J., Mujika, M., Lorenzo, E. P. & Arana, S. (2016). Electrochemical real-time analysis of bacterial biofilm adhesion and development by means of thin-film biosensors. IEEE Sensors Journal, 16(7), 1856–1864. doi:10.1109/JSEN.2015.2504495.

Belton, P. S. (1997). NMR and the mobility of water in polysaccharide gels. International Journal of Biological Macromolecules, 21(1–2), 81–88.

Belmar-Beiny, M. T. & Fryer, P. J. (1993). Preliminary stages of fouling from whey protein solutions. Journal of Dairy Research, 60, 467–483.

Bhushan, B. (2016). Bio- and inorganic fouling: in Bhushan B. (Ed.), Biomimetics: Bioinspired hierarchical-structured surfaces for green science and technology, Cham: Springer International Publishing, 423–456. doi: 10.1007/978-3-319-28284-8_12.

Bonsaglia, E. C. R., Silva, N. C. C., Fernades Júnior, A., Araújo Júnior, J. P., Tsunemi, M. H. & Rall, V. L. M. (2014). Production of biofilm by Listeria monocytogenes in different materials and temperatures. Food Control, 35(1), 386–391. doi: 10.1016/j.foodcont.2013.07.023.

Brooks, J. D. & Flint, S. H. (2008). Biofilms in the food industry: Problems and potential solutions. International Journal of Food Science & Technology, 43(12), 2163–2176. doi: 10.1111/j.1365-2621.2008.01839.x.

Brownson, D. A. C. & Banks, C. E. (2014). Interpreting electrochemistry. In: D. A. C. Brownson & C. E. Banks (Eds.), The handbook of graphene electrochemistry (23–77). London: Springer London. doi: 10.1007/978-1-4471-6428-9_2.

Bryers, J. D. (1987). Biologically Active Surfaces. Processes Governing the Formation and Persistence of Biofilms. Biotechnol Progress, 3(2), 57–68. doi: 10.1002/btpr.5420030202.

Bylund, G. (1995). Dairy processing handbook (1st ed.). Lund, Sweden: Tetra Pak.

Callaghan, P. T. (1991). Principles of nuclear magnetic resonance microscopy. Clarendon Press, Oxford.

Cappitelli, F., Polo, A., & Villa, F. (2014). Biofilm Formation in Food Processing Environments is Still Poorly Understood and Controlled. Food Eng Rev, 6(1-2), 29–42.

Characklis, W. G., Turakhia, M. H. & Zelver, N. (1990). Transport and interfacial transfer phenomena. Biofilms, 265–340.

Chmielewski, R. A. N. & Frank, J. F. (2003). Biofilm formation and control in food processing facilities. Comprehensive Reviews in Food Science and Food Safety, 2(1), 22–32. doi: 10.1111/j.1541-4337.2003.tb00012.x.

Christie, J. H., Turner, J. A., & Osteryoung, R. A. (1977). Square wave voltammetry at the dropping mercury electrode: Theory. Analytical chemistry, 49(13), 1899–1903.

Costerton, J. W., Cheng, K. J., Geesey, G. G., Ladd, T. I., Nickel, J. C., Dasgupta, M., & Marrie, T. J. (1987). Bacterial biofilms in nature and disease. Annual Reviews in Microbiology, 41(1), 435–464. doi: 10.1146/annurev.mi.41.100187.002251.

Cousin, M. A. (1982). Presence and Activity of Psychroptrophic Microorganisms in Milk and Dairy Products: A Review. Journal of Food Protection, 45(2), 172–207.

Crattelet, J., Ghnimi, S., Debreyne, P., Zaid, I., Boukabache, A., Esteve, D., Auret, L., & Fillaudeau L. (2013). On-line local thermal pulse analysis sensor to monitor fouling and cleaning: Application to dairy product pasteurisation with an ohmic cell jet heater. Journal of Food Engineering, 119(1), 72–83.

Dalitz, F., Cudaj, M., Maiwald, M. & Guthausen, G. (2012). Process and reaction monitoring by low-field NMR spectroscopy. Progress in Nuclear Magnetic Resonance Spectroscopy, 60, 52–70.

Dat, N. M., Hamanaka, D., Tanaka, F. & Uchino, T. (2010). Surface conditioning of stainless steel coupons with skim milk solutions at different pH values and its effect on bacterial adherence. Food Control, 21(12), 1769–1773. doi: 10.1016/j.foodcont.2010.06.012.

Denkhaus, E., Meisen, S., Telgheder, U., & Wingender, J. (2007). Chemical and physical methods for characterisation of biofilms. Microchim Acta, 158, 1–27. doi: 10.1007/s00604-006-0688-5.

Derlon, N., Gruetter, A., Brandenberger, F., Sutter, A., Kuhlicke, U., Neu, T. R. & Morgenroth, E. (2016). The composition and compression of biofilms developed on ultrafiltration membranes determine hydraulic biofilm resistance. Water Research, 102, 63–72.

Djordjevic, D., Wiedmann, M. & McLandsborough, L. A. (2002). Microtiter Plate Assay for Assessment of Listeria monocytogenes Biofilm Formation. Applied and Environmental Microbiology, 68(6), 2950–2958. doi: 10.1128/AEM.68.6.2950-2958.2002.

Doijad, S. P., Barbuddhe, S. B., Garg, S., Poharkar, K. V., Kalorey, D. R., Kurkure, N. V., Rawool S. P. & Chakraborty T. (2015). Biofilm-Forming Abilities of Listeria monocytogenes Serotypes Isolated from Different Sources. PLoS ONE 10(9), e0137046. doi: 10.1371/journal.pone.0137046.

Drenkard, E. & Ausubel, F. M. (2002). Pseudomonas biofilm formation and antibiotic resistance are linked to phenotypic variation. Nature, 416(6882), 740–743. doi: 10.1038/416740a.

Dunne, W. M. (2002). Bacterial Adhesion. Seen Any Good Biofilms Lately? In Clinical Microbiology Reviews, 15(2), 155–166. doi: 10.1128/CMR.15.2.155-166.2002.

EHEDG Guidelines: Document 8 Hygienic Equipment Design Criteria 2nd edition. (2004). [Internet document].URL:www.goudsmitmagnets.com/data/uploads/Standards%20and%20Guidelines/EHEDG_DOC_08_English.pdf

Eneroth, Å., Ahrné, S. & Molin, G. (2000a). Contamination of milk with Gram-negative spoilage bacteria during filling of retail containers. International Journal of Food Microbiology, 57(1-2), 99–106. doi: 10.1016/S0168-1605(00)00239-7.

Eneroth, Å., Ahrné, S. & Molin, G. (2000b). Contamination routes of Gram-negative spoilage bacteria in the production of pasteurised milk, evaluated by randomly amplified polymorphic DNA (RAPD). International Dairy Journal 10(5-6), 325–331. doi: 10.1016/S0958-6946(00)00055-8.

Epstein, N. (1981). Fouling in Heat Exchangers and Fouling: Technical Aspects, in Fouling of Heat Transfer Equipment, Somerscales EFC & Knudsen JG, eds., 701–734.

Faimali, M., Chelossi, E., Pavanello, G., Benedetti, A., Vandecandelaere, I., Vos, P. d., Vandamme P. & Mollica A. (2010). Electrochemical activity and bacterial diversity of natural marine biofilm in laboratory closed-systems. Bioelectrochemistry, 78(1), 30–38. doi: 10.1016/j.bioelechem.2009.04.012.

Feder, A. L. & Yarnitzky, C. (1984). Background compensation in fast scan square wave voltammetry and other pulse techniques at the dropping mercury electrode. Analytical chemistry, 56(4), 678–681.

Foster, M. A., Magnetic Resonance in Medicine and Biology, Pergamon Press, New York, 1984.

Flemming, H.-C. & Ridgway, H. (2009). Biofilm Control: Conventional and Alternative Approaches. In: Flemming, H.-C., Murthy, P.S., Venkatesan, R., Cooksey, K. (eds) Marine and Industrial Biofouling. Springer Series on Biofilms, vol 4. Springer, Berlin, Heidelberg. doi: 10.1007/978-3-540-69796-1_5.

Flemming, H.-C. (2002). Biofouling in water systems–cases, causes and countermeasures. Applied microbiology and biotechnology, 59(6), 629–640. doi: 10.1007/s00253-002-1066-9.

Flemming, H.-C. (2011). Microbial Biofouling: Unsolved Problems, Insufficient Approaches, and Possible Solutions, in Biofilm Highlights, Flemming, H.-C., Wingender, J., Szewzyk, U. (Eds.), Springer International, Heidelberg, New York. doi: 10.1007/978-3-642-19940-0_5.

Fletcher, M. (1976). The effects of proteins on bacterial attachment to polystyrene. Journal of general microbiology, 94(2), 400–404. doi: 10.1099/00221287-94-2-400.

Fratamico, P. M., Annous, B. A. & Gunther, N. W. (2009). Biofilms in the food and beverage industries. Boca Raton, FL: CRC Press, Woodhead publishing.

Fridjonsson, E. O., Vogt, S. J., Vrouwenvelder, J. S. & Johns, M. L. (2015). Early non-destructive biofouling detection in spiral wound RO membranes using a mobile earth′s field NMR. Journal of Membrane Science, 489, 227–236.

Garrett, T. R., Bhakoo, M. & Zhang, Z. (2008). Bacterial adhesion and biofilms on surfaces. Progress in Natural Science, 18(9), 1049–1056. doi: 10.1016/j.pnsc.2008.04.001.

Giao, M. S., Montenegro, M. I. & Vieira, M. J. (2003). Monitoring biofilm formation by using cyclic voltammetry-effect of the experimental conditions on biofilm removal and activity. Water Science and Technology, 47(5), 51–56.

Gopal, N., Hill, C., Ross, P. R., Beresford, T. P., Fenelon, M. A. & Cotter, P. D. (2015). The prevalence and control of bacillus and related spore-forming bacteria in the dairy industry. Frontiers in microbiology, 6, 1418. doi: 10.3389/fmicb.2015.01418.

Gründler. P., (2007). Chemical sensors. Berlin, Heidelberg: Springer Berlin Heidelberg. doi: 10.1007/978-3-540-45743-5.

Harnisch, F., Freguia, S. (2012). A basic tutorial on cyclic voltammetry for the investigation of electroactive microbial biofilms. Chemistry - An Asian journal, 7(3), 466–475. doi: 10.1002/asia.201100740.

Hauser, G. (2009). Allgemeine Grundlagen (Chapter 6), in Hygienische Produktionstechnologie, G. Hauser (Ed.). doi:10.1002/9783527626335.ch9.

Hood, S. K. & Zottola, E. A. (1997). Adherence to stainless steel by foodborne microorganisms during growth in model food systems. International Journal of Food Microbiology, 37(2-3), 145–153. doi: 10.1016/S0168-1605(97)00071-8.

Hoskins, B. C., Fevang, L., Majors, P. D., Sharma, M. M. & Georgiou, G. (1999). Selective Imaging of Biofilms in Porous Media by NMR Relaxation. Journal of Magnetic Resonance, 139(1), 67–73.

Hulanicki, A., Glab, S., & Ingman, F. (1991). Chemical sensors: Definitions and classifi cation. Pure and Applied Chemistry, 63(9). doi: 10.1351/pac199163091247.

Jain, A., Connolly, J. O., Woolley, R., Krishnamurthy, S. & Marsili, E. (2013). Extracellular electron transfer mechanism in shewanella loihica PV-4 biofilms formed at indium tin oxide and graphite electrodes. International Journal of Electrochemical Science, 8, 1778–1793.

Janknecht, P. & Melo, L. F. (2003). Online Biofilm Monitoring. Rev Environ Sci Biotechnol, 2(2-4), 269–283. doi: 10.1023/B:RESB.0000040461.69339.04.

Kang, J., Kim, T., Tak, Y., Lee, J.-H. & Yoon, J. (2012). Cyclic voltammetry for monitoring bacterial attachment and biofilm formation. Journal of Industrial and Engineering Chemistry, 18(2), 800–807. doi: 10.1016/j.jiec.2011.10.002

Katuri, K. P., Kavanagh, P., Rengaraj, S. & Leech, D. (2010). Geobacter sulfurreducens biofilms developed under different growth conditions on glassy carbon electrodes: Insights using cyclic voltammetry. Chemical communications (Cambridge, England), 46(26), 4758–4760. doi: 10.1039/C003342A.

Kelly, A. (2004). Dairy processing: improving quality: Gerrit Smit (Ed.), CRC Press Ltd., Boca Raton, FL, and Woodhead Publishing Ltd., Cambridge, 2003.

Kessler, H. G. (2006). Lebensmittel- und Bioverfahrenstechnik: Molkereitechnologie, 4th edn. München: Verl. A. Kessler.

Kim, Y. W., Sardari, S. E., Meyer, M. T., Iliadis, A. A., Wu, H. C., Bentley, W.E. & Ghodssi, R. (2012). An ALD aluminum oxide passivated Surface Acoustic Wave sensor for early biofilm detection. Sensors and Actuators B: Chemical, 163(1), 136–145.

Kirkland, C. M. & Codd, S. L. (2018). Low-field borehole NMR applications in the near-surface environment. Vadose Zone J. 17:170007. doi: 10.2136/vzj2017.01.0007.

Kirkland, C. M., Hiebert, R., Phillips, A., Grunewald, E., Walsh, D. O., Seymour, J. D. & Codd, S. L. (2015). Biofilm Detection in a Model Well-Bore Environment Using Low-Field NMR. Groundwater Monitoring & Remediation, 35(4), 36–44.

Kotwaliwale, N., Kalne, A., Singh, K. (2010), Radiography, CT and MRI. In: Jha S. (eds) Nondestructive Evaluation of Food Quality. Springer, Berlin, Heidelberg.

Krause, M. S. & Ramaley, L. (1969). Analytical application of square wave voltammetry. Analytical chemistry, 41(11), 1365–1369.

Kwak, Y. H., Lee, J., Lee, J, Kwak, S. H., Oh, S., Paek, S.-H., Ha, U.-H., Seo, S. (2014). A simple and low-cost biofilm quantification method using LED and CMOS image sensor, Journal of Microbiological Methods, 107, 150–156. doi: 10.1016/j.mimet.2014.10.004.

Lelieveld, H. L. M., Holah, J. T., Gabric, D. (2016). Handbook of hygiene control in the food industry (2nd edition). Woodhead publishing in food science and technology, Oxford.

Lewandowski, Z. & Beyenal, H. (2013). Fundamentals of biofilm research. Boca Raton: CRC Press/Taylor & Francis Group. doi: 10.1201/b16291.

Liu, X., Tang, B., Gu, Q., Yu, X. (2014). Elimination of the formation of biofilm in industrial pipes using enzyme cleaning technique. MethodsX, 1, 130–136. doi: 10.1016/j.mex.2014.08.008.

Mafu, A. A., Roy, D., Goulet, J., & Magny, P. (1990). Attachment of Listeria monocytogenes to Stainless Steel, Glass, Polypropylene, and Rubber Surfaces After Short Contact Times. Journal of Food Protection, 53, 742–746.

Maher, A. D. & Rochfort, S. J. (2014). Applications of NMR in dairy research. Metabolites, 4(1), 131–141.

Manz, B., Volke, F., Goll, D. & Horn, H. (2003). Measuring local flow velocities and biofilm structure in biofilm systems with Magnetic Resonance Imaging (MRI). Biotechnology and Bioengineering, 84(4), 424-432.

Marchand. S., De Block, J., De Jonghe, V., Coorevits, A., Heyndrickx, M. & Herman, L. (2012). Biofilm formation in milk production and processing environments: influence on milk quality and safety. Comprehensive reviews in Food Science and Food Safety, 11(2), 133–147. doi: 10.1111/j.1541-4337.2011.00183.x.

Marcone, M. F., Wang, S., Albabish, W., Nie, S., Somnarain, D. & Hill, A. (2003). Diverse food-based applications of nuclear magnetic resonance (NMR) technology. Food Research International, 51(2), 729–747.

Mariette, F. (2018) NMR Relaxometry and Imaging of Dairy Products. In: Webb, G. (eds) Modern Magnetic Resonance. Springer, Cham.

Marsili, E., Sun, J. & Bond, D. R. (2010). Voltammetry and growth physiology of geobacter sulfurreducens biofilms as a function of growth stage and imposed electrode potential. Electroanalysis, 22(7-8), 865–874. doi: 10.1002/elan.200800007.

Matsunaga, T. & Namba, Y. (1984). Detection of microbial cells by cyclic voltammetry. Analytical chemistry, 56(4), 798–801. doi: 10.1021/ac00268a047.

Meyer, B. (2003). Approaches to prevention, removal and killing of biofilms. International Biodeterioration & Biodegradation, 51(4), 249-253. doi:10.1016/S0964-8305(03)00047-7.

Mirceski, V., Guziejewski, D. & Lisichkov, K. (2013). Electrode kinetic measurements with square-wave voltammetry at a constant scan rate. Electrochimica acta, 114, 667–673. doi: 10.1016/j.electacta.2013.10.046.

Mogha, K. V., Shah, N. P., Prajapati, J. B., & Chaudhari, A. R. (2014). Biofilm - A threat to dairy industry. Indian J. Dairy Sci., 67(6) 459–466.

Molina, Á., Laborda, E., Rogers, E. I.; Martínez-Ortiz, F., Serna, C., Limon-Petersen, J. G., Rees N. V., Compton, R.G. (2009). Theoretical and experimental study of Differential Pulse Voltammetry at spherical electrodes. Measuring diffusion coefficients and formal potentials. Journal of Electroanalytical Chemistry, 634(2), 73–81. doi: 10.1016/j.jelechem.2009.07.011.

Moretto, L. M. & Kalcher, K. (2014). Environmental analysis by electrochemical sensors and biosensors. New York, NY: Springer New York. doi: 10.1007/978-1-4939-0676-5.

Nealson, K. H. & Finkel, S. E. (2011) Electron flow and biofilms. MRS Bull, 36(05), 380–384. doi: 10.1557/mrs.2011.69.

Nguyen, H. D., Renslow, R., Babauta, J., Ahmed, B. & Beyenal, H. (2012). A voltammetric flavin microelectrode for use in biofilms. Sensors and Actuators B: Chemical, 161(1), 929–937. doi: 10.1016/j.snb.2011.11.066.

Oligschläger, D., Kupferschläger, K., Poschadel, T., Watzlaw, J. & Blümich, B. (2014). Miniature mobile NMR sensors for material testing and moisture monitoring. Diffusion fundamentals, 22(8), 1–25. URN: http://nbn-resolving.de/urn:nbn:de:bsz:15-qucosa-178760

Osteryoung, J. G. & Osteryoung, R. A. (2012). Square wave voltammetry. Analytical chemistry, 57(1), 101A–110A. doi: 10.1021/ac00279a789.

O'Toole, G., Kaplan, H. B. & Kolter, R. (2000). Biofilm formation as microbial development. Annual review of microbiology, 54, 49–79. doi: 10.1146/annurev.micro.54.1.49.

Ozkan, S. A., Kauffmann, J.-M. & Zuman, P. (2015). Electroanalysis in biomedical and pharmaceutical sciences. Berlin, Heidelberg: Springer Berlin Heidelberg. doi: 10.1007/978-3-662-47138-8.

Parizzi, S. Q. F., Andrade, N. J. d., Silva, C. A. d. S., Soares, N. d. F. F. & Silva E. A. M. d. (2004). Bacterial adherence to different inert surfaces evaluated by epifluorescence microscopy and plate count method. Braz. arch. biol. technol., 47(1), 77–83. doi: 10.1590/S1516-89132004000100011.

Pasmore, M., Todd, P., Pfiefer, B., Rhodes, M. & Bowman, C. N. (2010). Effect of Polymer Surface Properties on the Reversibility of Attachment of Pseudomonas aeruginosa in the Early Stages of Biofilm Development. Biofouling, 18(1), 65–71. doi: 10.1080/08927010290017743.

Pavanello, G., Faimali, M., Pittore, M., Mollica, A., Mollica, A., Mollica, A. (2011). Exploiting a new electrochemical sensor for biofilm monitoring and water treatment optimization. Water research, 45, 1651–1658.

Pendlebury, J. M., Smith, K., Unsworth, P., Greene, G. L. & Mampe, W. (1979). Precision field averaging NMR magnetometer for low and high fields, using flowing water. The Review of scientific instruments, 50, 535-540. doi: 10.1063/1.1135904.

Pereira, M. O., Kuehn, M., Wuertz, S., Neu, T. & Melo, L. F. (2002). Effect of flow regime on the architecture of a Pseudomonas fluorescens biofilm. Biotechnology and bioengineering, 78(2), 164–171. doi: 10.1002/bit.10189.

Pinck, S., Jorand, F. & Etienne, M. (2017). Electrochemistry of biofilms. In: Wandelt K. (ed.) Encyclopedia of Interfacial Chemistry, Elsevier, 182–189. doi: 10.1016/B978-0-12-409547-2.13805-3.

Ramaley, L. & Krause, M. S. (1969). Theory of square wave voltammetry. Analytical chemistry, 41 (11), 1362–1365.

Ramaley, L. & Surette, D. P. (1977). Autoranging in high speed data acqui sition systems. Instrumentation Science & Technology, 8 (3), 181–196. doi: 10.1080/10739147708543448.

Randles, J. E. B. (1948). A cathode ray polarograph. Part II.-The current-voltage curves. Transactions of the Faraday Society, 44 (0), 327–338. doi: 10.1039/TF9484400327.

Reyes-Romero, D. F., Behrmann, O., Dame, G. & Urban, G. A. (2014). Dynamic thermal sensor for biofilm monitoring. Sensors and Actuators A: Physical, 213, 43-51. doi :10.1016/j.sna.2014.03.032.

Romney, A. J. D. (1990). CIP: Cleaning in Place, 2nd edn. The Society of Dairy Technology, Huntingdon.

Roscoe, S. G., Fuller, K. L., Robitaille, G. (1993). An Electrochemical Study of the Effect of Temperature on the Adsorption Behavior of β-Lactoglobulin. Journal of Colloid and Interface Science, 160(1), 243–251. doi: 10.1006/jcis.1993.1390.

Rosmaninho, R., Santos, O., Nylander, T., Paulsson, M., Beuf, M., Benezech, T., Yiantsios S., Andritsos, N., Karabelas, A., Rizzo, G., Müller-Steinhagen, H. & Melo F. L. (2007). Modified stainless steel surfaces targeted to reduce fouling – Evaluation of fouling by milk components. Journal of Food Engineering, 80(4), 1176–1187. doi: 10.1016/j.jfoodeng.2006.09.008.

Roßteuscher, T. (2009). Online monitoring of biofilm in microchannels with thermal lens microscopy. Doctoral thesis at Technical University of Munich.

Sanderlin, A. B., Vogt, S. J., Grunewald, E., Bergin, B. A. & Codd, S. L. (2013). Biofilm detection in natural unconsolidated porous media using a low-field magnetic resonance system. Environmental Science & Technology, 47(2), 987–992.

Sauer, K., Rickard A. H. & Davies D. G. (2007). Biofilms and Biocomplexity. Microbe, 2(7), 347–353. doi: 10.1128/microbe.2.347.1.

Scholz, F., et al. (Eds.). (2010). Electroanalytical methods. Berlin, Heidelberg: Springer Berlin Heidelberg. doi: 10.1007/978-3-642-02915-8.

Seth Yang-En Tan, Su Chuen Chew, Sean Yang-Yi Tan, Michael Givskov & Liang Yang. (2014). Emerging frontiers in detection and control of bacterial biofilms. Current Opinion in Biotechnology, 26, 1–6.

Ševcík, A. (1948). Oscillographic polarography with periodical triangular voltage. Collection of Czechoslovak Chemical Communications, 13, 349–377. doi: 10.1135/cccc19480349.

Simões, M., Simões, L. C. & Vieira, M. J. (2010). A review of current and emergent biofilm control strategies. LWT - Food Science and Technology, 43(4), 573-583. doi: 10.1016/j.lwt.2009.12.008.

Sørhaug, T. & Stepaniak, L. (1997). Psychrotrophs and their enzymes in milk and dairy products. Quality aspects. Trends in Food Science & Technology, 8(2), 35–41. doi: 10.1016/S0924-2244(97)01006-6.

Speers, J. G. S. & Gilmour, A. (1985). The influence of milk and milk components on the attachment of bacteria to farm dairy equipment surfaces. Journal of Applied Bacteriology, 59(4), 325–332. doi: 10.1111/j.1365-2672.1985.tb03326.x.

Srey, S., Jahid, I. K. & Ha, S.-D. (2013). Biofilm formation in food industries: A food safety concern. Food Control, 31(2), 572–585. doi: 10.1016/j.foodcont.2012.12.001.

Stoodley, P., Sauer, K., Davies, D., Costerton, J. W. (2002). Biofilms as complex differentiated communities. Ann Rev Microbiol, 56, 187-209. doi: 10.1146/annurev.micro.56.012302.160705.

Storgards, E., Simola, H., Sjoberg, A.-M. & Wirtanen, G. (1999). Hygiene of Gasket Materials used in Food Processing Equipment Part 2. Trans IChemE. doi: 10.1205/096030899532295.

Stone, L. S. & Zottola, E. A. (1985). Effect of cleaning and sanitizing onthe attachment of *Pseudomonas fragi* to stainnless steel. Journal of Food Science, 50, 951–956.

Stulik, K., Amatore, C., Holub, K., Marecek, V. & Kutner, W. (2000). Microelectrodes. definitions, characterization, and applications. Pure and Applied Chemistry, 72(8), 1438–1492. doi: 10.1351/pac200072081483.

Sultana, S. T., Babauta, J. T. & Beyenal, H. (2015). Electrochemical biofilm control: A review. Biofouling, 31(9-10), 745–758. doi: 10.1080/08927014.2015.1105222.

Teixeira, P., Lopes, Z., Azeredo, J., Oliveira, R. & Vieira, M. J. (2005). Physico-chemical surface characterization of a bacterial population isolated from a milking machine. Food Microbiology, 22(2–3), 247–251. doi: 10.1016/j.fm.2004.03.010.

Teh, K. H., Flint, S., Brooks, J. & Knight, G. (2015). Biofilms in the dairy. John Wiley & Sons, Ltd, UK. doi: 10.1002/9781118876282.

Todt, H., Guthausen, G., Burk, W., Schmalbein, D. & Kamlowski, A. (2006). Water/moisture and fat analysis by time-domain NMR. Food Chemistry, 96, 436–440.

Vert, M., Doi, Y., Hellwich, K.-H., Hess, M., Hodge, P., Kubisa, P., Rinaudo, M. & Schué, F. (2012). Terminology for biorelated polymers and applications (IUPAC Recommendations 2012)*. Pure Appl Chem, 84, 377–410.

Vieira, M. J., Pinho, I. A., Gião, S. & Montenegro, M. I. (2003). The use of cyclic voltammetry to detect biofilms formed by pseudomonas fluorescens on platinum electrodes. Biofouling, 19(4), 215–222.

Visser, J. & Jeurnink, T. J. M. (1997). Experimental Thermal and Fluid Science, 14, 407-424, Fouling of heat exchangers in the dairy industry. doi: 10.1016/S0894-1777(96)00142-2.

Vogt, M., Flemming, H.-C. & Veeman, W.S. (2000). Diffusion in Pseudomonas aeruginosa biofilms: a pulsed field gradient NMR study. Journal of Biotechnology, 77(1), 137–146.

Wallhäußer, E., Hussein, M. A., Becker, T. (2012). Detection methods of fouling in heat exchangers in the food industry. Food Control, 27(1), 1–10. doi: 10.1016/j.foodcont.2012.02.033.

Wang, J. (2006). Analytical electrochemistry. Hoboken, NJ, USA: John Wiley & Sons, Inc. doi: 10.1002/0471790303.

Webster, T. A., Sismaet, H. J. & Goluch, E. D. (2014). Electrochemical monitoring of pseudomonas aeroginosa biofilms in microfluidic channels. 18th International Conference on Miniaturized Systems for Chemistry and Life Sciences, MicroTAS 2014. 2119-2121.

Wilking, J. N., Zaburdaev, V., Volder, M. d., Losick, R., Brenner, M. P. & Weitz, D. A. (2013). Liquid transport facilitated by channels in Bacillus subtilis biofilms. In Proceedings of the National Academy of Sciences of the United States of America, 110(3), 848–852. doi: 10.1073/pnas.1216376110.

Wilson, M. & Devine, D. (Eds.). (2003). Medical Implications of Biofilms. Cambridge: Cambridge University Press. doi: 10.1017/CBO9780511546297.

Wolter, B. & Krus, M. (2005). Moisture Measuring with Nuclear Magnetic Resonance (NMR). In: Kupfer K. (eds) Electromagnetic Aquametry. Springer, Berlin, Heidelberg.

Wong, K. H. & Osteryoung, R. A. (1987). Real-time simplex optimization of square wave voltammetry. Electrochimica acta, 32(4), 629–631.

Xu, K., Dexter, S. C. & Luther, G. W. (1998). Voltammetric microelectrodes for biocorrosion studies. CORROSION, 54(10), 814–823. doi: 10.5006/1.3284801.

Yarnitzky, C., Osteryoung, R. A. & Osteryoung, J. (1980). Instrument design for a one-drop square wave analyzer. Analytical chemistry, 52(8), 1174–1178.

Xiao, Y. & Zhao, F. (2017). Electrochemical roles of extracellular polymeric substances in biofilms, Current Opinion in Electrochemistry, 4(1), 206-211. doi: 10.1016/j.coelec.2017.09.016.

Zoski, C. G. (2007). Handbook of electrochemistry. Amsterdam and Oxford: Elsevier.

Further peer reviewed papers

1. Fysun, O., Nöbel, S., Loewen, A. J., Hinrichs, J. (2018). Tailoring yield stress and viscosity of concentrated microgel suspensions by means of adding immiscible liquids. LWT - Food Science and Technology, 93, 51−57. doi: 10.1016/j.lwt.2018.03.013

2. Fysun, O., Stoeckel, M., Thienel, K. J. F., Waeschle, F., Palzer, S., Hinrichs. J. (2015). Prediction of Water Activity in Aqueous Polyol Solutions. Chemie Ingenieur Technik, 87(10), 1327−1333. doi: 10.1002/cite.201400134